An Application of artificial neural networks for rainfall forecasting. December 1998.

Author:
Luk, K. C.; Ball, J. E.; Sharma, A.

Publication details:
Report No. UNSW Water Research Laboratory Report No. 194
0959240319 (ISBN)

Publication Date:
1998

DOI:
https://doi.org/10.4225/53/57a4181590631

THE UNIVERSITY OF NEW SOUTH WALES
water
research
laboratory
Manly Vale N.S.W. Australia

AN APPLICATION OF ARTIFICIAL NEURAL NETWORKS FOR RAINFALL FORECASTING

by K C Luk, J E Ball and A Sharma

Research Report No. 194
December 1998

THE UNIVERSITY OF NEW SOUTH WALES
WATER RESEARCH LABORATORY

AN APPLICATION OF ARTIFICIAL NEURAL NETWORKS FOR RAINFALL FORECASTING

by

K C Luk, J E Ball and A Sharma

Research Report No. 194

December 1998

BIBLIOGRAPHIC DATA SHEET

Report No. 194	Report Date: December 1998	ISBN: 0/85824/031/9

Title

AN APPLICATION OF ARTIFICIAL NEURAL NETWORKS FOR RAINFALL FORECASTING

Author (s)

Kin C Luk, MEngSc, MIEAust, MHKIE
James E Ball, ME, PhD, MIEAust, MASCE, MIAHR
Ashish Sharma, MTech, PhD.

Sponsoring Organisation

Australian Research Council (ARC)

Supplementary Notes

The work reported was carried out and published under the direction of the Director of the Water Research Laboratory.

Abstract

Presented in this report is the development of artificial neural networks (ANNs) for rainfall forecasting. A four-stage network development procedure is adopted, which involves identifying appropriate networks, determining network complexity, estimating parameters and evaluating performance. Particular emphasis is made on the generalization issue of complex networks with large parameters. The Upper Parramatta River Catchment is used as a test case to compare the three alternative ANN, namely, multi-layer feedforward network (MLFN), partial recurrent neural network (PRNN) and time delay neural network (TDNN). It was found that with careful development, the three alternative types of network could produce reasonable predictions of the rainfall depth one time-step (15 min) in advance. In addition, various ways to improve the accuracy of forecasts were attempted. By integrating an ANN with a spatial model developed within a Geographic Information System environment, the rainfall forecasting model was able to forecast the spatially distributed rainfall patterns one time-step ahead for the study catchment.

Distribution Statement

For general distribution

Descriptors

Rainfall forecasting; Spatial and Temporal; Alternative Types of Artificial Neural Networks.

Identifiers

Number of Pages: 114	Price: On Application.

https://doi.org/10.4225/53/57a4181590631

CONTENTS

LIST OF TABLES

LIST OF FIGURES

ACKNOWLEDGMENT

The authors wish to acknowledge the Australian Research Council (ARC) for providing the funding and support for this study through the Small Grant Scheme.

In addition, the authors would like to express their sincere thanks to the people who contributed to this study. Dr Stephen Lees and Mr Stephen Lynch of The Upper Parramatta River Catchment Trust and Mr Roger Riley of Australian Water Technologies are gratefully acknowledged for providing data for this study.

SUMMARY

Flash flooding in the urban environment is a life-threatening phenomenon. One way to reduce the risk to life and to alleviate economic losses is to provide advance warnings to people affected by these flash floods. An effective flood warning must allow sufficient lead time for the people to respond (usually more than 1 hour). This poses a critical problem for flood warning systems in most urban catchments as these catchments are characterised by a fast hydrologic response due to the small catchment size and a high proportion of effective impermeable area. Flood forecasts produced solely with a rainfall-runoff model usually cannot provide a warning with sufficient lead-time for these fast responding catchments. Forecast of likely rainfall therefore is necessary to provide advance information in order to achieve the required lead-time for warning.

Lettenmaier and Wood (1993) noted that if the hydrologic response time of a catchment is shorter than the required lead time for warning then forecasting of rainfall is required. This is necessary as some of the runoff included in the flood forecast has yet to fall as rainfall on the catchment at the time the forecast is made. Quantitative rainfall forecasting is thus an important element of a flood warning system for most urban catchments. The aim of the present study was to develop a model for forecasting short-term rainfalls and their spatial distribution over a catchment.

There are two possible approaches to rainfall forecasting. One approach involves the study of the rainfall process in order to model the underlying physical laws. However, the complexity of the rainfall generation mechanism and the lack of available climatological data on the necessary temporal and spatial scales have limited the scope and applicability of this process-based modelling approach for urban catchments. An alternative approach is based on pattern recognition methodologies, which attempt to simulate the characteristics of rainfall patterns that are representative of the observed record. The logic behind this alternative approach is to find the spatial and temporal regularities in historical rainfall patterns and to use these regularities to reproduce the expected pattern for a new rainfall event.

The rainfall forecasting model developed in this study is based on the application of two powerful computer software systems, namely artificial neural networks (ANNs) and geographic information systems (GISs). These two systems were integrated to form a powerful model which is able to provide a forecast of spatially distributed rainfall prior to its occurrence. In essence, an ANN was developed to forecast rainfall at a number of rain gauge positions, whereas a GIS was used to estimate the spatial distribution of the forecasted rainfall over the catchment.

The application of GIS for modelling of the spatial distribution of rainfall is described in detail by Luk and Ball (1996). The focus of this report, therefore, is the forecasting of future rainfall which involves implementation of a pattern recognition methodology through an ANN.

ANNs are a form of artificial intelligence. Artificial intelligence systems are concerned with implementation of computer systems that exhibit intelligent behaviour. In this respect, ANNs adopt the brain metaphor which suggests that intelligence emerges through the combined effort of a large number of processing elements connected together, each of which performs a simple computation. With this parallel distributed processing architecture, ANNs have proven to be very powerful computational tools which excel in pattern recognition and function approximation. It has been shown by Hornik et al (1989) that an ANN with sufficient complexity is capable of approximating any smooth function to any desired degree of accuracy. In addition, ANNs are computationally robust, in the sense that they have the ability to learn and generalise from examples to produce meaningful solutions to problems even when input data contain errors or are incomplete. A further advantage of ANNs in relation to short-term rainfall forecasting is that ANNs can be designed to operate in real-time.

The application of ANNs for solving any practical problems, however, requires a substantial development efforts. A four-stage network development procedure was adopted in this study, with stages being

- network identification;
- network complexity determination;
- parameters estimation; and

- performance evaluation.

The Upper Parramatta River Catchment in the western suburbs of Sydney was used as a case study to illustrate the network development. It was shown that the rainfall forecasting model was capable of producing forecast of spatially distributed rainfall patterns for the study catchment with an acceptable level of accuracy.

1. INTRODUCTION

1.1 An Overview

Flash flooding is a life-threatening phenomenon which also results in huge economic losses. An indication of the magnitude of the economic losses associated with urban flood events can be obtained from Handmer et al (1988) who estimated the direct economic losses for residential property in the Toongabbie Creek catchment of New South Wales, Australia as being approximately A$ 5 million (1986 Australian dollars) for the 1% AEP (Annual Exceedance Probability) event with nearly 500 residential properties located within the predicted limits of the 1% AEP event. In addition to the residential losses, the economic losses associated with commercial and residential activities within the Toongabbie Creek catchment were estimated to be over A$ 5.1 million (1986 Australian dollars) for the same event. Substantial further development has occurred in this catchment since the study of Handmer et al (1988) which, with the general economic inflation that has occurred, would be expected to substantially increase the economic losses in this catchment.

Development of an effective flood warning system can be expected to reduce these estimated losses. For an effective flood warning system there needs to be a sufficient time period between the recognition of a likely flood problem and its occurrence for the dissemination of flood warning messages.

Urbanisation of a catchment, however, results in a decreased catchment response time to the occurrence of rainfall which is not a desirable effect from the viewpoint of the implementation of flood warning systems. This effect of catchment urbanisation can be countered, however, through accurate quantitative rainfall forecasts. These rainfall forecasts will increase the time period between recognition of a likely flood problem and its subsequent occurrence. This need prompts the development of a rainfall forecasting model.

Rainfall is a dynamic process which varies in both space and time. Given the same amount of rainfall, the impact on flow within and from a catchment depends very much on the spatial and temporal patterns of rainfall. This variability must be considered in order to provide accurate input for modelling the hydrologic response of a catchment.

There are two possible approaches to rainfall forecasting. The first approach involves the study of rainfall processes in order to model the underlying physical laws. However, this physical approach may not be feasible because

- rainfall is a complex dynamic system which varies both in space and time;
- even if the rainfall processes can be described concisely and completely, the volume of calculations involved may be prohibitive; and
- the data that is available to assist in definition of control variables for the models, such as pressure, evaporation, wind speed and direction are limited in both the spatial and temporal dimensions.

A second approach to forecasting rainfall is to apply a transformation to the input data (present and past rainfall) for production of the desired output data (predicted future rainfall). This transformation can be considered as a mapping between the inputs and outputs without a detailed consideration of the internal structure of the physical processes. This approach is essentially a pattern recognition technique which involves the analysis of historical spatial and temporal rainfall patterns. Since all important information is embedded in the rainfall data, appropriate models are developed to extract the essential features from these historical rainfall patterns.

ANNs, which emulate the parallel distributed processing of the human nervous system, have proven to be very successful in dealing with complicated problems, such as, function approximation and pattern recognition. It has been shown that an ANN with sufficient complexity is capable of approximating a smooth function to any desired degree of accuracy (Hornik et al 1989). An ANN, therefore, was adopted in this study to carry out the complex mapping of the rainfall time series. The inputs and outputs of the ANN developed during the study were the recorded and future rainfall values at a number of rain gauges of within the study catchment.

Rainfall forecasts at gauge positions, however, provide only scattered point values over a catchment. Although the rainfall forecasts may have a fine temporal resolution, the areal rainfall which produces runoff is not known. This highlights a critical problem in

conventional rainfall-runoff modeling where simplified approaches, such as Thiessen Polygons, are used without taking the spatial distribution nor the dynamic properties of the rainfall into account. These simplified approaches can result in large error in runoff estimation (Fontaine 1991; Urbonas 1992).

Due to the rapid development in computer technology, it is increasingly feasible to provide more accurate descriptions of the rainfall in the spatial dimension. There also has been a pressing need for user-friendly, informative systems that water system managers can use to evaluate the economic, environmental and social consequences of flood events. In response to this need, Luk and Ball (1996) developed a GIS approach to model the spatial variability of rainfall using point measurements of rainfall as the input information. Within a GIS environment, the rainfall forecast information produced by the ANN can be input to a rainfall distribution model for the determination of future rainfall patterns over a catchment.

With the integration of an ANN and a GIS, a powerful rainfall forecasting model has been developed in this study to provide forecasts of spatial distribution of rainfall over a catchment. The basic assumption of this forecast model, however, is that the future rainfall is a function of a finite number of past spatial and temporal patterns of rainfall. One of the important tasks in this study therefore was to determine how rainfall forecasts are influenced by knowledge of the past spatial and temporal patterns. To achieve this aim, a comparison test was made on the forecast accuracy among the ANNs configured with different temporal lags and different numbers of spatial inputs. The optimal number of temporal and spatial inputs was determined empirically from these tests.

1.2 Outline of the Report

Although the theory of ANNs has been developed for more than a decade and there are numerous applications of ANNs in many fields of science and engineering, the development of ANNs for forecasting rainfall at multiple spatial locations has not been attempted previously. To facilitate an understanding of the approach, therefore, an introduction to the fundamental theory of ANNs is given in Chapter 2. The intention is to

provide some background theory of ANNs in order to clarify the terminology used in subsequent chapters and to pave the way for further discussions.

The Upper Parramatta River Catchment of Western Sydney was used as a case study for testing the rainfall prediction models. The catchment characteristics, hydrometric network and available data, therefore, are described in Chapter 3.

A detailed discussion on the development of ANNs for rainfall forecasting is given in Chapter 4. First, a generic model for rainfall forecasting is formulated. Then, three alternative types of ANN are identified and developed to implement the rainfall forecasting model. Within this chapter, the properties of each individual ANN are discussed in detail. The alternative ANNs are compared with the rainfall data obtained from the catchment as described in Chapter 3. In addition, contained within this Chapter is a section describing an investigation of different combinations of temporal and spatial rainfall input.

Presented in Chapter 5 is the integration of the GIS and ANN to forecast the spatial distribution of rainfall over the study catchment. The integrated model is able to produce rainfall forecasts for every pixel of the study catchment at 15 minute increments. By averaging the relevant pixel rainfalls, forecasts of subcatchment rainfall can be determined also. Artificial rainfall events were generated to ascertain the accuracy of the integrated model under ideal conditions.

The main findings and conclusions are summarised in Chapter 6 which is the final chapter of this report. Following that are several appendices providing supplementary information from the study.

2. FUNDAMENTAL THEORY AND LITERATURE REVIEW

2.1 Introduction

An artificial neural network (ANN) is a computational approach inspired by studies of the brain and nervous systems in biological organisms. The human brain is an extremely powerful computational tool that has substantial pattern recognition abilities such as those necessary for speech. These tasks, however, are very difficult for conventional computers although their computational speed is much faster than human brains. In learning a language or recognising a face, a three year old child can do much better than any computer available at present.

There is a strong motivation therefore to study how a biological neural system works in order to emulate its powerful functionality. It is believed that the powerful functionality of a biological neural system is attributed to the distributed parallel processing nature of a network of cells, known as neurons. An ANN emulates this structure by distributing the computation to small and simple processing units, called artificial neurons. With this architecture, an ANN has proven to be a powerful mathematical model which excels at function approximation and pattern recognition.

In the following sections, the building blocks of an ANN are described by drawing an analogy to their biological equivalents. The mathematical formulation of an ANN is then explained in some detail. It is shown that an ANN is a general purpose mathematical model, which can be applied to solve a wide range of problems. Like developing a conventional model, a successful application of an ANN involves careful consideration of four stages of development which are

- selecting an appropriate network;
- determining network complexity;
- estimating parameters; and
- evaluating network performance.

There are various alternative approaches in each stage of the development. These alternative approaches are discussed in detail and guidelines are provided for selection among alternatives for different problems.

2.2 Basic Structure and Functions

An analogy between an ANN and a biological neuron is drawn in order to gain a better understanding of the structure and functions of an ANN. Presented in Figure 1 is a biological neuron.

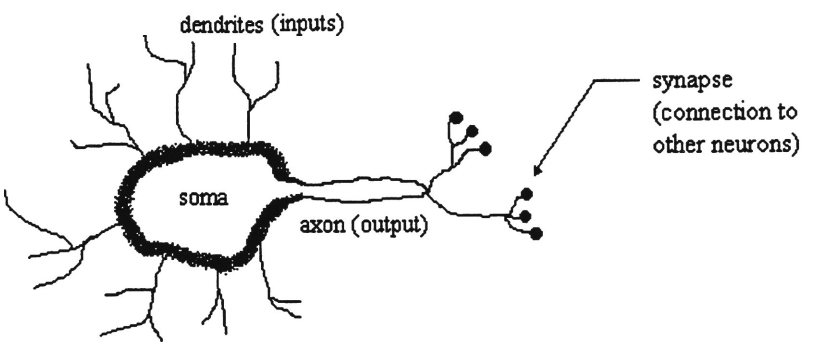

Figure 1 - A Biological Neuron

A neuron is composed of three major parts: a soma, an axon and dendrites. The soma is the central body of a neuron controlling the behaviour of the neuron. The dendrites act as a neuron's input receptors for signals coming from other neurons. The axon is the neuron's output channel and conveys signals to other neurons. The connection of a neuron's axon to the dendrite of another neuron is called a synapse. There are usually between 1000 and 10,000 synapses on each neuron.

The signal processing of a biological neural network involves three steps: First, the dendrites of a neuron receive signals (electric potentials) through its synaptic contacts with other neurons, and pass electric potentials to the soma. Second, the soma accumulates all incoming electric potentials over time. Note that some incoming electric potentials cause an increase in the soma potential, but others may lower the soma potential. Third, if the accumulated electric potential exceeds a threshold, the neuron is said to be "activated",

then an outgoing electric potential is triggered, and passed out through the axon. After transmitting the electric potential, the soma potential will fall to its resting potential level.

An outside simulate will trigger the above process. The neural system makes a response through the activation of a large number of neurons, forming a pattern of activation. Different stimulates cause different patterns of activation. As such, a biological neural system distinguishes the outside stimulates based on different patterns of activation of the neurons.

The essential features of neural processing are summarised by Schalkoff (1992) as:

- the overall processing consists of a variable interconnection of neurons;
- the processing is essentially parallel and distributed;
- local computation is simple; and
- biological neural networks are dynamic systems, whose state (e.g. neuron's outputs and inter-connection strengths) change over time, in response to external inputs or an initial state.

An ANN is constructed to mimic the structure of a biological neural network. Shown in Figure 2 is a simple ANN which consists of three layers of artificial neurons. A single output is used here for clarity of illustration. It is straightforward to extend to multiple output. Like the biological neuron, an artificial neuron, or node, consists of three main parts:

- a processing unit (soma);
- outgoing connections (axons); and
- incoming connections (dendrites).

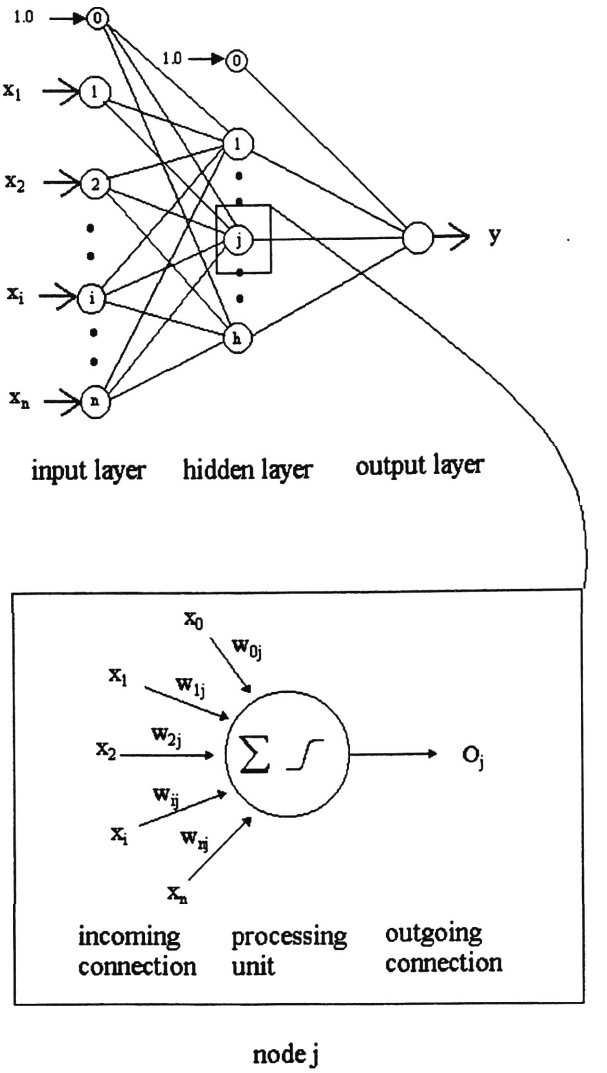

Figure 2 - A Three-layer Artificial Neural Network

The structure of an ANN is formed by nodes connected together through their connections (synaptic contacts). Nodes with similar characteristics are arranged into a layer. A layer can be seen as a group of nodes, which share the same input and output connections, but do not interconnect with themselves. In other words, connections occur only between layers and not within a layer. There are basically three types of layers. The first layer connected to the input variables is called an input layer. The last layer connected to the output variables is called an output. Layers in between the input and output layers are called hidden layers; there can be one or more hidden layers within an ANN. Information is transmitted through the connections between nodes of each layer.

Input and output nodes are used to store information. Computation relies mainly on hidden nodes, which usually contain a simple function to process information. In a simple situation, the information passes forward from the input to the output; a network of this type, therefore, is called a feedforward network with multiple layers, or simply a multi-layer feedforward network (MLFN).

Although a MLFN has a simple structure, it is a very powerful mathematical model. It was shown by Hornik et al, (1989) that given enough hidden nodes, a simple 3-layer MLFN can approximate any continuous function to any desired degree of accuracy. Mathematically, a three-layer MLFN with I input nodes, J hidden nodes, and one output node can be expressed as:

$$y = s_1\left(\sum_{j=0}^{J} w_j \cdot s_2\left(\sum_{i=0}^{I} w_i \cdot x_i\right)\right) \tag{1}$$

where
- y is the output from the ANN
- x_i are inputs to the ANN
- w_i are connection weights between nodes of input and hidden layers
- w_j are connection weights between nodes of the hidden and output layers
- $x_o = 1.0$ is a bias and w_o is weight for the bias (the bias is used to prevent the error surface from passing through the origin at all times)
- I is the total number of input nodes
- J is the total number of hidden nodes
- s_1 and s_2 are activation functions

The main control parameters of an MLFN and, in general, for any ANN, are the connection weights. The process of estimating these parameters is known as training where optimal connection weights are determined by minimising an objective function.

An ANN, therefore, is a powerful yet flexible non-linear model, which has at its core simple processing elements that collectively produce complex non-linear behaviour. The

flexibility of an ANN is due to the fact that one can vary the number of hidden layers and the number of hidden nodes in each hidden layer to adjust the computational power of an ANN. This flexibility allows one to model complex systems even though one has little knowledge about the form of relationship between the independent and dependent variables.

The non-linearity of an ANN comes from the use of non-linear activation function in the hidden nodes. The most commonly used activation function is a sigmoid (S-shaped) function, and the most popular sigmoid function is the logistic function.

$$s(x) = \frac{1}{1+e^{-x}} \tag{2}$$

One advantage of this function is that a derivative is easily found; this derivative is

$$s'(x) = s(x)(1-s(x)) \tag{3}$$

Other sigmoid functions, such as the hyperbolic tangent

$$\tanh(x) = \frac{e^{x}-e^{-x}}{e^{x}+e^{-x}} \tag{4}$$

and (scaled) arctangent, are sometimes used.

Note that many other functions can be used as the activation function. The choice depends mainly on the application. The popularity of sigmoid functions are, however, due to the following properties:

- they are continuous functions;
- they have a real-valued domain and bounded range; and
- their derivatives can be easily determined.

For the output nodes, an activation function should be chosen to suit the distribution of the target values. If the target values have no known bounded range, an unbounded activation

function such as an identity function (y = x) may be more appropriate than a sigmoid function.

2.3 Development of Artificial Neural Networks

Like conventional time series model development as described by Box and Jenkins (1976), a successful application of an ANN involves careful consideration of the stages in its development.

- selection of an appropriate network;
- determination of network complexity;
- estimation of parameters; and
- evaluation of performance.

The first stage of development involves the selection of a type of network appropriate to the problem. For example, a MLFN is suitable for function approximation while a network with feedback connections may be appropriate for modelling a dynamic system. Once an appropriate type of network is selected, the next stage is to determine the network complexity, namely to determine the number of hidden nodes and the number of hidden layers. The third stage is the estimation of the values of the parameters (connection weights). This involves the selection of an objective function, and an effective algorithm to adjust the connection weights to optimise the selected objection function. The final stage is the evaluation of the network performance.

2.3.1 Network Type

There are a considerable number of alternative types of ANN which have been developed due to the many different purposes to which they have been applied. According to Kosko (1990), an ANN can be classified by two criteria, namely, type of connection and mode of learning.

There are two main types of connections: (1) feedforward connections, and (2) feedback connections. The direction refers to the flow of information. A feedforward network only allows information to pass from input to output; whereas, a feedback network (also known

as a recurrent network) allows information to pass backwards. Feedback connections enable a recurrent network to retain information of the previous states. Thus, a recurrent network is sometimes referred to as a dynamic system containing memory. In general, feedforward networks are faster and provide a direct mapping between input and output while recurrent networks have memory and are better in simulating the dynamics of non-linear systems.

Learning is a technical term used in neural network literature. It refers to the process whereby an ANN adjusts its connection weights to achieve some predetermined criteria. There are two basic modes through which the learning process can be carried out. These are supervised and unsupervised learning.

In the supervised learning mode, a set of training data, with input and desired output, is presented to the network. The desired output serves as a teacher providing the desired response to the network. The network is thus given an indication of how it performs, and the weights are adjusted to achieve the maximum performance. A child learning to recite the alphabet at school is an example of this type of learning.

In the unsupervised learning mode, the desired output is not given. Weight adjustments are based on the responses to inputs. Often, this results in self-organisation of weights, trying to recognise patterns, regularities or separating properties in the given input data. For example, a child learning to ride a bicycle will do so with minimal help from outside. The child must learn independently how to find the balance required to ride the bicycle.

An ANN can be generally classified in quadrants shown in Figure 3. The upper left corner depicts the most transparent networks which required supervised training, such as the MLFN whereas the lower right corner area depicts recurrent networks which can self-organise to classify or associate input data, such as the Hopfield network.

Learning Mode	Connection: Feedforward	Connection: Feedback
Supervised	MLFN TDNN	PRNN
Unsupervised	Kohonen	Hopfield

Abbreviations:

MLFN - Multilayer Feedforward Neural Network

TDNN - Time Delay Neural Network

PRNN - Partial Recurrent Network

Figure 3 - Classification of ANN (after Kosko 1990)

2.3.2 Network Complexity

The network complexity is determined by the number of effective parameters within an ANN. The importance of determining the network complexity is due to the need to determine the optimal number of parameters (hidden nodes and connections) appropriate to the problem being investigated. This is similar to fitting data with a polynomial function where the order of the polynomial must be determined. Only a polynomial function with an appropriate order (complexity) can generalise the important data features and, consequently, will provide reasonable data interpolation or extrapolation.

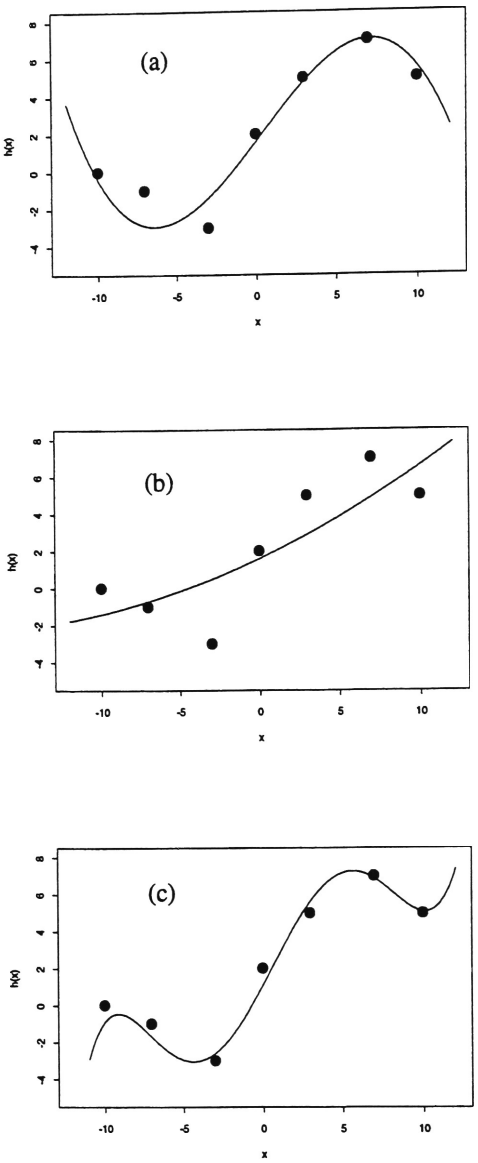

Figure 4- Polynomial Fitting

(a) Good Generalisation (b) Underfitting (c) Overfitting

Illustrated in Figure 4 are data fitted by polynomials with different order. The polynomial shown in Figure 4(a) has the right order, and thus achieves good generalisation of the data. However, the order of the polynomial shown in Figure 4(b) is too low and therefore, it is not able to fit the data points, leading to underfitting. On the other hand, the order of the polynomial shown in Figure 4(c) is too high and it passes through all the data points and ends up overfitting the data.

In most cases, the input and output nodes of a network are fixed by the problem. The network complexity, therefore, is determined by the number of hidden layers and the number of hidden nodes. There are several approaches to determine the network complexity.

- Trial and error;
- Cascade correlation;
- Pruning; and
- Genetic method.

In the trial and error approach, networks with different numbers of hidden nodes are tried and compared. The network with the best performance is finally adopted. One advantage of the trial and error approach is that it allows an observation of how the number of hidden nodes affects the performance of a network; this can be achieved by plotting the errors of the network against the number of hidden nodes to examine their relationship. The disadvantage of the trial and error method is that it is time consuming. Also this method does not guarantee to obtain the correct number of hidden nodes. Masters (1993) presented a detailed discussion on identifying the network complexity using a trial and error approach.

The cascade correlation algorithm (CasCor) was developed by Fahlman and Lebiere (1991). The CasCor is an approach which automatically increases the network complexity by increasing one hidden node at a time. A network starts without any hidden nodes and grows automatically to a more complex form. By gradually increasing the number of hidden nodes, the complexity of the network is increased. The process is stopped either when the required performance is achieved or the number of hidden nodes reaches a predetermined maximum number. The main advantage of this approach is that a network is automatically constructed according to the complexity of the problem. Thus, the CasCor is often referred to as a constructive approach. The drawback of CasCor is that it is not good for function approximation problems (Hwang et al, 1996).

Contrary to CasCor, the pruning method (LeCun et al, 1990) determines the network complexity in a destructive manner. It starts with an oversized network and gradually

deletes the unimportant nodes and connections. The main advantage of this approach is the discrimination of the important nodes and weights. This may help in analysing the properties of the network. However, in comparison with CasCor, the pruning method is slow and requires predetermination of a maximal network size.

The genetic method (Braun and Weisbrod, 1993) is a technique which mimics the evolution theory. In this approach, a network with maximal complexity is first specified. Within this specified limit, a pool of networks are then selected and compared. Like the evolution theory, the networks with poor performance are rejected; the ones with good performance are retained. Next, a second pool of networks is evolved from the retained networks, a second round of selection is made. This process of evolution and selection is repeated a number of times. Finally, the network with the best performance is adopted. The main advantage of this approach is that the ultimate network is evolved and selected from the better networks attempted. Furthermore, the network is not selected randomly, nor mechanically like the trial and error approach. However, a major drawback of this approach is that it is slow and computationally costly.

There are advantages and disadvantages in adapting any of the above methods. The choice depends on the available data, computer resources, time for completion of the task and expertise in using the alternative approaches.

2.3.3 Training

Training is a term used in the neural network literature to describe the selection of the connection weights. In conventional modelling terminology, training is similar to calibration of a model whereby the parameters of a model are adjusted to yield a desired, or target output. Hence, training is a process of determining the weights (parameters) of a network such that the network produces a particular response to a specific input.

There are generally two types of training for neural networks; these are supervised and unsupervised training. For rainfall forecasting, the network is trained with historical data, and undergoes a supervised training process. Therefore, only supervised training will be discussed here. During a supervised training process, the network is presented with input

and output patterns. Given the input patterns, the network will produce some outputs which are then compared with the target outputs. The objective of the training is to minimise the discrepancies between the network outputs and the target outputs by adjusting the parameters of the network.

An error function is a measure of the discrepancies between the network outputs and the desired outputs. The most commonly used error function is the sum of squared errors which is shown below:

$$E = \sum_{1}^{N} \sum_{1}^{P} (d_{np} - y_{np})^2 \tag{5}$$

where
- E is the sum of squared errors
- N is the total number of outputs
- P is the total number of training samples
- d_{np} are the target outputs
- y_{np} are the outputs produced by the network

The objective of training is to minimise this error function by adjusting the parameters. There are two important points to note:

- the only parameters in the error function are the weight values (the network outputs depend only on the weights as shown in equation (1), discussed in Section 2.2), and hence training proceeds by modifying the weights; and
- the error function defines an error surface in n dimensions (where n is the number of weights). This n-dimensional error surface contains many local minima which hinder the search for the global minimum point.

In essence, training of an ANN is a form of numerical optimisation, which is the search of the global minima on the n-dimensional error surface defined by the connection weights of the ANN. The search requires

- some starting positions;
- a direction towards the minimum point; and
- an appropriate step size.

Usually the starting positions are randomly selected. The direction and step size are the main concerns of all training algorithms. The most commonly used training algorithms include:

- backpropagation, or gradient descent and its variants;
- cascade correlation algorithm; and
- global training methods.

2.3.3.1 Backpropagation and its Variants

The backpropagation training algorithm (BP) was introduced by McClelland et al (1986). It was the first practical and is still the most widely used training algorithm. The name backpropagation, however, is sometimes misleading. Backpropagation training is not related to the network containing feedback connections. In fact, backpropagation is a training algorithm that enables the errors from the output layer to be successively propagated backwards through the network for adjustment of the values of the connection weights.

In essence, the BP algorithm is a gradient descent method. The search of a minimum point on the error surface is based on the direction of the steepest descent down the error surface, and the weights are modified by taking a step in this direction.

The application of the BP algorithm involves two phases. During the first phase the input is presented to the network and propagated forward through the network to compute the output value for each output node. This output is then compared with the target, resulting in an error signal for each output node. The second phase involves a backward pass through the network during which the error signal is passed to each node in the network and the appropriate weight changes are made in order to minimise the error signal.

The BP technique is a robust method which guarantees attainment of a local minimum point from a given starting position. However, it is slow and easily struck in local minima. In order to overcome its shortcomings, many variation algorithms have been developed.

One variant of the BP technique is the Quickprop algorithm developed by Fahlman (1988). The Quickprop speeds up training by using information about the curvature of the error surface. This requires the computation of second order derivatives of the error function. Quickprop assumes the error surface to be locally quadratic (approximated by a parabola) and attempts to jump in one step from the current position directly into the minimum of the parabola. However, Quickprop has the disadvantage of requiring a large number of parameters which require evaluation, and hence it can be hard to find the best parameter set.

Another variant of gradient descent technique is the Rprop which stands for Resilient backpropagation. The Rprop was introduced by Riedmiller et al (1993) to avoid the use of a fixed step size in BP. To achieve this aim, the Rprop uses an adaptive learning parameter (LP) and the sign of gradient to adjust the step size. The LP increases if the sign of gradient remains the same; otherwise LP decreases. In so doing, the training speed increases dramatically and Rprop becomes one of the fastest variants of the gradient descent techniques. In addition, there are only a few parameters that require evaluation (in general only the initial LP value). Moreover, Rprop is fairly insensitive to choices of LP since it is quickly adapted.

The last group of gradient descent variants are the methods using the rate of change of gradient, $\partial^2 E/\partial w^2$, to improve the speed of convergence. These methods include the conjugate gradient method and the Levenberg-Marquardt method. Masters (1995) has a detailed discussion of these more advanced training algorithms. In brief, these methods are often faster than the classical BP. However, they demand and require more computational resources.

2.3.3.2 Cascade Correlation Algorithm

The variants of gradient descent techniques improve the training speed. However, one major problem remains unsolved - these algorithms cannot avoid being trapped in local minima. The cascade correlation algorithm (CasCor), discussed in the previous section, can overcome the problem of local minima.

In the CasCor, new nodes are added progressively to the network. Accordingly, the number of connections increase. This means that each time when a new node is added, the error surface changes. Consequently, this gives the network the opportunity to escape from local minima by re-defining the error surface. Another advantage of the CasCor is that it is very fast computationally as only two layers of nodes are trained each time. The process of error backpropagation is avoided.

2.3.3.3 Global Training Algorithms

Global training algorithms use techniques to explore the whole error surface and thus do not get caught in local minima. However, they are much slower than gradient descent approaches, especially for large networks which have high dimensional error surfaces.

Genetic algorithms (GA) are one popular and efficient method of global searching for the optimal point. Masters (1993) has a detailed discussion on the use of GA to search for the optimal weights. The method involves three stages:

- initialisation;
- evaluation and selection; and
- crossover and mutation.

For a network with fixed number of hidden nodes, each weight (parameter) is treated as a gene. An initial population of weights is randomly generated. For a population size of n, there will be n networks. Next, the performance of each network is evaluated and the network with better performance will be assigned a higher probability for reproduction. Then, crossover and mutation are carried out from the networks. The process is repeated for a predetermined number of generations and at each generation the better parameters are preserved, and the worse die out. It can be seen that a GA involves a time consuming process, but has been shown to be an effective training approach for finding the global minimum (Braun and Weisbrod, 1993).

2.3.4 Evaluation of Performance

The final stage of network development is the evaluation of the performance of the network. The purpose of evaluation is to ensure that the network has extracted adequate detail to enable it to generalise the relevant characteristics from the measured data which, in this study, is the rainfall pattern in space and time.

A critical decision is when to stop training. In many reported studies, such as French et al (1992), training is stopped when a predetermined minimum error is reached. There are, however, two major problems of this approach. The first problem is that it is difficult to set a minimum error for training. The second problem is that this approach is inherently time consuming. After training has been completed, if an evaluation shows that the performance of the network is unsatisfactory, the network is required to be re-trained and then re-evaluated. This involves a lengthy trial and error process.

Two alternative approaches to solve this problem are discussed herein; these alternatives are: (1) the early stopping technique and (2) regularisation.

2.3.4.1 The Early Stopping Technique

The first of the two approaches to solve the above problems is the early stopping technique presented by Sarle (1995). In essence, this technique aims to monitor the progress of the network training using a separate data set. Therefore, the available data is divided into three sets: (1) training set, (2) monitoring set, and (3) validation set. The training set is used to train the network, that is to determine its parameters (connection weights). The monitoring set is used to check the progress of training and decide when to stop training while the validation set is used for final evaluation of the network performance.

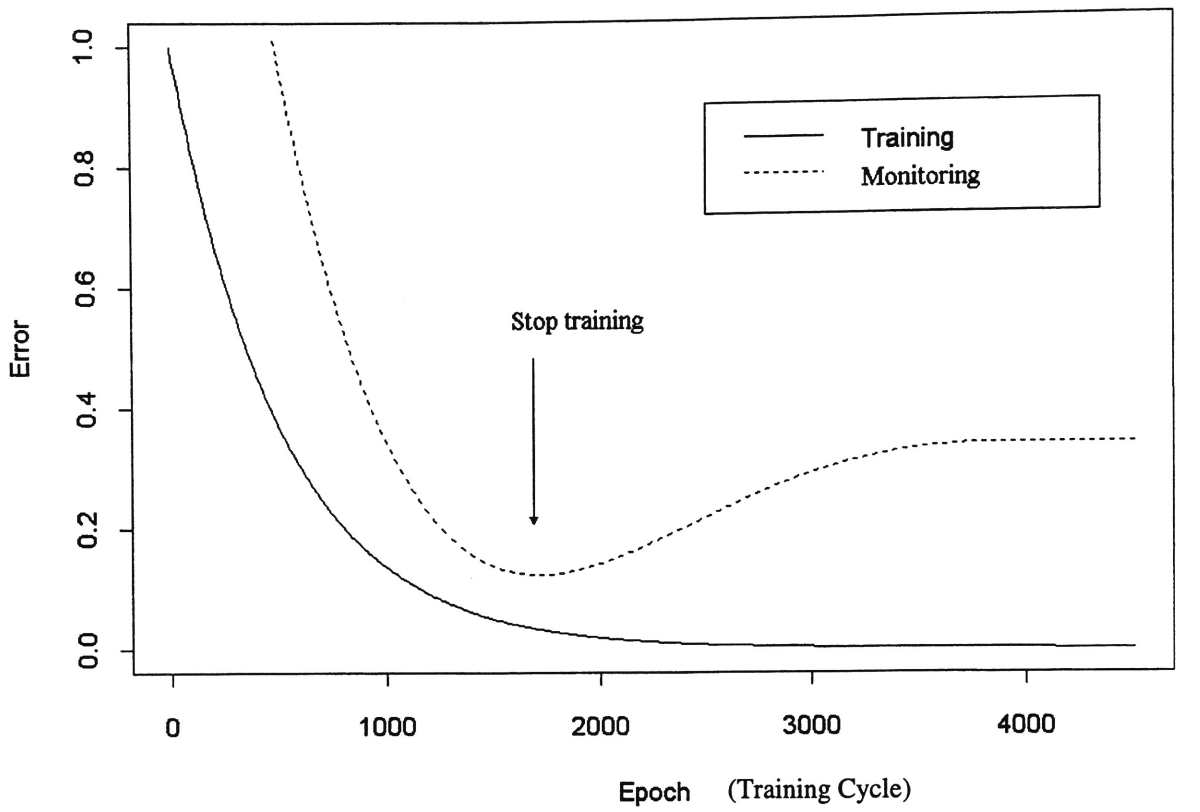

Figure 5 - Errors in Training and Monitoring

The concept of early stopping is illustrated in Figure 5 where typical error curves of a training set and a monitoring set are illustrated. Training is stopped when the monitoring set error reaches a minimum value. At this point the network has achieved the optimal generalisation. If training is not stopped, the network may be over-trained and the performance of the network will deteriorate despite the error on the training data decreasing. The network performance is finally evaluated by the validation set, which is not used at all during the training process.

The manner in which the early stopping technique avoids over-training is best explained through a discussion of the training of a network. Suppose a network is selected for training and initialised with small random parameter values. At the beginning of training, some parameters are adjusted to minimise the error between the target and network outputs. These adjusted parameters are called effective parameters because they contribute

to the performance of the network. As training progresses, the number of effective parameters grows. The error in both the training and the monitoring data set will gradually decrease as the network generalises features from the training data. As training progresses further and beyond a point, the network activates more parameters than necessary and starts to fit the noise of the training data. Consequently, a further decrease in the training error occurs but an increase in the validation error is observed. Therefore, the location of the minimum of the monitoring error determines when the network achieves an optimal number of effective parameters.

2.3.4.2 Regularisation

Another approach to ensure generalisation is regularisation (Chauvin, 1990) which is used to improve generalisation by constraining the network complexity. In most neural networks the weights are adjusted to minimise an error function which is commonly defined as the sum of squared errors. If a network pursues to minimise the sum of squared errors, it will eventually fit all the training data points. Consequently, the network will have poor performance when dealing with new data due to the problem of over-fitting.

To overcome this problem, an error function can be modified as

$$O = E + \lambda C \tag{6}$$

where E is the sum of squared errors
C is a function to penalise the complexity of the network
λ is a parameter specifying the importance of C relative to E

The inclusion of the penalty term (λC) is to prevent the network from fitting exactly to the data points. The penalty term thus has a smoothing effect to the network's complexity.

This approach requires the determination of the function C and the parameter λ. As regards the first decision, one way is to penalise the change in weights. For example, C can be defined as:

$$C = \frac{1}{2}\sum w_j^2 \tag{7}$$

where w_j are the weights of the networks. The derivative to the objective function results in

$$\frac{\partial O}{\partial w} = \frac{\partial E}{\partial w} + w \tag{8}$$

Recall that in the gradient descent method, the change in weight is based on the negative of $\partial E/\partial w$. Therefore, the penalty term reduces the change of weight proportional to the size of the weight. Consequently, this method is often referred to as weight decay.

As regards the second decision, if the value of λ is small, there is little penalty for complexity and the network is able to fit the training data closely. On the other hand, if the value of λ is large, the network is prevented from developing a complex mapping, and excessive error may result. An optimal λ must be carefully determined. One way is to try a series of λ and use a validation sample to evaluate the results. However, this method is computationally intensive.

Comparing the early stopping technique with the regularisation method, the former approach will usually be found to be computationally faster and easier to implement. For this reason, an early stopping technique was used in this study.

2.4 Application of Artificial Neural Networks in Hydrology

Recently enormous literature relating to the development and application of ANNs has evolved. From a review of this literature, it can be seen that ANNs have been successfully applied to many problems in civil engineering (Cheu et al, 1991; Moselhi et al, 1991; Furuta et al, 1991) and structural engineering (Kamarthi et al, 1992; Xihui et al, 1991) as well as time series predictions (Weigend et al, 1992; Wan, 1993).

Although ANNs have wide application in many fields of science and engineering, the review given here is confined to the application of ANN in hydrology, with particular reference given to rainfall forecasting. A good general review of the application of ANNs in hydrology and water resources engineering is provided by Daniell (1991) who also presented examples where ANNs had been used to determine water consumption and regional flood estimates.

With the rapid development of ANNs, there have been a growing number of studies applied ANN to solve problems in hydrology. These applications cover a wide range of areas, including rainfall forecasting (French et al, 1992; Tohma and Ando, 1995), river flow prediction (Karunanithi et al, 1994; Zhu and Fujita, 1994), modelling rainfall-runoff process (Hsu et al, 1995; Smith et al, 1995; Minns and Hall, 1996), hydraulic structure operation (Rasul and Paudyal, 1994), scheduling of hydroelectric power systems (Sadd et al, 1996), as well as geophysical log interpretation (Pezeshk et al, 1996).

Flood (1994a, b) pointed that several factors have stimulated research in the application of ANNs. One factor is that an ANN is able to learn and generalise from examples, without a detailed study of the underlying principles. The other factor is an ANN is a powerful non-linear model which in theory can approximate any continuous function to any degree of accuracy. Daniell (1991) also pointed out that the extremely uncertain nature of many hydrological data sets where a particular output is dependent on many unmeasurable variables results in many hydrological problems being suitable for analysis using neural networks.

Although an ANN is a powerful tool, the successful application of an ANN must involve careful consideration of four stages of ANN development which are

- Identification of network architecture;
- Determination of network complexity;
- Selection of training algorithms; and
- Validation of network performance.

However, this systematic approach has not been adopted in most of the previous reported studies in hydrology. The review presented in the following sections highlights that these studies have not given sufficient emphasis to each stage of the network development resulting in poor network design in many cases. In line with the network development discussed above, the review is organised into four sections.

It must be pointed out also that many hydrological applications have been illustrated only with synthetic data. In the present study, however, real data were used in order to evaluate the networks' performance for real life applications.

2.4.1 Identification of Network Architecture

The range of alternative ANNs is immense and growing rapidly. Each type has its own characteristics, often determining its suitability for solving certain classes of problems. For example, multi-layer feedforward networks (MLFN) are suitable for function approximation and static mapping of inputs and outputs (Sejnowski and Rosenberg, 1987; Pomerleau, 1989), while the radial basis function networks are more efficient in classification problems (Moody and Darken, 1989; Renals and Rohwer, 1989). Networks with feedback connections are more appropriate for modelling dynamic processes (Jordan, 1986; Elman, 1990). Time Delayed Neural Networks are specially designed for modelling temporal sequences (Waibel, 1989). For large and complex problems, Modular Neural Networks consisting of a group of ANN modules are used to decompose the problems into smaller and manageable tasks (Jacobs et al, 1991 (a, b); Happel and Murre, 1994).

Many reported studies in hydrology have used a multi-layer feedforward network (MLFN) without referencing other types of ANN. While a MLFN is a powerful non-linear model and has been shown to be an universal approximator, there are many other types of ANN which may have been more appropriate to the problem being considered. For example, Saad and Bigras (1996) applied a radial basis functions neural network (RBFN) to assist in determining the operating rules for reservoirs. They compared the RBFN with a MLFN trained with backpropagation technique and found that the RBFN outperformed the MLFN. They pointed out that the learning of the back propagation technique in the MLFN was time-consuming and that using the RBFN approach gave results at least 15 times faster.

A review on previously reported studies in rainfall forecasting showed that the only network type which had been applied to the problem was a MLFN. French et al (1992) applied a MLFN to forecast rainfall in space and time. They used the network to forecast artificial two-dimensional rainfall fields one time step ahead which was in one hour increments. The data were generated by a mathematical rainfall simulation model which was a modified version of the model developed Rodriguez-Iturbe and Eagleson (1987). They compared the rainfall forecast made by the MLFN with those obtained by the nowcasting technique and claimed that the MLFN could generalise and abstract the rainfall process. Their study, however, can be considered as a preliminary investigation only since there was a lack of consideration in various stages of development of the neural network and only artificial data were used.

Although their study was one of the first attempts in applying ANN to forecast rainfall and paved the way for subsequent development, a number of key issues were not properly addressed. Firstly, a MLFN was adopted without referencing other types of network. Secondly, the input data considered only rainfall one time-step in the past. The inclusion of more information from the past as input was not considered. Thirdly, the network complexity was determined arbitrarily.

Another problem was that the MLFN in their study was developed with a very large number of weights; a network with such a large number of weights was extremely difficult to optimise. In their study, the simulation domain was 100km × 100km at a resolution of 4km, yielding a regular grid of 25 × 25 points (625 points). The number of input and output nodes was 625 which was determined by the size of grid. The number of hidden nodes was arbitrarily chosen from 15 to 100, resulting in a network containing more than 20,000 connection weights. The training data set for the network, however, contained only 1000 training data points. Similar to fitting three data points with a ten-order polynomials, the network was bound to overfit the training data, resulting in a network with poor generalisation.

Along similar lines, Tohma and Ando (1995) used a MLFN to produce a 1-hour lead time forecast of rainfall fields using simulated rainfall inputs. Again, their network was very large consisting of 576 input nodes and 576 output nodes. The numbers of hidden nodes attempted were 90, 120 and 150. Twenty rainfall events were used for training and ten events for validation. Each event contained 20 data points. Obviously there were insufficient data to train the network. In brief, Tohma and Ando did not achieve any improvements over the work of French et al (1992). They did not provide any discussion on the choice of networks nor did they provide information on how to optimise the network performance.

In summary, there are various types of ANN developed to solve specific problems. One needs to identify a network architecture appropriate to the problem. Chapter 4 of this report contains a detailed discussion of the various types of networks and their suitability for rainfall forecasting.

2.4.2 Network Complexity

Given a particular type of network, say an MLFN, a critical problem is the determination of the number of hidden nodes. If there are too few hidden nodes, the network is not able to learn the features of a complex problem. On the other hand, if a network contains too many hidden nodes, it tends to learn not only the features but also the noise of the data.

However, the important issue of network complexity has not been properly addressed in many previous reported studies. For example, French et al (1992) used an arbitrary number of hidden nodes, while Rasual and Paudyal (1994) and Minns and Hall (1996) did not state how many hidden nodes were included in their networks. This indicated that the networks may not have been designed according to the complexity of the problem.

A study which took into account the network complexity was presented by Karunanithi et al (1994), who used the cascade correlation algorithm to train a MLFN for river flow prediction. The cascade correlation algorithm was an efficient training algorithm which combined the idea of incremental network building and learning in the training process. In essence, the training starts with a minimal network comprising only input and output

layers. Then, hidden nodes are added one at a time during the training process. The training is stopped when the specified error is reached. This ends up with an automatically structured network according to the complexity of the problem.

However, it is difficult to set a minimum error for training. Therefore, in the present study a trial and error approach was adopted. A number of networks were constructed and their performance compared. Finally, the best performed network was selected.

2.4.3 Selection of Training Algorithms

The training of neural networks involves minimising the discrepancies between the target outputs and network outputs. This can be achieved by adjusting the weights between connections. The most popular algorithm for adjusting the weights is the backpropagation (BP) method which has been adopted in many hydrological applications. However, many studies failed to point out that the BP approach is a gradient descent algorithm, which is computationally inefficient and is usually trapped in a local minimum.

Hsu et al (1995) was one of the first to avoid the use of BP. They applied a three-layer MLFN to model the rainfall-runoff process. A procedure (entitled linear least squares simplex, or LLSSIM) was developed in their study to optimise the parameters of the three-layer MLFN. The LLSSIM method, which used a combination of linear least squares and multi-start simplex optimisation techniques, was claimed to obtain the global or near-global solution of the problem. In addition, this study was one of the few hydrologic applications of ANN using real life data.

There have been rapid developments on training algorithms for neural networks. The objectives are to improve training speed and avoid local minima. An excellent review of the BP and its variants is presented by Riedmiller (1994). In addition, the earlier discussion in Section 2.3.3.3 of this Chapter provides an overview of global search training algorithms.

2.4.4 Generalisation

Even with the best training algorithms, the network may not be able to achieve good generalisation of the features of the system. In most cases, the better the network learns the training samples, the worse it will perform on the data it has not encountered during the training process. This problem is due to over-learning of the training samples. However, in many hydrologic applications, there is limited discussion about the important issue of generalisation. To some extent the networks were trained arbitrarily. For example, French et al (1992) trained the networks with 100-1000 iterations without specifying a reasonable stopping criterion.

Smith and Eli (1995) trained their network with predetermined error tolerances and then evaluated the performance of the network by some test data set. The problem with their approach is that there is no efficient way of pre-defining an error tolerance, and that the error tolerance of training samples is not related to the problem of generalisation.

In view of this, a strategy is required to make the best use of the available data to ensure generalisation. The early stopping technique discussed previously is one such strategy and was adopted in the present study. Our use of the early stopping technique in this study is thought to be one of the first attempts at its application in the field of hydrology.

2.5 Summary

From the above review, it can be concluded that the application of an ANN to solve a hydrological problem requires careful consideration at each stage of development, namely: selection of an appropriate network, identifying the network architecture, choosing appropriate training algorithms, and achieving good generalisation. A successful application requires sound engineering judgement and knowledge of the available techniques. The development of an ANN for rainfall forecasting is discussed in detail in Chapter 4 where a case study on forecasting rainfall at multi-locations in a catchment is included to illustrate the points discussed.

3. THE STUDY CATCHMENT

The Upper Parramatta River Catchment (UPRC) is used as a case study for development of the rainfall forecasting model. This Chapter provides some details of the catchment characteristics, hydrometric network and available data for the study.

3.1 Catchment Details

The UPRC, shown in Figure 6, is located in the western suburbs of Sydney, Australia. Total area of the catchment is approximately 112 km^2. The catchment is rather steep with the confining ridges being 180 metres Australian Height Datum (AHD) at Thompsons Corner, Castle Hill, and 100 metres AHD at Prospect. The average slope of the catchment is about 1.2%.

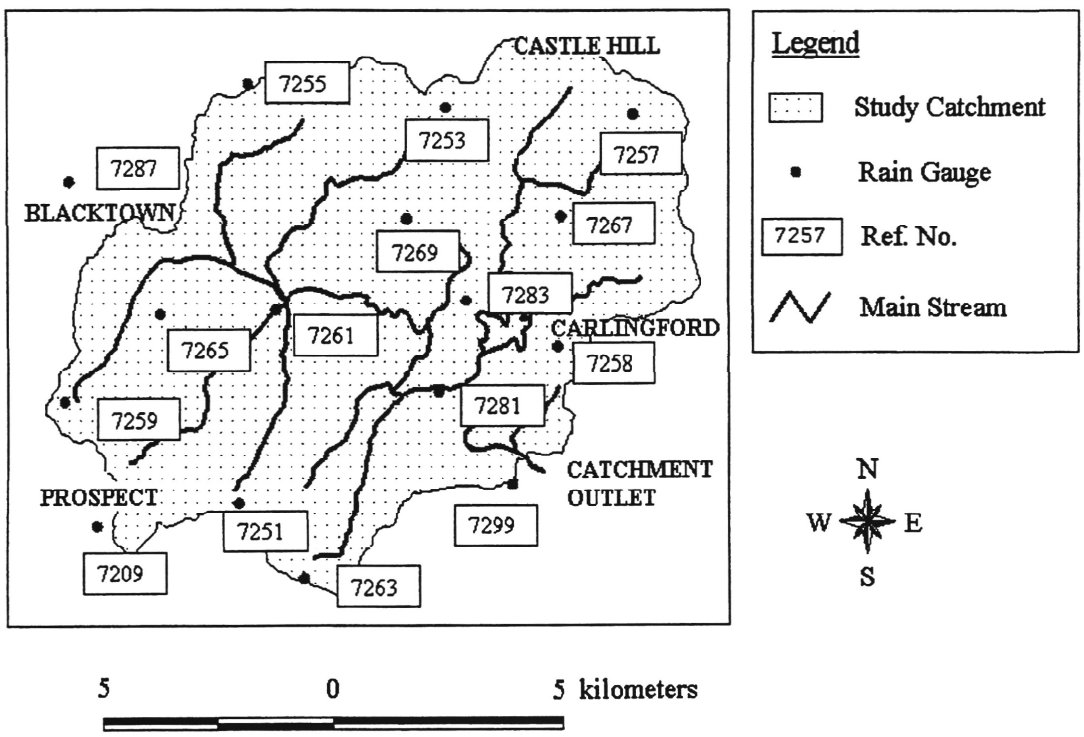

Figure 6 - The Upper Parramatta River Catchment

The Parramatta River drains into Sydney Harbour and is tidal to the Charles Street Weir located at the catchment outlet. The section of the Parramatta River immediately upstream of the Charles Street Weir passes through part of the Parramatta central business district.

There are two main tributaries, namely Toongabbie Creek and Darling Mills Creek. They join about 2.5 km upstream of the Charles Street Weir.

Within the catchment, the dominant land use is typical of urban environments with a mix of residential, commercial, industrial and open space (parkland) areas. Considerable development as a result of rapid increase in population and dwellings has occurred within the catchment over the past two decades. Details are shown in Table 1 which was obtained from Australian Bureau of Statistics, Census of Population and Housing (personal communication).

TABLE 1
POPULATION AND DWELLINGS IN PARRAMATTA

Year	Total Population	% Change to Previous 5 Years	Total Occupied Dwellings	% Change to Previous 5 Years
1976	348398	--	100246	--
1981	374190	7.4	111064	10.8
1986	384601	2.8	119229	7.4
1991	435478	13.2	140900	18.2

Shown in Table 1 are five year census report figures for years 1976, 1981, 1986 and 1991. The increase in dwellings from 1986 to 1991 by 18% in 5 years is significant. A rough estimation of the increase in impervious areas can be made by assuming an average dwelling size of 200 square metres and allowing 50% for associated roads and courtyards. The increase in paved area would be 6.5 km^2, which amounts to 6% of the total catchment area.

The effect of urbanisation and rapid development has led to increases in estimates of the peak level for frequently occurring floods. To mitigate the social and economic losses associated with flood events in this catchment, the Upper Parramatta River Catchment Trust (UPRCT) was instituted in 1989 with the task of managing flood mitigation measures within the catchment, among other duties.

3.2 Available Data

There are sixteen (16) telemetered rain gauges within the Upper Parramatta River Catchment; locations of these gauges are shown in Figure 6. The majority of these gauges have been installed by the UPRCT since its formation. Consequently, long-term records are not available from these gauges.

With 16 gauges in an area of 112 km^2 the study catchment has, on average, one point for rainfall sample for every seven (7) km^2 of catchment. While this is a high density of information from rain gauges for most catchments, Urbonas et al (1992) suggest that an even higher density of spatial information is required if accurate predictions of catchment response are to be obtained for convective storm events. Reproduced in Table 2 are the peak flow accuracies obtained by Urbonas et al (1992); the deviations presented in this table are referenced to the maximum gauge density of 1.6 km^2 of catchment per gauge. It is important to note that, while the mean error over a number of events may be within reasonable limits, the range of errors for individual events can be significant.

TABLE 2
ACCURACY OF RAINFALL-RUNOFF MODELS
(after Urbonas et al 1992)

Gauge Density (km^2/gauge)	Range (%)	Mean Deviation (%)
8.0	–100.0 to 150.0	–24.2
4.0	–75.3 to 94.5	0.5
2.7	–32.2 to 63.66	15.8
2.0	–32.2 to 18.8	–0.9
1.6	0.0 to 0.0	0.0

Records from the sixteen (16) rain gauges were obtained from January 1991 to September 1996. During this period, thirty four (34) storm events occurred with daily rainfall total greater than 20 mm. These were the storm events selected for the study. Among the selected storms, more than 70% were identified as convective, and the rest were frontal storms. The convective storms occurred mostly during summer and autumn, while the frontal storms were more evenly distributed over the four seasons. A detailed list of the storm events is given in Appendix A.

The data series are rainfall amounts during 15-minute intervals which are compatible with the time step used by the UPRCT for modelling runoff from the catchment. The total number of 15-minute rainfall values obtained was 1749. Shown in Table 3 are the number of events extracted for each year and the total number of events for the whole period of record.

TABLE 3
NUMBER OF STORM EVENTS EXTRACTED

Year	No. of events	No. of 15-min rainfall values
1992	2	105
1993	5	205
1994	6	302
1995	11	533
1996 (up to September)	10	604
Total	34	1749

Due to malfunctioning of gauges or errors in transmission, there were missing values in some events. These missing values were estimated from neighbouring rain gauges using the spatial rainfall model developed as part of this study and discussed by Luk and Ball (1996). Essentially, the model utilises the spline surface spatial interpolation method within the ARC/INFO geographic information system.

3.3 Sub-catchments

For catchment management purposes and particularly for flood management of the catchment, the UPRCT has been implementing a conceptual rainfall-runoff model for the catchment. This model is based on the RAFTS software package (WP Software, 1995) which uses the non-linear reservoir model of Laurenson (1964) to route flows through the catchment storage. For implementation of this model, the total catchment has been subdivided into twenty-four (24) sub-catchments. As expected, the area of each of these sub-catchments was not constant but rather differed according to the catchment characteristics. The largest sub-catchment was approximately 9 km^2 while the smallest was approximately 1km^2. The remaining sub-catchment areas were evenly distributed between these limits.

4. RAINFALL FORECASTING — THE ANN APPROACH

Presented in this chapter is the application of artificial neural networks to forecast rainfall at a number of gauge positions for the study catchment, as well as a comparison of various forms of artificial neural networks. In addition, an empirical test has been carried out for the networks constructed with different spatial and temporal architectures with a view to improving the accuracy of rainfall forecast. A number of further tests, such as those using more sophisticated training algorithms, incorporating time indices for the storm events, etc, have been carried out and the results of these tests are also detailed in this chapter.

4.1 Artificial Neural Network for Rainfall Forecasting

Rainfall is a natural process which has a high degree of variability in both time and space. For development of the proposed rainfall forecast model, the rainfall process was assumed to be a Markovian process, which means that the rainfall value at a given location in space and time is a function of a finite set of previous realisations. With this assumption, a simple model structure can be expressed as:

$$X(t+1) = f(X(t), X(t-1), X(t-2), ..., X(t-k+1)) + e(t) \tag{9}$$

where $X(t) = [x_{1t}, x_{2t}, \ldots, x_{Nt}]^T$ represents a vector of rainfall values $x_{1t}, x_{2t}, .., x_{Nt}$ at N different gauge sites at time t, where T denotes the transpose operator

$f(\,)$ is a nonlinear mapping function which shall be approximated using an ANN

$e(t)$ is a mapping error (to be minimised)

k is the unknown number of past realisations contributing to rainfall at the next time-step

Usually, k is referred to as the lag of a model. If k is equal to 1, the future rainfall is related only to the present rainfall, representing a lag-1 model.

A multi-layer feedforward neural network (MLFN) is a straightforward approach to represent the above rainfall model. The MLFN is presented with the current and past

rainfall values as inputs, e.g. X(t),.., X(t-k+1). The next rainfall value X(t+1) is used as output of the network. There are, however, several drawbacks associated with this approach. Firstly, since the model lag k is unknown, a lengthy trial process is required to determine the optimal value of k. Secondly, for a network with high order of lag, large numbers of input nodes are required. Consequently, the number of parameters will increase making the network unnecessary complex. Last but not least, the MLFN is a static model which may not be able to model the dynamic rainfall process.

An alternative type of network which can effectively model the rainfall process while keeping a minimum of parameters is a time delay neural network (TDNN). A distinctive feature of a TDNN is the use of partial connections; this dramatically reduces the number of weights presented in the network compared with a fully connected MLFN architecture. In addition, the TDNN has been developed for detecting local features within a larger pattern; this feature detection ability is very useful for the task of rainfall forecasting. A TDNN, however, is still a static model.

The need for a dynamic model leads to the consideration of a recurrent network which contains recurrent connections to feed past states of the system into the network. A recurrent network possesses the characteristic of a dynamic memory. In addition, a recurrent network reduces the number of inputs and consequently the number of parameters.

Recurrent networks can be classified as fully and partially recurrent. Fully recurrent networks can have arbitrary feedforward and feedback connections with all of these connections trainable. The training of these networks is very complicated. For practical applications, partially recurrent networks (PRNNs) are more appropriate because the training of such networks is similar to MLFNs. In partially recurrent networks, the main network structure is feedforward. The feedforward connections are trainable. The feedback connections are formed through a set of "context" units and are not trainable. This simplifies the training process. The context units store some past states of the system, and so the outputs of the networks depend on an aggregate of the previous states as well as the current input.

All networks have their strengths and weaknesses. They are powerful tools when used appropriately. The PRNN and TDNN are specifically developed to model the structure in time series. They are considered to be the most suitable candidates for the current study. The MLFN, however, is the most popular model and has a relatively simple structure. The MLFN was included in this study to provide a base line for comparison.

Other types of network were considered but were rejected because either the networks were not appropriate for rainfall forecasting or the networks required a large amount of data which the present study could not provide for. Two networks rejected were:

- radial basis function network; and
- modular neural network

Radial basis function networks (RBFNs) have been developed and used by some research workers (Moody and Darken 1989). A RBFN usually consists of three layers. The first layer represents the inputs. They are fully connected to the neurons in the second (hidden) layer. A hidden node has a radial basis function (RBF) as the activation function. The RBF is a radially symmetric function (e.g. Gaussian function).

The principal advantage of a RBFN is that the training speed is much faster than a MLFN trained with standard backpropagation technique. Training of a RBFN is carried out in two phases, first for the parameters of the hidden layer, then for the parameters of the output layer. The hidden-layer parameters control the centres and widths of the radial basis function. They can be trained by some unsupervised training algorithms, such as the Kohonen learning algorithm (Kohonen, 1990). The parameters of the output nodes are the values that produce the minimum error in the mapping function. They may be trained by gradient descent without any backpropagation since there is only one layer of weights to be trained. The speed of training is therefore much quicker.

A second advantage of the network is that the behaviour of the hidden units and the output can be more easily interpreted in statistical terms. If confidence estimates for the output of the network are required, a RBFN is a suitable network.

However, a RBFN has three major limitations for rainfall forecasting. First, because of the way it uses radial basis functions around clusters of training data, its performance depends strongly on having a thoroughly representative training set. If only a few training samples are available, a MLFN having very few hidden neurons can be trained to generalise features from data points. The RBFN however, may not be able to achieve good generalisation because a data set with good coverage is required. The other disadvantages stem from the fact that the entire training set must be stored, as well as processed, each time an unknown case is classified. This means that memory requirements are large, and execution speed is poor. A RBFN is rarely suitable for real time applications.

A RBFN would be chosen when the problem is one of classification and the training set is so extensive that training other models would be impracticably slow. This model would also be favourable when confidence is needed for classification decisions. However, for the nature of the current study, this model is excluded because the objective is rainfall forecasting, and the training data set is rather limited and contains noise.

Another type of neural network gaining increasing popularity is the modular neural network. This network has a modular structure to represent a large problem divided into smaller subtasks. This network is suitable for complex system consisting of different components. Several small networks can be trained for the corresponding components and then combined. For example, there are different types of rainfall processes, eg. convective, frontal and orographic. In principle, it is more effective to construct three relatively simple networks for the individual situations and apply a suitable network according to the prevailing situation.

In practice, the form of rainfall could be difficult to identify in real time. For the study catchment, some of the storms were a mixture of both frontal and convective storms. It was impractical to separate the data. In addition, in the current study, only 34 storm events are available. There is certainly not enough data for training a modular network.

4.2 Alternative Artificial Neural Networks

From the review of alternative categories of ANNs, suitable types of networks for the task of rainfall forecasting have been assessed as being:

- Multi-layer Feedforward Neural Network (MLFN);
- Partial Recurrent Neural Network (PRNN); and
- Time Delay Neural Network (TDNN).

Although intuitively the TDNN and PRNN networks are better models than MLFN for rainfall forecasting, it was necessary to empirically compare the performance of the alternative networks. These three alternative types of ANN were developed and compared. Detailed design of the networks for rainfall forecasting is presented in the following sections.

4.2.1 Multi-Layer Feedforward Neural Network

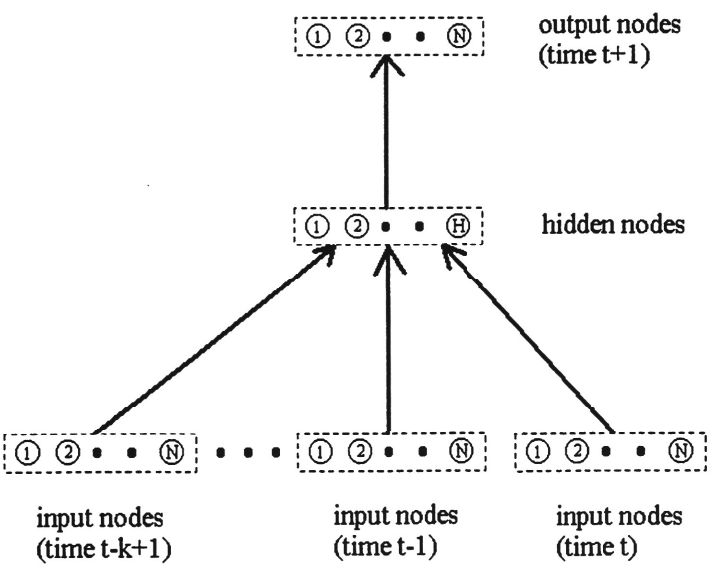

Figure 7 - A MLFN for Rainfall Forecasting

Presented in Figure 7 is a generic structure of a MLFN designed for rainfall forecasting. The output nodes of the network consist of the rainfall values for the next time step at each of the (N) locations considered in this study. For example, if a forecast of rainfall at 16

points in space is needed, then (N) is equal to 16. The number of hidden nodes (H), which defines the complexity of the network, is a key variable to be estimated. Note that the number of hidden layers can be more than one but only one is shown in Figure 7 for the purpose of illustrating the concepts. The input layer contains (k) sets of input nodes. The value of (k) as previously noted is referred to as the lag of the network and is another key variable to be determined.

As previously discussed, the MLFN is a very powerful nonlinear model despite its simple structure. In theory a 3-layer MLFN can approximate any continuous function to any desired degree of accuracy (Hornik et al, 1989). There are many successful applications of MLFN in engineering and science.

The crucial point for developing the MLFN is to determine the optimal complexity of the network to cope with the complex underlying rainfall process.

4.2.2 Time Delay Neural Network

The time delay neural network (TDNN) was developed by Waibel for speech recognition (Waibel, 1989). The main feature of a TDNN is the implementation of the concept of "invariance". In many practical applications it is known that the outputs in a classification or regression problem should be unchanged, or "invariant", when the input is subject to various transformations. An example is the classification of objects in two-dimensional images. A particular object should be assigned the same classification even if it is rotated or translated within the image or if it is linearly scaled (corresponding to the object moving towards or away from the camera). Such transformations produce significant changes in the raw data and yet should give rise to the same output from the classification system. One way to provide this invariance is to build the invariance properties into the neural network structure itself. A TDNN network makes use of the technique of "shared weights" to achieve this purpose. The following illustration of the technique is based on Bishop (1996).

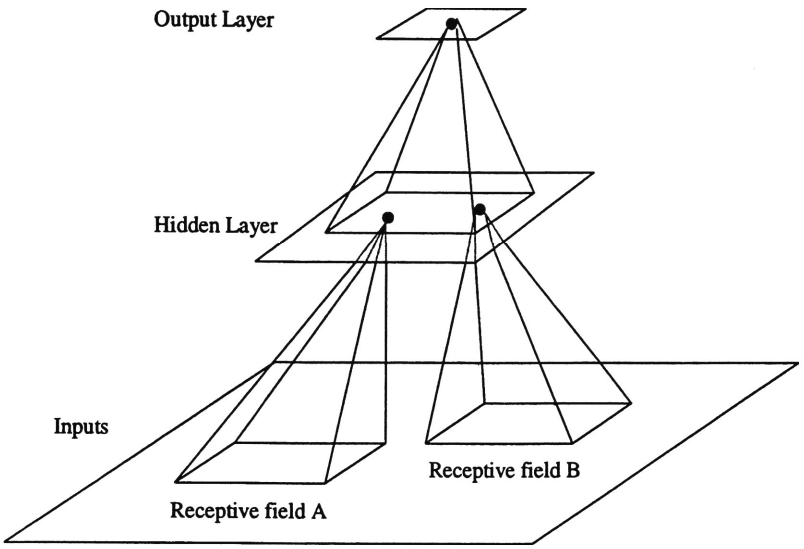

Figure 8 - Schematic Architecture of a Network for Translation-invariant Object Recognition in Two-dimensional Images (after Bishop, 1996)

The diagram shown in Figure 8 helps to explain the technique of "shared weights". The network is presented in a two-dimensional form. The inputs to the network are given by the intensities at each of the pixels in a two-dimensional array. Instead of having full interconnections between adjacent layers, each hidden unit receives inputs only from units in a small region in the input layer, known as receptive field. The network architecture is typically chosen so that there is some overlap between adjacent receptive fields.

The technique of shared weights can then be used to build in some degree of translation invariance into the response of the network (Lang et al, 1990). In the simplest case this involves constraining the weights from each receptive field of the other units in the same layer. Consider an object which falls within Receptive Field A shown in Figure 8, corresponding to a unit in the hidden layer, and which produces some activation level in that unit. If the same object falls at the corresponding position in Receptive Field B, then, as a consequence of the shared weights, the corresponding unit in the hidden layer will have the same activation level. The units in the output layer have fixed weights chosen so that each unit computes a simple average of the activations of the units that fall within its receptive field. This allows units in the output layer to be relatively insensitive to moderate translations within the input image. However, it does preserve some position information thereby allowing units in the output layer to detect more complex composite features.

Typically each successive layer has fewer units than previous layers, as information on the spatial location of objects is gradually eliminated. This corresponds to the use of a relatively high resolution to detect the presence of a feature in an earlier layer, while using a lower resolution to represent the location of that feature in a subsequent layer.

Another distinctive feature of the use of receptive fields is that they can dramatically reduce the number of weights present in the network compared with a fully connected architecture. In addition, the use of shared weights means that the number of independent parameters in the network is less than the number of weights, which allows much smaller data sets to be used than would otherwise be necessary.

The above technique can be applied to detect local features in time as well as space; time is simply a dimension in the same context as a co-ordinate system. The invariance of local features that occur in the time dimension is referred to as "time invariance". The time invariance property is relevant to rainfall forecasting because a rainfall time series usually contains local features, such as isolated peaks between prolonged periods with low to zero values of rainfall. Since these local features do not have a fixed position in time, a TDNN should be able to detect their occurrence.

The architecture of a TDNN essentially is feedforward, but the connections between layers are modified in order to achieve time invariance. Instead of having full interconnections between adjacent layers, each hidden node receives inputs only from nodes in a small region in the previous layer. This small region is called a "time window" which consists of several time frames as shown in Figure 9.

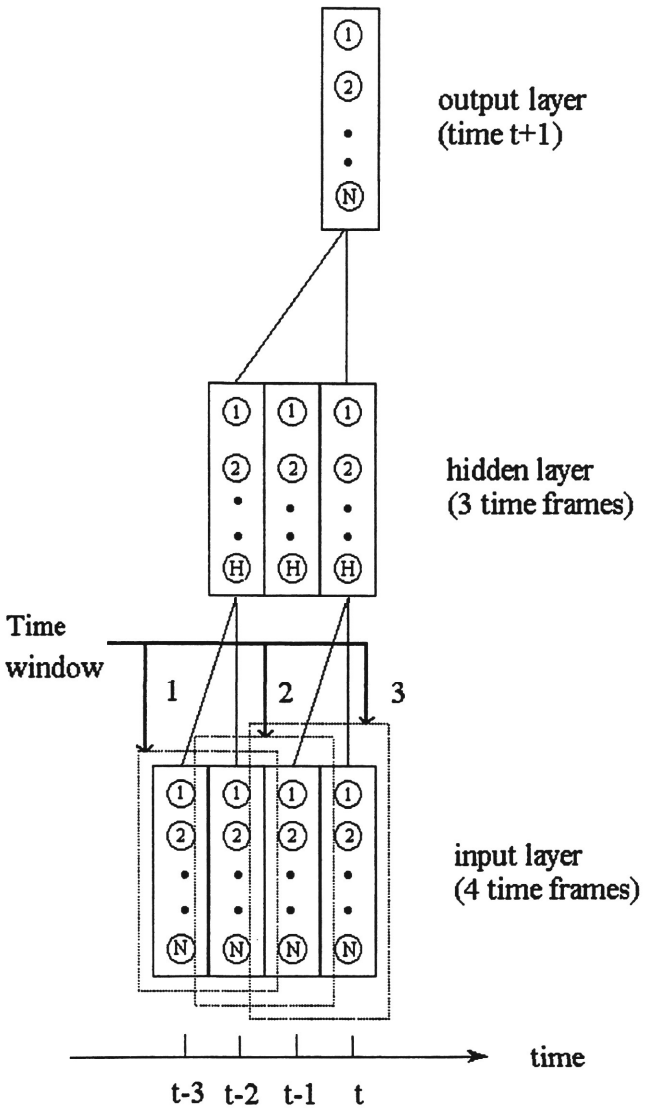

Figure 9 - A TDNN for Rainfall Forecasting

In this illustration of a TDNN, at the input layer there are three time windows, each of which consists of two time frames. At the hidden layer, however, there is only one time window consisting of three time frames. Presented in Equation (24) are the activations of the hidden nodes of the first time frame of the hidden layer which are connected to the input nodes of the first time window of the input layer.

$$O_1 = S(W_1 \cdot X(t-2) + W_1 \cdot X(t-3)) \tag{10}$$

where O_1 are the activations of the hidden nodes connected to the 1st time window of the input layer

W_1 is a weight matrix connected between inputs of the 1st time window and hidden nodes of the 1st time frame of the hidden layer

S is an activation function

$X(t-2)$ and $X(t-3)$ are rainfall at time t-2 and t-3 respectively; they constitute the 1st time window of the input layer

At the output layer, as with previous ANNs, the outputs are the rainfall depth at each gauge at time t+1. Algebraically, this is

$$X(t+1) = S\left(\sum_{m=1}^{3} W_m \cdot O_m\right) \tag{11}$$

where $X(t+1)$ are rainfall at time t+1

O_m are the activations of the hidden nodes

W_m is a weight matrix connected between hidden layer and output layer

S is an activation function

With this partial connection architecture, the technique of shared weights can be used to build in some degree of time invariance into the response of the network. The technique of shared weights involves constraining the weights from a time window to be equal to the corresponding weights from all other time windows in the same layer. For example, at the connections between input layer and hidden layer, the entries in the weight matrix are set equal, namely, $W_1=W_2=W_3$. As a consequence of the shared weights, a feature that falls in different time windows of the input layer will produce the same activation in the hidden layer. For the TDNN shown in Figure 9, each hidden node has the ability to detect local features within the range of the three time windows at the input layer. A shift in position of

the features at the input can be detected by the hidden nodes and subsequently by the output nodes.

The main variables of a TDNN that need to be defined are:

- number of time frames for input and hidden layers;
- size of time window; and
- number of hidden nodes.

4.2.3 Partial Recurrent Neural Network

The MLFN and TDNN use a static representation of past rainfall inputs whereby the past states of the rainfall system have to be represented externally by including a fixed number of past rainfall values as input. This static representation has several drawbacks. Firstly, if the rainfall process has a long term memory, a large number of input nodes are required, resulting in a network containing a large number of free parameters. Secondly, the number of past rainfall inputs has to be determined experimentally. A lengthy trial and error process is required. A dynamic model may overcome this problem. A dynamic model can be represented by a neural network with feedback connections to feed past states of the system back to the network. Such a network with feedback connections is called recurrent network. A recurrent network possesses the characteristic of dynamic memory. In addition, a recurrent network reduces the number of inputs and consequently the number of parameters.

As previously discussed, recurrent networks can be classified as fully and partially recurrent. A partially recurrent network (PRNN) is more appropriate for the present study because training of a PRNN is much easier than a fully recurrent network. In addition, a PRNN can be developed for real time applications.

Among the available partially recurrent networks, the Elman network (Elman, 1990) is one of the simplest types that can be trained using standard backpropagation learning algorithms (McCelland et al, 1986). This type of network was adopted and customised for

the present study. Shown in Figure 10 is the structure of an Elman network as used in this study for rainfall forecasting.

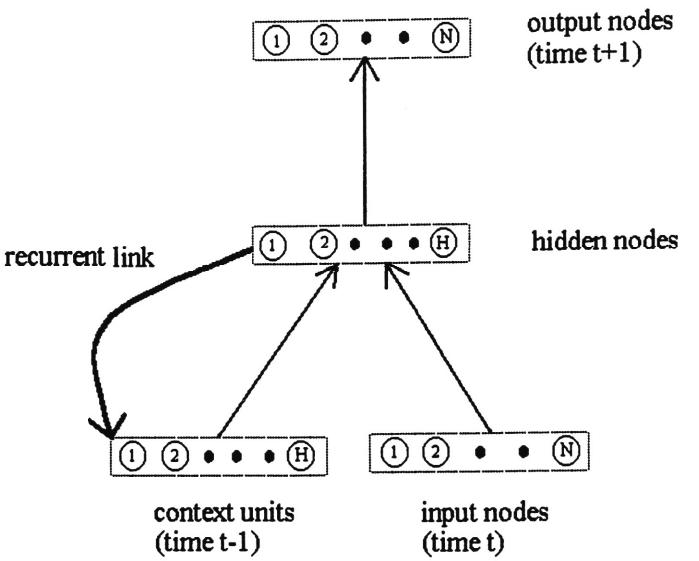

Figure 10 - An Elman Network for Rainfall Forecasting

As stated previously, an important feature of the Elman network is the inclusion of a special set of context units to receive feedback signals from the hidden nodes. The function of the context units is to store information about the previous time steps. To achieve this, the context units make a copy of the activation of hidden nodes in the previous time step. Therefore, at time (t) the context units have some signals related to the state of network at time (t-1). As a result, the rainfall at time (t+1) is a function of the rainfall at time (t) and the previous states of the system represented by the activation of the hidden nodes at time (t-1), as expressed in the following equation.

$$X(t+1) = g(X(t), O(t-1)) + e(t) \tag{12}$$

where

X(t+1)	are rainfall at time t+1, which are outputs of the network
X(t)	are rainfall at time t, which are inputs of the network
O(t-1)	are the activations of the hidden nodes at time t-1 and copied back to the context units for input at time t
g()	is a recurrent mapping function
e(t)	is the mapping error

As shown in Figure 10, the input nodes contain (N) elements, representing the spatial dimension of the rainfall. For example, if rainfall forecasts at 16 gauge positions are required, then the number N should be set to 16. The total number of hidden nodes is (H) which is the same as the number of context units. The key variable to be specified is (H). The number of hidden nodes controls the complexity of the network.

4.3 Comparison of Alternative Networks

The three alternative networks were developed and compared on their performance for forecasting the storm events collected from the UPRC. The following sub-section highlights the methodology for development of the network for rainfall forecasting. After that are the test results and discussions.

4.3.1 Methodology

The alternative networks were developed through the following major steps:

- data preparation, including data pre-processing;
- selection of training algorithm and performance indicators; and
- determination of the number of inputs and outputs.

It is necessary to select appropriate methods for each step of development. The various methods adopted in this study are summarised in Table 4.

TABLE 4
ADOPTED METHODS FOR NETWORK DEVELOPMENT

Category	Method Adopted in the Study	Main Reasons
Data preparation	(1) The data were randomly selected and split into 3 parts in order to implement the early stopping technique.	Straightforward, low computation cost.
	(2) Activation Functions: hidden nodes - logistic output nodes - linear	Logistic activation function to enable nonlinearity; linear activation function to avoid pre-setting a maximum value of rainfall.
	(3) The data were transformed by a log function	To meet the requirements of the logistic activation function, accelerate training speed and enhance convergence.
Selection of Training algorithm and Performance Indicators	(1) Training algorithm: Recilent propagation	Fast, very few parameters require setting and the performance is insensitive to choices of parameters
	(2) Performance indicators: SSE and NMSE	The most commonly used method for optimisation. It also yields a maximum likelihood estimation if the errors are normally distributed.
Input and output representation	The alternative networks are trained to forecast rainfall at 16 gauges simultaneously.	All the available information are used for forecasting.
Software	SNNSv4.1	Powerful and versatile.

4.3.1.1 Data Preparation

Data preparation includes:

- separation of data sets; and
- selection of activation function and data pre-processing.

It was necessary to separate the data into different data sets to implement the early stopping technique. In order to obtain unbiased samples for each of the data sets, the 34 storm events were divided randomly into three data sets which were:

- training set – 16 storm events with a total of 748 rainfall periods (15-minutes);
- monitoring set – 8 storm events with a total of 376 rainfall periods; and
- validation set – 10 storm events with a total of 625 rainfall periods.

As these events were randomly selected, they have similar characteristics. Presented in Table 5 below is a summary of the storm characteristics among the three data sets. A more detailed description is given in Appendix B.

TABLE 5
SUMMARY OF STORM CHARACTERISTICS

Characteristics	Training	Monitoring	Validation
Storm Type	10 convective 6 frontal	4 convective 4 frontal	8 convective 2 frontal
Storm Duration (hour)	3 to 22	2 to 21	6 to 24
Maximum Rainfall (mm/15min)	2 to 25	2.5 to 25	5 to 25
Time to Maximum Rainfall	30 min to 10 hr	1 hr to 18 hr	45 min to 21 hr

The training data set was used to calibrate the connection weights of the networks while the monitoring data set was used to check the performance of the training and provide an indication on when to stop training. Finally, the networks were evaluated by the validation data, which had not been involved in the training process.

The next step was to pre-process the data sets to cope with the requirements of the neural networks. All three alternative types of networks considered in this study adopted a sigmoid activation function in the hidden nodes, but a linear function in the output nodes. The use of sigmoid function was to enable non-linearity of the network. The sigmoid

function, however, was not adopted for output nodes because the sigmoid function forces an output bounded over a range of 0.0 to 1.0. This means that the output variable has to be scaled by a known maximum value. This is undesirable for rainfall forecasting because it was not desirable to set a maximum rainfall value. If the probable maximum rainfall was chosen all the rainfall values would be scaled down to a narrow range. To overcome this situation an identity (linear) function was used.

Since the sigmoid activation was used in the hidden nodes, the speed of training would be improved if the data were scaled down to the range between 0 and 1. The rainfall data, therefore, were transformed by the logarithmic function:

$$y = a \bullet \log_{10}(x+b) \tag{13}$$

where a is an arbitrary constant and a value of 0.5 was adopted in this study

b was set to 1 to avoid the entry of zero rainfall in the log function

The maximum rainfall value the data set used during in this study was 32.6 mm in a 15min period. Thus the rainfall values were in the range of [0, 32.6] and were transformed to a range of [0, 0.763].

A more general Box-Cox transformation (Box and Cox, 1964) was attempted but found to be inappropriate for this application.

A Box-Cox transformation is of the form of:

$$y = \frac{(x+c)^{\lambda} - 1}{\lambda} \qquad \text{if } \lambda \neq 0$$

$$y = \ln(x + c) \qquad \text{if } \lambda = 0$$

With a constant C of value 1.1, the parameter λ was estimated as -1.7 by maximising the log likelihood of a linear multiple regression on the rainfall data.

However, a rainfall series usually contains a large number of low values with occasional jumps of high values. The Box-Cox transformation normalises the data by stretching low values and compressing high values. For example, rainfall values of 10 mm and 20 mm will be transformed to 0.578 and 0.584. The difference is 0.006. On the other hand, rainfall values of 0.5 mm and 1.0 mm will be transformed to 0.324 and 0.422. The difference is 0.098 which is 16 times greater than 0.006. Consequently, with the transformed data, a network is trained to optimise low rainfall values and hence will give poor results in predicting high rainfall values.

4.3.1.2 Selection of Training Algorithm and Performance Indicators

The Rprop (as described in Section 2.3) was used for training the networks where appropriate because this is one of the fastest training algorithms available and is insensitive to the choice of initial parameter.

During training, the weights of the networks were adjusted in order to minimise the discrepancies between the network outputs and the target outputs. There are two general error functions, namely the sum of squared error and the cross entropy function to measure the network performance during training.

(i) Sum of squared error

$$SSE = \sum_{N}\sum_{P}(d_{np} - y_{np})^2 \tag{14}$$

where

	SSE	is the sum of squared errors
	N	is the total number of outputs
	P	is the total number of patterns
	d_{np}	are the target outputs
	y_{np}	are the outputs given by the network

The SSE is straightforward to compute. It also yields a maximum likelihood estimation if the errors are normally distributed. Because of its advantages, the SSE function was adopted in the study.

(ii) Cross entropy

$$E = \sum_{i=1}^{P} d_i \log(d_i/y_i) \tag{15}$$

where
- E is the cross entropy
- P is the number of patterns
- d_i are the target outputs
- y_i are the outputs given by the network

The cross entropy error function has a number of useful properties for pattern classification problems, however, it requires both the input and the output values in the range of [0,1] and therefore was considered inappropriate for this study.

The normalised mean squared error (NMSE) was chosen as the performance indicator for the comparison of the alternative types of network. One problem with the use of SSE for network comparison is that the rainfall series had different lengths. This problem can be overcome by using a normalised version of the SSE, namely the normalised mean squared error (NMSE). Weigend et al (1993) defined the NMSE as

$$\mathrm{NMSE} = \frac{\sum_N \sum_P (d_{np} - y_{np})^2}{\sum_N \sum_P (d_{np} - \bar{d}_{np})^2} \approx \frac{1}{NP\sigma^2} \sum_N \sum_P (d_{np} - y_{np})^2 \tag{16}$$

where
- N is the total number of output nodes
- P is the total number of data samples
- d_{np} are the target outputs
- y_{np} are the network's outputs
- σ^2 is the variance of the target outputs

In essence, the NMSE is the sum of squared errors normalised by the number of data samples over all output nodes and the estimated variance of the data. A NMSE of 0 indicates a perfect fit, while a NMSE of 1 implies that the network performance is no better than a simple model using the mean output as forecast.

4.3.1.3 Input and Output Representation

For the study catchment, there are a number of possible ways to determine the input and output information. The three most feasible approaches are:

- Divide the study catchment into grids (439 pixels of 500m × 500m) and use rainfall at the 439 pixels as inputs to forecast rainfall at all 439 pixels simultaneously. The resulting outputs will be rainfall at each pixel of the catchment.
- Use rainfall at the 16 gauges as inputs to forecast rainfall for the 16 gauges simultaneously. In this case, one network represents rainfall for all 16 gauges. After the rainfall forecasts for the 16 gauges are obtained, a spatial rainfall model is used to generate the rainfall at every point of the catchment.
- Use rainfall at the 16 gauges as inputs to forecast rainfall for a single gauge. This will end up with 16 networks for 16 gauges of the study catchment. Again, after the rainfall forecasts for the 16 gauges are obtained, a spatial rainfall model is used to generate the rainfall at every point of the catchment.

A preliminary assessment of the three methods had been carried out and the option of using 16 gauges for inputs and outputs was adopted. The reasons for this decision were:

- Information from all measurement points are used simultaneously to produce forecasts for each of the measurement points.
- The forecast results can be used readily in the spatial rainfall model developed by Luk and Ball (1996).

The option of forecasting a single gauge was rejected because the same process was required once for each prediction location and 16 networks were needed.

The option of using 439 pixels as both input and output also was rejected because it involved the use of a large number of input and output nodes; consequently, the network contained a large number of parameters (weights) to be estimated. For example, a 3-layer MLFN with 439 input nodes, 439 output nodes and 2 hidden nodes comprises 1756

connections (439×2 + 439×2, excluding the biases). The available rainfall data (max. 1749 data points) are not sufficient to train the network. The large number of free parameters are prone to overfitting the data. Moreover, training of such a large network is extremely time consuming.

4.3.1.4 Software for Implementation

The SNNS (Stuttgart Neural Network Simulator) version 4.1 was selected to implement the alternative networks. The SNNS is a simulator for neural networks developed at the Institute for Parallel and Distributed High Performance Systems at the University of Stuttgart since 1989. The SNNS is distributed by the University of Stuttgart as free software in a licensing agreement similar in some aspects to the GNU General Public License. The software is available for anonymous ftp from ftp.informatik.uni-stuttgart.de [129.69.211.2] in directory /pub/SNNS as SNNSv4.1.tar.gz.

The SNNS consists of four main components:

- Simulator kernel
- Graphical user interface
- Batch simulator
- Network compiler

The simulator kernel operates on the internal network data structures of the neural networks and performs all operations on them. The graphical user interface XGUI, built on top of the kernel, gives a graphical representation of the neural networks and controls the kernel during the simulation run. The batch simulator is designed to carry out batch jobs without user interactions. The simulators were written ANSI-C, all source codes are freely distributed. The simulator can be run on a variety of platforms, including SunSparc stations and IBM-Linux systems. The XGUI is based upon X11 Release 5. It also works under X11R6.

4.3.2 Test Results and Discussions

The three alternative types of networks considered in this study were trained and validated with rainfall data collected from the study catchment. There were a total of 34 storm events with each storm event divided into 15-minute intervals. Inputs from all 16 gauges were used in training the networks. After training, the networks were used to forecast future rainfall at the same 16 gauges during one time step or 15 minutes.

Various network configurations were attempted in order to determine the effect of two key variables, which were:

- lag of the network; and
- number of hidden nodes.

For the MLFN, networks with lags of 1, 2, 3 and 4 were attempted. In addition, the number of hidden nodes tried were 2, 4, 8, 16, 24, 32, 64, and 128. Also attempted were networks with two-layers of hidden nodes. For the TDNN the size of input windows used were 2, 3 and 4. Finally, for the Elman network, the lag was fixed at 1, while the numbers of context units tried were 2, 4, 8, 16, 24, 32 and 64.

All the results are tabulated in Appendix C. Some representative results are selected and presented here for discussion. First, the effects of hidden nodes and order of lag are discussed; then, a comparison of the three alternative types of networks is presented.

4.3.2.1 The Effect of Hidden Nodes

It was observed that networks with more hidden nodes were able to produce less training error at the maximum pre-set training epoch (1000 epochs). An epoch was defined as a complete sweep through the training patterns; the connection weights of the network were updated after each epoch. Therefore, a maximum epoch of 1000 means that the weights were allowed to be updated 1000 times at most. After sufficient training, the networks adjusted all available parameters to minimise the discrepancies between the target and network outputs. The networks with more hidden nodes have more free parameters, thus resulting in less training errors. As expected, these networks had poorer performance in validation because the networks over-learned the training samples.

This effect is clearly shown in Table 6 which shows a comparison of the results produced by a MLFN with 2 hidden nodes and a MLFN with 128 hidden nodes. The networks were trained to the maximum pre-set epoch (1000 epochs). It is noted that for all lags the MLFN with 128 hidden nodes have smaller NMSE in training but much higher NMSE in validation. For example, the lag-4 MLFN with 128 hidden nodes had the smallest training error where the NMSE was equal to 0.27, but the validation error was the highest with a value of 2.33.

TABLE 6
EFFECT OF HIDDEN NODES AND TIME LAG OF MLFN

Network	Normalised Mean Squared Error (NMSE)	
	Training	Validation
Lag-1 MLFN with 2 hidden nodes	0.53	0.71
Lag-1 MLFN with 128 hidden nodes	0.40	1.20
Lag-2 MLFN with 2 hidden nodes	0.51	0.73
Lag-2 MLFN with128 hidden nodes	0.36	0.96
Lag-3 MLFN with 2 hidden nodes	0.49	0.72
Lag-3 MLFN with 128 hidden nodes	0.32	1.26
Lag-4 MLFN with 2 hidden nodes	0.49	0.78
Lag-4 MLFN with 128 hidden nodes	0.27	2.33

Note: the networks were trained to 1000 epochs.

4.3.2.2 The Effect of Order of Lag

Also shown in Table 6, given the same number of hidden nodes, the MLFNs with higher order of lag tended to better learn the training data series but did worse in validation. These results do not suggest that a network with higher order lag will give poorer results. Rather the results indicate that a network with higher order of lag contained more connection weights, and hence more free parameters. Therefore, like a network with more hidden nodes, the network with higher lag tended to overfit the training samples.

It seemed that the performance of a network depended more on the network complexity than the inclusion of more information of the past time steps. The effect of using higher order of lag mainly increased the network complexity. It might suggest that the network

complexity depended on the combined effect of two variables: (1) number of hidden nodes and (2) order of lag.

4.3.2.3 Comparison of Alternative Networks

Shown in Table 7 are details of the eight best networks as determined by analysis of the results from testing of all the above network configurations as shown in Appendix C. Selection of the best network within a specific type was based on the minimum NMSE for the validation data.

Each row of Table 7 represents a network with a specific lag. For example, the first row shows the lag-1 MLFN with 24 hidden nodes; second row shows the lag-2 MLFN with 8 hidden nodes, and so on. The number of hidden nodes were determined as the optimum number for the network being considered.

TABLE 7
COMPARISON OF ALTERNATIVE NETWORKS

Network	Training (NMSE)	Monitoring (NMSE)	Validation (NMSE)	Stopping epoch	Training Error at 1000 epoch (NMSE)
MLFN Lag 1 (16-24-16)	0.50	0.68	0.64	200	0.49
MLFN Lag 2 (32-8-16)	0.51	0.69	0.66	100	0.47
MLFN Lag 3 (48-4-16)	0.48	0.69	0.67	700	0.47
MLFN Lag 4 (64-2-16)	0.52	0.71	0.65	200	0.49
Elman (16-4-16)	0.49	0.67	0.64	300	0.48
TDNN Lag 2 (32-16-16)	0.50	0.67	0.63	100	0.41
TDNN Lag 3 (48-32-16)	0.50	0.69	0.64	100	0.41
TDNN Lag 4 (64-32-16)	0.51	0.69	0.65	100	0.40

Notation: The network configuration is denoted by three figures (x-y-z), where x= no. of input nodes, y = no. of hidden nodes and z = no. of output nodes.

In general, all three alternative types of networks showed comparable performance. The NMSE of the validation samples for all networks were in the range of (0.63 - 0.67) with only very small differences among the networks. The comparable performance among the various networks under consideration was due to the networks shown in Table 7 being developed to their optimal complexity. For example, the lag-1 MLFN requires more hidden nodes to achieve an optimal complexity, whereas the more complicated lag-4 MLFN only requires two hidden nodes to offset the large number of parameters introduced by the higher order of lag. The reduction in number of hidden nodes with the increase in lag may indicate the existence of an optimal complexity of network for the problem.

It was noted also that networks with a lower lag had a slightly better performance, which suggests that the rainfall series does not have long time-dependence structures, although this is not conclusive since only limited data are available. While not conclusive, however, this result does tend to confirm the assumption outlined previously in Section 4.1 regarding the structure of rainfall time series.

In order to give some indications of the performance of the networks, selective plots of the forecasts are given in Figures 11 and 12. Also shown in these Figures are comparisons of the three alternative types of networks for forecasting of rainfall depth one time-step ahead at a gauge during two validation storm events. The histogram in each figure shows the actual rainfall temporal pattern at a gauge site. The forecast rainfalls of the three networks are represented by different symbols. There are similar plots for other gauges and storm events.

From Figure 11 it can be seen that all three types of network closely matched the actual rainfall pattern. The networks especially produced a good forecast for the decreasing parts of the rainfall histogram. However, none of the networks could pick up the highest peak of rainfall. This might be attributed to the fact that the peak occurred randomly which suddenly jumped from a low value of rainfall.

Similar observations were noted for Figure 12. However, on this storm event, because the rainfall depth gradually increased and then decreased, the networks were able to make good predictions for both the rising and falling parts of the rainfall histogram.

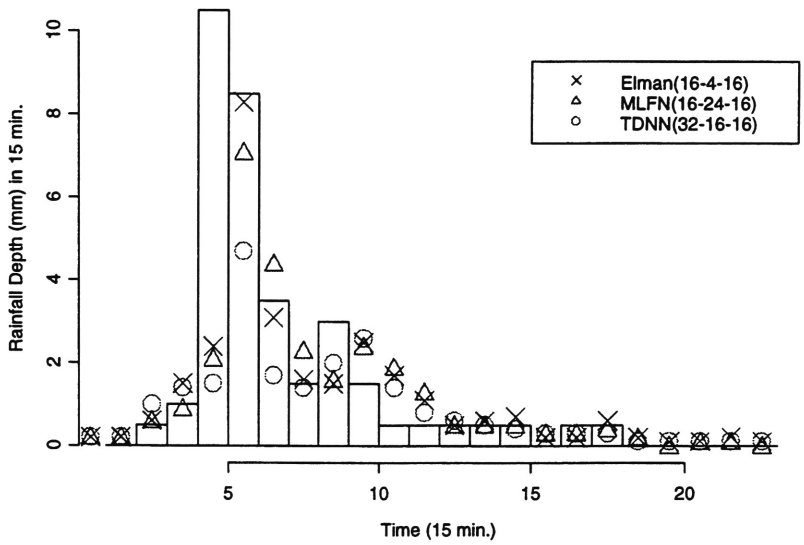

Figure 11 - Forecasting Rainfall at Gauge No. 7253 for the Storm Event on 2 Jan 1996

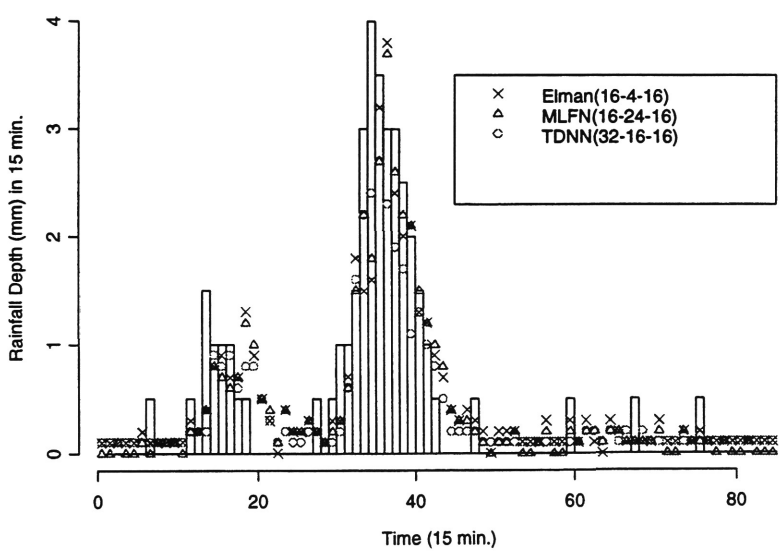

Figure 12 - Forecasting Rainfall at Gauge No. 7253 for the Storm Event on 6 Jan 1996

Observation of the forecast errors shown in Figures 11 and 12 reveals that there exists a functional relationship between the forecast errors and the rate of change of rainfall

intensity. A plot of the forecast error versus the rate of change of rainfall intensity is therefore made for each 10 validation storm events. Such plots are presented in Figures 13 and 14 for the storm events on 2 January 1996 and 6 January 1996 respectively. Similar figures for other storm events are given in Appendix D.

Each figure has three plots corresponding to three alternative artificial neural networks. At each plot, the y-axis represents the error of forecast, i.e. the forecast subtracted by the actual rainfall. A positive value means over-prediction, and vice versa. The x-axis represents the rate of change of rainfall depth (mm) in 15 minutes. A positive value means that the rainfall increases in the next time step (15 minutes), and vice versa. The data points are shown in dots; a line of best fit for the data points is produced by the cubic smoothing spline method with three degrees of freedom.

An interesting point to note from the figures is that there is a distinctive break of slope of the smoothing line at zero rate of change. The smoothing line slope is much steeper when the rate of change is positive (corresponding to the rising part of the rainfall hyetograph), whereas the slope is flatter when the rate of change is negative (corresponding to the decreasing part of the rainfall hyetograph). The following points are derived from observation of the figures:

- The forecast error increases as the rate of change of rainfall intensity increases. Thus it is shown in the figures that the rainfall was under-predicted when the rate of change of rainfall intensity increases, whereas the rainfall was over-predicted when the negative rate of change of rainfall intensity increases.
- The networks made better predictions when the rainfall reduced from peak values.
- The networks tended to under-predict the rainfall when the rate of change is positive, but over-predict the rainfall when the rate of change is negative.

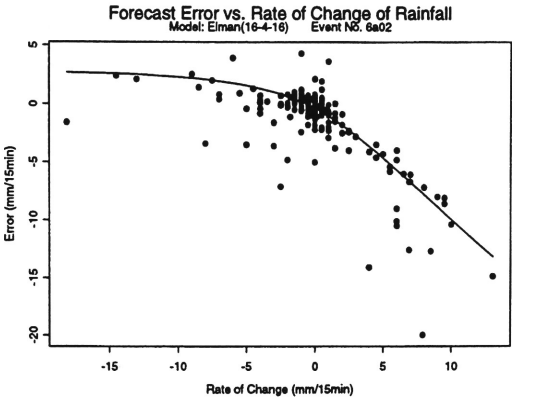

(a) Elman Network

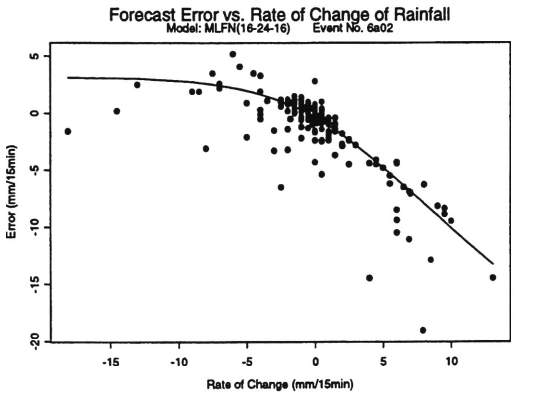

(b) MLFN

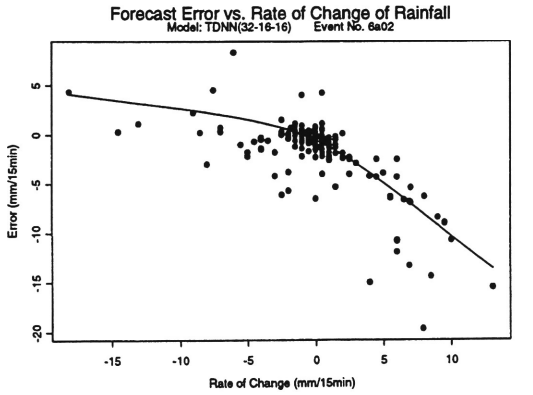

(c) TDNN

Figure 13 - Forecast Error Vs. Rate of Change of Rainfall: Date 2 Jan 1996

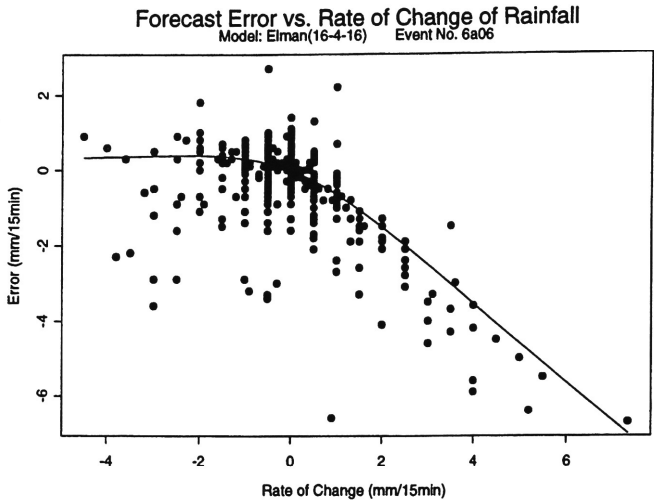

(a) Elman Network

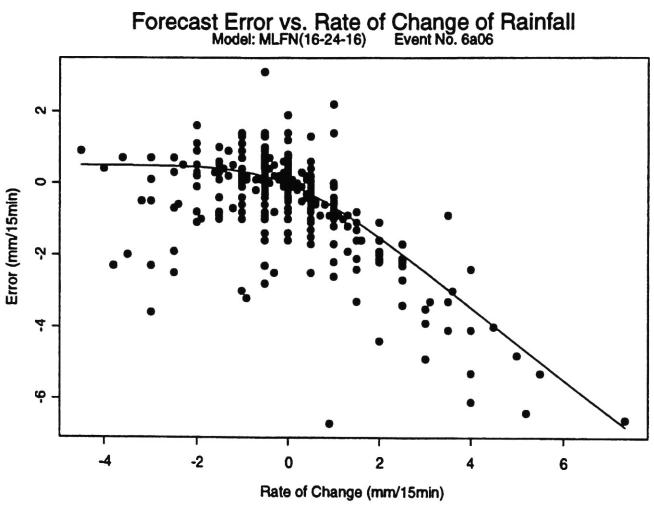

(b) MLFN

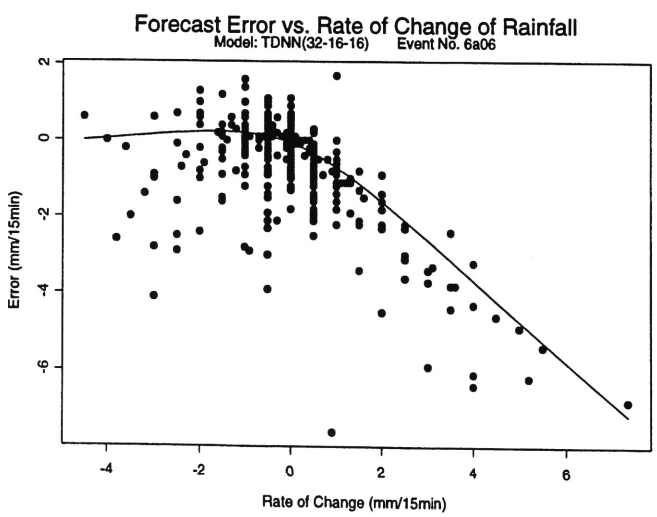

(c) TDNN

Figure 14 - Forecast Error Vs. Rate of Change of Rainfall: Date 6 Jan 1996

In summary, the following points were observed from these comparison test results.

- All three alternative types of networks have comparable performance.
- MLFN with lower order of lag showed slightly better test results than that of higher order of lag.
- MLFN with higher lags tended to over-learn the training data, resulting in smaller training but larger validation errors.
- MLFN with lower lags required more hidden nodes, and vice versa. An optimal level of network complexity needed to be maintained to cope with the complexity of the data.
- The Elman network showed comparable performance with the lag-1 MLFN and outperformed the MLFN with higher order of lag.
- Among all the networks, the lag-2 TDNN yielded the minimum validation error.
- For all three alternative networks, forecast errors increase as the rate of change of rainfall intensity increases. The networks tended to under-predict the rainfall when the rate of change is positive, but over-predict the rainfall when the rate of change is negative. Forecast errors are higher when the rate of change is positive.

For this pattern recognition approach, improvement of prediction is expected by collecting more data for training. Additionally, in order to predict the occurrence of the rainfall peak more accurately, it might be necessary to identify more control variables, such as wind speed and direction, and incorporate them into the input of networks.

4.4 Investigation of Optimal Spatial and Temporal Inputs

In the previous section the three alternative types of networks were compared based on rainfall input and output at all 16 gauges. It was found that all three types of networks showed comparable performance, and that there existed an optimal network complexity which depended on a combined effect of the order of lag and number of hidden nodes.

Apart from the order of lag and number of hidden nodes, it is of paramount importance to investigate how the spatial inputs affect the performance of the network. Tests on the effect

of spatial input can be undertaken by constructing networks with one single output, but with different numbers of neighbouring rainfall inputs added to the network.

The procedure is illustrated in Figure 15. A gauge (ref. no. 7261) located at the centre of the catchment is selected to demonstrate the procedure.

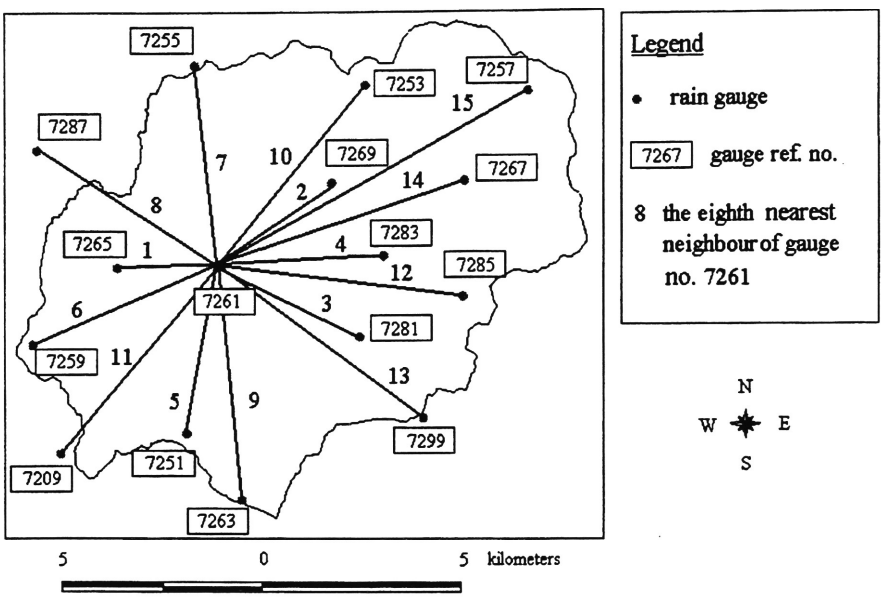

Figure 15 - Sequence of Neighbour Gauges

Shown in Figure 15 are the positions of the gauges and their distances relative to Gauge no. 7261. Initially, the input and the output of the network was rainfall at the gauge itself. Then, inputs from neighbouring gauges were gradually added to the network, with the only output being Gauge no. 7261. The number of neighbouring gauges used as input to the ANNs were 2, 4, 6, 8, 10, 12 and 15 respectively. The sequence of neighbouring gauges being used as input of network is shown in Figure 15; the priority was according to the shortest distance between the gauge and Gauge 7261. For example, the first two gauges added to the input were Gauge nos. 7265 and 7269.

The above procedure was carried out in turn for each of the 16 gauges. The results were summarized and are presented in Table 8. The value shown in Table 8 is the sum of normalised mean squared errors for the 16 gauges.

TABLE 8
COMPARISON OF DIFFERENT SPATIAL AND TEMPORAL INPUTS

Spatial variation	Normalised Mean Squared Error on Validation Events		
	Lag 1	Lag 2	Lag 3
No neighbouring inputs	0.679	0.686	0.678
2 neighbouring inputs	0.641	0.650	**0.655**
4 neighbouring inputs	0.635	**0.642**	0.662
6 neighbouring inputs	0.631	0.656	0.663
8 neighbouring inputs	**0.630**	0.659	0.665
10 neighbouring inputs	0.639	0.676	0.685
12 neighbouring inputs	0.650	0.682	0.691
15 neighbouring inputs	0.644	0.683	0.719

For ease of comparison and economy in computation, the network chosen for these tests was a MLFN with two hidden nodes.

The following points were observed from the test results:

- There existed an optimal limit of spatial information for inclusion into the network; and
- For the temporal domain, the lag-1 networks in general showed the best performance.

The inclusion of more neighbouring gauges may introduce the following side-effects:

- Additional gauge inputs require additional connection weights, resulting in a more complicated network; and
- More noise may be introduced to the network and this may undermine the network's performance.

4.5 Further Testing

Apart from temporal and spatial dependence of the rainfall inputs, there are many other factors which may improve the network performance. One of the possible ways to improve

the performance of networks is to use a more sophisticated training algorithm, like the cascade correlation algorithm to find the global minimum of the error function. The other way is to include additional variables to provide information about the pattern of rainfall. For example, the rainfall time series may have a seasonal behaviour. If a time index is added, it may help to improve the predictability of networks.

The following additional tests, therefore, are considered relevant.

- Use of more sophisticated training algorithms; and
- Incorporation of additional variables.

It is important also to compare ANNs with a multiple linear regression model to ascertain the advantage of using the more sophisticated non-linear ANNs. The results of these additional tests and the comparison with a multiple linear model are presented in the following sections.

4.5.1 Use of Cascade Correlation Algorithm

The cascade correlation algorithm (CasCor) as described in Section 2.3, is an effective training algorithm which automatically adds hidden nodes to the network to cope with the complexity of the problem. The CasCor, therefore, was applied to test whether it could improve the forecast performance.

The CasCor required the setting of the maximum number of context units and the maximum output unit error. Training stopped if either the maximum number of context units was added to the network or the output unit error was less than the maximum pre-set value. In order to avoid stopping the training prematurely, a low value of 0.2 was adopted as the maximum output node error. In this way, the training proceeded until all context units were added to the network. A number of context units were tried for comparison. The results are shown in Table 9.

TABLE 9
NETWORK ERROR USING
CASCADE CORRELATION ALGORITHM

Network	Normalised Mean Squared Error (NMSE)	
	Training	Validation
16-3cc-16	0.57	0.67
16-5cc-16	0.51	0.65
16-9cc-16	0.47	0.67
16-17cc-16	0.52	0.61
16-25cc-16	0.36	0.77
16-33cc-16	0.32	0.81
16-65cc-16	0.20	0.85

Note: each network is denoted as (x-ycc-z), where x is the no. of input nodes, y is the no. of context units, and z is the no. of output nodes.

These results were compared with those obtained from the network trained by early stopping technique as shown in Table 10.

TABLE 10
NETWORK ERROR USING
EARLY STOPPING TECHNIQUE

Network	Normalised Mean Squared Error (NMSE)	
	Training	Validation
16-2-16	0.59	0.64
16-4-16	0.56	0.66
16-8-16	0.59	0.64
16-16-16	0.56	0.64
16-24-16	0.56	0.64
16-32-16	0.55	0.65
16-64-16	0.54	0.65

The following points were noted from comparison of the two tables.

- CasCor networks could produce better results. The CasCor network with 17 context units showed the smallest error in the validation tests.

- CasCor networks showed larger variations in performance. Networks trained with the early stopping technique showed a more consistent performance. The test results of CasCor range from 0.61 to 0.85, with a mean of 0.72 and a standard deviation of 0.091. The test results of early stopping range from 0.64 to 0.65, with a mean of 0.65 and a standard deviation of 0.008.
- The CasCor network has the ability to fit the data very closely, especially when a lot of context units are used. However, there is no objective way to set a correct error tolerance. If the error tolerance is set too low, the CasCor network will tend to overfit the data; on the other hand, if the error tolerance is set too high, the network will stop prematurely.

4.5.2 Incorporation of an Indicator for Wet and Dry Periods

Rainfall for the next time step may be forecast by two steps. Firstly, to determine whether there is some rain or no rain for the next time step, an additional binary node for each gauge can be added to the network to distinguish the wet and dry period for the next time step. A value of (1) indicates there is some rain, while a value of (0) indicates that there is no rain. Secondly, if there is rain, then the amount of rainfall will be determined.

The advantage of this approach depends on the accuracy of the first step. If the wet and dry period of the next time step can be accurately predicted. The performance of the network will be enhanced. Otherwise, apart from the inaccuracy of prediction of wet and dry, the performance of networks would worsen by inclusion of more connection weights resulting from the additional nodes.

Shown in Table 11 are the results of networks having one additional node at each of the 16 gauges to predict the wet and dry of the next time step. The results show that the predications are generally less accurate than the networks without the indicators. The average NMSE was 0.78.

TABLE 11
NETWORKS WITH WET/DRY INDICATOR

MLFN	SSE for the 32 outputs			SSE and NMSE for 16 output nodes on validation		Stopping
Lag 1	Training	Monitoring	Validation	SSE	NMSE	Epoch
(16-2-32)	1823	1053	1726	81.52	0.77	800
(16-16-32)	1747	1088	1737	81.86	0.78	400
(16-24-32)	1765	1081	1739	82.09	0.78	200

4.5.3 Adding an Index to Indicate the Day of a Year

Rainfall time series usually display seasonality which is due to the seasonal variation of global weather conditions. It was considered worthwhile, therefore, to include an indicator for the time of year of a storm event in order to model the long-range seasonal effects. The indicator may be constructed in the following way. For example, a storm event occurred on 15 Feb 94. The position of this day was:

$$d = 31\ (\text{Jan}) + 15\ (\text{Feb}) = 46$$

This day can be represented by a set of sine and cosine indices using the following equations:

$$\text{sine\_index} = \sin\left[d\left(\frac{360}{365}\right)\left(\frac{\pi}{180}\right)\right]$$

$$\text{cos\_index} = \cos\left[d\left(\frac{360}{365}\right)\left(\frac{\pi}{180}\right)\right]$$

These two indices define the position of the day of the year on which the storm occurred. By including the indices as additional inputs to an ANN, the seasonality will be modelled.

Shown in Table 12 are the results from the network with the addition input of time indices. Although the results showed a comparable performance with those of the network without the time indices (NMSE of 0.64), they did not provide the expected better results. This may

be due to the rainfall series being considered in this study having a 15-min interval. For such a short duration time series, the process is governed by local fluctuations. The long term seasonal effect is a secondary factor and hence will have only a secondary influence on the prediction. Another reason may be due to insufficient data to completely cover each day of the year for training the network.

TABLE 12
NETWORKS WITH INDICES OF THE DAY OF A YEAR

Network	NMSE Training	Monitoring	Validation	Stopping Epoch
MLFN Lag 1 (18-24-16)	0.49	0.70	0.65	400

An index to indicate the month of an event was attempted also. The months were represented by a set of sine and cosine indices using the following equations:

$$\text{sine\_index} = \sin\left[m\left(\frac{360}{12}\right)\left(\frac{\pi}{180}\right)\right]$$

$$\text{cos\_index} = \cos\left[m\left(\frac{360}{12}\right)\left(\frac{\pi}{180}\right)\right]$$

where m denotes the month of a year, with the value ranges from 1 to 12 representing January to December respectively.

Presented in Table 13 are the results of the testing. The results show a small improvement over that of the network using day indices as input. There was, however, no significant improvement in predictability over the networks without the seasonal indicator.

TABLE 13
NETWORKS WITH INDICES OF THE MONTH OF A YEAR

Network	NMSE Training	Monitoring	Validation	Stopping Epoch
MLFN Lag 1 (18-24-16)	0.49	0.69	0.64	400

4.5.4 Comparison with Multiple Linear Regression Model

The neural networks were compared with a multiple linear regression model. The aim of this comparison is to evaluate the benefit of using nonlinear neural networks for the problem of rainfall forecasting.

The rainfall of time (t+1) at a gauge was forecast by using a multiple linear regression based on the rainfall recorded at the 16 gauges during the previous time step (t). For the 16 gauges in the catchment, there are a total of 16 linear multiple regression models. Presented in Table 14 are the prediction errors for the 16 gauges obtained from use of the multiple linear regression model. This model was calibrated with the training data set and validated with the validation data set.

TABLE 14
RESULTS OF MULTIPLE LINEAR REGRESSION

Model Type	Normalised Mean Squared Error (NMSE)	
	Calibration	Validation
Multiple Linear Regression	0.50	0.64

It was found that the linear model had comparable performance with many of the ANNs. The two ANNs which yielded better results than the linear regression model were the TDNN with two input windows and the MLFN trained with CasCor algorithm; the NMSE for their validation tests were 0.63 and 0.61 respectively.

The reasons why the other more complex non-linear networks do not show better results than the linear regression model may be due to the following factors.

- The performance of a model largely depends on the nature of the data. The rainfall data contains a lot of noise which makes generalisation of the time series features with the more sophisticated ANNs difficult. Although they approximated the training data more closely, they did not perform better in validation tests.

- The rainfall data was transformed by a log function. This transformation linearises the data, thus facilitating the modelling of the data by a multiple linear regression model.

4.6 Summary

Rainfall forecasting for a number of rain gauge positions using ANNs was the focus of this chapter. Three alternative types of ANN suitable for this task were identified, developed and compared in a systematic manner. These networks were:

- multilayer feedforward neural network (MLFN)
- Elman partial recurrent neural network (Elman)
- time delay neural network (TDNN)

All the above alternative networks were found suitable for provision of forecasts of rainfall one time step (15 minutes) ahead.

In addition, the following points were observed.

- For each type of network, there existed an optimal complexity which was determined by a combined effect of the number of hidden nodes and the lag of the network.
- All three alternative networks had comparable performance when they were developed and trained to reach their optimal complexities.
- Based on the available data, the 15-min rainfall time series did not seem to possess a long term memory. Therefore the networks with lower lag slightly outperformed the ones with higher lag.

An investigation of the effect of spatial inputs revealed that there existed an optimal limit of spatial information for inclusion into the network. Either too much or too little spatial information would result in a decreased performance. For the available rainfall data in this study, the optimal spatial input would be the eight nearest neighbouring gauges for a lag-1 network.

Further tests were carried out to ascertain the feasibility of improving the network performance. The following points were derived from these test results.

- The use of CasCor training algorithm showed an improvement of network performance. However, there is no objective way to set an optimal error tolerance.
- The use of additional nodes to predict the wet or dry period for the next time step did not give better results. On the contrary, the performance of the network was decreased due to additional errors introduced by incorrect prediction in wet or dry period together with an increase of connection weights.
- Adding an indicator for the time of year to model the seasonal effect was not successful because the short-term rainfall series is governed by local fluctuations rather than long term seasonal effects.
- A multiple linear regression model showed better performance than some ANNs with higher orders of lag. The linear regression model was outperformed by the TDNN with two input windows and the MLFN trained by the CasCor. The reason the more sophisticated ANNs did not produce better results than the linear model was that the former networks would tend to overlearn the training samples thus giving decreased performance in validation, and that the rainfall time series data had been linearised by a log function.

5. INTEGRATION OF AN ANN AND A GIS FOR RAINFALL FORECASTING

The ANN models developed in Chapter 4 are integrated with a spatial model developed within a Geographic Information System (GIS) environment to form a spatial rainfall forecasting model, which provides a rainfall forecast for each pixel within a catchment. Subcatchment rainfalls are obtained by averaging the rainfall values at pixels within the corresponding subcatchments. The accuracy of the model is ascertained by predicting artificial storm events generated for the study catchment.

5.1 Integrating an ANN and a GIS

The integration of ANN and GIS provides a powerful spatial rainfall forecasting model by merging the merits of the two separate models.

It is assumed that the rainfall measured at gauges is the only available rainfall data for the study catchment. In such a situation there are two alternate ways to integrate the two models. One approach is to use the GIS to estimate rainfall at each pixel of the study catchment based on measured rainfall at gauges. This generates hundreds of estimated pixel rainfall values within the catchment. The ANN is then used to map the estimates of rainfall at the pixels and to directly produce a rainfall forecast for each pixel within the catchment. The alternate approach is to use the ANN to forecast rainfall at the gauge sites and then to use the GIS to generate the forecast rainfall for all pixels within the study catchment. The latter approach was adopted in this study because the number of parameters for the ANN would be dramatically reduced as compared to the former approach. Moreover, the time required for training the ANN would be much faster.

The first approach (of using catchment pixels as both input and output) is not feasible because it involves the use of a large number of input and output nodes and, consequently, the ANN contains a large number of parameters (weights) for which values need to be estimated. For example, the total number of pixels (500m × 500m) of the study catchment is 439. A 3-layer MLFN with 439 input nodes, 439 output nodes and 2 hidden nodes comprises 1756 connections (439×2+439×2, excluding the biases). Training such a large

network is extremely time consuming. Moreover, a network with so many free parameters requires a large number of data sets which generally are not available in practice.

5.2 Methodology

There are 16 rain gauges in the study catchment. As such, the ANN was designed to contain 16 inputs and 16 outputs for the 16 rain gauges. After the forecast of rainfall at the 16 gauges were made, the information was passed forward to the GIS where a spline surface was generated to obtain rainfall at each pixel within the study catchment.

In order to test the accuracy of the model, artificial storm events were generated. The forecast rainfall at each pixel then was compared with the actual value of rainfall to ascertain the forecast accuracy.

5.2.1 Autoregressive Storm Events

The artificial storm events were assumed to be a random process with some memory. Accordingly, they were generated by a mixture of autoregressive and random equations which have the following characteristics.

First, a storm centre was randomly started at a point close to or within the study catchment. According to long term records, the predominant wind direction of Sydney is North East, so in generating the starting points of a storm event, a higher weighting was given to the North-East corner of the catchment. Once the starting position was generated the storm would move towards the centre of the catchment. During the movement, the storm centres would deviate from the initial direction and be governed by the following autoregressive equation:

$$\text{direction}(t) = 0.8 \cdot \text{direction}(0) + 0.2 \cdot \text{direction}(t-1) + e(t) \qquad (17)$$

where direction[t] is the direction of storm centre at time t

direction[0] is the initial direction of storm movement

e[t] is random deviation of storm movement which had a mean of 0° and a standard deviation of 15°

The intensity of the storm centre also was an autoregressive process and governed by the following expression.

$$p_{max}(t) = 0.2 \cdot p_{max}(t-1) + 0.8 \cdot e(t) \tag{18}$$

where $p_{max}(t)$ is the rainfall intensity at the storm centre (mm/hr) at time t;

$e(t)$ is the random fluctuation of intensity which has a mean of 30 mm/hr and a standard deviation of 5 mm/hr.

The spatial distribution of rainfall had a Gaussian pattern which was governed by the following expression:

$$p_t(x, y) = p_{max}(t)\, e^{-az^2} \tag{19}$$

where $p_t(x,y)$ is the rainfall intensity (mm/hr) at a pixel (x,y) at time t

$p_{max}(t)$ is rainfall intensity at centre of storm (mm/hr) at time t

a is a coefficient which controls the spread of the rainfall, a constant value of 2.25×10^{-8} was adopted in this study to limit the spatial extent of the storm event to the study catchment

z s a position variable defined as $(x^2+y^2)^{0.5}$

The speed of movement of the storm centre was a random process with a mean speed of 12km/hr, and a standard deviation of 2km/hr.

As an illustration, shown in Figure 16 is the storm centre track as a storm moves across the catchment. The catchment is coloured yellow while the initial position of the storm centre is labelled by 0, the next position is labelled by 1, and so on. This storm moved across the catchment form the north east corner to the south west corner during its life span which was 2.5 hours (15 min x 10 time steps).

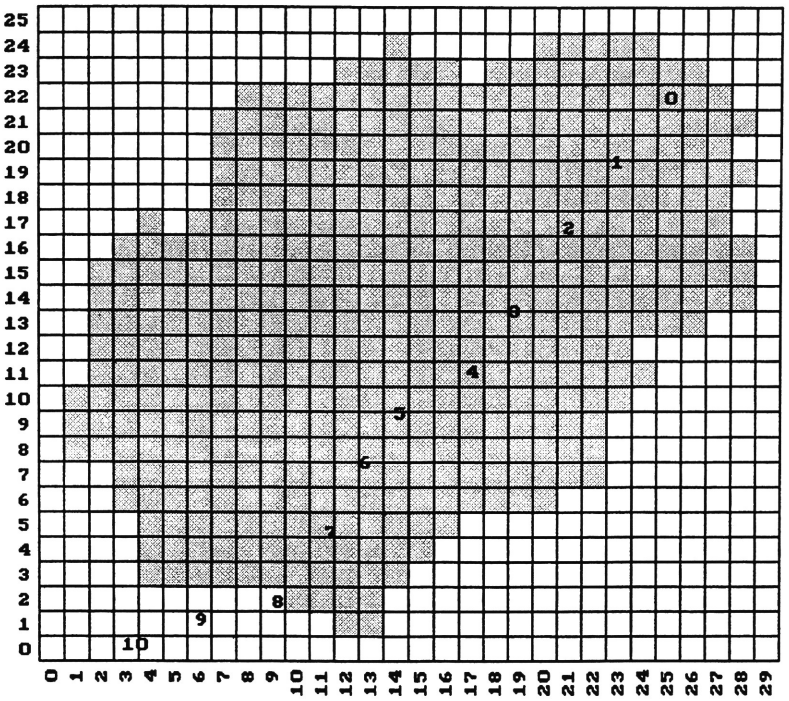

Figure 16 - Track of Storm Centres

In order to train and test the rainfall forecasting model, a total of 150 artificial storms were generated. Of these storm events, 100 were used for training, 25 for monitoring, and 25 for validation.

The storm centre tracks for all 25 validation events are shown in Appendix E; these tracks are representative of all the generated storm events.

5.2.2 Components of the Spatial Rainfall Forecasting Model

As previously discussed, the spatial rainfall forecasting model consists of two major components; these are the artificial neural network and a geographic information system.

The ANN adopted for this study was an Elman network with 16 inputs, 16 outputs and 4 context units. This network was adopted to avoid the need for determining the time lag explicitly.

There were 16 input nodes and 16 output nodes in the Elman network representing the present and future rainfall values at the 16 gauges of the catchment. Based on the present rainfall information, the network would produce one time step ahead (15 minute) forecasts for the 16 gauges. The procedure was first to extract rainfall values at the 16 gauge positions from the artificial storms as if they were recorded during the storm events. Then, the rainfall values at gauges were input to the Elman network. After processing, the forecast rainfalls at the gauge positions were obtained from the outputs of the network.

The rainfall forecasts at 16 gauges were then passed to the GIS where the spatial rainfall model was invoked to estimate the rainfall depth for each pixel within the catchment. The Spline model developed within the GIS environment was adopted since it was the best performed spatial model during the tests described in Luk and Ball (1996). Subcatchment rainfalls were determined by averaging pixel rainfall values within subcatchment boundaries.

All the above procedures were automated thus simulating real time operation.

5.3 Test Results and Discussions

In ascertaining the accuracy of the spatial rainfall forecasts, both visual and arithmetic comparisons were established. The spatial rainfall forecasting model was validated on the following aspects.

- Replicating the real rainfall patterns (visual inspection).
- Tracking the movement of storm centres (visual inspection).
- Predicted rainfall at individual pixels.
- Predicted rainfall for subcatchments.

5.3.1 Moving Storm Patterns (Visual Inspection)

Shown in Figures 17 to 26 are the distribution of rainfall over the study catchment during the life span of validation storm event no. 138. Similar maps were obtained for other events. For each map, the rainfall intensity was colour-coded to facilitate visual inspection. Each figure consists of three pieces of information: the actual distribution of rainfall is

shown at the top of the figure, the forecast rainfall pattern is shown in the middle, while shown at the bottom of the figure is the distribution of error obtained from subtracting the forecast rainfall by actual rainfall at each pixel.

As can be seen from the figures, the spatial rainfall forecasting model had good performance. The Gaussian spatial patterns were correctly preserved for all time steps.

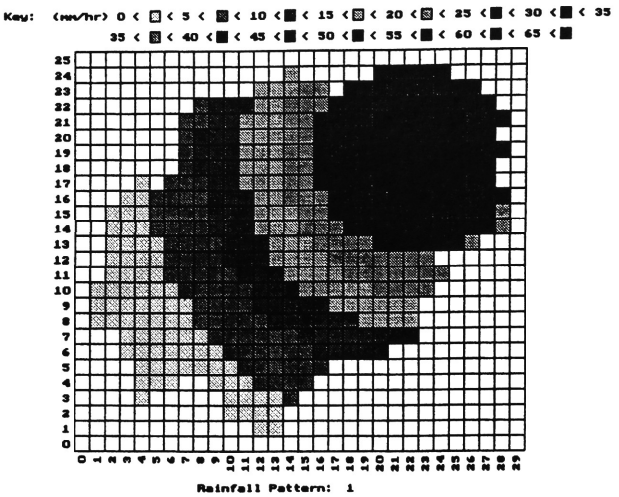

Distribution of Actual Rainfall

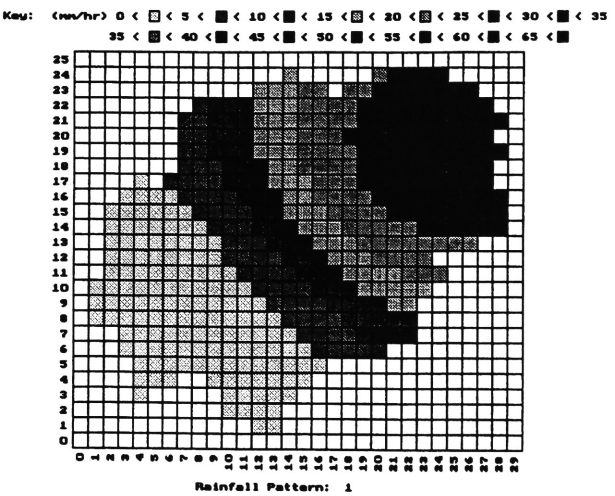

Distribution of Forecasted Rainfall

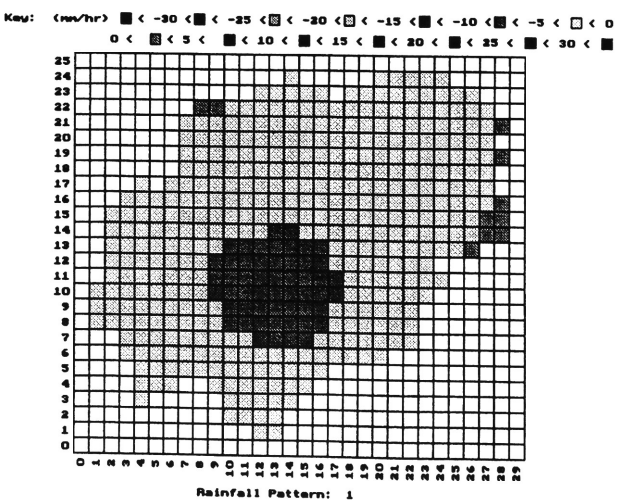

Distribution of Forecasted Error

Figure 17 - Artificial Storm Event No. 138 - Time Step 1

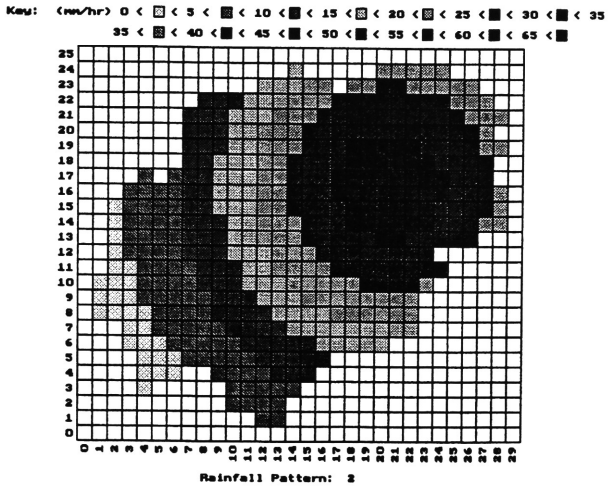

Distribution of Actual Rainfall

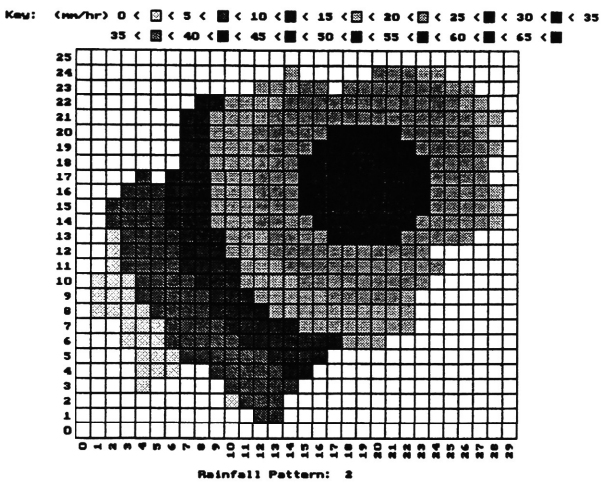

Distribution of Forecasted Rainfall

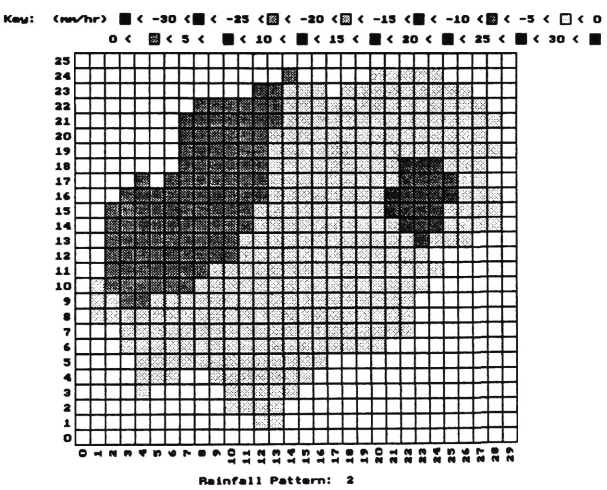

Distribution of Forecasted Error

Figure 18 - Artificial Storm Event No. 138 - Time Step 2

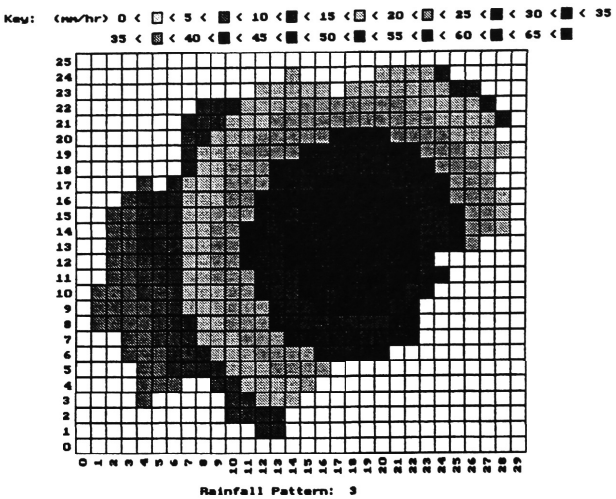

Distribution of Actual Rainfall

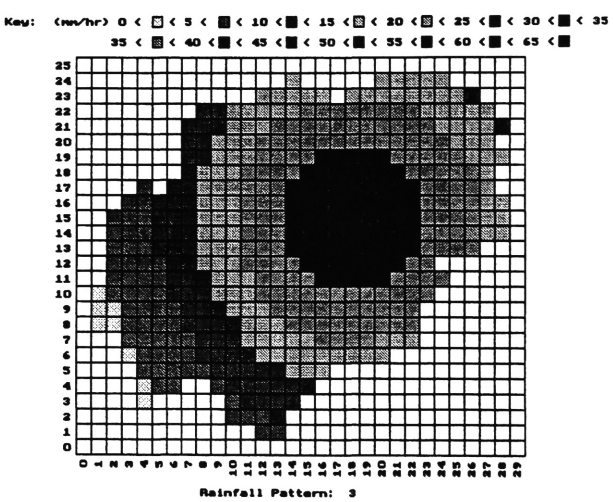

Distribution of Forecasted Rainfall

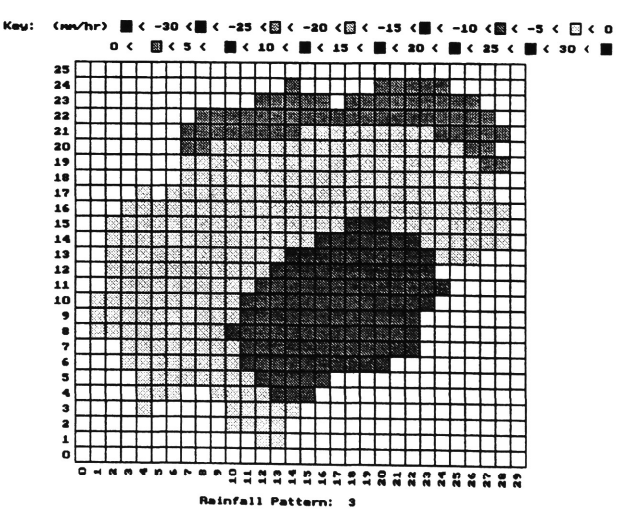

Distribution of Forecasted Error

Figure 19 - Artificial Storm Event No. 138 - Time Step 3

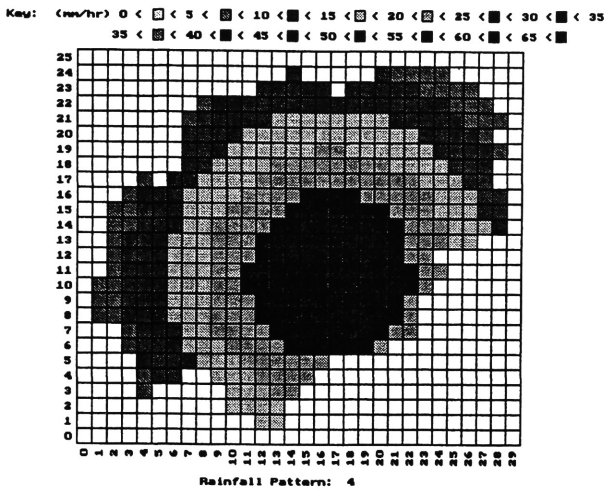

Distribution of Actual Rainfall

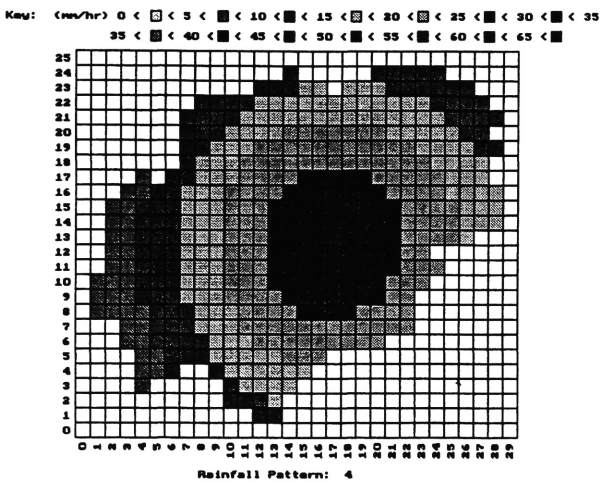

Distribution of Forecasted Rainfall

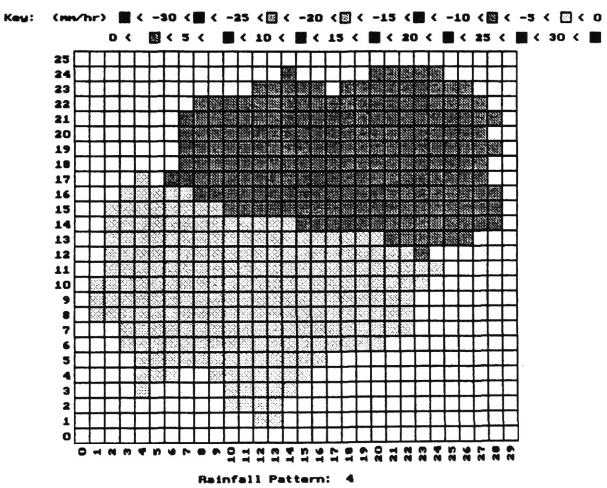

Distribution of Forecasted Error

Figure 20 - Artificial Storm Event No. 138 - Time Step 4

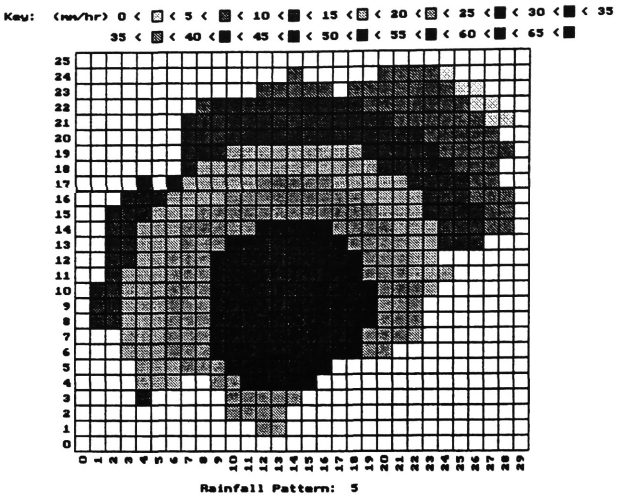

Distribution of Actual Rainfall

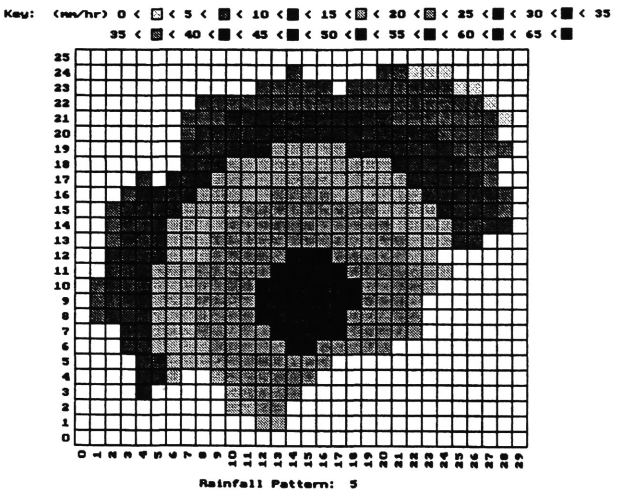

Distribution of Forecasted Rainfall

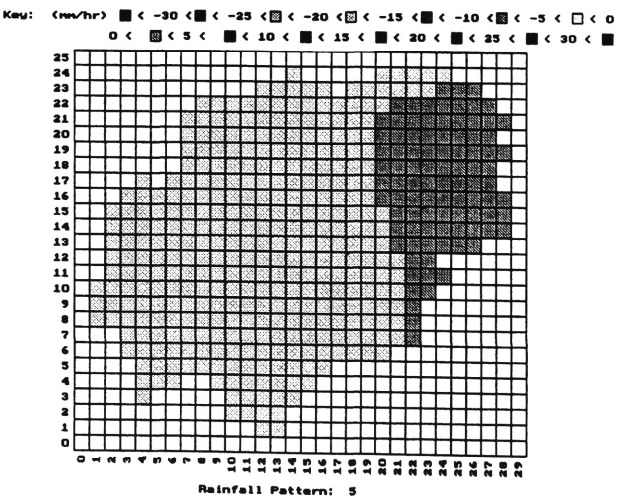

Distribution of Forecasted Error

Figure 21 - Artificial Storm Event No. 138 - Time Step 5

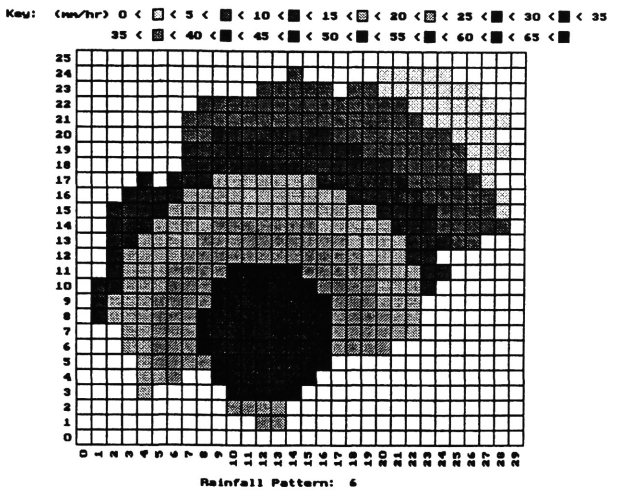

Distribution of Actual Rainfall

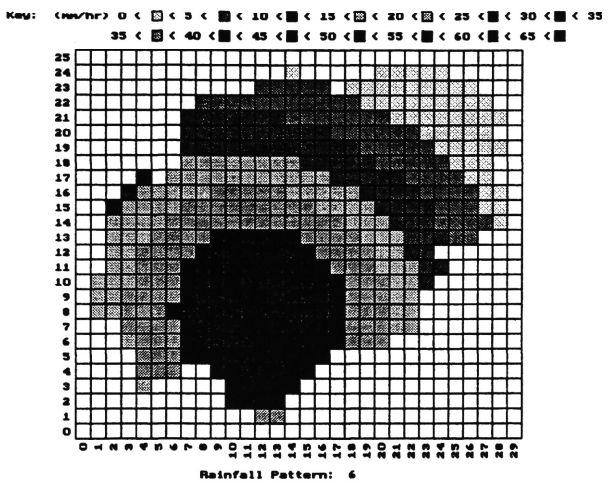

Distribution of Forecasted Rainfall

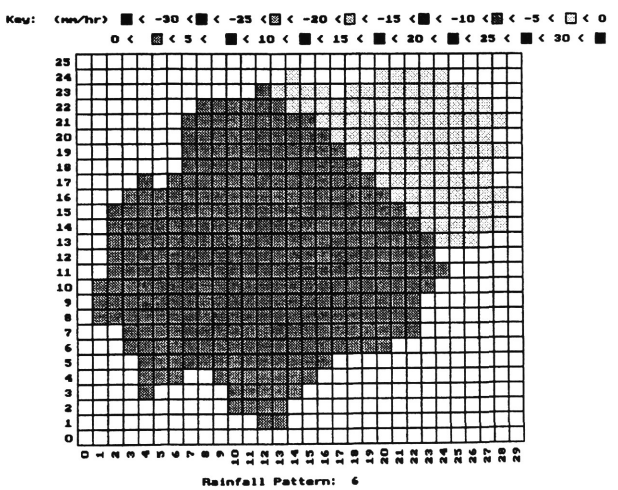

Distribution of Forecasted Error

Figure 22 - Artificial Storm Event No. 138 - Time Step 6

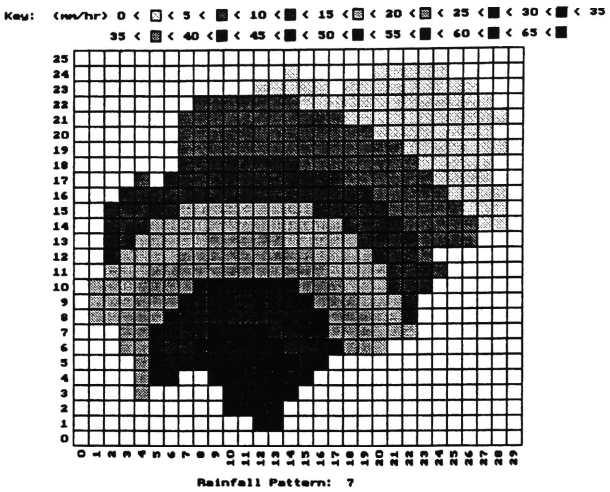

Distribution of Actual Rainfall

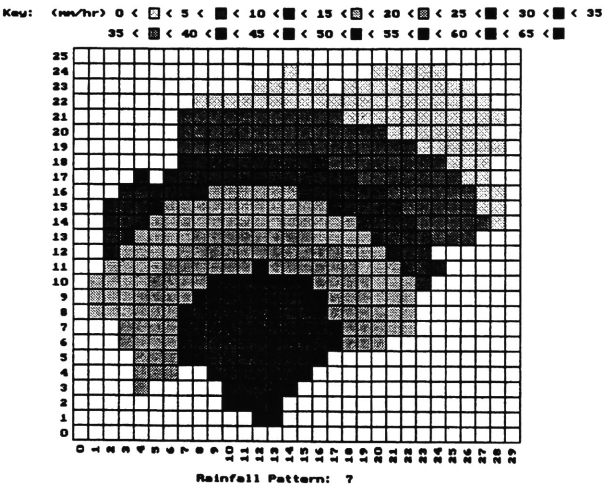

Distribution of Forecasted Rainfall

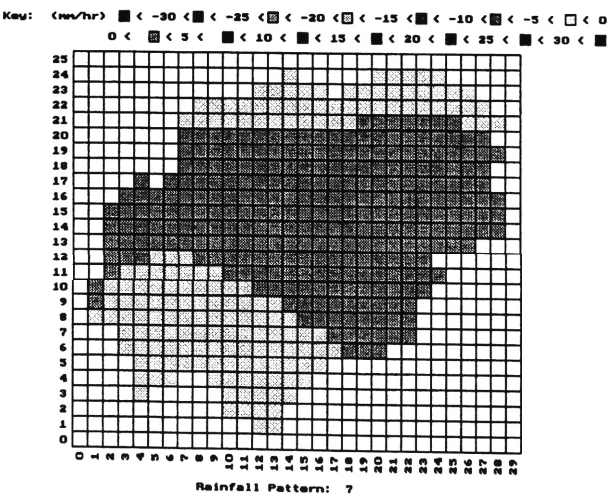

Distribution of Forecasted Error

Figure 23 - Artificial Storm Event No. 138 - Time Step 7

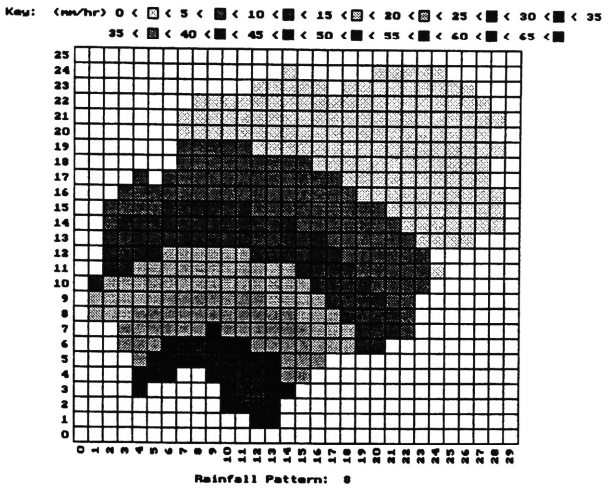

Distribution of Actual Rainfall

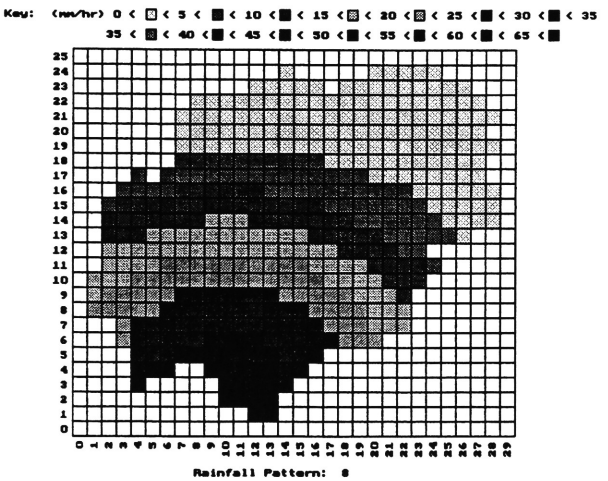

Distribution of Forecasted Rainfall

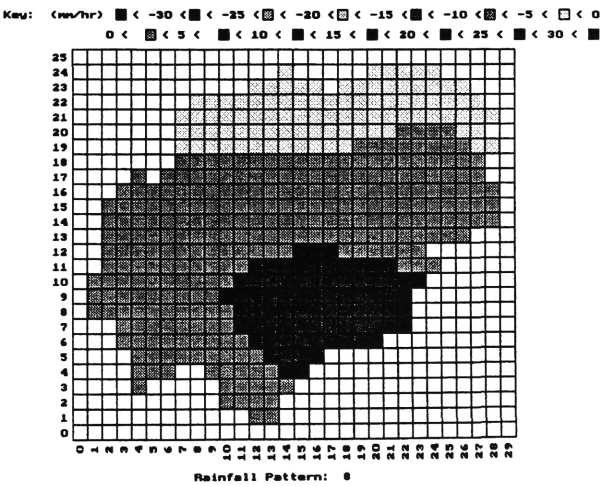

Distribution of Forecasted Error

Figure 24 - Artificial Storm Event No. 138 - Time Step 8

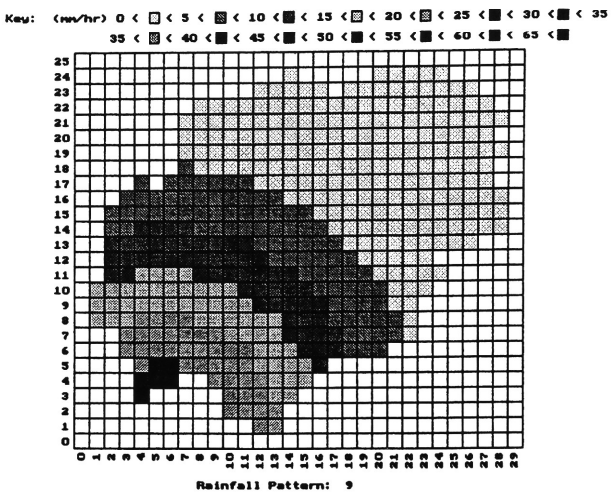

Distribution of Actual Rainfall

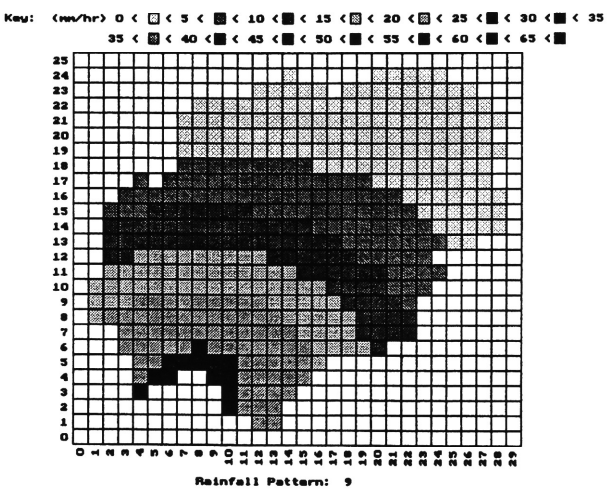

Distribution of Forecasted Rainfall

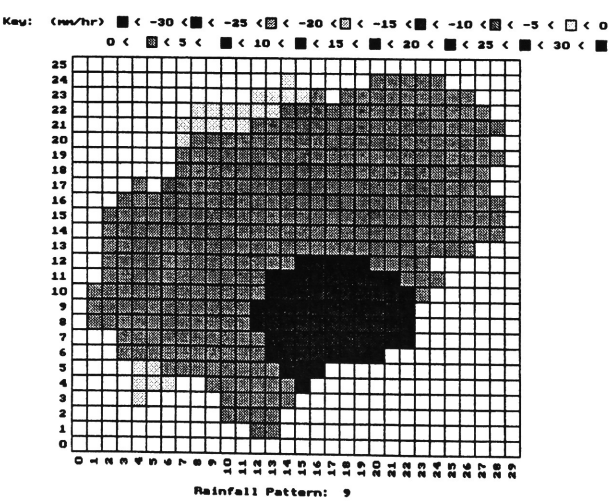

Distribution of Forecasted Error

Figure 25 - Artificial Storm Event No. 138 - Time Step 9

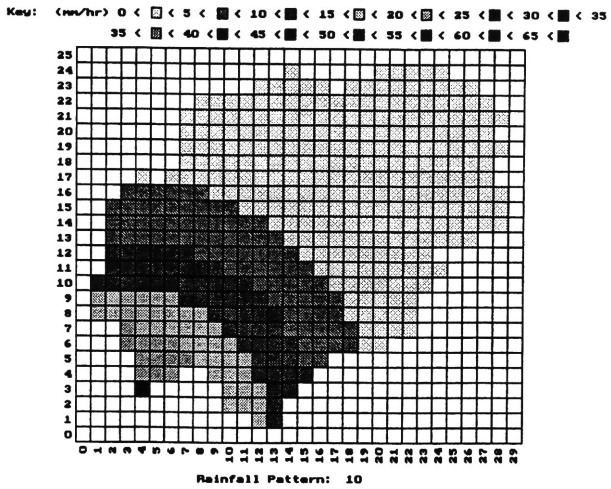

Distribution of Actual Rainfall

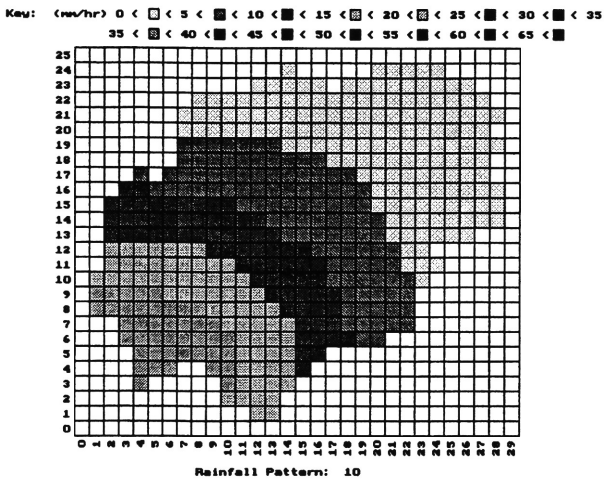

Distribution of Forecasted Rainfall

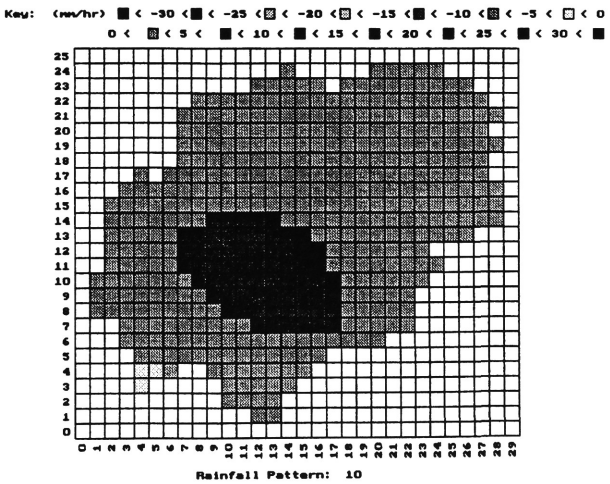

Distribution of Forecasted Error

Figure 26 - Artificial Storm Event No. 138 - Time Step 10

5.3.2 Tracking of Storm Centres (Visual Inspection)

Shown in Figure 27 is a comparison of the actual storm centre track with the predicted storm centre track.

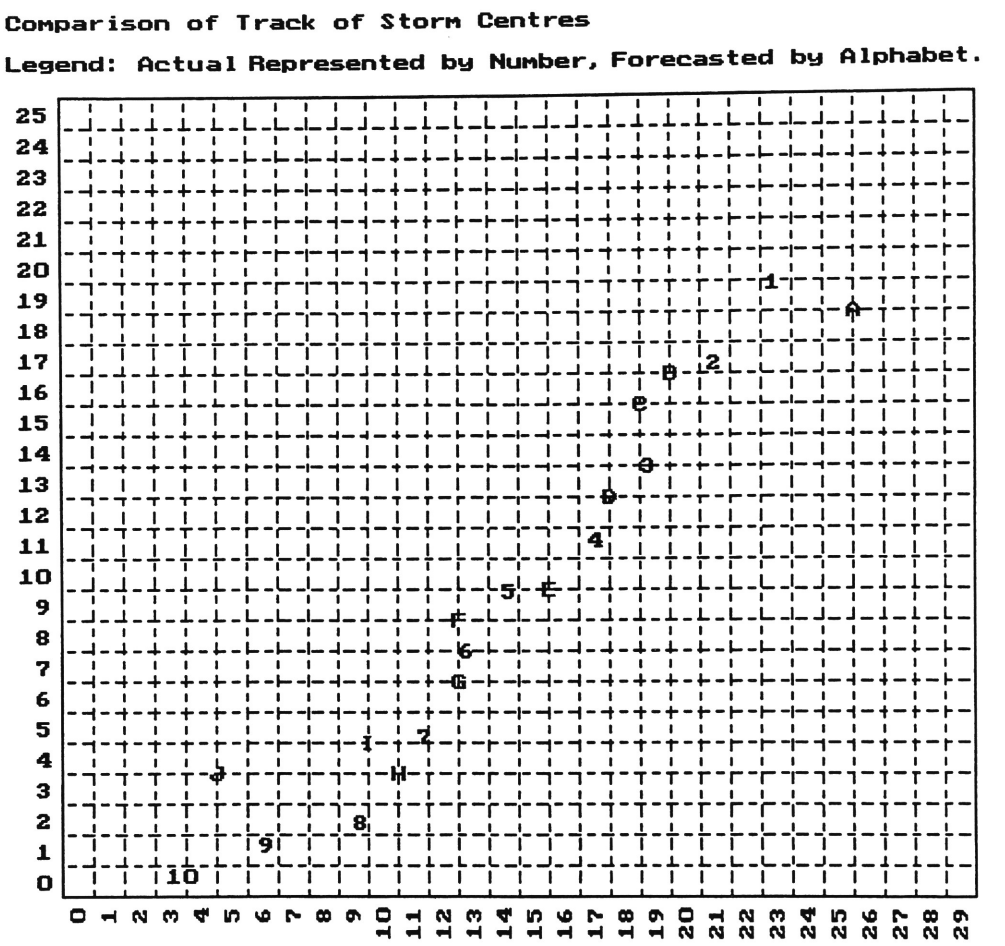

Figure 27 - Forecasting Movement of Storm Centres

The actual track of storm centres was represented by numbers, whereas the forecast track is shown by alphabetic characters. As shown in Figure 27 both tracks had similar characteristics. In particular, the forecasting model did very well in tracking the storm centres from time steps 2 to 8. There were, however, larger errors in forecasting the centres at time steps 9 and 10. These errors resulted in an overestimation of the spatial rainfall distribution as shown in Figures 25 and 26 previously.

Presented in Table 15 is the error in the predicted storm centre for each time step during storm event 138 while presented in Table 16 is a summary of the characteristics of the errors.

TABLE 15
FORECAST ERRORS FOR STORM NO. 138

Time Step	Intensity (mm/15-min)	Distance (km)	Angle (degree)
1	–4.0	0.11	–47.2
2	–4.6	0.64	12.3
3	–5.8	–0.61	28.3
4	–1.5	–0.66	16.4
5	–3.5	–0.56	–15.8
6	1.8	–0.22	25.4
7	–3.1	–1.05	–10.7
8	1.8	–1.00	–1.5
9	–2.0	–0.34	109.4
10	–3.6	–0.17	74.8

TABLE 16
ERROR STATISTICS FOR STORM NO. 138

Statistics	Intensity (mm/15-min)	Distance (km)	Angle (degree)
High	1.8	–0.22	28.3
Low	–5.8	–1.05	–15.8
Mean	–1.7	–0.68	7.0
Median	–2.3	–0.63	7.4
Standard Deviation	3.1	0.31	18.9
Skewness	0.1	0.18	–0.1

There are large errors in the first and the last two time steps. The errors might be due to initiation and boundary conditions for the model. Due to the uncertainty in these time steps, the error characteristics presented in Table 16 do not include values of the first and last two time steps.

Considering the fact that the average intensity of storm no. 138 was 28.9mm/15-min, the error in the forecast rainfall intensity was small. In addition, the prediction in distance was excellent; the range of error was only from –1.05 to –0.22 km with a mean error of –0.68,

which means that the storm centre was predicted in an adjacent pixel to that where it actually occurred. However, there was significant error in predicting the direction of storm centres. The range of error of storm direction was between −15.8° and 28.3° with a standard deviation as high as 18.9°.

Similar statistics were calculated for all 25 validation storm events and given in Appendix F. A summary of the results is presented in Table 17.

TABLE 17
ERROR STATISTICS FOR ALL 25 VALIDATION STORM EVENTS

Statistics	Intensity (mm/15-min)	Distance (km)	Angle (degree)
High	8.2	0.73	178.3
Low	−16.8	−1.68	−172.5
Mean	−2.8	−0.62	−0.9
Median	−2.9	−0.62	0.6
Standard Deviation	4.3	0.49	53.0
Skewness	−0.1	0.27	−0.03

The error statistics show that the ANN produced excellent prediction on the rainfall intensity and distance of the storm centre. The network, however, was not able to provide accurate prediction of the storm direction. The range of error was between −172° and 178° with a mean of 0.6° and standard deviation of 53°. The skew of −0.03 suggests that the error in angle is normally distributed which may be interpreted as white noise.

These results are encouraging because the mean distance error is 0.6 km which is only slightly larger than a pixel size of the catchment grid.

5.3.3 Rainfall at Pixels

The errors in forecast at each catchment pixel were quantitatively evaluated. Shown in Table 18 are the normalised mean squared errors of each time step for all 25 validation storm events.

TABLE 18
NORMALISED MEAN SQUARED ERRORS FOR ALL 25 VALIDATAION STORM EVENTS

	NMSE at Each Time Step										
Event	1	2	3	4	5	6	7	8	9	10	Mean
126	0.444	0.245	0.227	0.429	0.015	0.028	0.072	0.162	—	—	0.203
127	0.063	0.875	0.506	0.482	0.042	0.083	0.101	0.027	0.055	—	0.248
128	0.246	0.227	0.156	0.232	0.327	0.436	0.312	0.046	0.097	0.193	0.227
129	0.362	0.046	0.177	0.161	0.341	0.156	0.254	0.617	0.587	0.163	0.286
130	0.328	0.336	0.173	0.056	0.150	0.177	0.554	0.116	0.196	0.193 0.326	0.237
131	0.16	0.512	0.305	0.01	0.015	0.031	0.185	0.066	0.098	—	0.154
132	0.469	0.264	0.321	0.078	0.07	0.239	0.454	0.348	0.215	0.143 0.645	0.295
133	0.703	0.123	0.267	0.199	0.206	0.074	0.161	0.299	0.124	—	0.240
134	0.175	0.328	0.328	0.074	0.175	0.168	0.04	0.055	0.194	—	0.171
135	0.145	0.092	0.266	1.643	0.167	0.307	0.241	0.132	0.176	—	0.352
136	0.884	0.35	0.12	0.503	0.202	0.236	0.14	0.144	0.137	0.14	0.286
137	0.07	0.443	0.213	0.224	0.615	0.375	0.063	0.221	—	—	0.278
138	0.13	0.086	0.286	0.139	0.127	0.081	0.026	0.176	0.199	0.396	0.165
139	0.15	0.245	0.301	0.427	0.062	0.054	0.082	0.08	—	—	0.175
140	1.561	0.165	0.388	0.244	0.419	0.21	0.237	0.41	0.101	0.059 0.150 0.189	0.344
141	4.422	0.026	0.826	0.147	0.217	0.199	0.278	0.053	0.048	0.113 0.133	0.587
142	0.039	0.178	0.056	0.134	0.083	0.167	0.286	0.024	0.299	1.755	0.302
143	0.416	0.028	0.383	0.07	0.809	0.441	0.224	0.117	0.165	0.147	0.280
144	0.756	0.181	0.305	0.222	0.191	0.204	0.347	0.207	0.261	—	0.297
145	0.703	0.112	0.132	0.651	0.103	2.333	0.211	0.226	0.115	0.094 0.045	0.430
146	0.434	0.196	0.13	0.128	0.257	0.056	0.045	—	—	—	0.178
147	0.093	0.655	0.104	0.402	0.355	0.069	0.071	0.009	0.059	—	0.202
148	0.149	0.107	0.073	0.093	0.207	0.073	0.15	0.17	0.185	—	0.134
149	0.063	0.186	0.09	0.102	0.476	0.12	0.285	0.041	0.051	—	0.157
150	1.075	0.432	0.391	0.097	0.566	0.296	0.251	0.08	0.073	0.156	0.342
										Overall Mean NMSE	0.263

The overall mean NMSE is 0.263 which is considered remarkable. The spatial distribution of rainfall was accurately forecast. There were, however, several abnormal figures as summarised in the following table.

TABLE 19
ABNORMAL FORECAST ERRORS

Event	NMSE	Time Step
140	1.561	1
141	4.422	1
150	1.075	1

It is noted that all these incidents occurred at the first time step. After these incidents, the ANN accurately forecast the remainder of the storm movement and intensities. It is believed that the errors were due to the ANN not being able to recognise the initial position of the storm centres. An inspection of the storm tracks shown in Appendix E revealed that Event 140 started from the North West direction, Event 141 from the West, and Event 150 from the South East corner. These three initial positions received less weighting when generating the starting positions of the artificial storms. Consequently there is a lack of training samples for these events.

Shown in Figures 28 to 32 are plots of the forecast rainfall as a function of actual rainfall for validation event number 138. Similar plots were obtained for other events. A measure of error can be obtained from the vertical distance of the plotted forecasts from the line of exact agreement. Also shown in the figure are ±20% error bars from the line of exact agreement. With the aid of these lines, the magnitude and distribution of errors can be derived from the plots.

In general the forecasts showed good agreement with the actual rainfall. The best prediction was at time step no. 7 where the NMSE was 0.026, whereas the worst prediction occurred at time step no. 10 where the NMSE was 0.396. The error was due to incorrect prediction of the storm centre and as a result of this the distribution of rainfall intensity was forecast incorrectly.

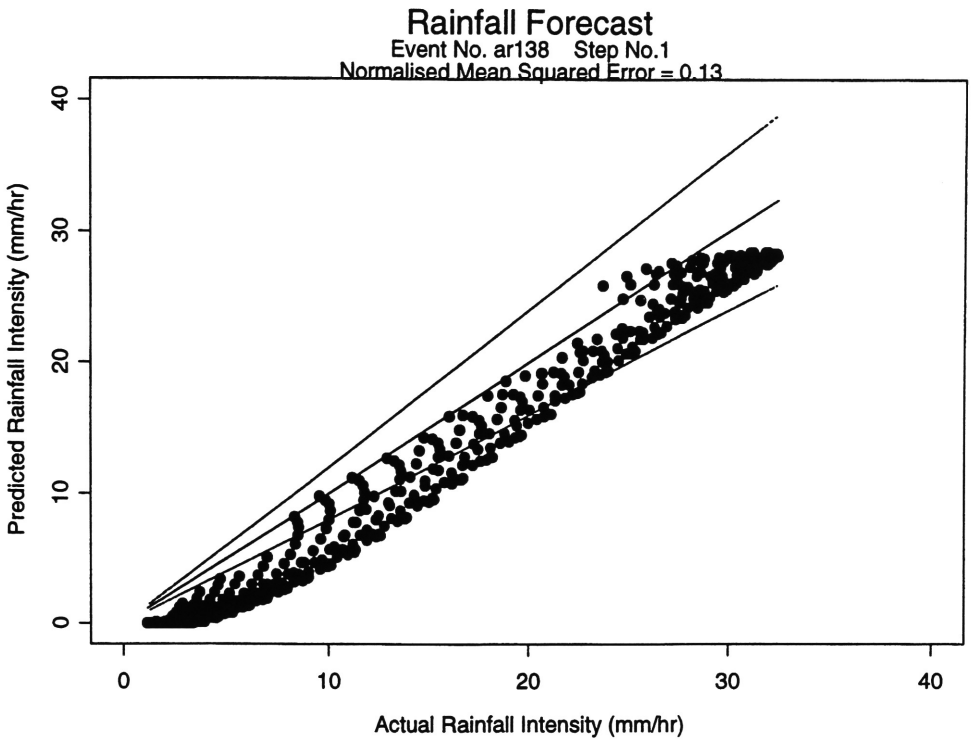

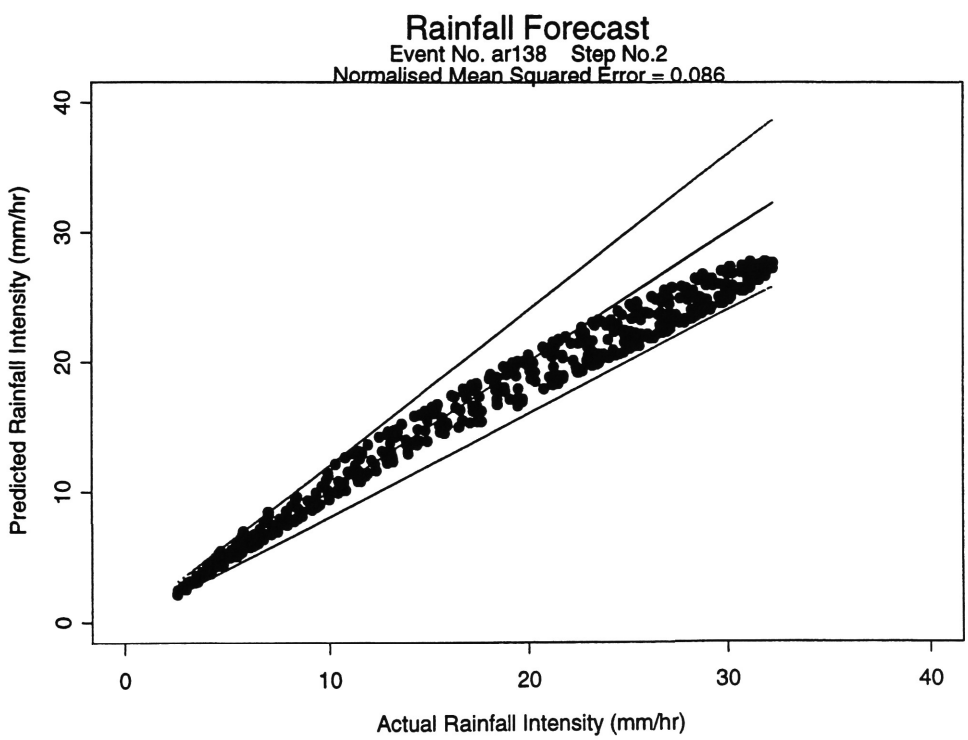

Figure 28 - Predicted vs. Actual Rainfall Intensity for Storm Event No. 138 (time steps 1 and 2)

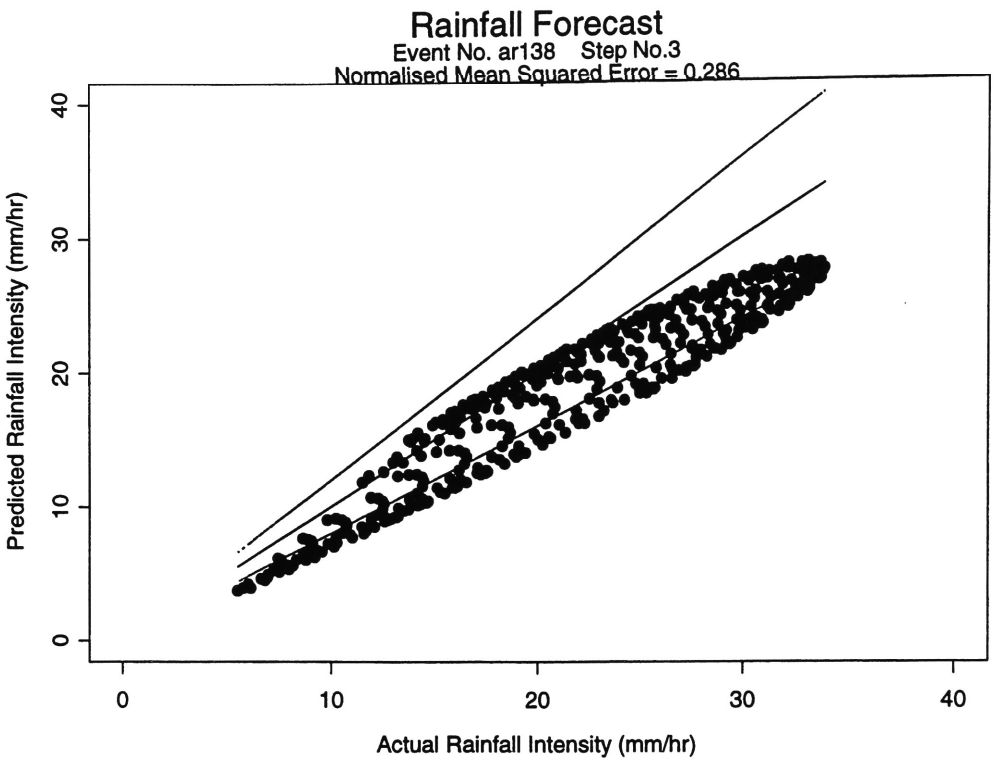

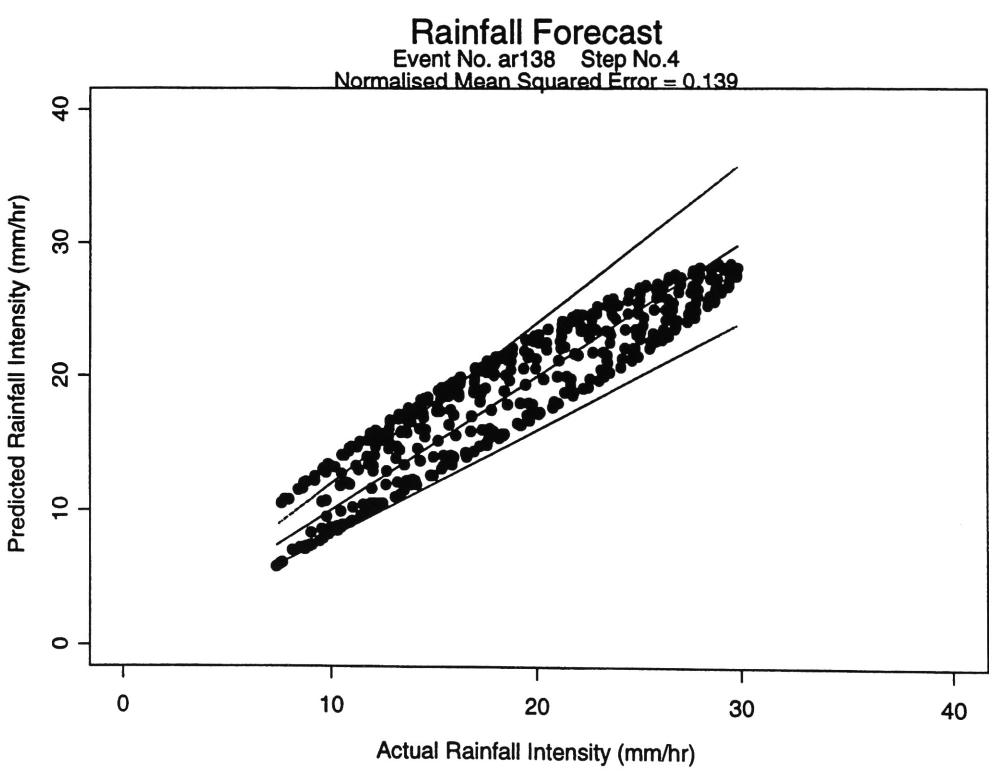

Figure 29 - Predicted vs. Actual Rainfall Intensity for Storm Event No. 138 (time steps 3 and 4)

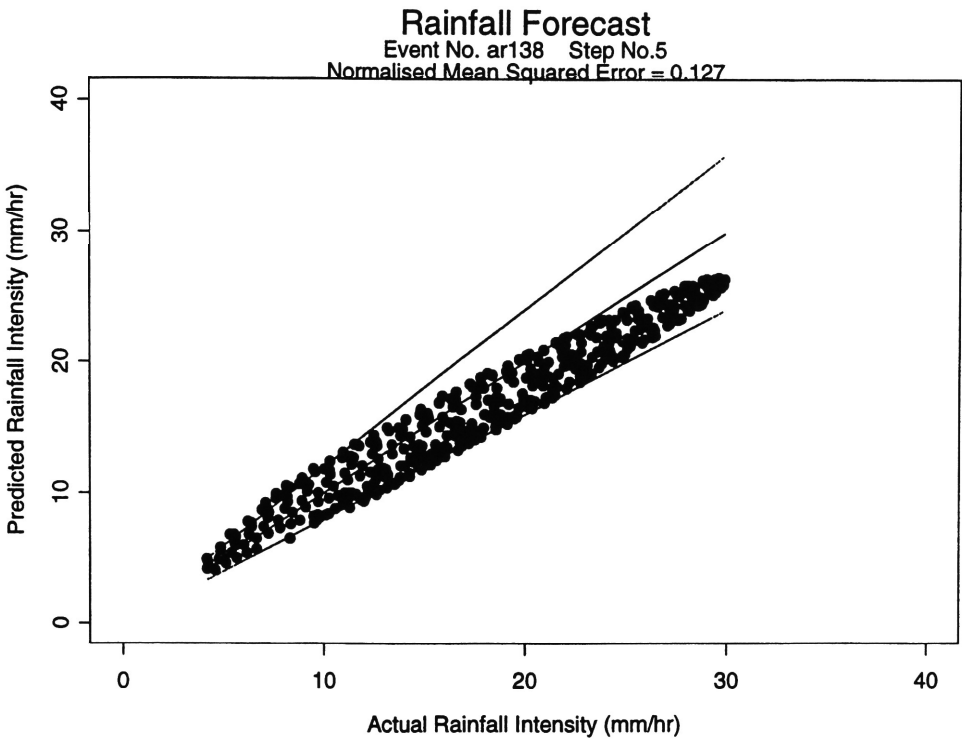

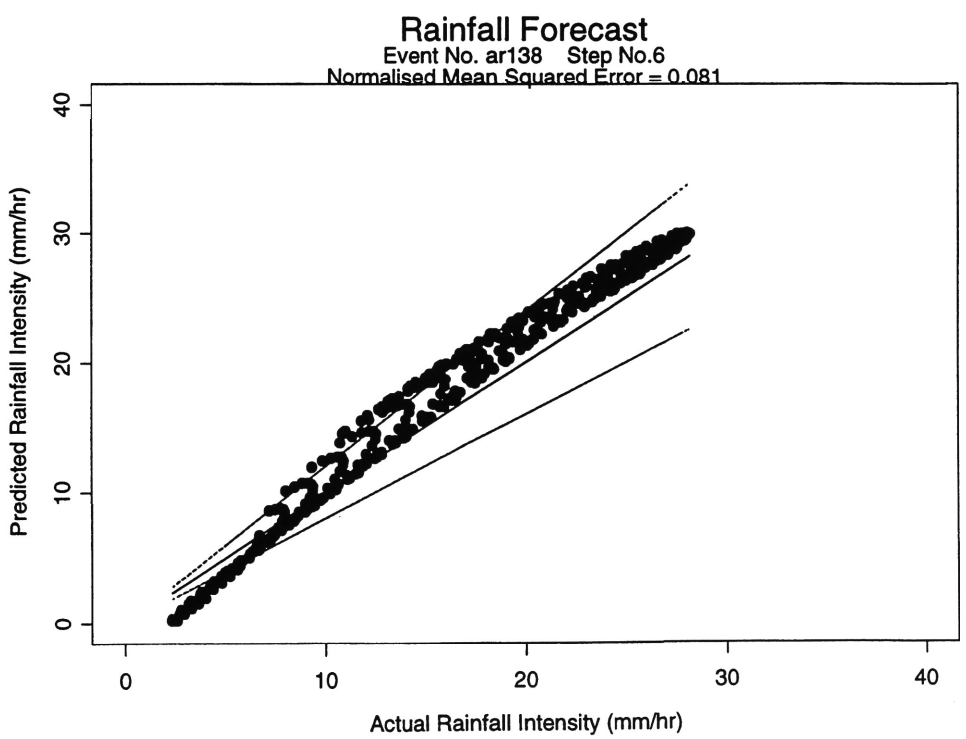

Figure 30 - Predicted vs. Actual Rainfall Intensity for Storm Event No. 138 (time steps 5 and 6)

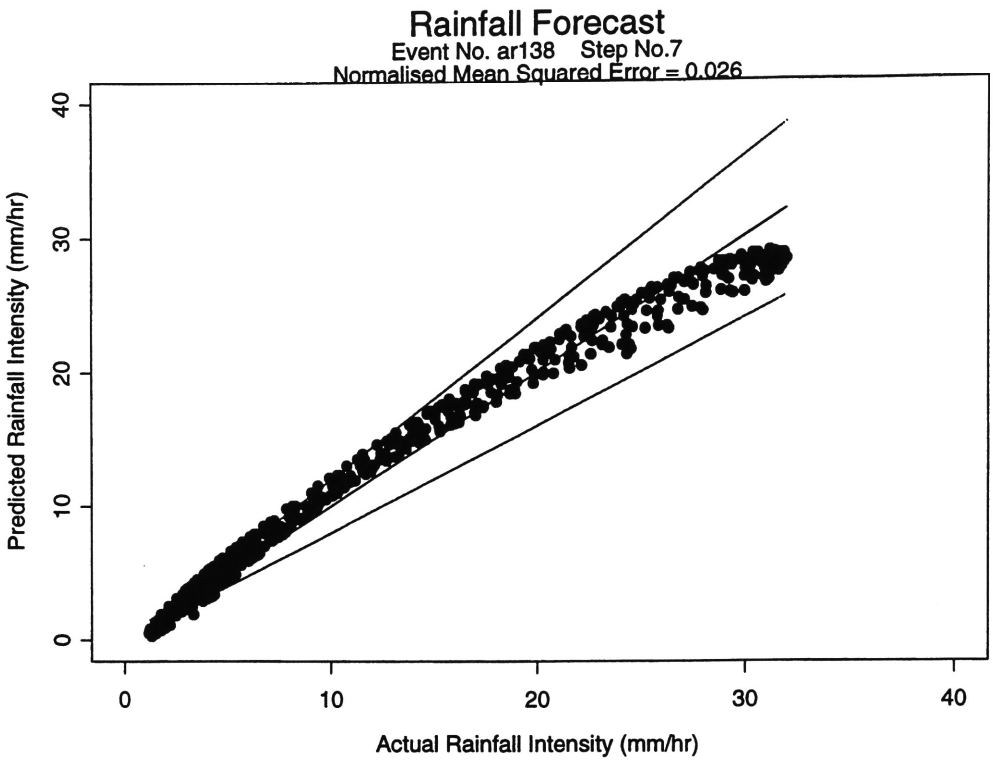

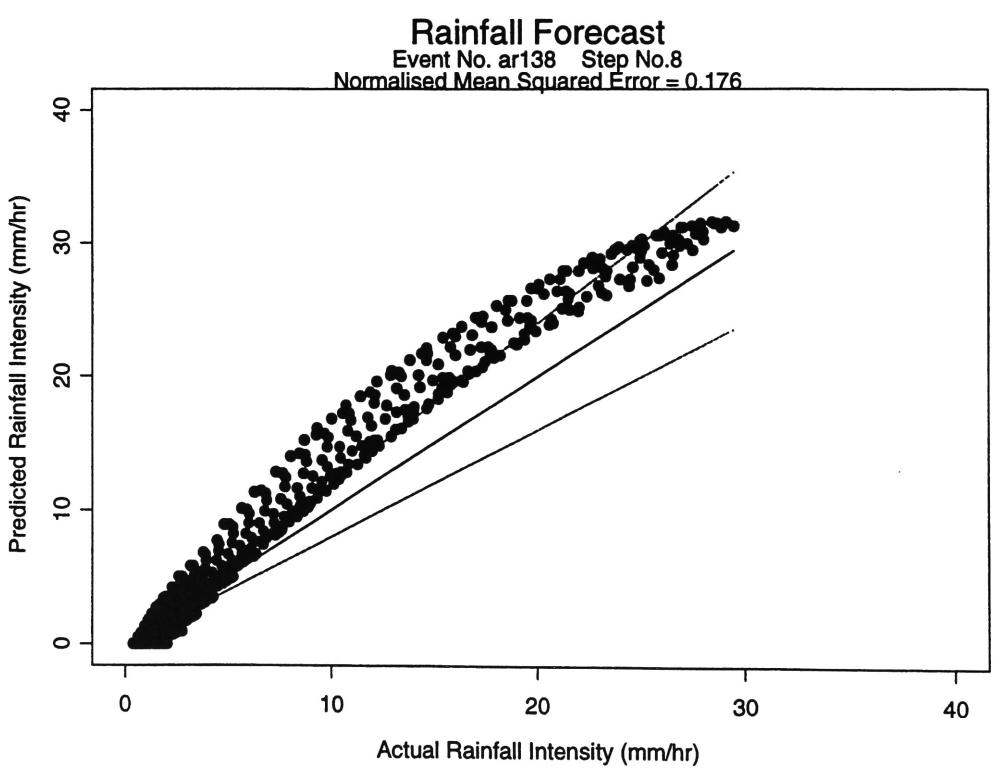

Figure 31 - Predicted vs. Actual Rainfall Intensity for Storm Event No. 138 (time steps 7 and 8)

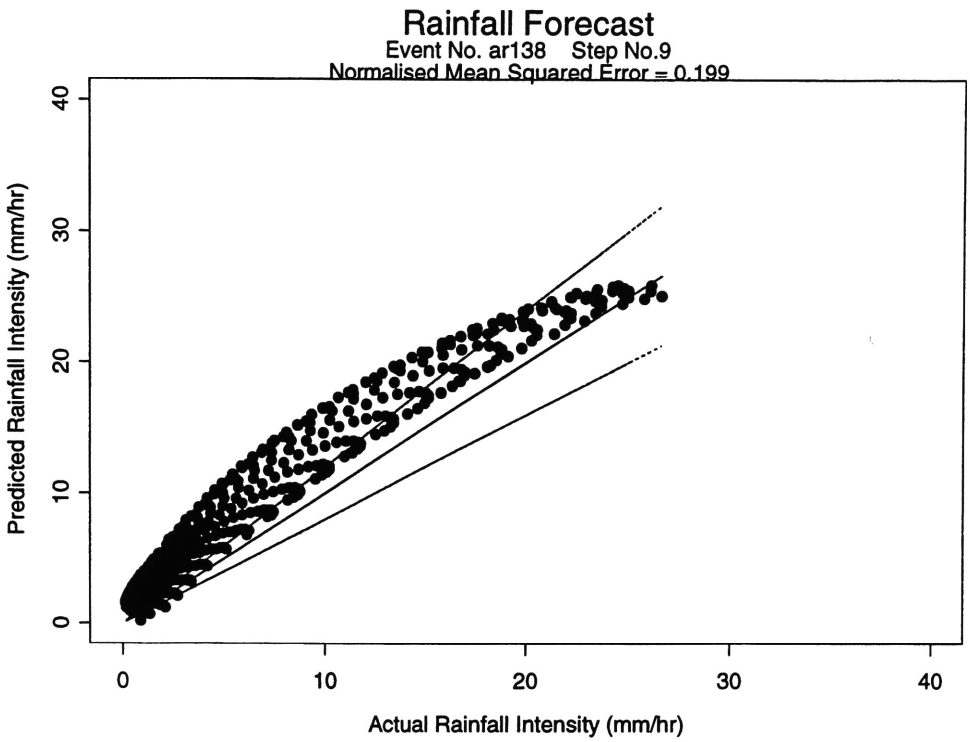

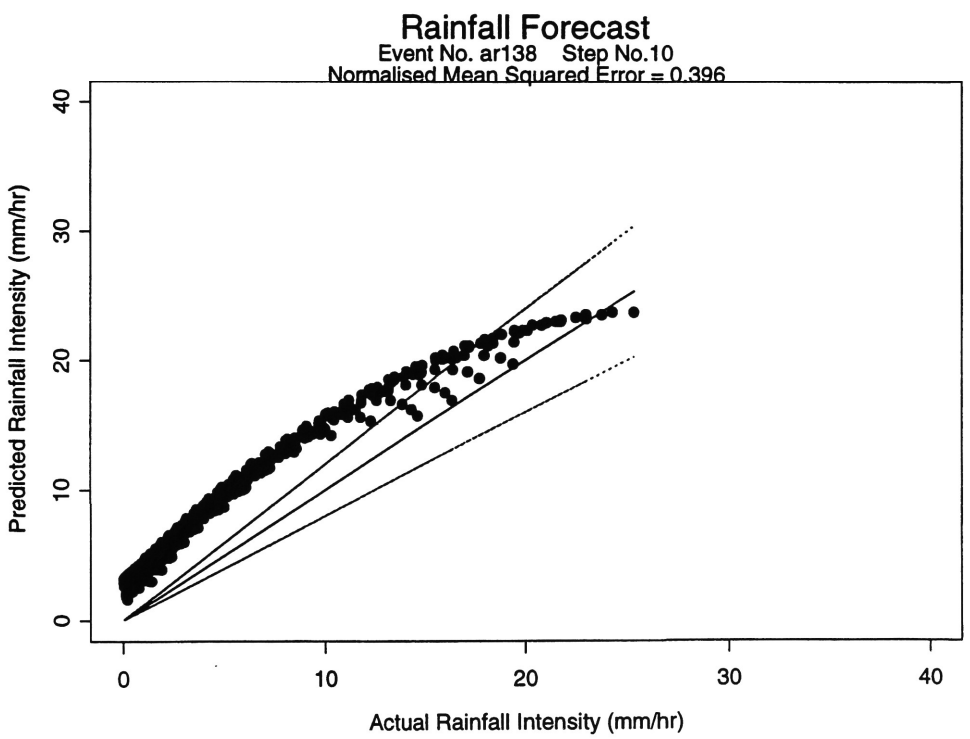

Figure 32 - Predicted vs. Actual Rainfall Intensity for Storm Event No. 138 (time steps 9 and 10)

5.3.3 Mean Rainfall at Subcatchments

In addition to the error measure based on pixel estimates, it is possible to obtain an error measure based on the forecast rainfall intensity at the centroid of each subcatchment. The subcatchment mean rainfalls forecasted by the spatial rainfall forecasting model for all 25 validation events are given in Appendix G.

Shown in Figures 33 and 34 are boxplots of relative errors of subcatchment rainfall for all 25 validation events. The boxplots are based on the information given in Appendix G. A boxplot, as used previously, consists of a line in the middle of the box denoting the 50% quantile (median), the box with edges representing 25% and 75% quantiles, and whiskers that extend to the 5% and 95% quantiles of the error statistics.

In general, over the 25 validation events the majority of relative errors are within ± 20%, which is considered a reasonable result. There are, however, quite a number of outliners. An inspection of the values shown in Appendix G revealed that these outliners occurred when the actual subcatchment rainfall values were very small. As such, a small error in estimation would result in a large percentage error. It should be noted that the small variation in absolute rainfall values would not severely affect the subsequent runoff estimation.

Storm No. 126 Storm No. 127 Storm No. 128

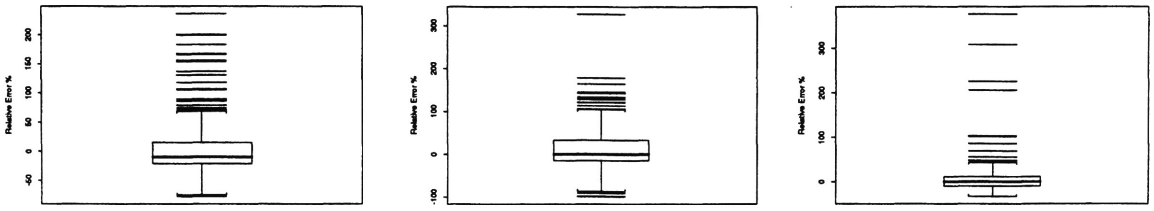

Storm No. 129 Storm No. 130 Storm No. 131

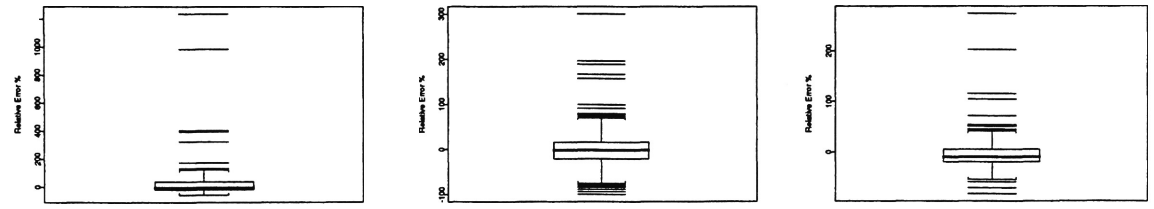

Storm No. 132 Storm No. 133 Storm No. 134

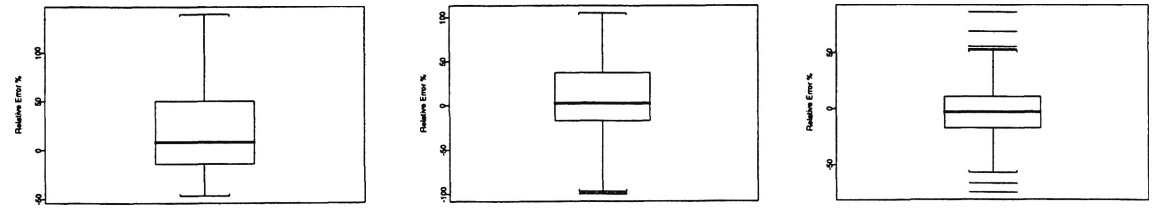

Storm No. 135 Storm No. 136 Storm No. 137

Figure 33 - Boxplots of Relative Error of Subcatchment Rainfall for Validation Event Nos. 126 - 137

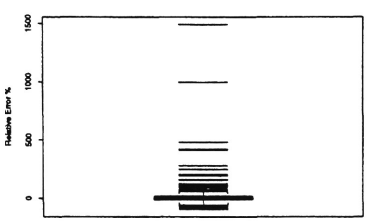

Storm No. 138

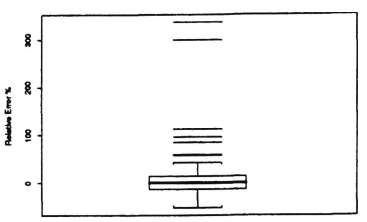

Storm No. 139

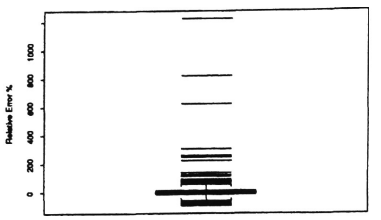

Storm No. 140

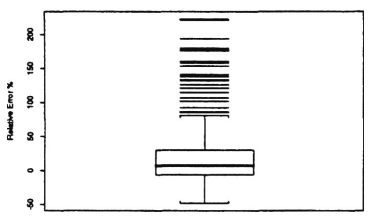

Storm No. 141

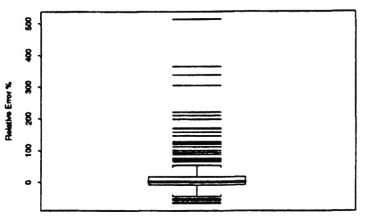

Storm No. 142

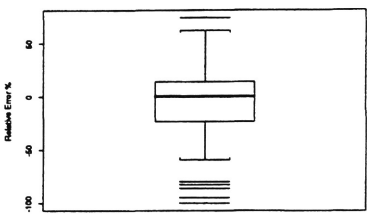

Storm No. 143

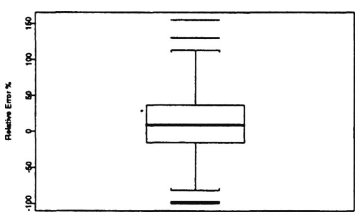

Storm No. 144

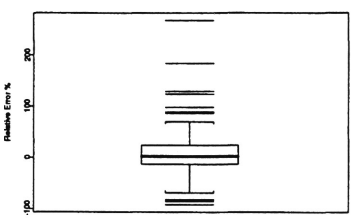

Storm No. 145

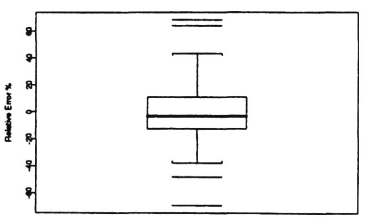

Storm No. 146

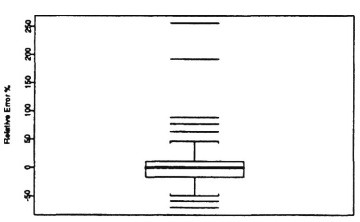

Storm No. 147

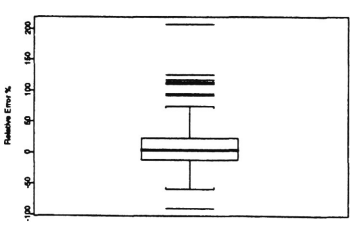

Storm No. 148

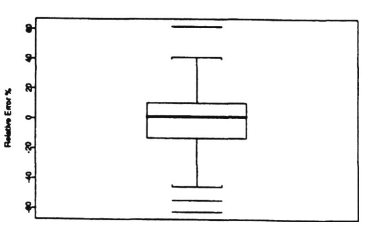

Storm No. 149

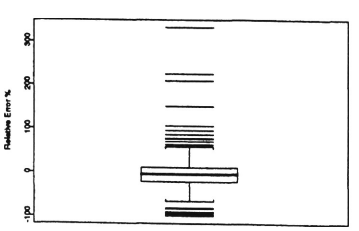

Storm No. 150

Figure 34 - Boxplots of Relative Error for Validation Event Nos. 138 - 150

In addition to subcatchment rainfalls, total volumes of rainfall were determined and are summarised in Table 20 below.

TABLE 20

TOTAL VOLUME OF RAINFALL FOR 25 VALIDATION EVENTS

Storm Event	Total Volume of Rainfall ($mm\text{-}km^2$)		% error
	Actual	Predicted	
126	13589.5	13435.0	-1.14
127	16346.8	15370.2	-5.97
128	17956.0	17647.5	-1.72
129	17496.5	15855.9	-9.38
130	18445.0	18166.7	-1.51
131	16197.8	15996.1	-1.25
132	18514.9	17684.5	-4.48
133	13851.3	13058.7	-5.72
134	16987.5	15804.5	-6.96
135	15142.8	15691.8	3.63
136	19046.4	17646.8	-7.35
137	14781.8	14187.5	-4.02
138	16482.0	16565.5	0.51
139	14990.6	14740.4	-1.67
140	18876.8	17643.8	-6.53
141	16277.2	16949.6	4.13
142	16823.8	17643.5	4.87
143	18962.4	18262.0	-3.69
144	15799.2	15694.5	-0.66
145	18290.4	17132.6	-6.33
146	12324.9	12278.4	-0.38
147	17346.8	16535.3	-4.68
148	14957.3	14837.1	-0.80
149	15992.7	15869.4	-0.77
150	16446.3	15086.7	-8.27

In general the neural network produced excellent forecast of the volume of rainfall for all 25 validation events. The error ranges from –9.38% to +4.87%, with a mean of –2.81%. The closest prediction was –0.38% for storm event no. 146.

5.4 Summary

A spatial rainfall forecasting model was developed. The forecasting model integrated an artificial neural network and a geographic information system, producing forecasts of the rainfall spatial distribution over a catchment one time step or 15 minutes ahead. The accuracy of the spatial rainfall forecasting model was ascertained empirically by testing artificial storm events with random movement and Gaussian spatial patterns.

The forecasting model accurately preserved the spatial rainfall patterns and produced forecasts with good agreement to the actual rainfall values. On forecasting rainfall at each pixel of the study catchment, the overall averaged normalised mean squared errors over 25 validation events was 0.263. This result was considered remarkable.

On forecasting subcatchment rainfalls, the model produced reasonable results. More than 50% of the forecasts were within ± 20% relative errors in percentage. In predicting the volume of rainfall, the range of error was (–9.4%, +4.9%), with a mean of –2.8%. The most accurate forecast for a storm event had a relative error as small as –0.38%.

6. CONCLUSION

Rainfall forecasting using Artificial Neural Networks (ANNs) has been the focus of this report. The ANNs are integrated with the thin plate spline spatial model developed within a Geographic Information System environment (Luk and Ball, 1996). The integrated model has enabled a reasonable forecast of the spatial distribution of rainfall over the study catchment for one time step into the future. The integrated model developed in this study has the following distinctive characteristics.

- The model has a spatially and temporally distributed architecture. It receives present rainfall values at multiple gauge positions and produces rainfall forecasts at every pixel of the study catchment. The accuracy of the model was validated empirically by artificial storm events with a random movement and a Gaussian spatial pattern.
- The model has been developed for real-time operation. The inputs to the model are ASCII rainfall data at multiple gauge positions. The output are ASCII rainfall values for each pixel as well as a plot of colour-coded rainfall pattern on the computer screen.
- With collection of new rainfall data, the model can be re-trained to improve its accuracy.

The accuracy of the model was good. The model accurately preserved the spatial rainfall patterns and produced forecasts with good agreement to the actual rainfall values. On forecasting rainfall at each pixel of the study catchment, the average normalised mean squared error over 25 validation events was 0.263. On forecasting subcatchment rainfalls, the model produced good results. More than 50% of the forecasts were within ±20% relative errors in percentage. In predicting the rainfall volume, the range of error was between –9.4% and 4.9%, with a mean of –2.8%. The most accurate forecast for a storm event had a relative error as small as –0.38%.

Another major aspect of this study is the investigation of the impact of temporal and spatial rainfall inputs on the accuracy of the rainfall model. The investigation was carried out empirically by comparing the results of networks with different numbers of temporal and

spatial inputs. Based on the results of a validation test on 34 real storm events, the following points were observed:

- there existed an optimal limit of spatial information for inclusion into the network. The optimal number of spatial inputs was rainfall values from eight gauges. Either too much or too little spatial information introduced to the network would result in decreased performance; and
- for the temporal domain, a lag-1 network in general showed the best performance.

During the development of the rainfall forecasting model, three alternative types of artificial neural networks were identified, developed and compared. These networks are:

- multilayer feedforward neural network;
- Elman partial recurrent neural network; and
- time delay neural network

It was found that with careful development all the above alternative networks were able to make reasonable forecast of rainfall one time step ahead for multiple locations of the study catchment. The following points were derived from the test results:

- for each type of network, there existed an optimal complexity which was determined by a combined effect of the number of hidden nodes and the lag of the network;
- all three alternative networks had comparable performance when they were developed and trained to reach their optimal complexities; and
- based on analysis of the available data, the 15-min rainfall time series did not seem to posses a long term memory, therefore the networks with lower lag slightly outperformed the ones with higher lag.

A systematic approach to develop the ANNs has been highlighted in the study. Four stages of development were identified:

- selection of appropriate network;
- determination of network complexity;

- estimation of parameters; and
- evaluation of performance.

A comprehensive review of the various alternative options/techniques for these four stages of development was presented in this study. A demonstration of the network development approach was made through a case study of forecasting rainfall for the Upper Parramatta River Catchment.

7. REFERENCES

Bishop, C. M. (1995), *Neural Networks for Pattern Recognition,* Oxford University Press, p. 482.

Box , G. E. P. and Cox. D. R. (1964), "An Analysis of Transformation", *Journal of the Royal Statistical Society,* Series B, 26:211-252.

Box, G. E. P. and Jenkins, G. M. (1976), *Time Series Analysis: Forecasting and Control,* Holden-Day, San Francisco.

Braun, H. and Weisbrod, J. (1993), "Evolving Neural Networks for Application Oriented Problems", *Proc., 2nd Conference in Evolutionary Programming,* San Diego, p. 62-71.

Chauvin, Y. (1990), "Dynamic Behavior of Constrained Back-Propagation Networks", in *Advances in Neural Information Processing Systems,* Volume 2, edited by David S. Touretzky, p. 642-649. San Mateo, California: Morgan Kaufmann Publishers.

Cheu, R. L., Ritchie, S. G., Recker, W. W. and Bavarian, B. (1991), "Investigation of a Neural Network Model for Freeway Incident Detection", *Proc., 2nd Int. Conf. on Applicability of AI to Civ. And Struct. Engrg.,* B. H. V. Topping, ed., Civil-Comp Press, Oxford, England, Vol. 1, 267-274.

Daniell, T. M. (1991), "Neural Networks - Applications in Hydrology and Water Resources Engineering", *International Hydrology and Water Resources Symposium,* p.797-802.

Elman, J. L. (1990), "Finding Structure in Time", *Cognitive Science,* 14, 179-211.

Fahlman, S. E. (1988), "Faster-learning Variations on Back-propagation: An Empirical Study", in T. J. Sejnowski, G. E. Hinton and D. S. Touretzky, editors, *1988 Connectionist Models Summer School,* San Mateo, CA, 1988. Morgan Kaufmann Publishers.

Fahlman, S. E. and Lebiere, C. (1991), "The Cascade-Correlation Learning Architecture", *Technical Report* CMU-CS-91-100, School of Computer Science, Carnegie Mellon University.

Flood, I. and Kartam, N. (1994a), "Neural Networks in Civil Engineering I: Principles and Understanding", *Journal of Computing in Civil Engineering*, 8(2), 131-148.

Flood, I. and Kartam, N. (1994b), "Neural Networks in Civil Engineering II: Systems and Application", *Journal of Computing in Civil Engineering*, 8(2), 149-162.

Fontaine, T. A. (1991), "Predicting Measurement Error of Areal Mean Precipitation During Extreme Events", *Water Resources Bulletin,* 27(3), 509-520.

French, M., Krajewski, W. and Cuykendall, R. R. (1992) "Rainfall Forecasting in Space and Time Using a Neural Network", *Journal of Hydrology,* 137, p. 1-31.

Furuta, H., Sugiura, K., Tonegawa, T. and Wanatabe, E. (1991), "A Neural Network System for Aesthetic Design of Dam Structures", *Proc., 2 nd Int. Conf. on Applicability of AI to Civ. And Struct. Engrg.,* B. H. V. Topping, ed., Civil-Comp Press, Oxford, England, Vol. 1, p. 273-278.

Handmer, J. W., Smith, D. I. and Lusting, T. (1988), "The Sydney Floods of 1986: Warnings, Damages, Policy and the Future", *Proc. Hydrology and Water Resources Symposium 1988,* Aust. Nat. Uni., Canberra, IEAust. Nat. Conf. Pub. 88/1, p. 206-210.

Happel, B. and Murre, J. M. J. (1994), "Design and Evolution of Modular Neural Network Architectures", *Neural Networks,* 7, p. 985-1004.

Hornik K., Stinchcombe M. and White, H. (1989), "Multilayer Feedforward Networks are Universal Approximators", *Neural Networks,* 2:359-366.

Hsu, K. L., Gupta, V. and Sorooshian, S. (1995), "Artificial neural network modeling of the rainfall-runoff process", *Water Resources Research,* 31(10), 2517-2530.

Hwang, J., Yau, S. and Jou, I. (1996), "The Cascade Correlation Learning: A Projection Pursuit Learning Perspective", *IEEE Trans. Neural Network,* 7(2), 278-289.

Jacobs, R., Jordan, M. I. and Barto, A. G. (1991a), "Task Decomposition Competition in a Modular Connectionist Architecture: The What and Where Vision Tasks", *Cognitive Science,* 15, 219-250.

Jacobs, R., Jordan, M. I., Nowlan, S. J. and Hinton, G. E. (1991b), "Adaptive Mixture of Local Experts", *Neural Computation,* p. 79-87.

Jordan M. (1986), "Attractor Dynamics and Parallelism in a Connectionist Sequential Machine", In *Proceedings of the Eighth Annual Conference of the Cognitive Science Society.* Hillsdale, NJ: Erlbaum, p. 531-546, IEEE, New York.

Kamarthi, S. V., Sanvido, V. E. and Kumara, S. R. T. (1992), "Neuroform - Neural Network System for Vertical Formwork Selection", *Journal of Computing in Civil Engineering,* Vol. 6, No. 2, p. 178-199.

Karunanithi, N., Grenney, W. J., Whitley D. and Bovee, K. (1994), "Neural Networks for River Flow Prediction", *Journal of Computing in Civil Engineering,* 8(2), 201-220.

Kohonen T. (1990), "The Self-Organisation Map", *Proceedings of the IEEE,* 78:1464-1497.

Kosko, B. (1990), "Unsupervised Learning in Noise", *IEEE Transactions on Neural Networks,* 1:44-57.

Lang, K. J., Waibel, A. H. and Hinton, G. E. (1990), "A Time-delay Neural Network Architecture for Isolated Word Recognition", *Neural Networks,* 3(1), 23-43.

Laurenson, E. M. (1964), "A Catchment Storage Model for Runoff Routing", *Journal of Hydrology,* 2:141-163.

LeCun, Y., Denker, J. S. and Solla S. A. (1990), "Optimal Brain Damage" in *Advances in Neural Information Processing Systems II,* D. S. Touretzky, Ed. San Mateo, CA: Morgan Kaufmann, p. 598-605.

Lettenmaier, D. L. and Wood, E. F. (1993), "Hydrologic Forecasting", Chapter 26 in *Handbook of Hydrology*, D. R. Maidment, Ed. McGraw-Hill, Inc. p. 26.1-26.30.

Luk, K. C. and Ball, J. E. (1996), "Application of GIS for Modelling of the Spatial Distribution of Rainfall", *Water Research Laboratory, Research Report,* No. 191.

Masters, T. (1993), *Practical Neural Network Recipes in C++,* Academic Press, New York.

Masters, T. (1995), *Advanced Algorithms for Neural Networks,* John Wiley & Sons, New York.

McCelland, J. E., Rumelhart, D. E. and Hinton, G. E. (eds.) (1986), *Parallel Distributed Processing: Explorations in the Microstructure of Cognition, Vol. 1: Foundations,* Cambridge, Mass, MIT Press.

Minns, A. W. and Hall M. A. (1996), "Artificial Neural Networks as Rainfall Runoff Models", *Hydrological Sciences,* 41(3), p. 399-417.

Moody, T. and Darken, C. (1989), "Fast Learning in Networks of Locally Tuned Processing Units", *Neural Computation,* 1:281-294.

Moselhi, O., Hagazy, T. and Fazio, P. (1991), "Markup Estimation using AI Methodology", *Proc., 2 nd Int. Conf. on Applicability of AI to Civ. and Struct. Engrg.,* B. H. V. Topping, ed., Civil-Comp Press, Oxford, England, Vol. 1, 257-266.

Pezeshk, S., Camp, C. V. and Karprapu, S. (1996), "Geophysical Log Interpretation Using Neural Network", *ASCE Journal of Computing in Civil Engineering,* Vol. 10, No. 2, p. 136-142.

Pomerleau, D. A. (1989), "ALVINN: An Autonomous Land Vehicle in a Neural Network", in *Advances in Neural Information Processing Systems I,* ed. D. S. Touretzky, 305-313. San Mateo: Morgan Kaufmann.

Rasul, A. Z. and Paudyal, G. N. (1994), "Neural Network Application in Hydraulic Structure Operation", *Hydroinformatics '94.* Verwey, Minns, Babovic & Maksimovic (eds).

Renals, S and Rohwer R. (1989), "Phoneme Classification Experiments using Radial Basis Functions", In *Proceedings of International Joint Conference on Neural Networks,* Washington, DC, June 1989, p. 461-467.

Riedmiller, M. and Braun, H. (1993), "A Direct Adaptive Method for Faster Backpropagation Learning: The Rprop Algorithm", *Proceedings of the IEEE International Conference on Neural Networks.*

Riedmiller, M. (1994), "Advanced Supervised Learning in Multi-layer Perceptrons - From Backpropagation to Adaptive Learning Algorithms", *International Journal of Computer Standards and Interfaces,* Special Issue on Neural Networks (5).

Rodriguez-Iturbe, I. and Eagleson, P. S. (1987), "Mathematical Models of Rain Storm Events in Space and Time", *Water Resources Research,* 23(1): 181-190.

Saad, M. and Bigras, P. (1996), "Fuzzy Learning Decomposition for the Scheduling of Hydroelectric Power Systems", *Water Resources Research,* Vol. 32, No. 1, p179-186.

Sarle, W. S. (1995), "Stopped Training and Other Remedies for Overfitting", *Proceedings of the 27th Symposium on the Interface of Computing Science and Statistics,* p. 352-360,

Schalkoff, R. (1992), *Pattern Recognition - Statistical, Structural and Neural Approaches,* John Wiley & Sons, Inc.

Sejnowski, T. J. and Rosenberg, C. R. (1987), "Parallel Networks that Learn to Pronounce English Text", *Complex Systems,* 1, 145-168.

Smith J. and Eli, R. N. (1995), "Neural-Network Models of Rainfall-Runoff Process", *Journal of Water Resources Planning and Management,* 121(6), 499-508.

Tohma, S. and Ando, Y. (1995) " Stochastic Modeling of Rainfall at the Meso-β Scale and Rainfall Forecasting in Space-Time Using a Neural Network", *International Congress on Modelling and Simulation Proceedings,* Vol. 3: Water Resources and Ecology, Editors P. Binning, et al.

Urbonas, B. R., Guo, J. C. Y. and Janesekok, M. P. (1992), "Hyetograph Density Effects on Urban Runoff Modelling", *Proc. International Conf. On Computer Applications in Water Resources,* Tamkang University, Tamsui, Taiwan, 32-37.

Waibel, A. (1989), "Modular Construction of Time-Delay Neural Networks for Speech Recognition", *Neural Computation,* 1, 39-46.

Wan, E. A. (1993), "Time Series Prediction Using a Connectionist Network with Internal Delay Lines", In *Time Series Prediction: Forecasting the Future and Understanding the Past,* edited by A. S. Weigend and N. A. Gershenfeld, p. 195-217. Reading, MA: Addison-Wesley.

Weigend, A. S., Huberman, B. A. and Rumelhart, D. E. (1992), "Predicting Sunspots and Exchange Rates with Connectionist Neworks", In Casdagli, M. and S. Eubank, editors, *Nonlinear Modeling and Forecasting,* p. 395-431. Addison Wesley.

Weigend, A. S. and Gershenfeld, N. A. (eds.) (1993), *Time Series Prediction: Forecasting the Future and Understanding the Past,* Santa Fe Institute Studies in the Sciences of Complexity, Proc. Vol. XV. Reading, MA: Addison-Wesley.

WP Software (1995), "RAFTS-XP: Runoff Analysis and Flow Training Simulation incorporating the Expert User Environment - Version 5", *Unpublished Report, WP Software,* Belconnen, ACT, Australia.

Xihui, L., Baocheng, S. and Wenyuan, F. (1991), "Fuzzy Reasoning with Engineering Applications using Neural Networks", *Proc., 2nd Int. Conf. on Applicability of AI to Civ. and Struct. Engrg.,* B. H. V. Topping, ed., Civil-Comp Press, Oxford, England, Vol. 1, p. 279-285.

Zhu, M. L. and Fujita, M. (1994), "Comparisons Between Fuzzy Reasoning and Neural Network Methods to Forecast Runoff Discharge", *Journal of Hydroscience and Hydraulic Engineering,* Vol. 12, No. 2, p. 131-141.

APPENDIX A

REAL STORM EVENTS

Table A.1 - Storm Type

No.	Date	Storm Type	Remark
1	5.11.92	Frontal	—
2	6.12.92	Frontal	—
3	17.2.93	Convective	—
4	7.3.93	Frontal	With convective cells
5	15.4.93	Convective	—
6	8.7.93	Convective	—
7	20.11.93	Frontal	With convective cells
8	12.2.94	Convective	—
9	15.2.94	Convective	—
10	7.3.94	Convective	—
11	13.4.94	Convective	—
12	27.6.94	Frontal	—
13	9.9.94	Convective	—
14	2.3.95	Convective	—
15	4.3.95	Convective	—
16	5.3.95	Convective	—
17	15.3.95	Frontal	—
18	13.5.95	Frontal	With convective cells
19	17.5.95	Frontal	—
20	16.6.95	Convective	—
21	24.9.95	Convective	—
22	25.9.95	Convective	—
23	5.12.95	Frontal	With convective cells
24	10.12.95	Frontal	With convective cells
25	2.1.96	Convective	—
26	6.1.96	Convective	—
27	24.1.96	Convective	—
28	11.4.96	Convective	—
29	12.4.96	Convective	—
30	2.5.96	Convective	—
31	3.5.96	Convective	—
32	4.5.96	Convective	—
33	27.7.96	Frontal	With convective cells
34	31.8.96	Frontal	—

Table A.2 Storm Type Statistics

Season	Frontal Storm	Convective Storm
Spring	3	3
Summer	2	6
Autumn	4	11
Winter	3	2
Total	12	22

APPENDIX A

REAL STORM EVENTS

Table A.3 - Detail of the Storm Events

No.	Date	File name	No. of 15-min rainfall values	Remark
1	5.11.92	2k05.16g	96	All gauges working.
2	6.12.92	2l06.16g	9	Gauge no. 7255 and 7285 not working. Use Spline to estimate the missing data.
3	17.2.93	3b17.16g	23	7209 not working. Use Spline to estimate missing data.
4	7.3.93	3c07.16g	16	7209 not working. Use Spline to estimate missing data.
5	15.4.93	3d15.16g	76	7209 not working. Use Spline to estimate missing data.
6	8.7.93	3g08.16g	53	7209 not working. Use Spline to estimate missing data.
7	20.11.93	3k20.16g	37	All gauges working.
8	12.2.94	4b12.16g	72	All gauges working.
9	15.2.94	4b15.16g	24	All gauges working.
10	7.3.94	4c07.16g	34	All gauges working.
11	13.4.94	4d13.16g	33	7209 not working. Use Spline to estimate missing data.
12	27.6.94	4f27.16g	86	All gauges working.
13	9.9.94	4i09.16g	53	All gauges working.
14	2.3.95	5c02.16g	22	All gauges working.
15	4.3.95	5c04.16g	70	All gauges working.
16	5.3.95	5c05.16g	96	All gauges working.
17	15.3.95	5c15.16g	20	7287 not working. Use spline to estimate missing data.
18	13.5.95	5e13.16g	33	7263 not working. Use spline to estimate missing data.
19	17.5.95	5e17.16g	85	All gauges working.
20	16.6.95	5f16.16g	51	All gauges working
21	24.9.95	5i24.16g	28	Gauges 7209, 7255, 7259 and 7299 not working. Use spline to estimate missing data.
22	25.9.95	5i25.16g	83	Gauges 7209, 7255, 7259 and 7299 not working. Use spline to estimate missing data.
23	5.12.95	5l05.16g	31	Gauges 7209 and 7299 not working. Use spline to estimate missing data.
24	10.12.95	5l10.16g	14	Gauges 7209 and 7299 not working. Use spline to estimate missing data.
25	2.1.96	6a02.16g	27	Gauge 7209 not working. Use Spline to estimate missing data.
26	6.1.96	6a06.16g	87	Gauge 7299 not working. Use spline to estimate missing data.
27	24.1.96	6a24.16g	44	All gauges working.
28	11.4.96	6d11.16g	26	All gauges working.
29	12.4.96	6d12.16g	36	All gauges working.
30	2.5.96	6e02.16g	89	All gauges working.
31	3.5.96	6e03.16g	79	All gauges working.
32	4.5.96	6e04.16g	96	All gauges working.
33	27.7.96	6g27.16g	68	7253 not working. Use spline to estimate missing data.
34	31.8.96	6h31.16g	52	All gauges working.

APPENDIX B
SUBDIVISON OF DATA FOR ARTIFICIAL NEURAL NETWORKS

Table B.1 - Training and Monitoring

No.	Ref. No.	Date	Duration	Max. Rainfall (mm/15min)	Time to Max. Rainfall[1]	No. of 15-min Rainfall Values (purpose)
1	6a24	24 Jan 96	11 hr	6	4 hr 30 min	44 (training)
2	5i24	24 Sep 95	7 hr	25	4 hr	28 (training)
3	3k20	20 Nov 93	9 hr 15 min	8	1 hr 15 min	37 (training)
4	3c07	7 Mar 93	4 hr	16	45 min	16 (training)
5	4f27	27 Jun 94	8 hr	3	1 hr 30 min	86 (training)
6	3g08	8 Jul 93	13 hr 15 min	5	1 hr 45 min	53 (training)
7	6h31	31 Aug 96	13 hr	18	5 hr 30 min	52 (training)
8	4b12	12 Feb 94	18 hr	20	10 hr	72 (training)
9	5c02	2 Mar 95	5 hr 30 min	25	3 hr 30 min	22 (training)
10	5f16	16 Jun 95	12 hr 45 min	9	1 hr 30 min	51 (training)
11	6d12	12 Apr 96	6 hr 30 min	10	1 hr 30 min	36 (training)
12	6e02	2 May 96	22 hr 15 min	10	2 hr 45 min	89 (training)
13	5c15	15 Mar 95	5 hr	8	30 min	20 (training)
14	4d13	13 Apr 94	16 hr 30 min	10	3 hr 30 min	33 (training)
15	3d15	15 Apr 93	3 hr 45 min	2	2 hr 45 min	76 (training)
16	5e13	13 May 95	3 hr	15	30 min	33 (training)
17	4c07	7 Mar 94	8 hr 30 min	18	2 hr 15 min	34 (monitoring)
18	5e17	17 May 95	21 hr 15 min	5	18 hr 30 min	85 (monitoring)
19	4b15	15 Feb 94	6 hr	25	2 hr 30 min	24 (monitoring)
20	5l10	10 Dec 95	7 hr 45 min	6	30 min	14 (monitoring)
21	2l06	6 Dec 92	2 hr 15 min	20	1 hr	9 (monitoring)
22	5c05	5 Mar 95	24 hr	6	6 hr 15 min	96 (monitoring)
23	5i25	25 Sep 95	20 hr 45 min	12	7 hr 30 min	83 (monitoring)
24	5l05	5 Dec 95	7 hr 45 min	6	1 hr 15 min	31 (monitoring)

APPENDIX B
SUBDIVISON OF DATA FOR ARTIFICIAL NEURAL NETWORKS

Table B.2 - Validation

No.	Ref. No.	Date	Duration	Max. Rainfall (mm/15min)	Time to Max. Rainfall[1]	No. of 15-min Rainfall Values (purpose)
25	6a02	2 Jan 96	6 hr 45 min	20	1 hr 30 min	27 (validation)
26	6e04	4 May 96	24 hr	14	20 hr 45 min	96 (validation)
27	4i09	9 Sep 94	11 hr 30 min	14	45 min	53 (validation)
28	3b17	17 Feb 93	5 hr 45 min	25	1 hr	23 (validation)
29	6e03	3 May 96	19 hr 45 min	9	5 hr	79 (validation)
30	5c04	4 Mar 95	17 hr 30 min	5	6 hr 30 min	70 (validation)
31	6d11	11 Apr 96	6 hr 30 min	14	1 hr 15 min	26 (validation)
32	6a06	6 Jan 96	21 hr 45 min	8	8 hr 45 min	87 (validation)
33	2k05	5 Nov 92	6 hr	9	4 hr 30 min	96 (validation)
34	6g27	27 Jul 96	12 hr 30 min	14	2 hr 15 min	68 (validation)

Remark [1] - the time to maximum rainfall is measured from the time that a gauge within the catchment started to receive rainfall to the time that maximum rainfall occurred at any rain gauge within the catchment.

There are totally 748 values of 15-min rainfall for training, 376 for monitoring and 625 for validation.

APPENDIX B
SUBDIVISON OF DATA FOR ARTIFICIAL NEURAL NETWORKS

Table B.3 – Properties of the Data Sets

	Training data set	Monitoring data set	Validation data set
Year			
92	0	1	1
93	4	0	1
94	3	2	1
95	5	5	1
96	4	0	6
Total	16	8	10
Month			
Jan	1	0	2
Feb	1	1	1
Mar	3	2	1
Apr	3	0	0
May	2	1	2
Jun	2	0	0
Jul	1	0	1
Aug	1	0	0
Sep	1	1	1
Oct	0	0	0
Nov	1	0	2
Dec	0	3	0
Total	16	8	10
Duration	From 3hr to 22hr 15min	From 2hr 15min to 21 hr 15 min	From 6hr to 24 hr
Max. Rainfall	From 2mm/15min to 25mm/15min	From 2.5mm/15min to 25mm/15min	From 5mm/15min to 25mm/15min
Time to Max. Rainfall	From 30min to 10hr	From 1hr to 18hr 30min	From 45min to 20hr 45min

Table B.3 provides some further information about the 3 data sets. First, the number of storm events selected on a particular year and month are compared. Next, the duration of storm, maximum rainfall and the time to maximum are compared. Because the data sets were selected randomly, so these properties are very similar.

APPENDIX B
SUBDIVISON OF DATA FOR ARTIFICIAL NEURAL NETWORKS

Table B.4 – Storm Type of the Data Sets

Data Set	Date	Storm Type	Remark
training	24.1.96	Convective	—
training	24.9.95	Convective	—
training	20.11.93	Frontal	With convective cells
training	7.3.93	Frontal	With convective cells
training	27.6.94	Frontal	—
training	8.7.93	Convective	—
training	31.8.96	Frontal	—
training	12.2.94	Convective	—
training	2.3.95	Convective	—
training	16.6.95	Convective	—
training	12.4.96	Convective	—
training	2.5.96	Convective	—
training	15.3.95	Frontal	—
training	13.4.94	Convective	—
training	15.4.93	Convective	—
training	13.5.95	Frontal	With convective cells
monitoring	7.3.94	Convective	—
monitoring	17.5.95	Frontal	—
monitoring	15.2.94	Convective	—
monitoring	10.12.95	Frontal	With convective cells
monitoring	6.12.92	Frontal	—
monitoring	5.3.95	Convective	—
monitoring	25.9.95	Convective	—
monitoring	5.12.95	Frontal	With convective cells
validation	2.1.96	Convective	—
validation	4.5.96	Convective	—
validation	9.9.94	Convective	—
validation	17.2.93	Convective	—
validation	3.5.96	Convective	—
validation	4.3.95	Convective	—
validation	11.4.96	Convective	—
validation	6.1.96	Convective	—
validation	5.11.92	Frontal	—
validation	27.7.96	Frontal	With convective cells

APPENDIX C

COMPARISON OF ALTERNATIVE TYPE OF ARTIFICIAL NEURAL NETWORKS

Table C.1 - Variance of the Data Sets

Lag	Training		Monitoring		Validation	
	No. of values	Variance	No. of values	Variance	No. of values	Variance
1	732	0.01011933	368	0.01189492	615	0.01071373
2	716	0.01021899	360	0.01201465	605	0.01081855
3	700	0.01026982	352	0.01192159	595	0.01092872
4	684	0.01036357	344	0.01130262	585	0.01102358

APPENDIX C

COMPARISON OF ALTERNATIVE TYPE OF ARTIFICIAL NEURAL NETWORKS

Note: (1) Training errors were recorded at every 20 epochs; Monitoring errors were recorded at every 100 epochs. The values shown in the bracket () under the training and Monitoring columns indicates the range of errors.

(2) The data are transformed with the log function so that results are also in the log domain.

Table C.2 - Results of the Lag-1 MLFN

Lag-1 MLFN	Sum of Squared Error			NMSE	Stopping epoch
	Training	Monitoring	Validation	Validation	
16-2-16	62.6 (77.3 at 20 epoch 62.8 at 1000 epoch)	48.5 (48.7 at 100 epoch 49.6 at 1000 epoch)	67.7	0.642	300
16-4-16	59.1 (65.6 at 20 epoch 55.6 at 1000 epoch)	49.8 (49.8 at 100 epoch 55.3 at 1000 epoch)	70.0	0.664	100
16-8-16	61.7 (119.6 at 20 epoch 57.7 at 1000 epoch)	49.5 (49.5 at 100 epoch 52.6 at 1000 epoch)	67.9	0.644	100
16-16-16	58.9 (104.2 at 20 epoch 58.9 at 1000 epoch)	48.7 (49.9 at 100 epoch 48.7 at 1000 epoch)	67.9	0.644	1000
16-24-16	59.3 (122.5 at 20 epoch 57.7 at 1000 epoch)	47.9 (48.5 at 100 epoch 49.3 at 1000 epoch)	66.9	0.635	200
16-32-16	58.2 (154.7 at 20 epoch 56.3 at 1000 epoch)	48.9 (50.1 at 100 epoch 49.8 at 1000 epoch)	68.4	0.649	300
16-64-16	57.1 (272.4 at 20 epoch 52.8 at 1000 epoch)	49.3 (49.9 at 100 epoch 52.7 at 1000 epoch)	68.3	0.648	300
16-128-16	60.4 (717.0 at 20 epoch 47.6 at 1000 epoch)	53.7 (53.7 at 100 epoch 83.8 at 1000 epoch)	74.4	0.706	100
16-12-12-16	58.0 (82.9 at 20 epoch 52.5 at 1000 epoch)	48.9 (48.9 at 100 epoch 54.4 at 1000 epoch)	68.5	0.650	200

APPENDIX C

COMPARISON OF ALTERNATIVE TYPE OF ARTIFICIAL NEURAL NETWORKS

Table C.3 - Results of the Lag-2 MLFN

Lag-2 MLFN	Sum of Squared Error			NMSE	Stopping epoch
	Training	Monitoring	Validation	Validation	
32-2-16	59.9 (81.7 at 20 epoch 59.4 at 1000 epoch)	48.6 (50.2 at 100 epoch 50.2 at 1000 epoch)	69.1	0.660	300
32-4-16	56.8 (92.9 at 20 epoch 55.4 at 1000 epoch)	48.7 (50.0 at 100 epoch 49.3 at 1000 epoch)	69.3	0.662	500
32-8-16	59.5 (127.3 at 20 epoch 54.9 at 1000 epoch)	48.0 (48.0 at 100 epoch 48.5 at 1000 epoch)	69.0	0.659	100
32-16-16	57.0 (136.2 at 20 epoch 52.1 at 1000 epoch)	50.4 (52.0 at 100 epoch 57.3 at 1000 epoch)	70.0	0.668	200
32-24-16	54.0 (164.4 at 20 epoch 52.3 at 1000 epoch)	49.1 (51.3 at 100 epoch 49.3 at 1000 epoch)	70.9	0.677	500
32-32-16	54.8 (127.1 at 20 epoch 49.6 at 1000 epoch)	51.3 (53.4 at 100 epoch 57.1 at 1000 epoch)	69.1	0.660	200
32-64-16	53.6 (350.0 at 20 epoch 40.0 at 1000 epoch)	54.9 (55.6 at 100 epoch 243.0 at 1000 epoch)	78.0	0.745	200
16-128-16	60.4 (717.0 at 20 epoch 47.6 at 1000 epoch)	53.7 (53.7 at 100 epoch 83.8 at 1000 epoch)	74.4	0.802	100
16-12-12-16	58.0 (82.9 at 20 epoch 52.5 at 1000 epoch)	48.9 (48.9 at 100 epoch 54.4 at 1000 epoch)	68.5	0.696	200

APPENDIX C

COMPARISON OF ALTERNATIVE TYPE OF ARTIFICIAL NEURAL NETWORKS

Table C.4 - Results of the Lag-3 MLFN

Lag-3 MLFN	Sum of Squared Error			NMSE	Stopping epoch
	Training	Monitoring	Validation	Validation	
48-2-16	57.9 (99.6 at 20 epoch 56.9 at 1000 epoch)	47.8 (47.9 at 100 epoch 48.6 at 1000 epoch)	70.6	0.679	600
48-4-16	54.8 (138.0 at 20 epoch 54.2 at 1000 epoch)	46.0 (47.5 at 100 epoch 46.3 at 1000 epoch)	69.9	0.672	700
48-8-16	55.9 (134.4 at 20 epoch 53.3 at 1000 epoch)	46.7 (48.0 at 100 epoch 47.2 at 1000 epoch)	70.8	0.680	300
48-16-16	53.1 (138.8 at 20 epoch 48.1 at 1000 epoch)	49.5 (50.8 at 100 epoch 56.6 at 1000 epoch)	75.3	0.724	200
48-24-16	53.4 (217.7 at 20 epoch 51.1 at 1000 epoch)	48.3 (54.0 at 100 epoch 48.3 at 1000 epoch)	72.9	0.701	400
48-32-16	51.5 (257.3 at 20 epoch 48.9 at 1000 epoch)	49.1 (57.0 at 100 epoch 49.7 at 1000 epoch)	71.1	0.683	500
48-64-16	42.3 (496.6 at 20 epoch 40.1 at 1000 epoch)	71.0 (74.7 at 100 epoch 75.3 at 1000 epoch)	90.4	0.869	700
48-128-16	44.2 (1111.0 at 20 epoch 37.0 at 1000 epoch)	79.4 (85.6 at 100 epoch 84.9 at 1000 epoch)	108.4	1.042	400
48-2-2-16	58.2 (69.6 at 20 epoch 55.8 at 1000 epoch)	48.3 (48.3 at 100 epoch 56.8 at 1000 epoch)	70.6	0.679	100

APPENDIX C

COMPARISON OF ALTERNATIVE TYPE OF ARTIFICIAL NEURAL NETWORKS

Table C.5 - Results of the Lag-4 MLFN

Lag-4 MLFN	Sum of Squared Error			NMSE	Stopping epoch
	Training	Monitoring	Validation	Validation	
64-2-16	58.9 (73.9 at 20 epoch 55.1 at 1000 epoch)	44.1 (44.8 at 100 epoch 48.4 at 1000 epoch)	67.4	0.653	200
64-4-16	54.6 (66.8 at 20 epoch 47.0 at 1000 epoch)	51.5 (51.5 at 100 epoch 60.5 at 1000 epoch)	75.1	0.728	100
64-8-16	54.2 (138.5 at 20 epoch 48.9 at 1000 epoch)	45.3 (47.5 at 100 epoch 48.6 at 1000 epoch)	70.9	0.687	200
64-16-16	51.0 (at 20 epoch at 1000 epoch)	48.5 (52.8 at 100 epoch 54.5 at 1000 epoch)	75.7	0.733	300
64-24-16	50.2 (229.1 at 20 epoch 46.0 at 1000 epoch)	48.6 (56.8 at 100 epoch 53.1 at 1000 epoch)	76.4	0.740	400
64-32-16	46.5 (253.7 at 20 epoch 43.3 at 1000 epoch)	54.2 (63.3 at 100 epoch 55.3 at 1000 epoch)	74.0	0.717	600
64-64-16	44.6 (420.9 at 20 epoch 37.7 at 1000 epoch)	59.5 (71.4 at 100 epoch 67.3 at 1000 epoch)	90.0	0.872	400
64-128-16	44.2 (1020.2 at 20 epoch 30.4 at 1000 epoch)	104.0 (117.2 at 100 epoch 138.6 at 1000 epoch)	133.2	1.291	300
64-1-1-16	60.0 (68.7 at 20 epoch 58.6 at 1000 epoch)	47.2 (47.2 at 100 epoch 49.5 at 1000 epoch)	70.7	0.685	100

APPENDIX C

COMPARISON OF ALTERNATIVE TYPE OF ARTIFICIAL NEURAL NETWORKS

Table C.6 - Results of the Lag-1 Elman Network

Lag-1 Elman	Sum of Squared Error			NMSE	Stopping epoch
	Training	Monitoring	Validation	Validation	
16-2-16	61.4 (79.9 at 20 epoch 61.3 at 1000 epoch)	47.8 (48.4 at 100 epoch 48.2 at 1000 epoch)	67.7	0.642	500
16-4-16	58.5 (78.1 at 20 epoch 57.3 at 1000 epoch)	46.8 (46.9 at 100 epoch 47.4 at 1000 epoch)	67.1	0.636	300
16-8-16	59.5 (110.3 at 20 epoch 54.6 at 1000 epoch)	48.3 (49.6 at 100 epoch 49.3 at 1000 epoch)	69.6	0.660	200
16-16-16	61.1 (115.4 at 20 epoch 51.9 at 1000 epoch)	63.0 (63.0 at 100 epoch 24601.3 at 1000 epoch)	71.5	0.678	100
16-24-16	50.9 (157.6 at 20 epoch 48.9 at 1000 epoch)	62.1 (5412.3 at 100 epoch 101.6 at 1000 epoch)	85.7	0.813	300
16-32-16	57.6 (180.3 at 20 epoch 42.3 at 1000 epoch)	89.5 (89.5 at 100 epoch 1574.2 at 1000 epoch)	82.6	0.784	100
16-64-16	77.3 (683.3 at 20 epoch 123.6 at 1000 epoch)	73.5 (73.5 at 100 epoch 1605.4 at 1000 epoch)	153.0	1.451	100
16-2-2-16	61.7 (101.6 at 20 epoch 59.3 at 1000 epoch)	50.6 (50.6 at 100 epoch 51.8 at 1000 epoch)	68.7	0.652	100

APPENDIX C

COMPARISON OF ALTERNATIVE TYPE OF ARTIFICIAL NEURAL NETWORKS

Table C.7 - Results of the TDNN with Linear Output Nodes

	Sum of Squared Error			NMSE	Stopping epoch
	Training	Monitoring	Validation	Validation	
TDNN with 2-input windows (32-16-16)	112.5 (119.4 at 20 epoch 109.6 at 1000 epoch)	78.3 (78.3 at 100 epoch 80.9 at 1000 epoch)	99.1	0.946	100
TDNN with 3-input windows (48-32-16)	98.0 (103.0 at 20 epoch 97.2 at 1000 epoch)	71.8 (72.3 at 100 epoch 72.1 at 1000 epoch)	99.7	0.958	300
TDNN with 4-input windows (64-32-16)	94.6 (98.4 at 20 epoch 91.9 at 1000 epoch)	68.2 (68.2 at 100 epoch 73.6 at 1000 epoch)	94.9	0.920	100

Table C.8 - Results of the TDNN with Sigmoid Output Nodes

	Sum of Squared Error			NMSE	Stopping epoch
	Training	Monitoring	Validation	Validation	
TDNN with 2-input windows (32-16-16)	58.6 (65.9 at 20 epoch 48.2 at 1000 epoch)	46.1 (46.1 at 100 epoch 52.0 at 1000 epoch)	66.3	0.633	100
TDNN with 3-input windows (48-32-16)	57.9 (70.1 at 20 epoch 47.8 at 1000 epoch)	46.2 (46.2 at 100 epoch 51.7 at 1000 epoch)	66.9	0.643	100
TDNN with 4-input windows (64-32-16)	57.9 (73.1 at 20 epoch 45.8 at 1000 epoch)	42.9 (42.9 at 100 epoch 49.7 at 1000 epoch)	66.5	0.645	100

APPENDIX D
FORECAST ERROR VS. RATE OF CHANGE OF RAINFALL INTENSITY FOR TEN REAL STORM EVENTS

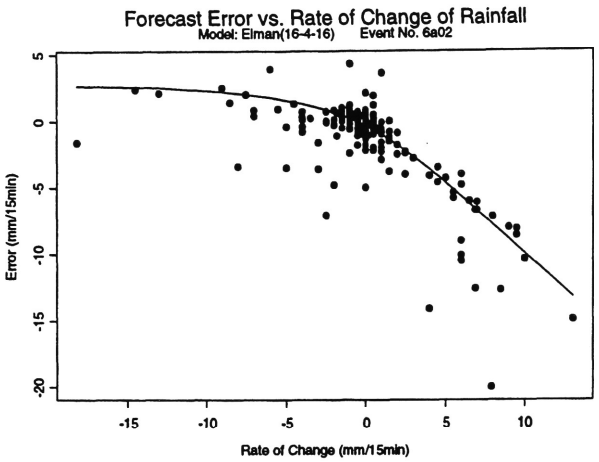

(a) Elman Network

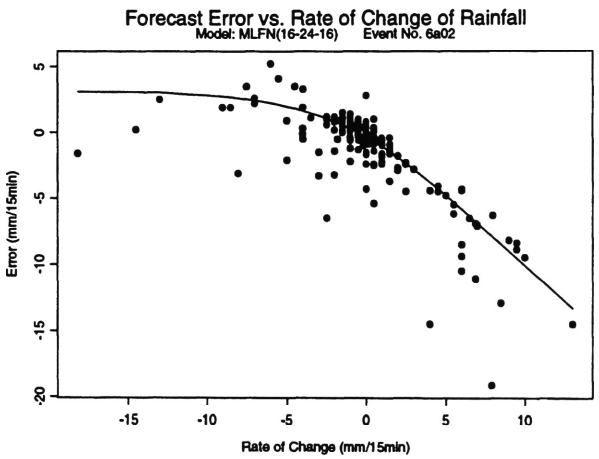

(b) MLFN

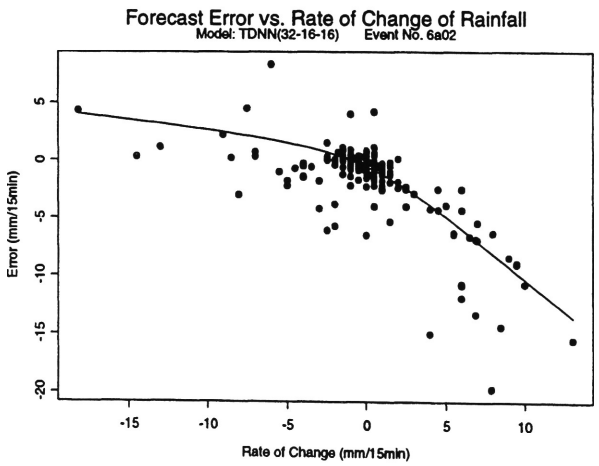

(c) TDNN

Figure D.1 - Event No. 1 : 2 Jan 1996

APPENDIX D
FORECAST ERROR VS. RATE OF CHANGE OF RAINFALL INTENSITY FOR TEN REAL STORM EVENTS

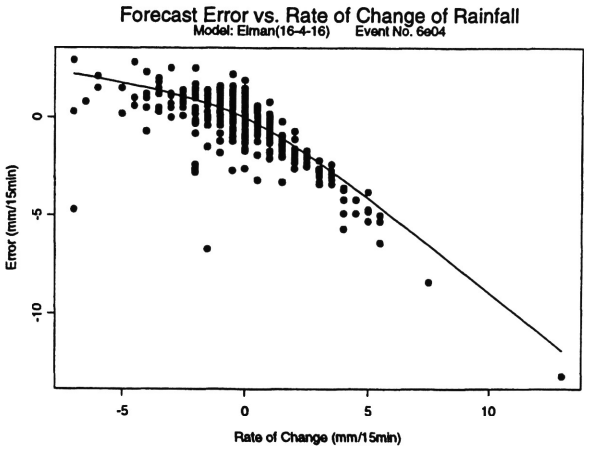

(a) Elman Network

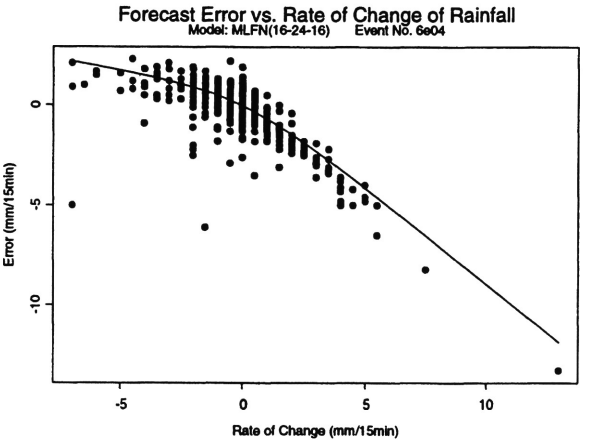

(b) MLFN

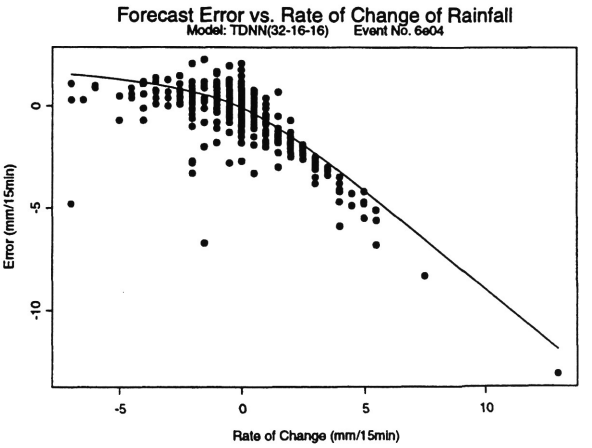

(c) TDNN

Figure D.2 - Event No. 2 : 4 May 1996

APPENDIX D
FORECAST ERROR VS. RATE OF CHANGE OF RAINFALL INTENSITY FOR TEN REAL STORM EVENTS

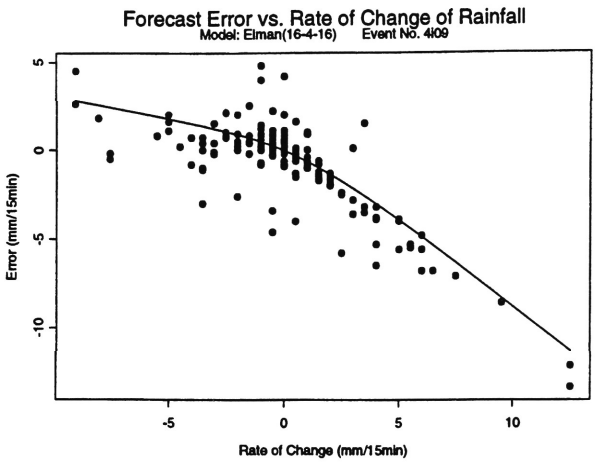

(a) Elman Network

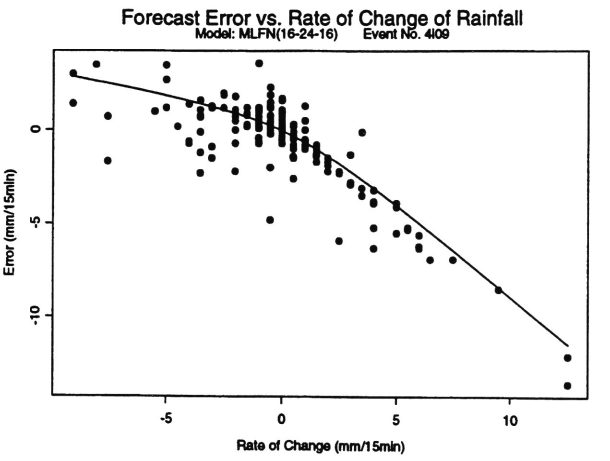

(b) MLFN

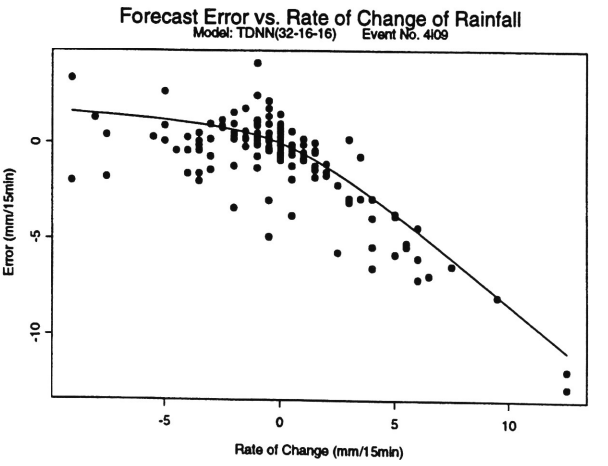

(c) TDNN

Figure D.3 - Event No. 3 : 9 Sep 1994

APPENDIX D
FORECAST ERROR VS. RATE OF CHANGE OF RAINFALL INTENSITY FOR TEN REAL STORM EVENTS

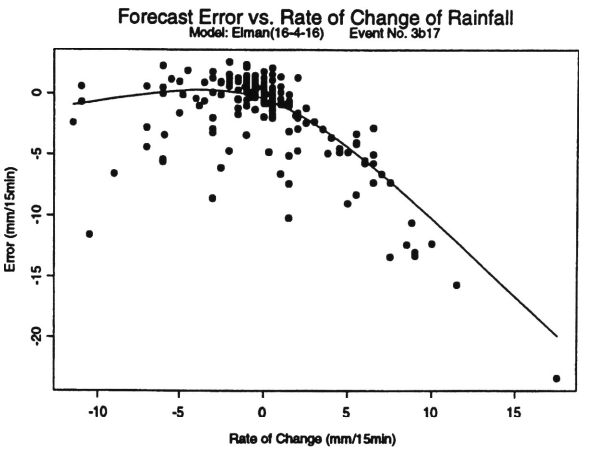

(a) Elman Network

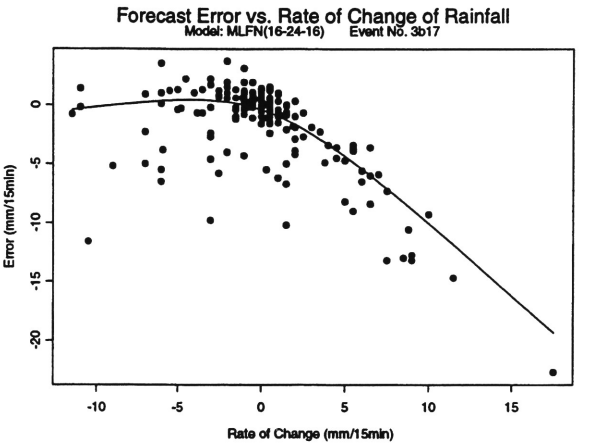

(b) MLFN

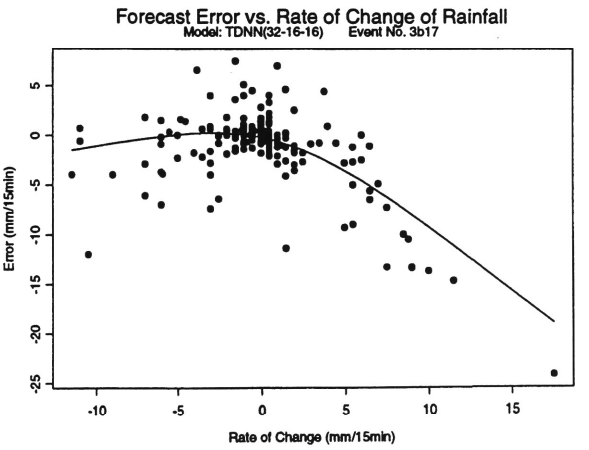

(c) TDNN

Figure D.4 - Event No. 4 : 17 Feb 1993

APPENDIX D
FORECAST ERROR VS. RATE OF CHANGE OF RAINFALL INTENSITY FOR TEN REAL STORM EVENTS

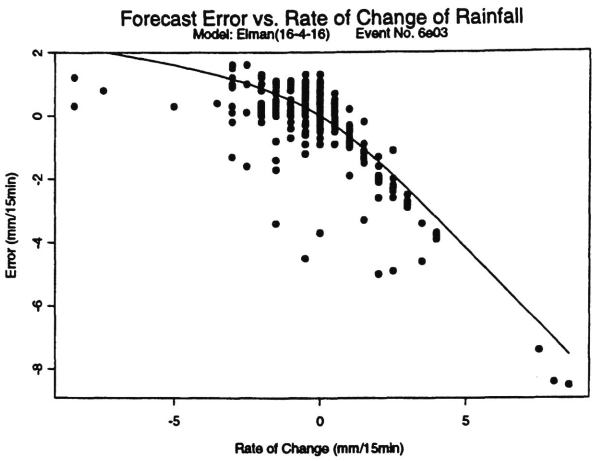

(a) Elman Network

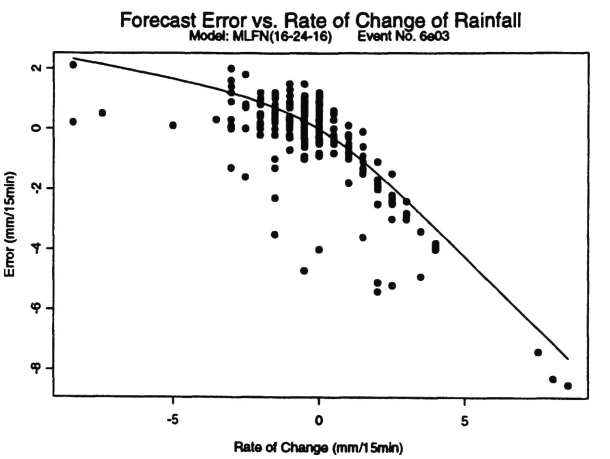

(b) MLFN

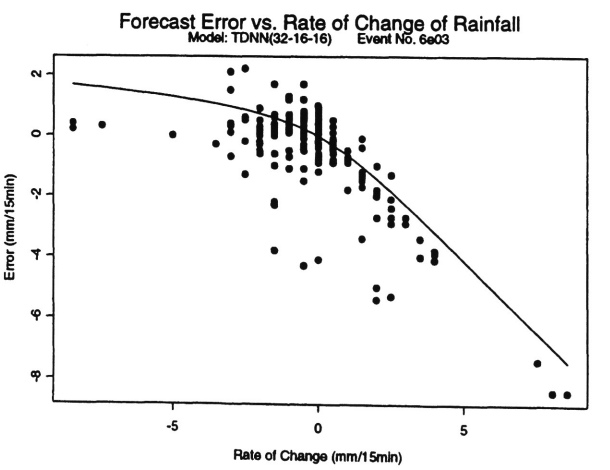

(c) TDNN

Figure D.5 - Event No. 5 : 3 May 1996

APPENDIX D
FORECAST ERROR VS. RATE OF CHANGE OF RAINFALL INTENSITY FOR TEN REAL STORM EVENTS

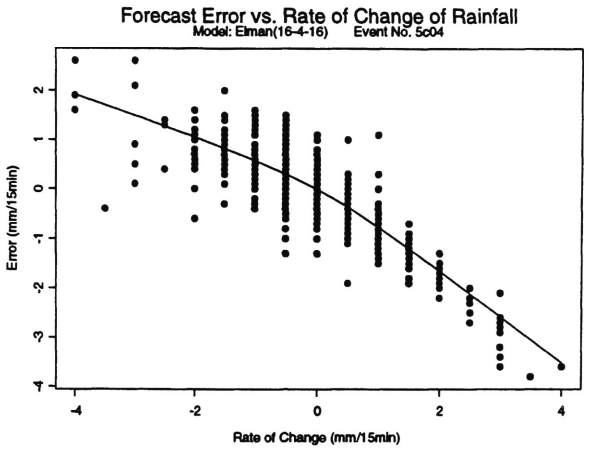

(a) Elman Network

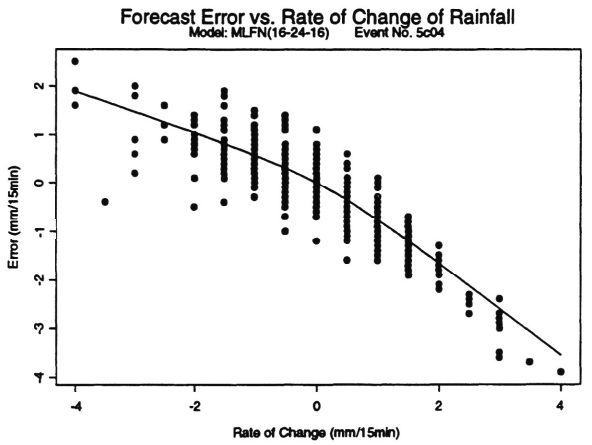

(b) MLFN

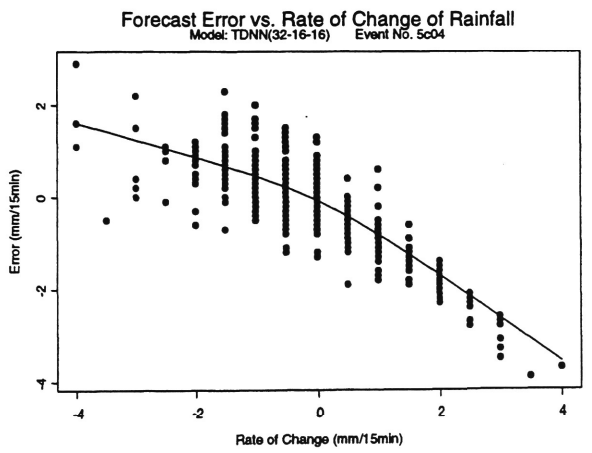

(c) TDNN

Figure D.6 - Event No. 6 : 4 Mar 1995

APPENDIX D
FORECAST ERROR VS. RATE OF CHANGE OF RAINFALL INTENSITY FOR TEN REAL STORM EVENTS

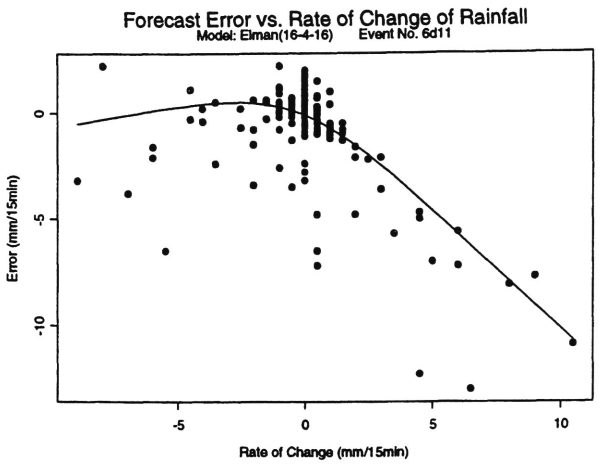

(a) Elman Network

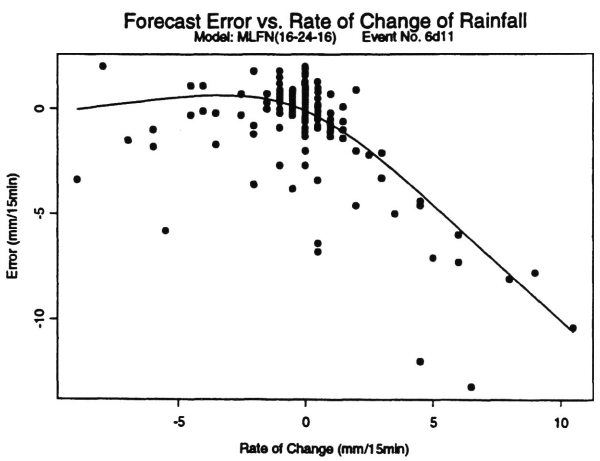

(b) MLFN

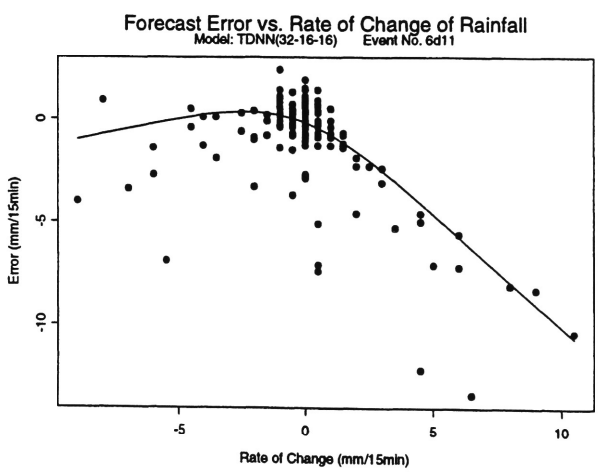

(c) TDNN

Figure D.7 - Event No. 7 : 11 Apr 1996

APPENDIX D
FORECAST ERROR VS. RATE OF CHANGE OF RAINFALL INTENSITY FOR TEN REAL STORM EVENTS

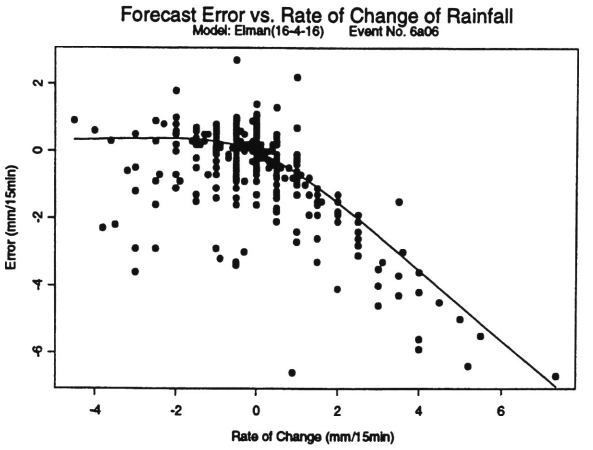

(a) Elman Network

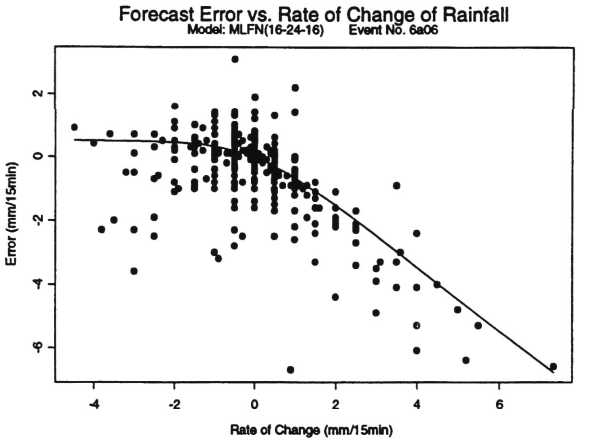

(b) MLFN

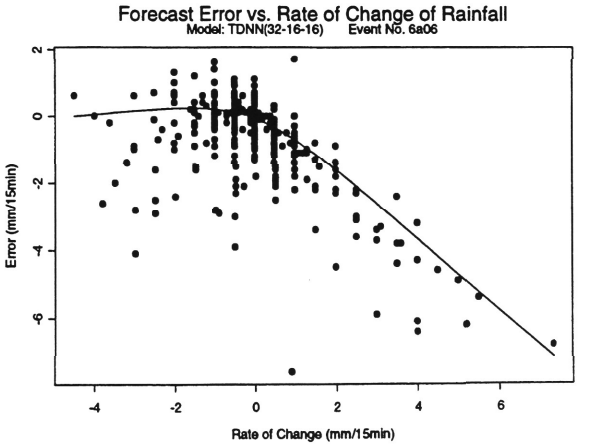

(c) TDNN

Figure D.8 - Event No. 8 : 6 Jan 1996

APPENDIX D
FORECAST ERROR VS. RATE OF CHANGE OF RAINFALL INTENSITY FOR TEN REAL STORM EVENTS

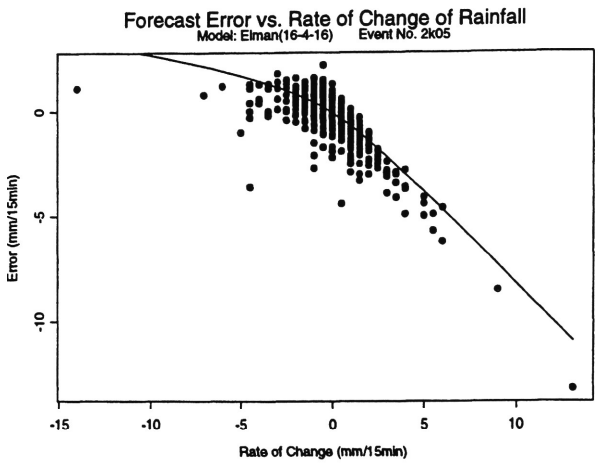

(a) Elman Network

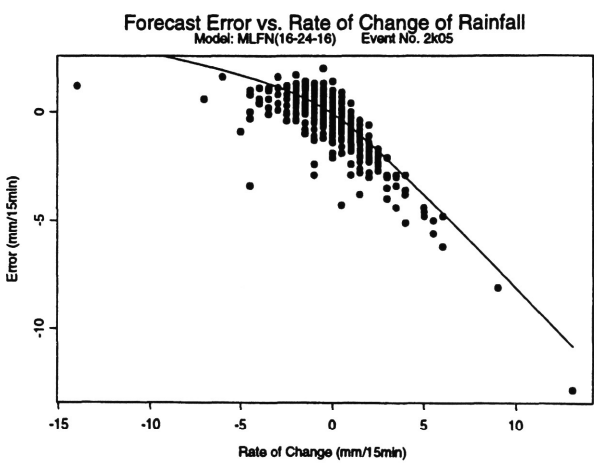

(b) MLFN

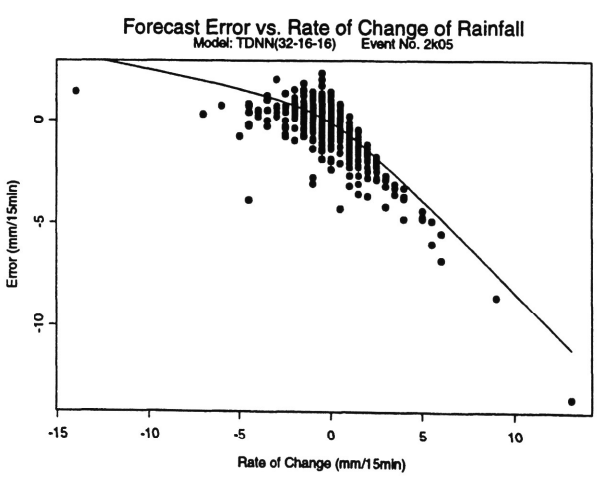

(c) TDNN

Figure D.9 - Event No. 9 : 5 Nov 1992

APPENDIX D
FORECAST ERROR VS. RATE OF CHANGE OF RAINFALL INTENSITY FOR TEN REAL STORM EVENTS

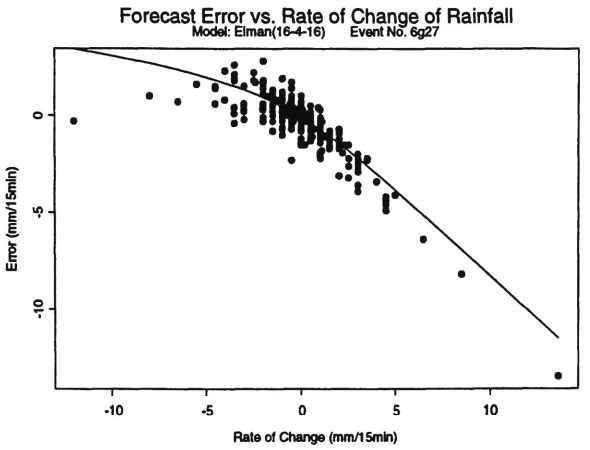

(a) Elman Network

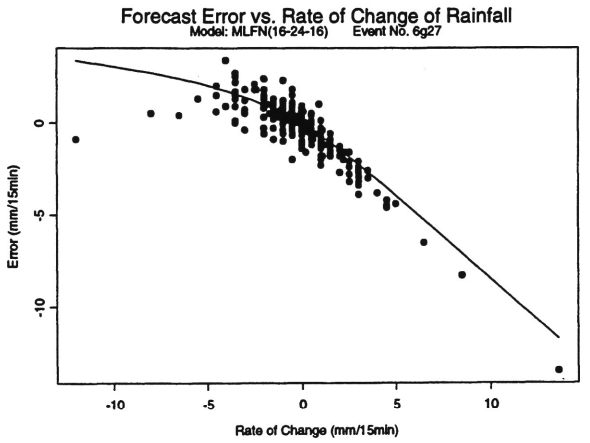

(b) MLFN

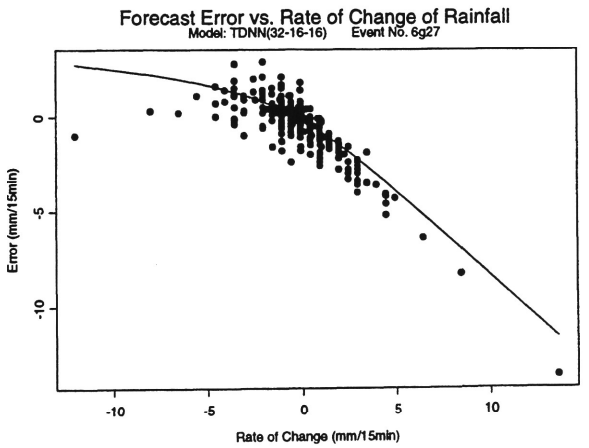

(c) TDNN

Figure D.10 - Event No. 10 : 27 Jul 1996

APPENDIX E

STORM CENTRE TRACKS FOR 25 ARTIFICIAL STORM EVENTS

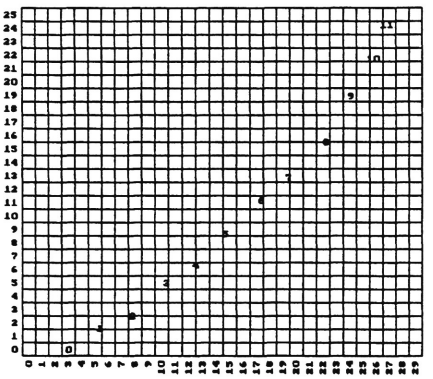

Storm 132

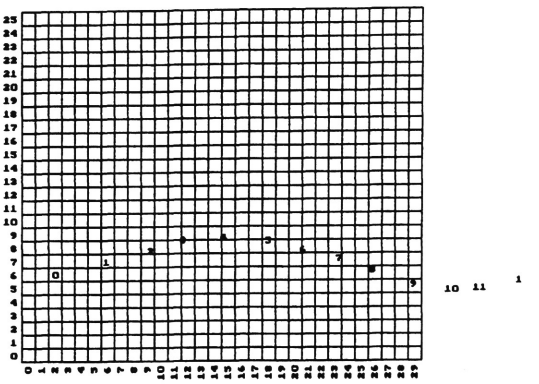

Storm 133

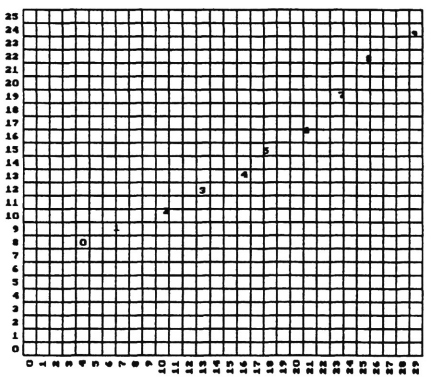

Storm 134

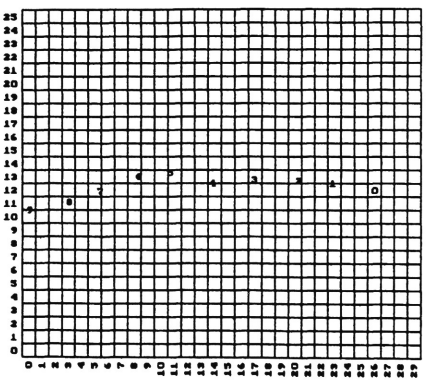

Storm 135

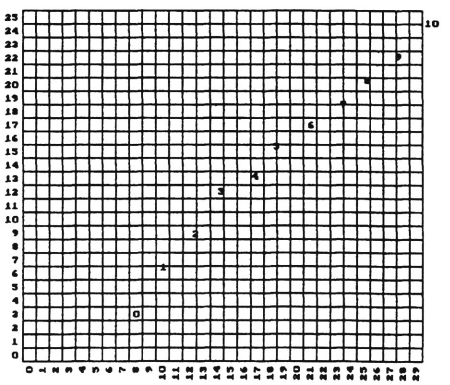

Storm 136

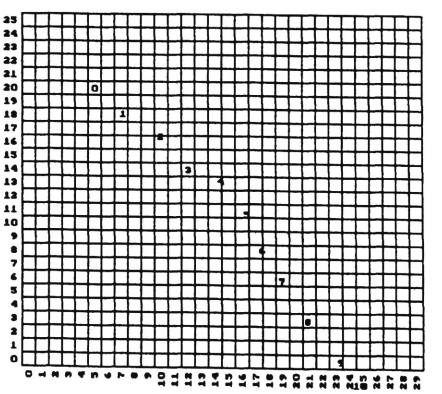

Storm 137

APPENDIX E

STORM CENTRE TRACKS FOR 25 ARTIFICIAL STORM EVENTS

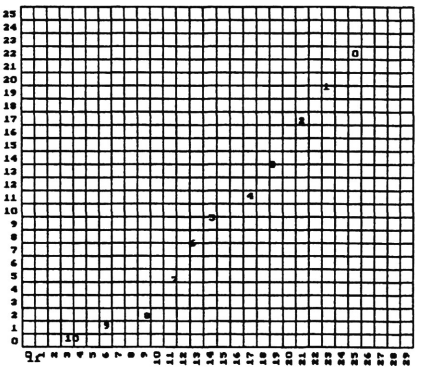

Storm 138

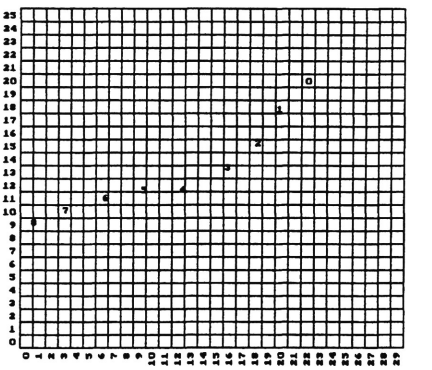

Storm 139

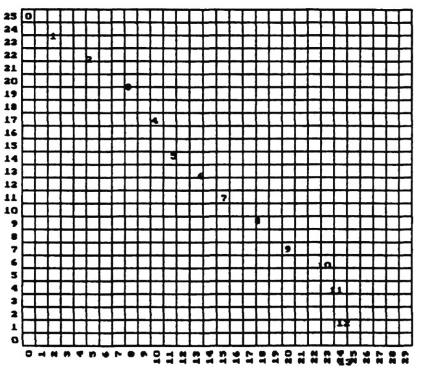

Storm 140

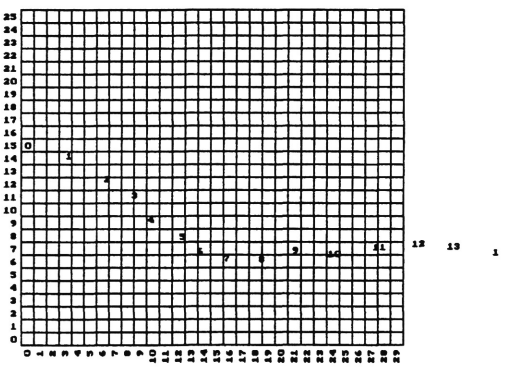

Storm 141

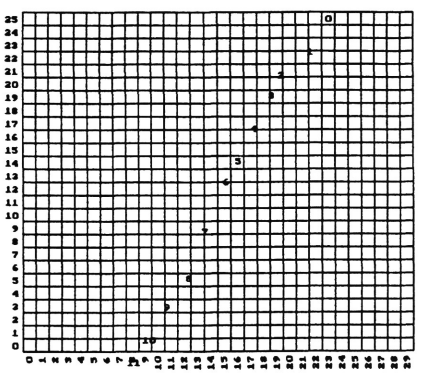

Storm 142

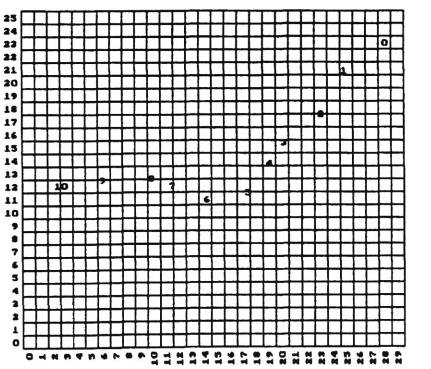

Storm 143

APPENDIX E
STORM CENTRE TRACKS FOR 25 ARTIFICIAL STORM EVENTS

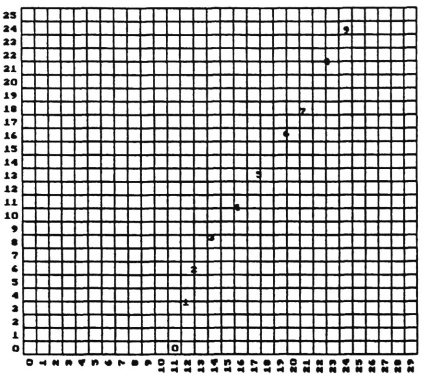

Storm 144

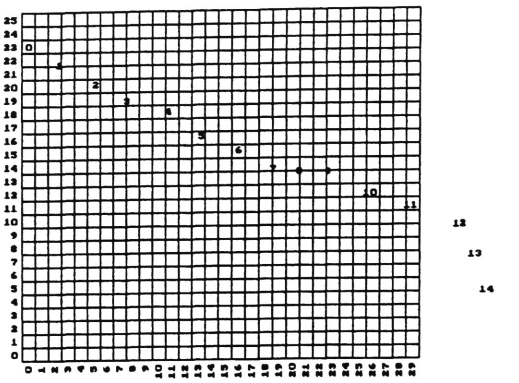

Storm 145

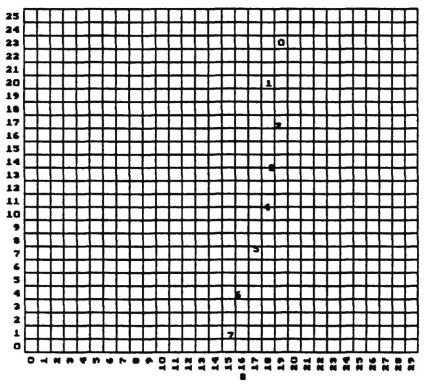

Storm 146

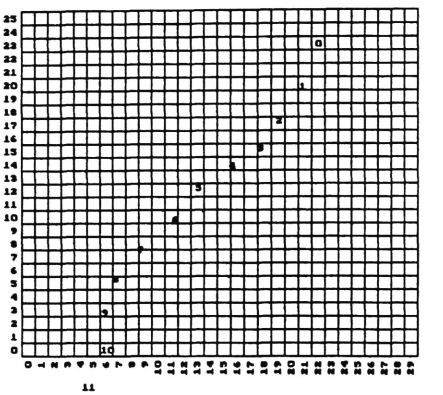

Storm 147

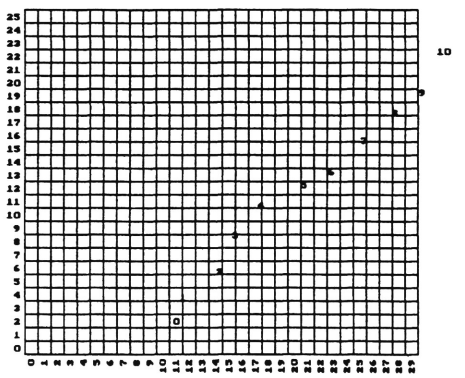

Storm 148

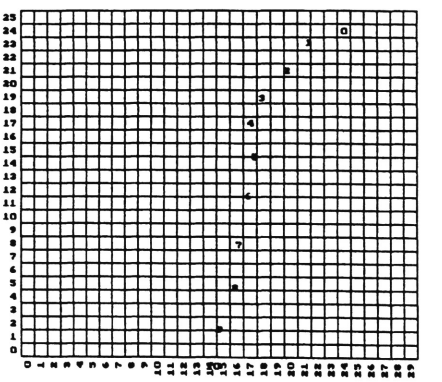

Storm 149

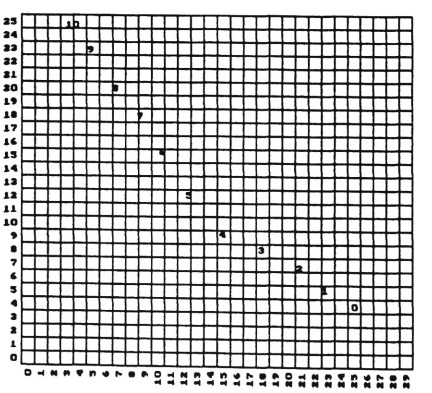

Storm 150

APPENDIX F

ERROR IN PREDICTION OF STORM CENTRES

Event no.	Error in Prediction		
126	Intensity	Distance	Angle
Time Step	(mm/15min)	(km)	(degree)
1	3.71	0.90	-52.31
2	-0.75	-1.01	-33.71
3	-4.47	-0.13	-2.57
4	2.28	-1.23	-6.62
5	-0.34	-0.28	3.40
6	-2.36	-1.23	-11.47
7	-7.56	-0.34	-27.29
8	-12.04	-0.39	44.71

Event no.	Error in Prediction		
127	Intensity	Distance	Angle
Time Step	(mm/15min)	(km)	(degree)
1	-4.65	0.58	-1.55
2	6.24	-0.31	-28.01
3	-7.32	-0.71	-25.62
4	-8.13	-0.64	-41.09
5	-2.78	-0.71	5.98
6	-2.11	-1.34	10.95
7	-5.46	0.43	22.83
8	-4.28	-0.29	-14.98
9	-6.89	-0.82	-88.85

Event no.	Error in Prediction		
128	Intensity	Distance	Angle
Time Step	(mm/15min)	(km)	(degree)
1	3.67	0.88	-9.00
2	-7.08	-0.70	-8.52
3	1.07	0.30	26.72
4	-5.64	-0.14	18.86
5	-5.67	-0.54	33.80
6	3.56	-0.61	28.85
7	-9.96	-0.58	22.47
8	-2.34	0.27	-9.57
9	-1.20	-1.02	44.13
10	-0.35	-0.20	174.62

Event no.	Error in Prediction		
129	Intensity	Distance	Angle
Time Step	(mm/15min)	(km)	(degree)
1	-6.80	-0.73	242.84
2	-2.79	-0.36	-0.78
3	-7.41	-0.39	-24.61
4	-9.22	-1.06	-31.58
5	-10.40	-0.87	13.62
6	-4.59	0.73	29.13
7	3.19	-1.06	-7.92
8	-16.78	-0.87	224.04
9	-0.14	0.86	215.69
10	-2.58	-0.75	87.43

Event no.	Error in Prediction		
130	Intensity	Distance	Angle
Time Step	(mm/15min)	(km)	(degree)
1	5.08	0.26	-4.20
2	0.44	1.99	-3.39
3	-3.23	-0.85	251.93
4	-3.29	-0.04	12.14
5	-3.95	-0.30	7.48
6	-2.53	-1.06	7.90
7	4.09	-0.69	-10.88
8	-2.18	-0.93	7.93
10	-2.90	-0.91	187.53
11	-5.87	-0.50	205.99
12	-1.28	-0.91	192.64

Event no.	Error in Prediction		
131	Intensity	Distance	Angle
Time Step	(mm/15min)	(km)	(degree)
1	2.92	0.26	5.54
2	-6.64	-0.50	-0.62
3	-2.93	-0.89	-7.68
4	0.12	-0.10	17.74
5	-1.64	-0.32	-6.01
6	-3.37	-0.97	-4.24
7	3.08	-0.38	-15.98
8	-6.10	-1.08	40.84
9	-10.44	0.49	122.16

APPENDIX F

ERROR IN PREDICTION OF STORM CENTRES

Event no.	Error in Prediction		
132	Intensity	Distance	Angle
Time Step	(mm/15min)	(km)	(degree)
1	-11.99	2.27	-28.18
2	-3.94	-0.25	266.16
3	-12.15	-0.05	-16.21
4	0.12	-0.65	7.51
5	-3.00	-0.11	-0.95
6	-4.33	-1.24	-3.82
7	-9.85	-0.66	-45.03
8	-1.36	-1.43	204.69
9	-3.82	-1.40	135.96
10	-5.21	-0.82	177.91
11	3.98	-0.75	156.13

Event no.	Error in Prediction		
133	Intensity	Distance	Angle
Time Step	(mm/15min)	(km)	(degree)
1	-7.04	-1.20	-5.37
2	0.25	-0.86	-7.10
3	-8.32	-0.06	-0.25
4	2.54	-1.07	4.48
5	0.88	-0.66	-27.42
6	-2.18	-0.59	-16.48
7	-11.17	-0.42	-5.91
8	-0.68	-0.93	187.71
9	-14.90	0.17	182.81

Event no.	Error in Prediction		
134	Intensity	Distance	Angle
Time Step	(mm/15min)	(km)	(degree)
1	-4.31	-0.77	-27.32
2	-6.79	-0.62	-3.97
3	-4.05	-0.76	-7.01
4	-0.78	-0.83	-4.68
5	1.98	-0.77	-51.52
6	-6.62	-0.44	-27.31
7	-2.84	-1.07	-11.03
8	-6.06	-0.39	-37.73
9	-1.03	-0.69	-58.42

Event no.	Error in Prediction		
135	Intensity	Distance	Angle
Time Step	(mm/15min)	(km)	(degree)
1	-3.99	-0.59	94.60
2	-0.95	-0.79	-16.79
3	-5.69	0.15	9.98
4	7.10	-0.81	-0.52
5	-3.49	-0.46	31.19
6	-0.13	-1.52	144.14
7	-3.19	-1.40	154.07
8	-6.60	-0.88	138.97
9	-5.32	-1.40	45.85

Event no.	Error in Prediction		
136	Intensity	Distance	Angle
Time Step	(mm/15min)	(km)	(degree)
1	-5.06	-0.24	246.23
2	-6.16	-0.81	9.25
3	0.73	-0.52	21.17
4	-7.85	-0.45	-26.83
5	0.00	-1.15	274.88
6	-0.36	-1.47	293.97
7	-3.81	-1.11	83.24
8	-8.34	-0.55	178.29
9	-12.58	-0.50	151.33
10	-6.75	-1.18	81.97

Event no.	Error in Prediction		
137	Intensity	Distance	Angle
Time Step	(mm/15min)	(km)	(degree)
1	1.04	0.32	40.46
2	-2.03	-0.28	73.30
3	-2.94	-0.62	23.82
4	-2.26	-0.95	25.01
5	3.11	-0.99	-70.45
6	-10.18	-0.31	19.82
7	-3.02	-1.04	32.51
8	-2.68	-0.94	-79.95

APPENDIX F

ERROR IN PREDICTION OF STORM CENTRES

Event no.	Error in Prediction		
138	Intensity	Distance	Angle
Time Step	(mm/15min)	(km)	(degree)
1	-4.04	0.11	-47.22
2	-4.62	0.64	12.32
3	-5.81	-0.61	28.31
4	-1.47	-0.66	16.35
5	-3.51	-0.56	-15.79
6	1.78	-0.22	25.39
7	-3.12	-1.05	-10.70
8	1.82	-1.00	-1.52
9	-1.98	-0.34	-250.62
10	-3.64	-0.17	74.78

Event no.	Error in Prediction		
139	Intensity	Distance	Angle
Time Step	(mm/15min)	(km)	(degree)
1	3.15	0.24	-0.63
2	-4.04	-0.60	12.11
3	2.22	-0.58	15.45
4	-7.41	-0.79	-27.99
5	-2.00	-0.41	-31.20
6	-4.87	-1.14	2.07
7	0.25	-0.73	-0.77
8	-3.68	-0.21	-24.11

Event no.	Error in Prediction		
140	Intensity	Distance	Angle
Time Step	(mm/15min)	(km)	(degree)
1	-16.83	3.17	-22.79
2	-3.72	1.26	-13.68
3	-7.77	0.37	32.29
4	-0.68	0.38	42.20
5	5.05	-0.36	35.77
6	-2.40	-0.44	47.25
7	-5.04	-0.66	-37.88
8	-10.61	-1.25	10.66
9	-2.48	-1.05	-6.59
10	-6.56	-0.12	-39.12
11	-5.55	-0.14	-152.61
12	-4.84	0.62	177.53

Event no.	Error in Prediction		
141	Intensity	Distance	Angle
Time Step	(mm/15min)	(km)	(degree)
1	14.44	1.55	-9.42
2	-1.74	-0.13	-18.68
3	8.18	-0.55	7.92
4	-5.65	-0.13	-38.03
5	2.46	-0.90	20.01
6	-7.76	0.25	-53.63
7	4.31	-0.43	82.99
8	-4.67	-0.29	-37.55
9	-3.00	-0.33	4.78
10	-2.32	-0.60	-31.35
11	-2.85	-0.95	223.47

Event no.	Error in Prediction		
142	Intensity	Distance	Angle
Time Step	(mm/15min)	(km)	(degree)
1	-3.37	1.31	-23.45
2	3.26	0.11	-30.32
3	-3.17	0.29	-2.34
4	1.72	-0.45	7.19
5	-1.16	-0.72	10.67
6	-4.05	-0.09	-9.79
7	-5.15	-1.46	11.14
8	-2.64	-0.22	0.06
9	6.18	-0.57	-41.96
10	4.99	-0.72	138.96

Event no.	Error in Prediction		
143	Intensity	Distance	Angle
Time Step	(mm/15min)	(km)	(degree)
1	9.19	-0.15	-63.81
2	-1.64	0.46	17.27
3	-8.49	-0.18	-0.60
4	0.19	0.41	37.81
5	-10.95	-0.45	15.70
6	-5.44	-1.18	15.12
7	3.40	-0.61	-34.62
8	2.33	-0.35	-47.03
9	-7.53	-1.78	-9.16
10	0.05	-1.62	17.49

APPENDIX F

ERROR IN PREDICTION OF STORM CENTRES

Event no.	Error in Prediction		
144	Intensity	Distance	Angle
Time Step	(mm/15min)	(km)	(degree)
1	-4.44	-0.52	333.76
2	1.67	0.93	7.74
3	-5.56	-1.06	331.24
4	-4.48	-0.44	14.82
5	2.08	-0.90	6.20
6	-2.56	-1.61	-23.74
7	2.53	-0.49	201.26
8	-4.30	-1.41	165.64
9	1.24	-0.89	153.32

Event no.	Error in Prediction		
145	Intensity	Distance	Angle
Time Step	(mm/15min)	(km)	(degree)
1	-18.63	2.43	-19.96
2	-5.42	0.74	35.04
3	-1.92	0.56	41.12
4	-6.06	0.04	77.26
5	-2.28	-0.38	4.26
6	7.87	-0.78	6.96
7	-4.48	-0.66	-6.17
8	1.55	-0.84	107.32
9	-0.50	-0.56	89.10
10	-7.56	-1.61	179.96
11	-9.70	-0.62	-77.25

Event no.	Error in Prediction		
146	Intensity	Distance	Angle
Time Step	(mm/15min)	(km)	(degree)
1	5.89	-0.33	-4.42
2	-1.09	-0.18	46.89
3	-2.30	-1.00	6.27
4	-2.51	-0.89	31.28
5	-9.16	-0.77	41.17
6	-6.05	-0.66	20.59
7	-5.46	-0.92	64.23

Event no.	Error in Prediction		
147	Intensity	Distance	Angle
Time Step	(mm/15min)	(km)	(degree)
1	-2.74	-0.27	11.11
2	-12.95	0.09	12.11
3	1.11	0.35	23.58
4	2.44	-0.89	-34.17
5	-6.19	-0.27	1.21
6	-2.83	-0.63	30.72
7	1.34	-0.55	-29.83
8	-1.47	-0.29	-10.56
9	-1.87	-0.57	38.82

Event no.	Error in Prediction		
148	Intensity	Distance	Angle
Time Step	(mm/15min)	(km)	(degree)
1	-5.68	-0.13	0.19
2	0.96	-0.69	-26.47
3	0.56	-0.42	9.88
4	-2.01	-0.34	-14.17
5	-5.86	-1.43	-58.98
6	-4.59	-0.97	254.95
7	-3.36	-1.52	262.39
8	-9.17	-1.04	120.73
9	-6.07	0.32	111.84

Event no.	Error in Prediction		
149	Intensity	Distance	Angle
Time Step	(mm/15min)	(km)	(degree)
1	1.10	-0.60	-53.11
2	-7.81	0.05	-19.07
3	2.10	-0.43	-0.67
4	-2.99	-0.31	-7.71
5	3.44	-0.90	53.99
6	-2.81	-0.39	14.13
7	-8.52	-1.30	8.71
8	-0.42	-0.14	29.80
9	-4.76	-0.74	29.51

APPENDIX F

ERROR IN PREDICTION OF STORM CENTRES

Event no.	Error in Prediction		
150	Intensity	Distance	Angle
Time Step	(mm/15min)	(km)	(degree)
1	3.10	4.27	-278.40
2	-8.58	0.07	-9.14
3	-3.95	-0.70	-228.88
4	2.23	-0.38	-11.70
5	-5.18	-1.20	-39.00
6	1.33	-1.68	-309.87
7	-8.91	-1.00	-99.67
8	-7.27	-0.44	-99.57
9	-9.02	-0.04	-103.96
10	-12.26	0.29	-199.66

APPENDIX G
Forecast of Spatial Distribution of Subcatchment Rainfall

Artificial Event No.126

Sub-Catchment No.	No. of Cell	Area	Time step 1			Time step 2			Time step 3			Time step 4			Time step 5			Time step 6			Time step 7			Time step 8		
			Actual	Predicted	% error	Actual	Predicted	% error	Actual	Predicted	% error	Actual	Predicted	% error	Actual	Predicted	% error	Actual	Predicted	% error	Actual	Predicted	% error	Actual	Predicted	% error
	(no.)	(km^2)	(mm/hr)	(mm/hr)	(%)	(mm/hr)	(mm/hr)	(%)	(mm/hr)	(mm/hr)	(%)	(mm/hr)	(mm/hr)	(%)	(mm/hr)	(mm/hr)	(%)	(mm/hr)	(mm/hr)	(%)	(mm/hr)	(mm/hr)	(%)	(mm/hr)	(mm/hr)	(%)
1	27	6.75	21.78	27.16	24.70	19.30	23.00	19.13	18.71	17.84	-4.67	10.84	16.83	55.17	6.31	5.83	-7.63	3.57	3.90	9.35	2.06	3.43	66.16	1.24	3.17	155.82
2	35	8.75	22.85	24.83	8.67	24.17	23.61	-2.34	25.99	23.15	-10.95	18.49	23.73	28.33	13.60	14.37	5.67	9.36	11.21	19.81	6.28	7.87	25.45	4.26	5.30	24.42
3	28	7.00	16.19	16.21	0.08	20.12	18.44	-8.35	23.70	21.76	-8.17	20.80	23.00	10.55	19.65	21.17	7.76	16.73	18.78	12.28	13.20	13.84	4.81	10.25	9.40	-8.37
4	36	9.00	16.01	24.85	55.20	14.09	19.49	38.30	13.90	13.66	-1.70	7.47	12.45	66.72	3.91	2.71	-30.71	2.02	1.30	-35.49	1.10	1.24	12.74	0.64	1.59	147.15
5	14	3.50	19.50	26.38	35.28	20.84	22.53	8.10	23.20	20.73	-10.64	15.05	21.46	42.60	9.67	9.44	-2.37	5.90	6.21	5.32	3.70	3.86	4.29	2.41	2.55	5.77
6	23	5.75	17.75	19.49	9.80	23.39	20.66	-11.69	29.21	25.28	-13.47	25.01	28.09	12.31	22.35	23.31	4.29	18.04	20.00	10.87	13.95	13.98	0.23	10.77	9.27	-13.94
7	13	3.25	18.69	24.02	28.51	22.95	21.97	-4.29	27.99	23.93	-14.49	20.86	26.42	26.63	15.62	15.99	2.36	10.82	11.93	10.27	7.55	7.34	-2.74	5.41	4.58	-15.18
8	23	5.75	11.99	20.87	74.05	12.86	16.07	24.97	14.73	13.40	-9.02	8.91	13.47	51.28	5.18	3.84	-25.86	2.90	1.76	-39.39	1.74	0.75	-57.12	1.12	0.37	-67.32
9	19	4.75	6.37	6.96	9.19	11.13	10.66	-4.23	16.48	16.01	-2.91	19.51	18.05	-7.52	25.27	25.26	-0.06	27.84	26.25	-5.71	27.44	23.20	-15.46	26.00	19.42	-25.29
10	6	1.50	10.42	10.92	4.77	16.44	14.48	-11.88	22.83	20.85	-8.69	23.95	23.65	-1.26	26.96	27.32	1.31	26.36	26.47	0.39	23.62	21.23	-10.11	20.62	16.08	-21.99
11	23	5.75	13.40	19.59	46.19	17.39	16.96	-2.44	22.46	19.12	-14.86	16.61	21.80	31.26	12.09	12.41	2.68	8.15	8.65	6.17	5.70	4.71	-17.31	4.16	2.67	-35.75
12	17	4.25	12.11	13.22	9.23	19.05	15.69	-17.65	27.02	23.09	-14.52	26.56	27.36	3.01	27.30	27.69	1.44	24.68	25.80	4.55	21.23	19.34	-8.91	18.15	14.07	-22.47
13	8	2.00	7.86	8.29	5.50	13.78	11.86	-13.91	20.77	18.76	-9.66	23.51	22.16	-5.73	28.53	28.05	-1.70	29.69	28.49	-4.06	28.41	24.15	-14.99	26.49	19.71	-25.59
14	14	3.50	14.34	17.41	21.43	20.91	17.77	-15.01	28.58	23.91	-16.33	25.03	28.24	12.79	22.35	23.14	3.51	17.92	19.64	9.63	14.16	13.15	-7.12	11.34	8.82	-22.18
15	10	2.50	7.40	7.70	4.04	13.62	10.81	-20.65	21.46	18.43	-14.14	24.26	22.82	-5.92	28.88	28.27	-2.10	29.43	28.64	-2.69	28.09	23.90	-14.91	26.36	19.60	-25.64
16	4	1.00	12.59	16.40	30.27	18.70	15.93	-14.86	26.19	21.75	-16.95	22.42	26.20	16.84	19.26	20.25	5.17	14.89	16.55	11.13	11.58	10.48	-9.51	9.21	6.83	-25.88
17	12	3.00	8.12	13.05	60.81	11.55	10.77	-6.78	16.19	13.33	-17.63	12.30	15.97	29.77	9.04	9.40	3.99	6.12	6.24	2.04	4.39	2.88	-34.39	3.33	1.38	-58.43
18	12	3.00	3.09	3.51	13.39	6.70	6.53	-2.42	11.58	11.17	-3.60	16.01	13.47	-15.89	24.15	23.03	-4.64	30.08	26.49	-11.92	33.47	26.35	-21.27	35.65	25.08	-29.67
19	17	4.25	5.97	6.11	2.29	11.50	8.22	-28.53	19.07	15.49	-18.77	21.61	20.37	-5.72	25.47	25.18	-1.13	25.76	25.67	-0.35	25.04	21.44	-14.40	24.26	18.18	-25.07
20	18	4.50	7.88	10.82	37.38	12.71	10.18	-19.94	19.18	15.56	-18.90	16.79	19.79	17.88	14.49	15.84	9.38	11.21	12.75	13.78	8.92	7.71	-13.59	7.34	5.04	-31.39
21	18	4.50	6.47	7.13	10.10	12.01	8.49	-29.25	19.62	15.71	-19.97	20.86	20.85	-0.05	22.75	23.27	2.28	21.56	22.59	4.80	20.08	17.63	-12.16	18.86	14.32	-24.09
22	31	7.75	3.66	3.66	0.01	7.74	6.10	-21.19	13.60	11.69	-14.04	17.64	15.23	-13.64	24.53	23.29	-5.07	28.64	26.13	-8.75	31.04	24.98	-19.52	32.86	23.47	-28.57
23	11	2.75	7.50	9.25	23.47	13.05	9.71	-25.62	20.57	16.58	-19.39	19.84	21.67	9.26	19.19	20.51	6.87	16.37	18.25	11.46	14.03	12.55	-10.54	12.29	9.24	-24.84
24	19	5.00	3.21	2.92	-9.12	6.91	3.84	-44.42	12.67	9.59	-24.32	14.59	14.06	-3.63	16.99	17.83	4.92	16.92	17.98	6.26	16.75	14.49	-13.52	16.80	12.52	-25.50
	Area (km^2)	109.75																								
Volume of Rainfall (mm-km^2/hr)			1364.39	1696.37	24.33	1722.70	1657.15	-3.81	2211.86	1939.65	-12.31	1928.34	2189.07	13.52	1853.24	1863.17	0.54	1668.58	1699.85	1.87	1489.19	1331.35	-10.60	1351.22	1058.35	-21.67
Root Mean Square Error (mm/hr)					3.93			2.63			3.00			3.50			0.86			1.50			2.81			4.52

APPENDIX G
Forecast of Spatial Distribution of Subcatchment Rainfall

Artificial Event No.127

Sub-Catchment No.	No. of Cell	Area	Time step 1			Time step 2			Time step 3			Time step 4			Time step 5			Time step 6			Time step 7			Time step 8			Time step 9		
			Actual	Predicted	% error	Actual	Predicted	% error	Actual	Predicted	% error	Actual	Predicted	% error	Actual	Predicted	% error	Actual	Predicted	% error	Actual	Predicted	% error	Actual	Predicted	% error	Actual	Predicted	% error
	(no.)	(km^2)	(mm/hr)	(mm/hr)	(%)	(mm/hr)	(mm/hr)	(%)	(mm/hr)	(mm/hr)	(%)	(mm/hr)	(mm/hr)	(%)	(mm/hr)	(mm/hr)	(%)	(mm/hr)	(mm/hr)	(%)	(mm/hr)	(mm/hr)	(%)	(mm/hr)	(mm/hr)	(%)	(mm/hr)	(mm/hr)	(%)
1	27	6.75	31.10	26.53	-14.69	18.30	25.33	38.44	19.27	17.83	-7.46	16.30	17.15	5.19	9.43	9.17	-2.76	4.37	4.95	13.33	2.26	2.86	26.41	1.13	2.88	154.36	0.56	3.46	514.59
2	35	8.75	30.55	26.92	-11.90	21.98	27.17	23.58	26.97	21.10	-21.79	27.47	24.12	-12.19	19.53	20.10	2.94	10.80	14.15	31.01	6.25	6.24	-0.16	3.50	4.76	35.98	1.99	4.21	112.18
3	28	7.00	19.65	19.02	-3.19	17.38	20.24	16.41	25.00	18.50	-26.00	30.81	23.89	-22.48	27.22	27.00	-0.78	18.02	23.36	29.64	11.67	11.18	-4.18	7.35	7.82	6.38	4.83	6.11	26.43
4	36	9.00	26.64	23.68	-11.13	14.14	21.86	54.68	13.74	14.66	6.76	10.80	12.34	14.29	5.72	4.15	-27.43	2.61	1.37	-47.35	1.36	1.19	-12.17	0.67	1.89	181.79	0.32	2.75	755.11
5	14	3.50	32.44	28.37	-12.54	20.49	28.00	36.62	22.70	20.00	-11.89	21.12	20.87	-1.19	13.46	13.14	-2.39	7.34	6.96	-5.13	4.30	3.35	-22.00	2.37	3.34	41.04	1.26	3.39	163.63
6	23	5.75	25.58	23.89	-6.63	21.38	25.84	20.84	29.36	21.79	-25.77	35.18	27.90	-20.68	29.87	29.33	-1.79	20.42	23.50	15.11	13.70	11.85	-13.49	8.75	9.19	5.03	5.70	7.41	30.01
7	13	3.25	31.25	28.08	-10.15	22.32	29.03	30.09	27.10	21.85	-19.37	28.52	25.44	-10.80	20.83	20.92	0.40	13.13	13.25	0.93	8.49	6.45	-23.98	5.14	5.76	12.01	3.09	5.06	63.71
8	23	5.75	23.83	22.01	-7.65	13.49	20.72	53.66	13.73	14.00	1.97	11.90	12.60	5.87	6.99	4.83	-30.89	3.83	1.45	-62.12	2.30	0.76	-67.13	1.28	1.27	-0.27	0.68	1.66	144.23
9	19	4.75	8.41	8.87	5.41	9.59	10.85	13.08	16.67	13.06	-21.65	26.75	18.63	-30.36	31.48	28.27	-10.19	28.88	29.87	3.45	23.41	21.01	-10.29	18.04	17.07	-5.34	14.69	14.66	-0.20
10	6	1.50	14.19	14.32	0.91	14.46	16.77	15.95	23.06	17.15	-25.63	33.19	23.98	-27.75	34.54	31.85	-7.80	28.24	30.52	8.06	21.21	18.67	-11.99	15.14	14.60	-3.56	11.26	11.97	6.24
11	23	5.75	26.03	23.72	-8.86	17.76	24.45	37.72	20.81	17.85	-14.22	21.59	20.26	-6.15	15.48	15.33	-0.98	10.31	8.55	-17.08	7.04	4.54	-35.51	4.42	4.66	5.44	2.71	4.13	52.44
12	17	4.25	19.09	18.25	-4.37	17.69	21.38	20.90	26.21	19.28	-26.43	35.38	26.60	-24.83	34.19	32.22	-5.76	27.84	28.54	2.51	21.23	17.52	-17.45	15.13	14.62	-3.36	11.01	12.10	9.85
13	8	2.00	11.58	11.50	-0.68	12.35	14.30	15.78	20.39	15.29	-25.01	31.28	22.04	-29.54	34.93	31.40	-10.10	31.99	31.59	-1.27	26.22	22.24	-15.19	20.16	18.66	-7.43	16.14	15.96	-1.07
14	14	3.50	24.66	22.96	-6.88	20.19	25.57	26.66	27.20	20.71	-23.87	33.00	26.84	-18.69	26.24	27.77	-1.66	21.19	21.22	0.15	15.44	12.04	-22.02	10.45	10.54	0.90	7.09	8.77	23.80
15	10	2.50	12.11	11.54	-4.73	12.63	14.79	17.15	20.43	15.07	-26.22	31.16	22.00	-29.41	34.41	31.00	-9.90	32.64	30.69	-5.97	27.66	22.65	-18.11	21.68	19.94	-8.04	17.46	17.26	-1.02
16	4	1.00	23.68	21.98	-7.19	18.62	24.35	30.74	24.30	19.08	-21.50	28.79	24.38	-15.34	23.91	24.00	0.39	18.12	17.03	-6.06	13.42	9.93	-26.02	9.12	9.25	1.46	6.13	7.83	27.58
17	12	3.00	18.32	16.84	-8.05	12.35	17.38	40.78	14.31	12.71	-11.21	15.12	14.16	-6.36	11.01	10.39	-5.64	8.02	5.19	-35.23	5.91	3.14	-46.84	3.93	3.73	-5.11	2.51	3.28	30.92
18	12	3.00	4.67	4.59	-1.73	5.93	6.63	11.86	11.16	9.24	-17.18	20.44	13.48	-34.06	27.74	23.82	-14.15	31.32	28.38	-9.38	29.60	25.63	-13.39	25.95	23.28	-10.29	23.99	21.48	-10.49
19	17	4.25	11.03	9.93	-9.95	11.09	13.13	18.34	17.48	12.81	-26.71	26.55	18.78	-29.25	29.18	26.63	-8.73	29.54	26.02	-11.89	26.68	21.35	-19.96	21.96	20.18	-8.12	18.38	17.93	-2.43
20	18	4.50	17.08	15.68	-8.17	13.23	17.67	33.62	17.03	13.84	-18.69	20.45	17.65	-13.67	17.16	17.46	1.70	14.11	11.86	-16.01	11.23	7.92	-29.45	8.05	8.14	1.15	5.63	6.96	23.60
21	18	4.50	12.73	11.49	-9.68	11.89	14.62	22.93	17.72	13.18	-25.60	25.36	18.88	-25.55	26.07	24.77	-5.01	25.44	22.33	-12.22	22.59	17.76	-21.39	18.19	17.16	-5.64	14.72	15.12	2.68
22	31	7.75	6.39	5.62	-12.13	7.24	8.17	12.83	12.59	9.66	-23.13	21.62	14.37	-33.53	27.45	23.76	-13.44	31.32	26.75	-14.61	30.44	25.02	-17.83	27.05	23.74	-12.25	24.91	21.93	-11.96
23	11	2.75	15.60	14.35	-7.99	13.28	17.17	29.32	18.39	14.25	-22.52	24.10	19.45	-19.32	22.36	22.35	-0.06	19.98	17.63	-11.78	16.73	12.73	-23.94	12.65	12.53	-0.94	9.45	10.78	14.08
24	19	5.00	7.34	6.00	-18.30	7.12	8.46	18.69	10.90	8.10	-25.67	16.65	11.98	-28.05	18.31	17.40	-4.94	20.41	18.33	-20.02	20.07	15.57	-22.44	17.50	16.13	-7.84	15.16	14.55	-4.08
	Area (km^2)	109.75																											
Volume of Rainfall (mm-km^2/hr)			2188.32	1988.85	-9.12	1642.89	2120.80	29.09	2145.86	1742.05	-18.82	2579.42	2116.93	-17.93	2318.17	2181.63	-5.89	1897.63	1835.83	-3.26	1515.71	1249.00	-17.60	1149.67	1128.37	-1.85	909.08	1006.78	10.75
Root Mean Square Error					2.03			4.69			4.53			5.91			1.96			2.57			3.29			1.27			1.62

APPENDIX G
Forecast of Spatial Distribution of Subcatchment Rainfall

Artificial Event No.128																																			
Sub-Catchment No.	No. of Cell	Area		Time step 1			Time step 2			Time step 3			Time step 4			Time step 5			Time step 6			Time step 7			Time step 8			Time step 9			Time step 10		
			Actual	Predicted	% error	Actual	Predicted	% error	Actual	Predicted	% error	Actual	Predicted	% error	Actual	Predicted	% error	Actual	Predicted	% error	Actual	Predicted	% error	Actual	Predicted	% error	Actual	Predicted	% error	Actual	Predicted	% error
	(no.)	(km²)	(mm/hr)	(mm/hr)	(%)	(mm/hr)	(mm/hr)	(%)	(mm/hr)	(mm/hr)	(%)	(mm/hr)	(mm/hr)	(%)	(mm/hr)	(mm/hr)	(%)	(mm/hr)	(mm/hr)	(%)	(mm/hr)	(mm/hr)	(%)	(mm/hr)	(mm/hr)	(%)	(mm/hr)	(mm/hr)	(%)	(mm/hr)	(mm/hr)	(%)
1	27	6.75	24.68	28.19	14.23	31.53	26.39	-16.32	21.96	23.73	8.06	20.05	19.40	-3.24	16.47	17.20	4.42	9.28	13.04	40.53	7.33	5.77	-21.28	4.81	2.50	-48.04	2.34	1.95	-16.51	1.46	0.80	-45.50
2	35	8.75	19.83	24.27	22.39	27.78	23.29	-16.15	21.28	25.21	18.45	21.58	20.06	-7.06	20.46	19.59	-4.28	12.57	17.05	35.71	11.38	9.44	-17.01	8.32	5.01	-39.77	4.40	4.28	-2.80	2.79	1.94	-30.54
3	28	7.00	10.58	14.43	36.36	15.84	14.33	-9.54	13.05	18.13	38.92	14.47	13.49	-6.73	15.81	14.14	-10.58	10.51	14.07	33.86	10.77	9.86	-8.39	8.78	5.51	-37.22	4.97	5.12	3.02	3.14	2.70	-14.05
4	36	9.00	22.11	27.18	22.88	29.60	24.94	-15.74	21.33	21.25	-0.35	19.68	19.04	-3.24	15.52	16.81	8.35	8.73	12.44	42.52	6.98	6.14	-12.07	4.49	3.64	-18.81	2.29	2.91	27.35	1.51	2.28	49.07
5	14	3.50	22.00	27.61	25.54	33.30	26.03	-21.85	27.01	27.37	1.35	27.99	24.50	-12.48	25.29	24.01	-5.06	15.55	20.41	31.26	14.39	11.98	-16.73	10.24	8.80	-14.03	5.76	7.64	32.56	3.93	5.16	31.26
6	23	5.75	13.50	17.69	31.01	22.23	18.01	-19.00	19.80	24.43	23.38	23.05	20.25	-12.13	25.10	22.01	-12.32	17.10	22.05	28.92	18.48	15.70	-15.04	15.13	12.28	-18.83	9.22	11.48	24.52	6.23	7.22	15.87
7	13	3.25	18.40	24.00	30.46	30.39	23.40	-23.00	26.86	28.52	6.15	30.37	25.66	-15.51	30.41	26.86	-11.66	20.06	24.96	24.59	20.87	16.75	-19.75	16.14	14.17	-12.21	9.93	12.86	29.47	7.01	8.95	27.73
8	23	5.75	16.91	23.74	40.41	27.08	21.50	-20.60	22.93	21.24	-7.37	24.20	21.10	-12.85	21.09	20.49	-2.82	13.04	16.79	28.77	12.43	10.85	-12.70	8.73	9.07	3.78	5.26	7.82	48.61	3.86	6.64	71.99
9	19	4.75	3.25	4.58	41.10	6.20	5.84	-5.82	6.42	9.69	50.82	8.84	7.42	-16.02	12.09	8.86	-26.75	9.47	11.39	20.36	12.78	11.79	-7.76	12.48	10.66	-14.52	8.77	11.12	26.77	6.06	8.57	40.99
10	6	1.50	6.13	8.37	36.58	11.06	9.46	-14.42	10.86	15.35	41.40	14.02	12.12	-13.60	17.63	14.13	-19.84	13.08	16.32	24.71	16.17	14.40	-10.96	14.73	12.20	-17.20	9.74	12.17	24.94	6.64	8.37	25.98
11	23	5.75	15.07	20.59	36.64	27.01	19.83	-26.56	25.60	25.01	-2.31	30.39	24.49	-19.41	30.63	26.16	-14.60	20.82	24.56	17.96	23.18	18.09	-21.96	18.27	17.71	-3.06	12.29	16.29	32.51	9.33	13.05	39.95
12	17	4.25	8.59	10.68	24.33	16.25	12.16	-25.17	16.48	20.64	25.26	21.58	17.99	-16.60	26.22	21.24	-19.00	19.51	23.56	20.78	24.63	19.96	-19.95	22.14	19.85	-10.31	15.47	19.44	25.67	11.21	14.69	31.07
13	8	2.00	4.56	5.58	21.62	9.07	7.21	-20.49	9.66	13.35	38.14	13.44	11.09	-17.50	17.97	13.60	-24.32	14.10	16.80	19.17	19.31	16.30	-15.58	18.65	16.61	-10.91	13.59	16.91	24.40	9.81	13.53	37.89
14	14	3.50	12.27	15.92	29.78	22.75	16.76	-26.31	22.47	25.39	12.96	28.29	23.30	-17.63	31.87	26.43	-17.08	22.86	27.31	19.49	27.41	21.47	-21.67	23.35	21.42	-8.25	16.04	20.41	27.26	11.83	15.58	31.69
15	10	2.50	4.69	4.96	6.05	9.88	6.95	-29.69	11.14	14.43	29.58	16.10	12.99	-19.34	21.73	16.42	-24.45	17.45	20.28	16.23	25.08	19.84	-20.88	24.52	22.59	-7.88	18.96	22.87	20.49	14.38	19.41	34.94
16	4	1.00	11.81	15.58	31.87	22.81	16.23	-28.88	23.28	24.83	6.63	29.86	24.03	-19.53	33.36	27.33	-18.10	24.13	28.00	16.02	29.59	22.53	-23.89	25.16	23.83	-5.32	17.92	22.70	26.65	13.68	18.30	33.73
17	12	3.00	10.02	14.58	45.49	19.95	13.84	-30.62	20.74	18.89	-8.90	26.41	20.60	-21.99	27.53	22.83	-17.10	19.63	22.01	12.12	24.03	18.39	-23.46	19.69	20.23	2.71	14.75	18.87	27.93	12.08	16.72	38.41
18	12	3.00	1.50	1.28	-14.96	3.41	2.95	-13.52	4.16	6.16	48.11	6.59	5.28	-19.86	10.21	6.93	-32.07	8.87	10.29	16.02	14.43	12.54	-13.08	15.67	15.57	-0.68	13.03	16.70	28.17	9.90	15.89	60.60
19	17	4.25	4.21	3.91	-7.16	9.48	5.90	-37.74	11.31	13.57	20.01	17.08	13.64	-20.12	23.34	17.86	-24.32	19.34	21.90	13.22	29.86	22.16	-25.78	30.04	28.25	-5.94	25.53	28.59	12.00	20.75	26.08	25.68
20	18	4.50	8.11	10.73	32.30	17.28	11.33	-34.46	19.25	19.09	-0.79	26.39	20.54	-22.14	30.38	24.17	-20.45	22.99	25.36	10.28	30.92	22.56	-27.06	27.27	26.53	-2.71	21.65	25.54	17.99	17.91	22.63	26.36
21	18	4.50	5.14	5.31	3.27	11.51	7.14	-37.96	13.62	15.46	13.55	20.20	16.08	-20.39	26.48	20.37	-23.08	21.57	24.16	11.96	32.60	23.59	-27.63	31.93	29.96	-6.17	27.16	29.93	10.25	22.44	27.18	21.12
22	31	7.75	2.22	1.66	-25.27	5.15	3.39	-34.21	6.38	8.25	29.27	10.14	8.17	-19.40	15.08	10.95	-27.39	13.13	15.10	15.00	21.93	17.10	-22.02	23.65	23.06	-2.52	21.03	24.10	14.60	17.08	23.23	36.02
23	11	2.75	6.80	8.10	19.18	14.95	9.51	-36.41	17.23	18.36	6.55	24.63	19.38	-21.29	30.25	23.68	-21.70	23.73	26.27	10.70	33.73	24.25	-28.09	31.26	29.58	-5.33	25.52	29.01	13.68	21.02	25.82	22.86
24	19	5.00	2.64	1.80	-31.96	6.82	3.32	-51.33	9.16	9.82	7.24	15.05	12.00	-20.26	21.15	16.20	-23.41	18.48	20.32	9.96	31.75	22.06	-30.52	33.09	31.13	-5.93	31.86	31.36	-1.64	28.52	30.44	6.71
	Area (km²)	109.75																																	
Volume of Rainfall (mm-km²/hr)			1309.35	1634.50	24.83	2102.79	1642.90	-21.87	1871.69	2078.90	11.07	2199.20	1887.22	-14.19	2374.17	2041.25	-14.02	1688.48	2055.13	21.71	2082.48	1845.43	-20.99	1853.43	1672.70	-9.75	1390.77	1625.85	16.90	1083.67	1363.57	25.83
Root Mean Square Error					3.54			4.71			2.71			3.67			4.26			3.43			5.27			1.89			3.03			3.66

APPENDIX G
Forecast of Spatial Distribution of Subcatchment Rainfall

Artificial Event No.129

Sub-Catchment No.	No. of Cell	Area	Time step 1			Time step 2			Time step 3			Time step 4			Time step 5			Time step 6			Time step 7			Time step 8			Time step 9			Time step 10		
			Actual	Predicted	% error	Actual	Predicted	% error	Actual	Predicted	% error	Actual	Predicted	% error	Actual	Predicted	% error	Actual	Predicted	% error	Actual	Predicted	% error	Actual	Predicted	% error	Actual	Predicted	% error	Actual	Predicted	% error
	(no.)	(km^2)	(mm/hr)	(mm/hr)	(%)	(mm/hr)	(mm/hr)	(%)	(mm/hr)	(mm/hr)	(%)	(mm/hr)	(mm/hr)	(%)	(mm/hr)	(mm/hr)	(%)	(mm/hr)	(mm/hr)	(%)	(mm/hr)	(mm/hr)	(%)	(mm/hr)	(mm/hr)	(%)	(mm/hr)	(mm/hr)	(%)	(mm/hr)	(mm/hr)	(%)
1	27	6.75	2.90	1.30	-55.06	4.86	4.46	-8.20	8.32	7.10	-14.59	9.51	9.13	-4.05	13.18	9.56	-27.46	15.20	14.55	-4.26	15.60	15.59	-0.06	34.21	15.66	-54.21	24.96	21.62	-13.39	24.21	24.17	-0.20
2	35	8.75	6.11	3.00	-50.91	8.49	6.53	-23.00	12.15	9.85	-18.98	11.66	10.12	-13.24	13.00	7.49	-42.38	13.88	11.30	-18.58	12.94	14.46	11.68	25.59	15.33	-40.09	17.22	21.09	22.50	14.10	17.59	24.74
3	28	7.00	8.08	5.95	-26.32	9.12	6.39	-30.01	10.74	8.50	-20.82	8.37	6.41	-23.41	7.43	2.50	-66.34	7.48	4.17	-44.23	6.55	7.76	18.47	12.08	9.64	-20.16	7.66	13.04	70.17	5.45	7.88	44.56
4	36	9.00	2.41	0.94	-60.86	4.39	5.03	14.58	8.25	7.73	-6.24	10.90	11.20	2.77	16.86	14.24	-14.50	18.72	19.61	4.73	18.12	18.74	3.44	37.61	17.66	-53.03	26.67	21.87	-17.96	25.96	26.01	0.21
5	14	3.50	6.46	2.62	-59.40	10.01	9.86	-3.50	16.18	13.88	-14.22	18.72	16.86	-9.96	23.66	17.36	-26.63	24.34	22.04	-9.48	20.86	22.80	9.32	37.90	21.61	-42.97	24.29	26.67	9.82	19.60	23.96	22.24
6	23	5.75	12.80	8.07	-36.98	15.18	12.76	-16.95	18.99	16.08	-15.29	16.67	14.68	-11.96	15.60	9.46	-39.35	14.86	10.90	-26.72	11.75	14.50	23.39	19.50	15.15	-22.30	11.56	19.83	71.61	7.71	11.50	49.27
7	13	3.25	11.55	5.38	-53.44	15.72	14.22	-9.53	22.62	18.81	-16.86	23.72	20.49	-13.62	25.88	16.38	-28.96	24.86	21.16	-14.93	19.41	22.89	17.94	32.02	21.71	-32.20	19.11	26.77	40.07	13.58	19.38	42.67
8	23	5.75	4.93	1.30	-73.65	8.23	8.50	3.33	14.54	12.37	-14.91	19.51	16.91	-13.35	27.09	20.99	-22.54	26.97	25.70	-4.71	21.55	24.15	12.07	36.73	21.93	-40.30	22.76	23.98	5.35	18.46	23.60	27.85
9	19	4.75	14.51	15.86	9.29	12.69	11.28	-11.06	11.92	10.62	-10.93	7.91	6.62	-16.35	5.23	2.08	-60.12	4.41	1.09	-75.20	3.00	3.10	3.31	4.23	4.47	5.54	2.21	5.67	156.53	1.14	1.82	59.75
10	6	1.50	15.20	13.38	-11.94	14.94	12.53	-16.12	15.63	13.43	-14.03	11.46	9.72	-15.23	8.61	4.00	-53.55	7.63	3.55	-53.50	5.51	6.63	20.47	8.26	8.02	-2.93	4.52	10.42	130.61	2.54	3.97	55.95
11	23	5.75	12.43	5.38	-56.90	17.22	16.10	-6.55	25.66	20.50	-20.13	29.53	23.48	-20.47	33.13	23.74	-28.34	30.12	25.58	-15.06	21.36	25.47	19.26	32.09	22.99	-28.34	18.09	25.93	43.31	12.25	18.60	51.83
12	17	4.25	20.64	14.66	-28.95	21.75	19.25	-11.48	24.66	21.10	-14.45	20.64	18.32	-11.21	16.89	11.58	-31.45	14.55	9.86	-32.26	9.89	12.80	29.36	14.06	12.87	-8.49	7.48	16.31	117.96	4.23	6.61	56.02
13	8	2.00	20.19	18.24	-9.66	18.56	16.66	-10.21	18.46	16.36	-11.36	13.42	12.14	-9.54	9.41	5.76	-38.78	7.80	3.83	-53.53	5.09	6.11	20.20	6.89	6.96	1.01	3.52	8.95	154.10	1.81	2.65	46.67
14	14	3.50	19.15	11.08	-42.14	22.56	20.29	-10.06	28.59	23.74	-16.97	27.20	23.31	-14.28	25.29	18.44	-27.09	22.28	17.69	-20.59	15.41	19.81	28.57	22.39	18.62	-16.82	12.18	22.72	86.51	7.40	11.96	61.65
15	10	2.50	25.56	20.70	-19.01	23.86	21.87	-8.34	24.32	21.39	-12.05	18.84	17.50	-7.10	13.41	10.46	-22.01	10.66	8.51	-38.91	6.45	8.53	32.24	8.12	8.50	4.74	3.96	10.59	167.89	1.93	2.85	47.78
16	4	1.00	19.86	10.53	-46.46	23.89	21.80	-8.74	31.39	25.40	-19.09	31.88	26.15	-17.96	30.67	22.83	-25.57	26.40	21.70	-17.82	17.46	22.65	29.72	24.25	20.48	-15.57	12.84	23.83	85.53	7.65	12.88	68.33
17	12	3.00	13.15	5.46	-58.49	17.97	16.73	-6.90	26.89	20.42	-24.06	32.96	23.88	-27.54	36.54	26.02	-28.79	30.94	26.55	-14.18	19.51	24.96	27.94	26.07	21.69	-16.90	13.63	22.01	61.43	8.49	14.85	74.83
18	12	3.00	20.10	23.23	15.56	15.47	16.42	6.12	13.14	13.36	1.81	8.43	9.12	8.17	4.84	4.01	-17.14	3.61	0.79	-78.06	2.03	1.88	-7.70	2.36	2.41	2.07	1.06	3.23	199.46	0.45	0.45	-0.90
19	17	4.25	30.58	22.52	-26.34	28.39	26.47	-6.76	29.34	25.51	-13.07	24.28	22.62	-6.86	17.43	16.28	-6.59	13.16	10.10	-23.26	7.34	10.82	47.46	8.55	9.58	11.94	3.99	11.30	183.30	1.88	3.09	64.17
20	18	4.50	20.81	10.67	-48.74	25.04	22.77	-9.09	33.22	25.49	-23.25	36.20	27.14	-25.03	34.63	26.13	-24.54	27.78	23.59	-15.08	16.34	22.73	39.06	20.25	19.49	-3.75	9.98	20.53	105.68	5.50	10.45	89.84
21	18	4.50	30.22	20.04	-33.67	29.82	27.34	-8.31	32.81	27.31	-16.78	29.39	25.84	-12.76	22.70	20.35	-10.34	17.28	14.27	-17.38	9.84	14.46	49.94	11.30	12.46	10.19	5.32	14.15	166.14	2.61	4.69	79.61
22	31	7.75	27.78	26.25	-9.09	22.60	22.77	0.74	20.65	19.81	-4.11	15.10	15.99	5.87	9.51	10.08	6.05	8.95	4.52	-34.99	3.75	5.11	36.31	4.23	4.72	11.38	1.93	5.81	200.72	0.87	1.17	34.15
23	11	2.75	26.42	15.38	-41.77	28.95	26.20	-9.50	35.12	27.78	-20.89	34.78	27.77	-20.16	30.00	24.31	-18.98	23.45	19.72	-15.93	13.42	19.48	45.19	16.10	16.70	3.74	7.71	18.30	137.20	3.96	7.54	89.14
24	19	5.00	31.96	20.31	-36.47	29.94	27.48	-8.23	31.93	26.27	-17.73	29.50	25.34	-14.13	21.53	21.91	1.78	14.92	14.13	-5.32	7.16	12.76	78.25	7.17	10.06	40.62	3.03	10.20	236.64	1.29	2.68	107.16
	Area (km^2)	109.75																														
Volume of Rainfall (mm-km^2/hr)			1662.21	1151.22	-30.74	1777.29	1630.48	-8.26	2154.57	1817.90	-15.63	2069.59	1797.27	-13.16	2008.52	1520.93	-24.28	1820.83	1520.96	-16.47	1354.61	1633.06	20.56	2227.92	1556.38	-30.14	1363.99	1885.68	38.25	1056.97	1342.08	26.97
Root Mean Square Error					6.38			1.87			4.08			3.97			5.57			3.46			3.47			8.18			7.07			3.51

APPENDIX G

Forecast of Spatial Distribution of Subcatchment Rainfall

Artificial Event No.130

Sub-Catchment No.	No. of Cell	Area		Time step 1			Time step 2			Time step 3			Time step 4			Time step 5			Time step 6			Time step 7			Time step 8			Time step 9			Time step 10			Time step 11	
			Actual	Predicted	% error	Actual	Predicted	% error	Actual	Predicted	% error	Actual	Predicted	% error	Actual	Predicted	% error	Actual	Predicted	% error	Actual	Predicted	% error	Actual	Predicted	% error	Actual	Predicted	% error	Actual	Predicted	% error	Actual	Predicted	% error
	(no.)	(km²)	(mm/hr)	(mm/hr)	(%)	(mm/hr)	(mm/hr)	(%)	(mm/hr)	(mm/hr)	(%)	(mm/hr)	(mm/hr)	(%)	(mm/hr)	(mm/hr)	(%)	(mm/hr)	(mm/hr)	(%)	(mm/hr)	(mm/hr)	(%)	(mm/hr)	(mm/hr)	(%)	(mm/hr)	(mm/hr)	(%)	(mm/hr)	(mm/hr)	(%)	(mm/hr)	(mm/hr)	(%)
1	27	6.75	0.64	0.96	48.52	1.60	3.94	145.33	3.10	2.61	-15.67	5.89	5.29	-10.16	9.47	7.61	-19.69	14.25	11.83	-16.98	13.88	16.48	18.76	19.14	15.35	-19.80	24.06	19.14	-20.44	29.30	20.68	-29.41	25.60	24.42	-4.62
2	35	8.75	1.96	0.02	-99.12	4.24	9.35	120.31	7.21	4.59	-36.40	11.66	10.35	-11.20	15.64	13.57	-13.25	18.74	16.49	-12.04	16.90	19.11	24.86	18.50	15.60	-15.69	19.84	19.58	-0.30	22.05	18.67	-15.33	17.30	20.98	21.28
3	28	7.00	3.98	0.52	-86.89	7.42	14.17	90.95	10.99	7.19	-34.57	14.94	13.46	-9.90	16.40	15.55	-5.19	15.40	14.66	-4.83	10.43	13.92	33.48	11.17	9.99	-10.56	10.07	12.80	27.20	10.69	10.45	-2.29	7.77	11.82	52.13
4	36	9.00	0.42	1.78	327.31	1.07	2.07	92.54	2.14	2.02	-5.49	4.31	3.59	-16.68	7.70	5.59	-27.44	12.96	10.49	-19.17	13.86	15.99	16.34	19.41	16.72	-13.87	25.79	19.53	-24.26	30.01	22.01	-26.66	26.13	24.51	-2.48
5	14	3.50	1.49	0.01	-99.52	3.38	6.90	104.27	5.97	4.10	-31.32	10.40	9.09	-12.56	16.01	12.64	-19.77	22.18	18.55	-16.38	20.36	23.48	15.32	24.94	21.57	-13.52	28.27	24.90	-11.91	29.51	25.24	-14.47	21.50	25.88	20.29
6	23	5.75	5.21	0.46	-91.16	9.75	17.40	78.42	14.49	9.64	-33.47	20.18	18.03	-10.67	23.81	21.46	-9.87	23.82	22.50	-5.91	17.10	22.22	29.88	17.87	16.64	-6.84	18.25	19.53	20.18	15.81	16.67	5.48	10.40	16.59	59.42
7	13	3.25	3.33	0.04	-98.85	6.75	12.28	81.95	10.79	7.05	-34.65	16.78	14.62	-12.78	23.08	19.12	-17.14	27.62	23.93	-13.36	22.66	26.79	18.28	26.11	22.78	-9.28	25.36	25.75	1.56	24.51	24.35	-0.65	18.22	23.47	44.98
8	23	5.75	0.90	0.60	-33.69	2.06	2.97	43.96	3.70	2.26	-38.44	6.76	5.03	-25.56	11.54	7.91	-31.49	17.87	13.98	-21.76	17.99	19.71	9.67	22.26	20.63	-7.30	26.68	22.56	-15.46	28.40	23.97	-9.19	18.31	23.14	26.39
9	19	4.75	10.64	8.81	-16.28	15.78	21.55	36.55	18.95	15.81	-16.59	20.32	18.12	-5.88	17.98	18.52	2.89	12.61	13.76	9.13	8.62	9.45	36.54	5.79	5.77	-0.29	4.04	6.29	55.74	3.46	4.12	19.04	1.92	4.37	127.46
10	6	1.50	8.91	4.00	-55.12	14.52	21.96	51.21	18.97	14.06	-25.77	22.51	20.46	-9.01	22.20	21.53	-3.01	17.79	18.27	2.71	10.66	14.68	37.74	9.77	8.60	-1.73	7.51	10.98	46.25	6.74	7.97	18.27	3.98	7.88	98.19
11	23	5.75	3.18	0.07	-97.86	8.24	10.42	66.85	9.79	6.64	-32.20	15.20	13.14	-13.52	21.96	17.37	-20.89	27.37	22.83	-16.57	23.31	26.12	12.06	25.09	23.69	-5.59	25.43	25.34	-0.35	22.77	24.37	7.05	13.91	21.60	55.33
12	17	4.25	9.75	3.41	-65.07	18.18	23.76	46.86	21.56	15.63	-27.52	26.79	23.89	-10.80	29.00	26.29	-9.32	25.66	25.29	-1.44	16.69	22.21	33.07	15.46	15.64	1.11	12.49	16.89	35.22	10.72	13.25	23.60	6.06	11.61	90.91
13	8	2.00	12.68	8.70	-31.41	19.06	25.04	31.20	23.26	18.34	-21.16	25.78	23.41	-9.19	24.41	23.61	-3.26	18.34	19.49	6.26	10.51	14.60	38.90	8.97	9.28	3.40	6.48	9.73	50.07	5.36	6.75	26.00	2.88	6.15	113.47
14	14	3.50	7.02	1.23	-82.51	12.52	19.68	57.18	17.84	12.44	-30.27	24.28	21.47	-11.58	29.56	25.41	-14.05	30.06	27.69	-7.91	21.81	27.16	24.62	21.47	21.19	-1.27	19.00	22.81	20.09	16.57	19.72	19.02	9.67	17.19	77.86
15	10	2.50	14.57	9.88	-32.19	21.68	26.93	24.19	26.18	20.62	-21.25	29.09	26.06	-10.45	28.47	26.53	-6.83	21.96	23.14	5.39	12.86	17.84	38.73	10.69	11.71	9.53	7.68	11.58	50.99	5.97	8.31	39.24	3.00	6.61	120.41
16	4	1.00	6.46	0.98	-84.91	11.58	17.93	54.86	16.58	11.78	-28.99	22.97	20.35	-11.41	29.23	24.48	-16.28	31.04	27.83	-10.36	23.33	28.05	20.28	22.82	22.90	0.33	20.48	24.00	17.20	17.20	21.25	23.55	9.64	17.68	83.38
17	12	3.00	3.11	0.27	-91.43	5.86	8.68	48.36	8.80	6.22	-29.35	13.29	11.33	-14.78	19.57	14.83	-24.19	24.44	19.93	-18.45	20.95	22.83	8.99	21.34	21.92	2.70	21.03	22.10	5.10	17.11	21.24	24.17	9.40	16.81	78.88
18	12	3.00	17.00	20.33	19.55	21.94	24.04	9.57	23.27	21.94	-5.69	21.95	21.50	-2.04	17.82	19.17	7.56	10.93	13.56	24.08	5.36	8.08	50.53	3.95	4.55	15.10	2.42	3.92	61.85	1.77	2.30	30.19	0.81	2.15	163.96
19	17	4.25	16.24	12.20	-24.87	23.12	26.40	14.17	26.97	22.00	-18.44	29.47	26.50	-10.06	29.66	27.02	-8.88	23.33	24.71	5.91	13.97	19.45	39.20	11.28	13.43	19.01	8.10	12.40	53.06	5.93	9.35	57.75	2.61	6.56	133.74
20	18	4.50	6.32	1.52	-75.90	10.80	15.44	42.99	14.87	11.27	-24.25	20.12	17.98	-10.64	26.20	21.42	-18.23	26.03	24.77	-11.64	21.30	24.93	17.01	19.80	21.53	8.71	17.36	21.16	21.86	13.30	16.92	42.24	6.75	13.91	106.24
21	18	4.50	13.90	8.95	-35.61	20.47	24.36	19.02	24.66	19.78	-19.76	28.24	25.37	-10.19	30.41	26.86	-11.67	25.90	26.17	1.06	16.54	22.07	33.44	13.78	16.26	18.01	10.42	15.22	45.98	7.65	12.15	58.73	3.66	8.43	130.27
22	31	7.75	19.52	20.05	2.70	25.20	25.88	2.68	26.88	23.91	-11.04	26.21	24.53	-6.43	23.17	22.97	-0.88	15.65	18.53	18.41	8.38	12.59	50.15	8.32	7.88	24.60	4.17	8.69	60.66	2.98	4.82	56.17	1.37	3.32	141.88
23	11	2.75	9.76	4.14	-57.64	15.60	20.64	32.28	20.19	15.68	-22.34	25.24	22.66	-10.21	29.99	25.46	-15.09	28.71	26.99	-6.00	20.03	24.96	24.61	17.62	19.91	13.02	14.33	19.23	34.19	10.69	16.29	52.36	5.22	11.57	121.52
24	19	6.00	14.74	10.92	-25.92	20.10	21.25	5.70	22.58	19.26	-14.71	24.28	22.36	-7.94	25.63	22.93	-10.55	20.80	22.20	6.72	12.86	17.97	39.78	9.78	13.67	39.72	6.89	11.47	66.47	4.44	9.14	105.55	1.83	6.09	178.22
	Area (km²)	109.75																																	
Volume of Rainfall (mm-km²/hr)			792.80	525.20	-33.75	1221.51	1660.72	35.98	1563.67	1218.90	-22.05	1937.14	1741.23	-10.11	2223.34	1960.80	-11.81	2225.50	2090.20	-6.08	1671.15	2061.42	24.55	1759.54	1704.35	-3.14	1749.81	1651.42	5.81	1715.91	1704.35	-0.67	1584.66	1628.07	2.74
Root Mean Square Error					3.88			4.94			3.88			2.09			3.06			2.55			4.09			1.97			3.59			3.85			5.08

APPENDIX G
Forecast of Spatial Distribution of Subcatchment Rainfall

Artificial Event No.131																														
Sub-Catchment No.	No. of Cell	Area		Time step 1			Time step 2			Time step 3			Time step 4			Time step 5			Time step 6			Time step 7			Time step 8			Time step 9		
			Actual	Predicted	% error	Actual	Predicted	% error	Actual	Predicted	% error	Actual	Predicted	% error	Actual	Predicted	% error	Actual	Predicted	% error	Actual	Predicted	% error	Actual	Predicted	% error	Actual	Predicted	% error
	(no.)	(km^2)	(mm/hr)	(mm/hr)	(%)	(mm/hr)	(mm/hr)	(%)	(mm/hr)	(mm/hr)	(%)	(mm/hr)	(mm/hr)	(%)	(mm/hr)	(mm/hr)	(%)	(mm/hr)	(mm/hr)	(%)	(mm/hr)	(mm/hr)	(%)	(mm/hr)	(mm/hr)	(%)	(mm/hr)	(mm/hr)	(%)
1	27	6.75	22.17	25.57	15.34	21.47	20.04	-6.64	15.69	18.99	21.05	10.66	10.59	-0.70	7.29	7.06	-3.13	4.75	4.09	-13.96	1.81	1.91	5.70	0.99	3.21	225.14	0.78	2.39	205.36
2	35	8.75	25.50	28.79	12.89	26.89	23.33	-13.25	22.86	24.32	6.42	17.47	18.18	4.07	13.62	13.94	2.36	10.07	10.23	1.61	4.48	5.54	23.77	2.67	4.52	69.65	2.18	2.15	-1.25
3	28	7.00	19.16	22.93	19.66	21.74	19.31	-11.14	21.40	20.93	-2.18	18.46	19.83	7.38	16.48	17.16	4.11	13.86	14.78	6.61	7.24	9.29	28.33	4.67	6.11	30.86	3.90	2.80	-28.29
4	36	9.00	17.93	21.02	17.20	17.66	16.74	-5.22	12.52	15.53	24.09	8.16	7.65	-6.23	5.36	4.88	-9.17	3.42	2.43	-28.91	1.27	1.24	-2.76	0.72	2.96	308.30	0.60	2.84	376.86
5	14	3.50	25.30	28.03	10.77	27.53	23.09	-16.14	22.65	24.50	8.18	16.44	16.66	1.36	12.19	12.31	0.94	8.83	8.49	-3.77	3.80	5.06	33.10	2.40	4.85	101.91	2.06	3.21	56.00
6	23	5.75	24.59	27.99	13.84	29.34	24.03	-18.09	29.25	27.67	-5.39	24.89	25.84	3.80	22.02	22.26	1.10	18.76	19.25	2.62	9.90	13.15	32.84	6.84	8.90	30.04	6.00	5.09	-15.10
7	13	3.25	27.07	29.73	9.83	31.75	25.24	-20.50	29.21	28.72	-1.70	23.01	23.37	1.57	18.75	18.86	0.60	15.01	14.87	-0.93	7.33	9.89	35.04	5.09	7.45	46.36	4.56	4.72	3.44
8	23	5.75	17.53	19.53	11.39	19.58	16.45	-15.99	15.75	17.30	9.82	11.01	10.41	-5.49	7.90	7.37	-6.70	5.69	4.54	-20.17	2.44	2.88	17.97	1.65	3.36	103.09	1.49	2.78	86.02
9	19	4.75	10.34	13.07	26.46	14.17	12.69	-10.43	17.98	14.68	-18.36	18.45	19.43	5.29	20.16	19.89	-1.33	21.16	20.94	-1.03	14.43	18.10	25.42	11.65	13.58	16.58	10.79	10.68	-1.07
10	6	1.50	15.95	19.42	21.75	20.75	17.70	-14.71	24.05	20.87	-13.25	23.01	24.02	4.38	23.19	23.00	-0.82	22.43	22.50	0.32	13.81	17.67	27.94	10.42	12.20	17.09	9.40	8.23	-12.41
11	23	5.75	22.34	24.19	8.29	27.54	21.14	-23.23	25.90	25.03	-3.38	20.36	20.56	0.99	16.69	16.83	0.86	13.78	13.57	-1.50	6.96	9.95	42.51	5.31	7.42	39.68	5.04	5.28	4.77
12	17	4.25	20.37	23.44	15.03	27.03	21.29	-21.22	30.61	26.51	-13.39	28.28	28.68	1.44	27.60	26.83	-2.80	26.44	25.79	-2.45	16.09	20.81	29.34	12.82	14.34	11.90	12.06	10.24	-15.08
13	8	2.00	13.74	16.51	20.18	19.14	15.83	-17.31	23.92	19.53	-18.37	23.96	24.45	2.05	25.59	24.50	-4.28	26.68	25.36	-4.92	18.02	22.10	22.63	15.08	16.24	7.67	14.37	12.86	-10.50
14	14	3.50	24.11	26.79	11.10	31.07	23.84	-23.28	32.64	29.39	-9.98	28.24	28.57	1.17	25.68	25.33	-1.36	23.14	22.84	-1.31	13.06	17.61	34.77	10.21	12.16	19.13	9.63	8.47	-11.99
15	10	2.50	14.39	16.57	15.16	20.83	16.23	-22.09	26.54	21.15	-20.31	26.59	26.59	0.01	28.53	26.74	-6.26	30.32	27.96	-7.78	20.93	25.39	21.31	18.55	18.81	1.43	18.34	15.66	-14.60
16	4	1.00	22.77	24.90	9.34	29.97	22.45	-25.09	31.46	28.30	-10.04	26.89	27.23	1.25	24.21	24.10	-0.43	21.87	21.63	-1.12	12.36	17.15	38.74	10.00	11.93	19.24	9.67	8.68	-10.29
17	12	3.00	16.03	16.48	2.84	21.17	15.34	-27.53	20.95	19.33	-7.77	16.78	16.83	0.27	14.17	14.38	1.54	12.34	12.16	-1.49	6.68	9.93	48.62	5.67	7.13	25.73	5.74	5.61	-2.32
18	12	3.00	6.45	7.93	22.93	10.07	8.81	-12.56	14.82	10.80	-27.12	16.67	17.10	2.59	20.36	19.23	-5.54	24.50	22.43	-8.43	19.72	23.21	17.71	18.93	19.63	3.74	19.17	18.91	-1.36
19	17	4.25	13.02	14.02	7.68	19.70	14.38	-27.03	25.76	19.98	-22.45	25.95	25.76	-0.72	28.27	26.32	-6.88	31.27	28.10	-10.14	22.76	27.24	19.68	22.29	20.75	-6.89	23.43	18.73	-20.08
20	18	4.50	16.68	17.38	4.21	23.40	16.66	-28.80	25.71	22.35	-13.08	22.32	22.71	1.73	20.62	20.78	0.79	19.60	19.43	-0.84	11.78	16.89	43.33	10.63	11.77	10.77	10.98	9.49	-13.51
21	18	4.50	14.29	15.15	6.00	21.38	15.30	-28.42	26.87	21.43	-20.27	26.12	26.09	-0.10	27.42	26.02	-5.09	29.47	27.04	-8.23	20.72	25.76	24.32	20.29	19.11	-5.85	21.50	16.92	-21.33
22	31	7.75	8.25	9.09	10.19	13.05	10.10	-22.57	18.70	13.70	-26.75	20.36	20.36	0.01	24.22	22.27	-8.05	29.15	25.49	-12.57	23.57	26.67	13.16	24.28	22.12	-8.89	25.87	21.58	-16.65
23	11	2.75	16.36	17.33	5.89	23.77	16.95	-28.70	27.95	23.38	-16.34	25.65	25.92	1.05	25.21	24.69	-2.05	25.40	24.35	-4.13	16.42	22.05	34.24	15.33	15.65	2.14	15.96	13.09	-17.99
24	19	5.00	8.76	8.29	-5.40	14.44	9.63	-33.33	19.87	14.97	-24.67	20.25	20.62	1.81	22.58	21.68	-3.99	26.38	23.85	-9.60	20.47	24.89	21.55	22.75	18.93	-16.78	25.82	18.19	-29.58
	Area (km^2)	109.75																												
Volume of Rainfall (mm-km^2/hr)			1960.60	2203.90	12.41	2390.53	1948.30	-18.50	2436.29	2263.25	-7.10	2123.92	2154.90	1.46	1997.82	1948.95	-2.45	1917.95	1816.50	-5.29	1218.13	1522.93	25.02	1072.91	1179.25	9.91	1079.66	958.15	-11.25
Root Mean Square Error					2.41			4.88			3.55			0.55			0.88			1.49			3.64			1.87			2.58

APPENDIX G
Forecast of Spatial Distribution of Subcatchment Rainfall

Artificial Event No.132

Sub-Catchment No.	No. of Cell (no.)	Area (km^2)	Time step 1 Actual (mm/hr)	Time step 1 Predicted (mm/hr)	Time step 1 % error (%)	Time step 2 Actual (mm/hr)	Time step 2 Predicted (mm/hr)	Time step 2 % error (%)	Time step 3 Actual (mm/hr)	Time step 3 Predicted (mm/hr)	Time step 3 % error (%)	Time step 4 Actual (mm/hr)	Time step 4 Predicted (mm/hr)	Time step 4 % error (%)	Time step 5 Actual (mm/hr)	Time step 5 Predicted (mm/hr)	Time step 5 % error (%)	Time step 6 Actual (mm/hr)	Time step 6 Predicted (mm/hr)	Time step 6 % error (%)	Time step 7 Actual (mm/hr)	Time step 7 Predicted (mm/hr)	Time step 7 % error (%)	Time step 8 Actual (mm/hr)	Time step 8 Predicted (mm/hr)	Time step 8 % error (%)	Time step 9 Actual (mm/hr)	Time step 9 Predicted (mm/hr)	Time step 9 % error (%)	Time step 10 Actual (mm/hr)	Time step 10 Predicted (mm/hr)	Time step 10 % error (%)	Time step 11 Actual (mm/hr)	Time step 11 Predicted (mm/hr)	Time step 11 % error (%)
1	27	6.75	0.72	7.86	984.96	1.33	1.73	29.96	3.74	4.11	10.07	4.96	2.43	-51.03	8.59	8.00	-6.89	14.50	11.06	-23.75	22.09	16.36	-25.91	22.55	18.13	-19.60	26.04	19.47	-25.23	27.43	22.79	-16.91	19.45	25.61	31.64
2	35	8.75	2.14	9.05	323.83	3.35	1.39	-58.54	7.80	5.92	-24.09	8.91	5.20	-41.61	13.07	11.11	-15.00	18.06	14.44	-19.98	23.54	18.43	-21.70	19.41	19.86	2.32	18.88	17.44	-7.61	17.44	18.54	6.33	11.10	18.28	64.61
3	28	7.00	4.14	9.13	120.40	5.40	2.52	-53.33	10.28	6.76	-34.07	9.94	6.68	-32.79	12.30	9.73	-20.93	13.84	11.77	-14.97	15.43	12.84	-16.82	10.34	13.05	26.19	8.69	9.33	7.36	7.21	9.34	29.45	4.22	8.04	90.37
4	36	9.00	0.50	6.73	1237.32	1.02	2.00	96.71	3.03	3.96	31.62	4.31	2.67	-37.97	7.81	8.18	4.69	14.06	11.04	-21.47	22.63	16.61	-27.06	24.90	18.36	-25.36	28.48	21.62	-24.46	29.78	24.40	-18.06	20.84	27.17	30.34
5	14	3.50	1.79	8.85	394.65	3.17	1.77	-44.18	7.99	7.19	-10.02	9.98	7.26	-27.22	15.51	14.66	-5.51	23.17	18.37	-20.72	32.38	23.66	-26.92	28.73	25.40	-11.60	27.69	24.94	-9.91	24.96	25.17	0.85	15.39	24.33	58.11
6	23	5.75	5.63	11.93	104.78	8.13	3.90	-51.99	15.62	11.26	-28.84	15.94	12.63	-20.76	19.66	17.36	-12.71	22.74	19.86	-12.66	25.63	21.20	-17.61	17.40	21.63	24.32	13.78	16.01	16.14	10.76	14.34	33.36	5.92	11.38	92.35
7	13	3.25	4.00	10.68	171.60	6.41	2.89	-54.91	14.04	10.78	-23.16	15.83	12.49	-21.09	21.76	19.66	-9.56	29.15	23.06	-18.11	36.35	26.62	-24.72	27.00	27.83	3.07	22.80	24.27	6.44	18.55	22.39	20.74	10.50	19.18	82.70
8	23	5.75	1.17	5.90	404.61	2.26	1.32	-41.44	5.92	5.43	-8.30	7.87	6.05	-23.09	12.95	12.42	-1.64	19.96	15.58	-21.94	29.40	20.74	-29.46	27.71	22.44	-19.02	26.67	24.56	-7.90	23.62	24.40	2.46	14.48	23.59	62.89
9	19	4.75	11.41	13.10	14.79	12.32	11.53	-6.47	17.62	13.06	-25.85	13.91	13.63	-2.07	13.26	11.43	-13.80	10.99	10.81	-1.63	9.77	8.25	-15.51	4.70	7.46	59.20	2.85	3.55	24.42	1.82	2.82	55.12	0.85	1.72	102.69
10	6	1.50	9.67	13.03	34.79	11.53	8.06	-29.91	18.62	12.96	-30.26	16.15	14.32	-11.34	17.07	14.55	-14.78	15.96	15.03	-5.92	15.55	13.35	-14.17	8.46	12.80	51.25	5.96	7.30	28.96	3.86	5.88	51.83	1.91	3.78	97.63
11	23	5.75	4.06	9.33	129.07	6.77	3.04	-55.06	14.63	11.23	-23.25	16.79	14.40	-14.26	22.74	20.68	-9.05	29.27	23.46	-19.84	36.97	26.56	-28.15	26.09	27.66	-1.44	22.60	25.18	11.90	17.42	22.03	26.43	9.41	17.91	90.26
12	17	4.25	11.35	14.60	30.45	14.64	8.88	-39.36	24.66	17.19	-30.27	22.66	20.59	-9.11	24.78	22.01	-11.21	24.42	22.65	-7.27	24.94	21.01	-15.76	14.33	20.64	44.03	9.59	13.12	36.80	6.52	9.86	51.17	3.19	6.09	91.07
13	8	2.00	14.28	15.31	7.23	16.32	12.98	-21.13	24.09	17.06	-29.13	19.84	19.16	-3.40	19.38	17.18	-11.37	16.65	16.43	-1.36	15.30	13.24	-13.48	7.63	12.35	61.76	4.62	6.43	39.00	2.92	4.51	54.65	1.34	2.36	75.72
14	14	3.50	8.62	13.50	56.47	12.19	6.28	-48.51	22.75	16.24	-28.62	22.86	20.21	-11.66	27.31	24.44	-10.51	30.00	26.21	-12.63	33.39	26.54	-20.52	21.47	26.61	24.06	15.44	20.02	29.69	11.05	16.02	45.04	5.61	11.27	100.87
15	10	2.50	17.20	16.73	-2.74	20.30	15.00	-26.10	29.86	20.78	-30.41	24.93	24.45	-1.94	24.12	21.92	-9.14	20.59	20.58	-0.07	18.92	16.59	-12.30	9.22	15.58	67.25	6.37	8.39	56.25	3.23	5.29	63.53	1.43	2.34	64.16
16	4	1.00	8.15	12.68	55.55	12.13	8.10	-49.73	23.00	16.58	-27.96	23.76	21.43	-9.78	28.62	25.73	-10.11	31.94	27.36	-14.36	36.12	27.53	-22.96	23.53	29.20	19.54	16.61	22.10	33.04	11.64	17.35	49.04	5.79	11.98	106.98
17	12	3.00	4.30	7.32	70.25	7.24	3.23	-55.36	14.96	10.98	-26.56	17.02	15.59	-8.38	22.06	19.83	-6.62	27.20	21.78	-19.96	33.58	23.77	-29.23	24.37	24.57	0.79	17.88	22.81	27.53	12.62	18.60	44.32	6.46	13.72	112.48
18	12	3.00	19.28	16.29	-15.51	19.21	20.53	6.86	23.36	18.90	-20.38	16.71	16.53	10.91	13.73	13.71	-0.18	9.64	11.16	16.06	7.62	6.97	-8.53	3.07	6.90	92.48	1.52	2.06	36.44	0.62	1.10	34.30	0.33	0.33	1.01
19	17	4.25	20.44	16.97	-16.97	24.43	17.39	-28.81	34.63	23.70	-31.57	28.88	28.94	0.20	27.16	25.48	-6.32	22.73	22.26	2.26	20.61	18.54	-10.09	10.18	17.46	72.31	5.59	9.99	78.70	3.28	5.80	61.53	1.39	2.40	72.98
20	18	4.50	8.54	10.67	24.93	12.93	8.86	-48.48	23.61	16.53	-29.71	24.16	22.78	-5.69	27.95	25.06	-10.36	30.06	25.70	-14.50	33.38	25.31	-24.16	20.90	25.48	21.92	13.50	20.52	51.06	8.86	14.86	67.71	4.12	9.22	123.54
21	18	4.50	18.01	15.66	-13.06	22.79	14.54	-34.87	34.01	23.04	-32.26	29.80	28.27	-1.79	29.30	27.07	-7.63	26.01	25.42	-2.30	24.99	21.48	-14.04	12.97	20.63	59.13	7.43	13.16	77.09	4.43	8.18	84.50	1.93	3.79	96.29
22	31	7.75	23.79	17.85	-24.22	25.24	21.86	-13.03	31.39	22.79	-27.39	23.54	26.62	9.68	19.84	19.78	-0.24	14.63	16.09	14.06	12.21	11.53	-5.59	6.31	10.31	64.01	2.74	4.86	77.17	1.53	2.56	66.57	0.64	0.67	3.63
23	11	2.75	12.90	13.44	4.14	17.96	10.34	-42.46	29.83	20.45	-31.42	26.42	27.18	-4.34	30.44	27.48	-9.72	29.83	27.06	-9.27	30.84	24.83	-19.49	17.57	24.48	39.38	10.67	17.66	65.48	6.62	11.85	78.92	2.98	6.39	115.77
24	19	5.00	20.29	13.60	-32.97	25.23	16.05	-36.39	34.67	22.70	-34.53	29.22	29.70	1.63	26.50	25.37	-4.26	21.54	22.61	4.94	19.51	17.79	-8.80	9.16	16.77	83.06	4.56	10.57	131.89	2.41	5.60	132.75	0.94	1.78	89.82
	Area (km^2)	109.75																																	
Volume of Rainfall (mm-km^2/hr)			964.90	1256.75	30.45	1207.24	839.27	-30.48	1936.96	1411.62	-27.12	1805.61	1840.25	-9.15	2039.08	1867.66	-8.41	2229.79	1978.57	-11.27	2583.35	2038.73	-21.08	1871.26	2075.25	10.90	1597.18	1704.53	6.72	1368.80	1538.96	12.66	913.79	1330.90	45.66
Root Mean Square Error					4.76			4.75			6.51			2.16			2.05			3.24			5.87			4.89			4.15			3.61			5.26

APPENDIX G
Forecast of Spatial Distribution of Subcatchment Rainfall

Artificial Event No.133

Sub-Catchment No.	No. of Cell	Area		Time step 1			Time step 2			Time step 3			Time step 4			Time step 5			Time step 6			Time step 7			Time step 8			Time step 9		
			Actual	Predicted	% error	Actual	Predicted	% error	Actual	Predicted	% error	Actual	Predicted	% error	Actual	Predicted	% error	Actual	Predicted	% error	Actual	Predicted	% error	Actual	Predicted	% error	Actual	Predicted	% error
	(no.)	(km^2)	(mm/hr)	(mm/hr)	(%)	(mm/hr)	(mm/hr)	(%)	(mm/hr)	(mm/hr)	(%)	(mm/hr)	(mm/hr)	(%)	(mm/hr)	(mm/hr)	(%)	(mm/hr)	(mm/hr)	(%)	(mm/hr)	(mm/hr)	(%)	(mm/hr)	(mm/hr)	(%)	(mm/hr)	(mm/hr)	(%)
1	27	6.75	2.55	1.83	-28.30	4.27	1.79	-58.01	7.37	6.93	-5.99	7.54	7.28	-3.48	7.93	10.36	30.60	7.81	9.99	27.83	9.25	8.43	-8.94	5.67	9.63	69.79	5.11	4.55	-10.93
2	35	8.75	6.77	2.44	-63.94	9.14	6.96	-23.68	13.51	11.27	-16.57	11.51	12.35	7.33	9.90	12.32	24.37	8.44	10.06	19.12	8.60	7.61	-11.46	4.58	5.73	25.01	3.50	4.83	38.05
3	28	7.00	12.00	5.49	-54.27	12.70	13.71	7.93	15.79	12.33	-21.96	10.87	13.04	19.94	7.40	9.21	24.49	5.28	6.02	13.88	4.47	3.82	-14.61	2.00	0.78	-61.04	1.23	3.55	188.58
4	36	9.00	1.61	1.11	-30.99	3.08	0.55	-82.15	5.82	5.65	-2.84	6.83	6.21	-9.19	8.45	11.20	32.56	9.58	12.74	33.04	13.10	12.46	-4.85	9.29	16.60	78.74	9.97	8.51	-14.59
5	14	3.50	4.96	0.77	-84.45	8.03	3.94	-50.88	13.34	11.71	-12.24	13.59	13.57	-0.16	14.46	17.19	18.91	14.78	17.06	15.46	18.13	15.54	-14.29	11.65	16.91	45.15	11.10	10.85	-2.26
6	23	5.75	14.73	5.12	-65.24	17.26	16.11	-6.64	22.83	18.28	-19.93	17.51	20.26	15.68	13.62	16.75	22.92	10.99	12.63	14.88	10.54	9.40	-10.88	5.37	5.39	0.30	3.87	6.69	72.77
7	13	3.25	9.66	1.82	-81.14	13.77	9.35	-32.08	20.78	17.11	-17.69	19.09	19.88	4.14	18.18	20.87	14.76	17.24	18.92	9.75	19.49	16.38	-15.95	11.84	15.19	30.53	10.11	11.48	13.60
8	23	5.75	2.80	0.01	-99.53	5.19	1.12	-78.48	9.41	7.84	-16.72	11.04	9.71	-12.03	13.90	15.67	12.75	16.45	18.44	12.09	23.44	19.20	-18.12	17.53	24.39	39.12	19.99	16.17	-19.12
9	19	4.75	23.69	16.44	-30.59	19.79	24.37	23.15	20.46	16.10	-21.30	11.73	15.88	35.37	6.65	8.69	30.66	4.26	4.73	11.04	3.20	2.72	-15.11	1.30	0.00	-100.00	0.71	2.84	300.62
10	6	1.50	21.94	11.77	-46.36	20.83	23.45	12.56	23.64	18.35	-22.37	15.08	19.13	26.85	9.58	12.13	26.67	6.85	7.48	12.61	5.43	4.77	-12.26	2.38	0.42	-82.48	1.42	4.22	196.08
11	23	5.75	8.33	0.91	-89.09	12.71	7.78	-38.80	19.95	18.24	-18.57	19.89	19.49	-2.01	21.04	22.14	5.22	22.05	22.10	0.19	27.61	21.01	-23.92	18.36	22.03	20.01	18.13	18.55	-8.70
12	17	4.25	22.97	9.68	-57.88	24.61	24.21	-1.63	30.20	23.47	-22.28	21.82	25.66	17.62	16.08	19.41	20.68	12.70	14.04	10.59	11.86	10.47	-11.73	5.95	5.39	-9.38	4.19	7.42	77.21
13	8	2.00	27.41	16.11	-41.23	24.96	27.50	10.10	27.31	21.10	-22.74	17.10	21.79	27.38	10.76	13.73	27.60	7.53	8.51	13.11	6.19	5.64	-8.99	2.75	0.96	-65.01	1.67	4.30	157.24
14	14	3.50	17.34	5.06	-70.83	21.46	18.27	-14.88	29.12	23.02	-20.94	23.98	26.23	9.37	20.46	23.32	14.01	18.10	19.32	6.77	19.01	16.01	-15.79	10.66	12.36	15.93	8.58	11.26	31.32
15	10	2.50	29.72	16.23	-45.38	28.49	29.29	2.81	32.05	24.58	-23.32	21.25	25.94	22.07	14.35	17.86	24.46	10.75	12.11	12.70	9.47	8.75	-7.65	4.52	3.60	-20.42	3.00	5.95	98.56
16	4	1.00	15.45	3.80	-75.40	20.32	16.20	-20.27	28.62	22.73	-20.60	25.08	26.38	5.15	23.04	24.96	8.38	21.77	22.15	1.76	24.43	19.50	-20.17	14.65	17.13	16.92	12.75	14.30	12.13
17	12	3.00	7.24	0.46	-93.67	11.47	6.70	-41.60	18.28	14.43	-21.04	19.23	17.88	-7.06	21.88	21.23	-2.96	24.72	22.85	-7.55	33.34	23.42	-29.76	24.00	26.13	8.84	25.99	20.83	-19.84
18	12	3.00	30.36	24.48	-19.40	23.23	28.24	21.56	22.25	18.40	-17.31	12.14	17.58	44.87	6.62	9.77	47.49	4.23	5.33	26.06	3.16	3.18	0.42	1.29	0.22	-83.23	0.71	1.89	166.64
19	17	4.25	29.61	15.92	-46.24	29.56	28.62	-3.18	33.96	26.14	-23.03	23.85	26.11	17.85	17.39	21.08	21.27	14.04	15.63	11.33	13.35	12.34	-7.62	6.91	7.65	10.79	5.03	8.03	59.75
20	18	4.50	13.39	3.08	-77.01	18.34	14.17	-22.71	26.30	20.66	-21.47	24.43	24.46	0.12	24.30	24.34	0.20	24.93	23.35	-6.32	30.42	22.28	-26.74	19.99	21.83	9.23	19.41	18.22	-6.10
21	18	4.50	25.66	11.96	-53.30	27.82	25.60	-7.99	33.84	26.07	-22.95	25.70	26.83	12.15	20.49	23.39	14.13	17.79	18.73	5.31	18.23	15.73	-13.71	10.14	11.74	15.77	8.06	10.83	34.39
22	31	7.75	32.63	22.79	-30.16	27.73	29.59	6.71	28.46	22.67	-20.36	17.47	22.95	31.34	11.05	15.14	37.02	8.06	9.96	23.48	6.94	7.17	3.38	3.28	3.13	-4.71	2.16	4.13	90.97
23	11	2.75	19.48	6.78	-65.19	23.87	20.44	-14.38	31.63	24.55	-22.37	26.65	28.13	5.53	23.80	25.18	5.79	22.50	22.10	-1.79	25.21	19.78	-21.52	15.26	17.17	12.54	13.41	14.82	10.46
24	19	5.00	23.40	11.58	-50.54	25.15	23.07	-8.27	30.04	23.31	-22.40	23.20	25.95	11.85	19.14	21.56	12.61	17.49	18.25	4.33	18.88	16.35	-13.29	11.15	13.80	23.71	9.51	11.81	24.13
	Area (km^2)	109.75																												
Volume of Rainfall (mm-km^2/hr)			1658.59	820.02	-50.56	1790.73	1630.60	-8.94	2265.80	1813.03	-19.98	1790.84	1991.28	11.20	1531.14	1797.17	17.37	1403.89	1539.10	9.63	1571.20	1323.45	-15.77	959.62	1174.42	22.38	879.71	969.67	10.23
Root Mean Square Error					9.54			3.22			5.17			2.99			2.61			1.51			3.69			2.99			2.43

APPENDIX G
Forecast of Spatial Distribution of Subcatchment Rainfall

Artificial Event No.134

Sub-Catchment No.	No. of Cell	Area		Time step 1			Time step 2			Time step 3			Time step 4			Time step 5			Time step 6			Time step 7			Time step 8			Time step 9		
			Actual	Predicted	% error	Actual	Predicted	% error	Actual	Predicted	% error	Actual	Predicted	% error	Actual	Predicted	% error	Actual	Predicted	% error	Actual	Predicted	% error	Actual	Predicted	% error	Actual	Predicted	% error
	(no.)	(km^2)	(mm/hr)	(mm/hr)	(%)	(mm/hr)	(mm/hr)	(%)	(mm/hr)	(mm/hr)	(%)	(mm/hr)	(mm/hr)	(%)	(mm/hr)	(mm/hr)	(%)	(mm/hr)	(mm/hr)	(%)	(mm/hr)	(mm/hr)	(%)	(mm/hr)	(mm/hr)	(%)	(mm/hr)	(mm/hr)	(%)
1	27	6.75	16.85	15.23	-9.58	18.74	15.27	-18.50	16.64	16.15	-2.93	12.57	13.09	4.11	9.53	7.63	-19.95	8.82	6.85	-22.35	4.96	5.10	2.96	2.81	4.32	53.53	1.13	4.21	273.90
2	35	8.75	14.61	13.34	-8.70	19.03	15.07	-20.82	20.68	18.16	-12.20	19.01	18.91	-0.54	17.21	15.79	-8.27	18.44	15.37	-16.63	12.62	14.94	18.35	8.34	10.09	20.98	4.04	8.70	115.39
3	28	7.00	7.56	6.93	-8.41	11.80	8.98	-23.94	16.12	12.76	-20.85	18.44	17.48	-5.20	20.52	19.55	-4.74	25.89	21.38	-17.45	22.00	24.05	9.33	17.21	17.51	1.75	10.34	15.00	45.07
4	36	9.00	20.48	19.22	-6.10	20.02	17.73	-11.47	15.23	16.61	9.08	10.01	11.32	13.13	6.46	5.07	-21.54	5.40	3.53	-34.66	2.72	1.51	-44.63	1.42	1.31	-7.28	0.50	1.52	202.30
5	14	3.50	25.09	21.84	-12.96	27.85	22.45	-18.81	24.55	23.45	-4.50	18.81	20.19	7.35	13.74	13.56	-1.30	12.87	10.69	-16.93	7.65	7.90	3.23	4.51	4.29	-4.76	1.85	3.79	104.29
6	23	5.75	14.55	12.10	-16.86	20.46	15.71	-23.19	24.71	20.45	-17.26	25.42	24.61	-3.17	24.63	24.74	0.45	28.78	23.98	-16.69	22.60	25.05	9.86	16.81	16.47	-2.00	9.22	14.10	52.89
7	13	3.25	24.49	20.57	-16.00	29.44	23.16	-21.32	29.23	25.96	-11.18	24.99	25.56	2.27	19.84	20.83	4.99	20.15	17.27	-14.30	13.51	15.01	11.11	8.71	8.02	-7.92	3.99	6.83	71.36
8	23	5.75	27.30	24.91	-8.75	26.25	22.99	-12.41	19.78	21.17	6.99	13.09	15.32	17.03	8.02	8.08	0.68	6.76	4.72	-30.17	3.61	1.95	-46.11	1.95	0.57	-71.08	0.71	0.49	-30.78
9	19	4.75	3.96	1.92	-51.84	7.17	4.20	-41.45	11.89	7.62	-35.94	16.59	14.29	-13.88	21.06	21.15	0.43	30.86	24.47	-20.69	33.29	30.04	-9.77	31.15	26.29	-15.58	22.97	24.14	5.09
10	6	1.50	7.10	4.72	-33.56	11.73	8.02	-31.66	17.37	12.62	-27.35	21.69	19.65	-9.42	24.97	25.02	0.19	33.63	26.98	-19.76	32.26	31.35	-2.82	27.54	24.50	-11.05	18.12	21.80	20.32
11	23	5.75	28.71	23.66	-17.61	31.68	25.17	-20.55	28.50	26.18	-8.13	22.42	23.94	6.79	15.85	18.43	16.27	15.18	13.55	-10.73	9.73	10.29	5.78	6.04	4.34	-28.11	2.60	3.65	40.69
12	17	4.25	13.34	9.32	-30.13	19.55	14.19	-27.44	25.09	19.60	-21.89	27.59	25.83	-6.38	27.34	28.83	5.46	33.58	27.88	-16.97	29.31	30.31	3.39	23.20	21.19	-8.66	13.70	18.65	36.15
13	8	2.00	6.96	3.71	-46.63	11.55	7.43	-35.69	17.31	12.01	-30.60	22.07	19.48	-11.76	25.15	25.85	2.78	34.47	27.54	-20.11	34.73	32.41	-6.66	30.73	26.58	-13.51	20.91	24.25	15.98
14	14	3.50	20.75	16.10	-22.40	27.13	20.72	-23.63	30.16	25.22	-16.36	28.94	28.41	-1.86	24.99	27.43	9.77	27.72	23.95	-13.61	21.32	23.50	10.22	15.27	13.91	-8.89	7.91	12.00	51.76
15	10	2.50	9.26	5.07	-45.25	14.55	9.81	-32.56	20.46	14.81	-27.60	24.70	22.06	-10.69	26.03	27.83	6.93	34.27	27.90	-18.59	33.43	31.98	-4.33	28.74	25.18	-12.39	18.65	23.09	23.83
16	4	1.00	24.25	18.93	-21.97	29.93	23.15	-22.64	31.02	26.60	-14.24	27.97	28.20	0.82	22.31	25.96	16.45	23.62	21.20	-10.25	17.36	19.48	12.18	11.97	10.33	-13.77	5.86	8.88	51.51
17	12	3.00	28.24	23.93	-15.27	29.39	24.28	-17.40	24.76	23.72	-4.20	18.48	20.68	11.95	11.91	15.63	31.18	10.98	10.24	-6.70	6.92	6.78	-2.14	4.23	1.92	-54.65	1.75	1.55	-11.21
18	12	3.00	3.00	0.51	-83.08	5.57	2.72	-51.20	9.66	5.69	-41.07	14.28	11.70	-18.07	18.17	18.99	4.52	27.86	22.01	-20.99	33.28	28.16	-15.38	33.51	27.78	-17.12	26.58	26.78	0.77
19	17	4.25	11.11	6.56	-40.95	16.36	11.81	-27.82	21.36	16.35	-23.46	24.27	22.29	-8.15	23.34	26.81	14.87	29.44	24.95	-15.27	27.98	27.72	-0.93	23.54	21.05	-10.59	14.66	19.61	33.77
20	18	4.50	24.44	19.57	-19.92	28.28	22.69	-19.77	27.30	24.35	-10.80	23.26	24.45	5.10	16.91	22.13	30.90	17.22	16.55	-3.89	12.43	14.16	13.94	8.42	6.54	-22.27	3.96	5.69	43.58
21	18	4.50	14.67	9.88	-32.63	20.10	15.26	-24.07	24.01	19.38	-19.29	25.12	23.99	-4.48	22.18	26.74	20.56	26.34	23.32	-11.48	23.32	24.48	4.94	18.56	16.69	-10.09	10.74	15.37	43.16
22	31	7.75	5.74	2.32	-59.57	9.30	5.96	-35.90	13.86	9.62	-30.60	16.02	15.65	-13.18	19.80	21.95	10.85	27.84	22.58	-18.88	30.62	27.31	-10.83	28.91	24.99	-13.55	20.90	24.12	15.42
23	11	2.75	20.27	15.15	-25.28	25.47	19.94	-21.73	27.29	23.19	-15.02	25.70	25.75	0.22	20.52	25.90	26.23	22.51	20.97	-6.84	17.94	20.13	12.20	13.13	11.45	-12.75	6.82	10.24	50.15
24	19	5.00	11.94	8.54	-28.51	15.88	13.12	-17.37	18.49	15.80	-14.56	19.11	19.07	-0.23	15.95	21.69	35.92	18.85	17.73	-5.95	17.22	18.27	6.10	13.96	12.41	-11.13	8.13	11.81	45.18
	Area (km^2)	109.75																												
Volume of Rainfall (mm-km^2/hr)			1748.75	1420.23	-18.79	2131.82	1674.37	-21.46	2255.14	1949.12	-13.57	2158.54	2125.20	-1.45	1941.92	2073.13	6.76	2277.47	1907.20	-16.26	1950.16	1957.73	0.39	1583.14	1413.02	-9.60	962.57	1264.48	33.44
Root Mean Square Error					3.62			4.65			3.80			1.63			2.76			4.09			2.02			2.54			3.36

APPENDIX G
Forecast of Spatial Distribution of Subcatchment Rainfall

Artificial Event No.135

Sub-Catchment No.	No. of Cell	Area	Time step 1			Time step 2			Time step 3			Time step 4			Time step 5			Time step 6			Time step 7			Time step 8			Time step 9		
			Actual	Predicted	% error	Actual	Predicted	% error	Actual	Predicted	% error	Actual	Predicted	% error	Actual	Predicted	% error	Actual	Predicted	% error	Actual	Predicted	% error	Actual	Predicted	% error	Actual	Predicted	% error
	(no.)	(km^2)	(mm/hr)	(mm/hr)	(%)	(mm/hr)	(mm/hr)	(%)	(mm/hr)	(mm/hr)	(%)	(mm/hr)	(mm/hr)	(%)	(mm/hr)	(mm/hr)	(%)	(mm/hr)	(mm/hr)	(%)	(mm/hr)	(mm/hr)	(%)	(mm/hr)	(mm/hr)	(%)	(mm/hr)	(mm/hr)	(%)
1	27	6.75	3.02	5.19	71.62	6.54	5.51	-15.76	12.31	10.58	-14.05	12.17	14.85	21.96	18.09	15.12	-16.44	22.20	19.22	-13.44	26.07	20.38	-21.83	28.50	23.17	-18.71	23.58	26.02	10.35
2	35	8.75	7.47	7.26	-2.87	12.62	11.50	-8.82	19.75	16.56	-16.15	15.95	21.00	31.65	20.81	16.95	-18.54	20.59	21.91	6.37	19.71	19.47	-1.23	18.16	18.91	4.10	11.71	18.30	56.25
3	28	7.00	12.39	9.38	-24.32	15.87	16.13	1.63	20.39	17.23	-15.47	13.24	19.34	46.09	15.19	12.87	-16.59	12.05	16.46	36.59	9.52	11.82	24.15	7.54	9.72	28.81	3.83	7.88	105.66
4	36	9.00	1.87	3.87	107.57	4.65	3.03	-34.83	9.57	7.99	-16.42	10.57	11.88	12.40	16.26	14.81	-8.90	22.16	17.79	-19.74	27.41	20.91	-23.71	30.75	24.34	-20.83	28.41	27.50	-3.20
5	14	3.50	5.32	5.96	12.11	10.83	8.37	-22.70	18.97	15.75	-16.97	17.66	21.19	19.95	23.97	20.53	-14.36	27.07	24.89	-8.05	27.41	25.08	-8.52	25.77	25.03	-2.86	18.98	24.30	28.03
6	23	5.75	14.59	11.34	-22.26	20.62	19.19	-6.95	27.82	23.21	-16.57	19.37	26.70	37.82	22.21	18.98	-14.53	18.63	23.37	25.48	14.58	18.29	25.45	11.17	14.59	30.65	5.92	11.13	88.16
7	13	3.25	9.66	8.52	-11.76	16.90	13.60	-18.33	26.25	21.50	-18.08	21.54	26.85	24.61	26.62	22.80	-14.36	26.25	27.31	4.05	23.03	25.03	8.68	19.15	22.26	16.28	12.08	18.93	56.76
8	23	5.75	2.90	3.17	9.42	6.78	3.61	-46.74	12.92	9.95	-22.98	13.44	14.50	7.84	18.79	17.53	-6.70	23.67	20.26	-14.41	25.27	22.83	-9.66	24.41	23.66	-3.10	20.42	23.41	14.65
9	19	4.75	20.76	16.05	-22.67	19.84	22.00	10.91	19.97	17.71	-11.34	10.10	16.27	60.99	9.42	8.86	-5.91	5.65	9.80	73.54	3.21	5.45	69.50	1.89	3.21	69.71	0.69	1.65	140.31
10	6	1.50	20.22	14.93	-26.15	22.41	23.00	2.63	25.19	21.53	-14.53	14.34	21.82	52.10	14.44	12.95	-10.33	9.78	15.32	56.66	6.24	9.70	55.43	4.03	6.28	55.78	1.67	3.58	114.94
11	23	5.75	7.86	6.94	-11.94	14.69	11.12	-24.31	23.45	18.95	-19.17	20.19	23.92	18.44	24.72	22.09	-10.64	25.40	25.37	-0.13	22.06	24.46	10.91	17.87	21.43	19.90	11.80	17.49	48.21
12	17	4.25	20.62	15.64	-24.14	25.90	24.46	-5.55	31.40	26.25	-16.40	19.73	27.98	41.77	20.44	18.46	-9.67	15.22	21.32	40.06	10.19	15.24	49.63	6.75	10.12	49.96	3.11	5.84	87.87
13	8	2.00	23.57	17.96	-23.79	24.65	25.30	2.63	26.19	22.56	-13.85	14.21	21.83	53.60	13.50	12.65	-6.29	8.65	13.95	61.31	5.07	6.53	68.04	3.03	4.91	62.27	1.18	2.24	89.70
14	14	3.50	15.90	12.57	-20.95	23.48	20.51	-12.61	31.83	26.23	-17.60	22.73	29.93	31.64	25.19	22.46	-10.83	21.37	26.02	21.77	15.87	21.26	33.99	11.39	16.01	40.56	6.06	10.93	80.48
15	10	2.50	24.68	19.16	-22.38	27.04	26.62	-1.54	29.25	24.96	-14.66	16.36	24.39	49.12	15.38	14.81	-3.66	10.05	15.82	57.36	5.78	10.21	76.62	3.34	5.64	68.79	1.32	2.22	68.60
16	4	1.00	13.89	11.30	-18.62	21.78	18.38	-15.64	30.52	25.10	-17.76	22.79	29.05	27.47	25.40	23.08	-9.14	22.39	26.13	16.66	16.75	22.45	34.02	11.96	17.05	42.58	6.60	11.53	74.67
17	12	3.00	6.39	5.38	-15.81	12.23	8.63	-29.48	19.45	15.38	-20.90	16.99	19.28	13.47	20.11	19.18	-4.66	20.74	20.94	1.00	17.12	20.93	22.21	13.07	17.52	34.01	8.63	13.16	52.51
18	12	3.00	23.60	20.32	-13.90	19.99	23.21	16.13	17.94	16.95	-5.52	8.17	13.93	70.48	6.78	7.34	8.22	3.59	6.75	87.87	1.71	3.48	103.22	0.85	1.53	80.65	0.27	0.40	50.82
19	17	4.25	23.17	19.05	-17.81	26.30	25.28	-3.89	28.74	24.74	-13.94	16.56	24.16	46.00	15.36	15.65	1.90	10.33	15.81	53.03	5.88	11.07	88.26	3.34	6.09	82.22	1.37	2.26	64.40
20	18	4.50	11.26	9.51	-15.53	18.20	14.97	-17.72	25.51	20.98	-17.77	19.41	24.05	23.89	20.99	20.36	-3.02	18.88	21.84	16.92	13.37	19.54	46.16	9.04	14.22	57.24	5.02	8.71	73.53
21	18	4.50	20.19	16.77	-16.92	25.10	23.25	-7.35	29.20	24.87	-14.81	18.12	25.34	39.85	17.43	17.64	1.22	12.66	18.09	42.91	7.65	13.72	79.46	4.55	8.17	79.80	2.04	3.56	73.90
22	31	7.75	24.45	21.01	-14.05	23.11	24.51	6.04	22.21	20.26	-8.79	11.16	17.87	60.14	9.57	10.45	9.20	5.69	9.69	70.50	2.95	6.01	104.03	1.58	2.92	85.03	0.61	0.85	40.68
23	11	2.75	15.89	13.27	-16.49	22.64	19.88	-12.19	29.00	24.26	-16.32	19.97	26.30	31.70	20.36	20.08	-1.39	16.37	21.25	29.75	10.74	17.51	63.10	6.77	11.53	70.21	3.37	6.01	78.18
24	19	5.00	16.90	14.90	-11.85	20.40	19.25	-5.66	22.68	20.06	-11.54	13.64	19.59	43.57	12.27	14.07	14.70	8.50	13.09	53.97	4.61	10.21	121.16	2.45	5.45	122.33	1.03	1.59	53.46
	Area (km^2)	109.75																											
Volume of Rainfall (mm-km^2/hr)			1427.86	1225.40	-14.18	1847.76	1713.30	-7.28	2384.71	2018.40	-15.36	1695.55	2262.73	33.45	1947.85	1782.97	-8.46	1818.50	2043.05	12.35	1604.83	1785.40	11.25	1410.81	1542.12	9.31	1004.91	1318.45	31.20
Root Mean Square Error					3.24			2.26			3.83			5.94			2.08			4.14			4.36			3.45			3.63

APPENDIX G
Forecast of Spatial Distribution of Subcatchment Rainfall

Artificial Event No.136

Sub-Catchment No.	No. of Cell	Area		Time step 1			Time step 2			Time step 3			Time step 4			Time step 5			Time step 6			Time step 7			Time step 8			Time step 9			Time step 10		
			Actual	Predicted	% error	Actual	Predicted	% error	Actual	Predicted	% error	Actual	Predicted	% error	Actual	Predicted	% error	Actual	Predicted	% error	Actual	Predicted	% error	Actual	Predicted	% error	Actual	Predicted	% error	Actual	Predicted	% error
	(no.)	(km^2)	(mm/hr)	(mm/hr)	(%)	(mm/hr)	(mm/hr)	(%)	(mm/hr)	(mm/hr)	(%)	(mm/hr)	(mm/hr)	(%)	(mm/hr)	(mm/hr)	(%)	(mm/hr)	(mm/hr)	(%)	(mm/hr)	(mm/hr)	(%)	(mm/hr)	(mm/hr)	(%)	(mm/hr)	(mm/hr)	(%)	(mm/hr)	(mm/hr)	(%)
1	27	6.75	4.61	0.14	-97.03	9.36	3.46	-63.05	12.61	11.19	-11.27	20.32	16.13	-20.61	21.96	18.83	-14.25	23.22	20.36	-12.31	25.59	21.06	-17.68	29.40	22.19	-24.52	30.19	23.94	-20.70	23.23	26.47	9.85
2	35	8.75	9.54	0.61	-93.65	16.28	9.62	-40.93	18.60	16.23	-12.76	25.26	20.95	-17.07	23.82	22.64	-4.94	20.94	21.89	4.53	19.39	19.45	0.28	19.35	18.50	-4.37	16.62	18.16	9.22	10.63	15.91	49.57
3	28	7.00	12.80	2.97	-76.45	17.94	13.63	-24.07	17.48	14.66	-16.15	19.78	17.81	-9.93	16.38	17.41	6.29	11.95	15.36	28.52	9.33	11.48	23.13	8.16	9.58	17.43	5.93	8.38	41.14	3.23	5.16	59.94
4	36	9.00	3.57	0.03	-99.30	7.80	2.26	-70.29	10.38	9.86	-5.08	18.30	13.90	-24.02	20.23	17.01	-15.90	23.18	19.31	-16.73	27.45	21.63	-21.23	32.81	23.58	-28.11	35.88	25.63	-28.57	28.77	28.48	-1.01
5	14	3.50	9.21	0.40	-95.65	16.66	9.11	-45.34	19.28	18.43	-4.39	29.33	22.45	-23.45	28.30	25.68	-9.26	27.47	25.68	-6.52	27.77	25.04	-9.82	28.91	24.97	-13.63	26.73	24.78	-7.30	17.77	23.39	31.66
6	23	5.75	16.40	4.74	-74.26	26.40	19.87	-24.72	24.93	23.14	-7.15	29.74	25.19	-15.30	24.21	25.85	6.75	18.29	22.43	22.59	14.67	17.54	19.58	12.78	14.93	16.78	9.40	12.83	36.48	4.99	8.33	66.90
7	13	3.25	16.78	2.74	-82.65	25.08	16.56	-33.96	25.43	24.47	-3.78	34.71	26.94	-22.40	30.25	29.50	-2.47	26.04	27.35	5.00	23.52	24.39	3.71	22.23	22.73	2.24	18.30	20.95	14.48	10.72	16.95	58.07
8	23	5.75	6.46	0.31	-95.22	12.07	5.40	-55.23	13.94	13.74	-1.43	23.18	16.74	-27.80	22.75	20.18	-11.29	24.00	21.35	-11.04	26.19	22.82	-12.85	28.45	23.81	-16.29	28.26	24.01	-15.04	19.76	24.38	23.42
9	19	4.75	20.11	14.36	-28.59	21.72	20.38	-6.16	15.70	14.43	-8.06	14.29	13.45	-5.89	9.37	11.44	22.13	5.30	8.53	60.76	3.25	5.05	55.41	2.28	3.33	46.20	1.27	2.25	76.44	0.51	0.22	-56.76
10	6	1.50	21.49	10.70	-50.21	25.92	22.50	-13.19	20.78	19.10	-8.08	20.90	19.03	-8.91	14.85	17.62	18.60	9.33	13.82	48.02	6.29	9.02	43.25	4.76	6.52	36.77	2.93	4.80	63.59	1.30	1.40	7.91
11	23	5.75	15.59	3.88	-75.12	24.32	16.29	-33.02	23.49	23.57	0.32	33.23	24.61	-25.95	28.28	27.50	-2.78	24.97	25.58	2.45	23.06	23.85	2.61	21.74	22.33	2.72	18.16	20.26	11.56	10.54	16.63	57.75
12	17	4.25	27.20	12.38	-54.47	33.92	27.91	-17.73	27.30	26.76	-1.96	29.72	25.38	-14.60	21.49	25.18	17.14	14.53	19.98	37.46	10.47	14.12	34.85	8.23	10.86	32.00	5.39	8.15	51.23	2.49	3.82	45.56
13	8	2.00	26.65	16.85	-36.78	29.50	26.25	-11.02	21.37	20.79	-2.73	20.57	18.58	-9.69	13.63	16.96	24.41	8.12	12.53	54.33	5.20	7.79	49.75	3.73	5.30	42.06	2.18	3.55	63.21	0.90	0.58	-35.80
14	14	3.50	24.74	8.81	-64.40	33.82	25.88	-23.48	29.31	29.10	-0.73	35.49	28.50	-19.70	27.41	29.84	8.85	20.64	25.24	22.29	16.43	20.06	22.09	13.88	16.97	22.25	10.02	13.97	39.46	5.06	8.74	72.73
15	10	2.50	31.85	20.25	-36.41	34.88	30.36	-12.95	24.40	25.00	2.44	24.00	21.06	-12.25	16.57	19.98	27.54	9.36	14.44	54.32	6.03	9.20	52.63	4.27	6.32	47.89	2.48	4.09	64.85	1.00	0.69	-30.73
16	4	1.00	24.35	9.03	-62.94	33.60	25.45	-24.26	28.85	29.35	1.75	36.15	28.13	-22.20	27.86	29.98	7.58	21.56	25.60	18.76	17.56	21.15	20.44	14.94	18.30	22.48	10.97	15.08	37.47	5.55	9.80	76.50
17	12	3.00	15.02	5.42	-63.96	22.31	15.58	-30.16	19.89	20.82	4.66	28.32	20.28	-28.48	22.92	22.92	-0.03	20.08	21.10	5.10	18.34	19.91	8.57	16.80	18.75	11.63	13.76	16.44	19.45	7.84	13.14	72.08
18	12	3.00	24.88	24.35	-2.13	22.92	23.07	0.63	13.72	14.80	7.84	11.36	10.93	-3.77	6.49	8.93	37.65	3.26	5.85	79.40	1.78	3.13	75.53	1.11	1.72	54.82	0.56	0.89	63.16	0.19	0.00	-100.00
19	17	4.25	35.07	23.91	-31.81	37.12	32.15	-13.37	24.56	27.08	10.22	24.68	21.13	-14.38	15.61	20.51	31.36	9.54	14.74	54.58	6.24	9.92	58.87	4.42	7.06	59.55	2.81	4.59	75.89	1.05	1.12	7.18
20	18	4.50	23.48	10.99	-53.19	30.96	24.17	-21.95	24.65	26.44	7.29	31.22	23.59	-24.42	22.99	25.42	10.57	17.73	21.44	20.98	14.36	18.16	26.47	11.91	15.72	31.95	8.82	12.52	45.22	4.19	7.93	89.00
21	18	4.50	33.99	21.42	-36.97	37.68	31.84	-15.49	25.83	28.61	10.75	27.80	22.83	-17.26	18.07	22.93	26.94	11.76	17.17	46.02	8.16	12.36	51.68	6.04	9.39	55.48	3.78	6.49	71.82	1.80	2.41	50.08
22	31	7.75	31.83	27.43	-13.83	29.95	28.06	-6.26	17.89	20.51	14.64	16.05	14.68	-8.53	9.40	13.19	40.31	5.18	8.81	70.03	3.12	5.34	71.10	2.09	3.43	63.93	1.17	2.04	74.69	0.46	0.30	-34.26
23	11	2.75	29.84	16.05	-46.20	36.25	29.48	-18.68	28.84	29.16	8.66	31.27	24.70	-21.02	21.70	25.76	18.74	15.36	20.50	33.44	11.51	16.04	39.34	8.99	13.03	44.87	6.03	9.65	60.09	2.72	4.90	79.86
24	19	5.00	32.61	24.00	-26.40	33.12	29.42	-11.16	20.11	24.78	23.17	20.81	17.49	-15.97	12.49	17.51	40.15	7.71	12.43	61.29	5.07	8.99	77.31	3.50	6.67	90.42	2.05	4.20	105.30	0.78	1.12	42.30
	Area (km^2)	109.75																															
Volume of Rainfall (mm-km^2/hr)			2057.37	1063.42	-48.31	2584.68	1991.92	-22.93	2174.67	2179.33	0.21	2662.26	2170.15	-18.48	2165.84	2276.42	5.06	1798.30	2013.00	11.94	1635.13	1728.85	5.73	1602.01	1579.40	-1.41	1423.32	1447.10	1.67	942.81	1198.18	27.08
Root Mean Square Error					10.64			5.88			1.82			5.27			3.03			3.81			3.19			3.45			3.53			3.29

APPENDIX G
Forecast of Spatial Distribution of Subcatchment Rainfall

Artificial Event No.137																											
Sub-Catchment No.	No. of Cell	Area		Time step 1			Time step 2			Time step 3			Time step 4			Time step 5			Time step 6			Time step 7			Time step 8	
			Actual	Predicted	% error	Actual	Predicted	% error	Actual	Predicted	% error	Actual	Predicted	% error	Actual	Predicted	% error	Actual	Predicted	% error	Actual	Predicted	% error	Actual	Predicted	% error
	(no.)	(km^2)	(mm/hr)	(mm/hr)	(%)	(mm/hr)	(mm/hr)	(%)	(mm/hr)	(mm/hr)	(%)	(mm/hr)	(mm/hr)	(%)	(mm/hr)	(mm/hr)	(%)	(mm/hr)	(mm/hr)	(%)	(mm/hr)	(mm/hr)	(%)	(mm/hr)	(mm/hr)	(%)
1	27	6.75	8.38	5.26	-37.29	12.72	5.44	-57.24	13.68	12.30	-10.07	15.26	13.41	-12.12	10.44	16.23	55.46	10.14	8.85	-12.70	6.40	8.32	30.00	3.38	5.12	51.61
2	35	8.75	17.66	14.72	-16.69	23.09	15.27	-33.86	22.60	21.53	-4.75	21.99	21.06	-4.22	13.90	20.77	49.36	13.12	10.70	-18.43	7.87	8.55	8.58	3.90	4.83	24.10
3	28	7.00	25.73	25.19	-2.11	28.30	24.91	-11.98	24.52	25.48	3.94	20.31	22.02	8.41	11.48	17.46	52.18	10.18	8.34	-18.09	5.59	4.81	-13.92	2.46	2.35	-4.61
4	36	9.00	4.32	1.86	-57.08	7.73	1.94	-74.94	9.69	7.29	-24.72	12.31	9.37	-23.90	9.74	13.95	43.19	10.64	9.98	-6.21	7.62	11.19	46.93	4.75	8.86	86.52
5	14	3.50	9.64	6.74	-30.11	15.78	7.95	-49.62	19.09	15.97	-16.34	22.10	18.49	-16.35	17.02	22.30	31.01	18.79	15.32	-18.48	13.28	15.97	20.26	8.14	12.04	47.93
6	23	5.75	23.27	21.53	-7.49	29.80	23.66	-20.62	30.19	28.12	-6.85	28.02	27.42	-2.15	18.41	24.90	35.21	18.60	15.00	-19.39	11.65	12.37	6.19	6.09	7.91	29.84
7	13	3.25	14.03	11.31	-19.40	21.85	13.81	-36.82	26.08	22.15	-15.04	28.35	24.62	-13.15	21.59	26.70	23.67	24.22	18.73	-22.68	17.07	18.87	10.53	10.41	14.02	34.71
8	23	5.75	4.08	2.27	-44.27	8.06	2.67	-66.83	11.65	7.75	-33.50	15.55	10.84	-30.29	14.12	16.46	16.52	17.82	14.60	-18.05	14.46	17.40	20.31	10.62	15.90	49.80
9	19	4.75	24.38	27.24	11.71	25.25	27.90	10.49	22.46	23.74	5.70	16.93	19.98	18.02	9.92	13.41	35.25	9.62	8.35	-13.15	5.56	5.03	-9.43	2.61	3.32	27.15
10	6	1.50	26.91	28.12	4.50	30.13	29.48	-2.16	28.05	28.02	-0.10	22.79	24.92	9.34	13.86	18.83	35.92	13.56	11.25	-17.03	8.01	7.63	-4.73	3.87	4.82	24.45
11	23	5.75	8.66	6.94	-19.83	15.41	9.37	-39.21	21.17	16.75	-20.91	25.34	20.46	-19.25	22.09	24.29	9.98	27.95	20.42	-26.93	22.18	22.78	2.70	15.83	19.39	22.51
12	17	4.25	22.65	22.65	0.00	29.61	26.35	-11.02	31.92	28.93	-9.38	29.29	28.82	-1.61	20.49	25.22	23.10	22.47	17.75	-21.03	14.98	15.71	4.88	8.49	11.19	31.74
13	8	2.00	23.91	25.81	7.95	27.80	28.36	2.01	27.57	26.68	-3.24	22.68	24.56	8.29	14.68	18.59	26.63	15.42	12.84	-16.73	9.67	9.94	2.79	5.05	6.96	37.91
14	14	3.50	17.42	16.06	-7.76	25.87	20.09	-22.33	30.82	26.41	-14.31	31.52	28.59	-9.30	24.11	28.29	17.33	28.00	21.22	-24.21	20.01	21.05	5.21	12.42	15.91	28.17
15	10	2.50	20.76	22.02	6.07	26.41	26.10	-1.17	28.83	26.14	-9.32	25.30	25.88	2.30	17.98	21.15	17.66	20.53	16.60	-19.15	13.99	15.06	7.64	8.16	11.28	38.26
16	4	1.00	13.29	12.08	-9.14	21.56	16.18	-24.96	27.99	23.13	-17.39	30.53	26.58	-12.96	25.29	27.90	10.31	31.39	22.98	-26.81	23.98	24.43	1.86	16.23	19.75	21.68
17	12	3.00	5.04	4.31	-14.51	10.13	6.35	-37.29	15.94	11.43	-28.33	20.62	15.41	-25.29	20.44	19.83	-2.98	29.15	20.23	-30.62	25.89	24.16	-6.69	21.39	23.03	7.67
18	12	3.00	17.27	20.03	15.98	18.77	22.39	19.31	18.40	18.63	1.20	13.95	16.74	19.97	9.01	11.27	25.04	9.82	9.34	-4.85	6.23	7.47	19.86	3.30	5.58	68.95
19	17	4.25	14.92	15.25	2.23	21.21	20.41	-3.81	26.09	22.02	-15.57	24.71	23.96	-3.02	19.65	21.32	8.51	24.88	19.63	-21.10	18.74	20.37	8.72	12.47	16.42	31.69
20	18	4.50	7.93	7.49	-5.53	14.40	11.22	-22.10	21.30	16.61	-22.02	25.12	20.78	-17.28	23.66	23.30	-1.53	33.17	22.95	-30.82	28.52	26.42	-7.37	22.61	23.88	5.60
21	18	4.50	12.59	12.54	-0.39	19.42	17.79	-8.39	25.57	20.96	-18.01	25.92	24.00	-7.41	21.93	22.94	4.58	28.99	21.82	-24.74	22.94	23.64	3.08	16.28	19.71	21.07
22	31	7.75	14.51	15.69	8.14	18.33	19.81	8.05	20.80	18.68	-10.18	17.79	19.07	7.19	13.22	15.09	14.08	16.18	14.23	-12.04	11.60	14.03	20.88	7.25	11.12	53.39
23	11	2.75	10.50	10.25	-2.31	17.66	15.09	-14.56	24.75	19.92	-19.51	27.13	23.81	-12.25	24.28	24.60	1.31	33.06	23.55	-28.78	27.25	26.30	-3.50	20.40	22.70	11.28
24	19	5.00	7.19	7.10	-1.22	12.14	11.80	-2.84	18.04	13.93	-22.82	19.25	17.60	-8.58	18.35	17.64	-3.89	27.38	20.45	-25.31	24.15	24.14	-0.06	19.77	21.78	10.16
	Area (km^2)	109.75																								
Volume of Rainfall (mm-km^2/hr)			1542.93	1450.48	-5.99	2093.22	1694.80	-19.03	2354.45	2079.78	-11.67	2349.78	2191.88	-6.72	1780.97	2162.18	21.40	2093.59	1650.95	-21.14	1542.98	1650.93	7.00	1023.94	1306.55	27.60
Root Mean Square Error					1.80			4.65			3.30			2.92			3.89			5.43			1.58			2.89

APPENDIX G
Forecast of Spatial Distribution of Subcatchment Rainfall

Artificial Event No.138

Sub-Catchment No.	No. of Cell	Area		Time step 1			Time step 2			Time step 3			Time step 4			Time step 5			Time step 6			Time step 7			Time step 8			Time step 9			Time step 10		
			Actual	Predicted	% error	Actual	Predicted	% error	Actual	Predicted	% error	Actual	Predicted	% error	Actual	Predicted	% error	Actual	Predicted	% error	Actual	Predicted	% error	Actual	Predicted	% error	Actual	Predicted	% error	Actual	Predicted	% error
	(no.)	(km^2)	(mm/hr)	(mm/hr)	(%)	(mm/hr)	(mm/hr)	(%)	(mm/hr)	(mm/hr)	(%)	(mm/hr)	(mm/hr)	(%)	(mm/hr)	(mm/hr)	(%)	(mm/hr)	(mm/hr)	(%)	(mm/hr)	(mm/hr)	(%)	(mm/hr)	(mm/hr)	(%)	(mm/hr)	(mm/hr)	(%)	(mm/hr)	(mm/hr)	(%)
1	27	6.75	29.56	26.21	-11.35	26.54	23.14	-12.79	20.69	20.82	0.65	13.24	16.65	25.78	8.91	8.74	-2.00	5.64	4.27	-24.29	3.39	3.14	-7.22	1.38	0.76	-44.90	0.69	2.00	190.67	0.31	3.39	995.48
2	35	8.75	22.92	20.43	-10.86	24.18	23.11	-4.41	22.74	22.21	-2.34	16.79	19.51	16.17	13.83	12.58	-9.03	9.77	10.00	2.31	6.68	6.69	0.29	3.23	2.44	-24.40	1.95	2.85	45.79	1.07	4.03	277.97
3	28	7.00	11.42	10.18	-10.88	13.93	15.28	9.64	15.56	15.37	-1.21	13.16	14.44	9.71	13.43	11.44	-14.82	10.80	12.90	21.84	8.20	8.45	3.07	4.73	4.16	-12.01	3.82	3.84	6.24	2.47	5.28	113.57
4	36	9.00	30.19	27.79	-7.93	26.42	22.16	-16.11	20.23	19.89	-1.66	12.85	16.09	27.25	7.76	8.87	14.34	4.82	3.53	-26.64	2.89	3.28	13.34	1.14	1.25	9.50	0.50	2.55	412.44	0.20	3.18	1492.33
5	14	3.50	30.65	26.50	-13.54	31.61	26.99	-14.63	29.38	26.24	-10.67	21.17	23.72	12.06	15.49	15.81	2.05	10.72	10.49	-2.16	7.34	8.52	16.12	3.40	4.49	32.26	1.73	4.51	160.34	0.81	4.22	421.57
6	23	5.75	17.01	13.37	-21.42	21.33	21.31	-0.10	24.84	22.52	-9.35	21.39	22.57	5.55	20.74	18.50	-10.80	16.54	19.10	15.45	13.23	14.30	8.11	7.65	8.99	17.54	5.29	7.43	40.36	3.32	7.48	125.63
7	13	3.25	26.02	21.61	-16.97	30.18	27.00	-10.54	32.38	27.76	-14.27	26.00	27.05	4.02	21.74	20.63	-5.11	16.41	17.28	5.31	12.54	13.97	11.38	6.63	8.90	34.15	3.82	7.30	90.96	2.02	6.14	204.02
8	23	5.75	27.34	26.20	-4.20	27.53	22.83	-17.05	25.32	22.07	-12.86	17.96	19.99	11.26	12.02	13.74	14.26	8.25	7.67	-7.06	5.76	7.19	24.84	2.63	4.52	71.88	1.16	4.10	246.45	0.50	2.89	479.50
9	19	4.75	3.90	1.83	-53.00	6.28	7.02	11.73	9.85	8.16	-17.18	10.66	9.53	-10.61	14.24	11.35	-20.26	13.62	17.37	27.54	13.47	13.98	3.75	10.29	12.27	19.19	9.81	11.27	14.91	8.39	12.90	53.72
10	6	1.50	7.47	4.43	-40.63	11.00	12.02	9.26	15.44	13.58	-12.02	15.33	14.90	-2.78	18.17	15.05	-17.19	18.20	20.05	23.78	14.71	15.43	4.92	10.05	11.80	17.40	8.48	10.03	18.39	6.42	10.93	70.27
11	23	5.75	24.34	20.53	-15.64	28.94	24.77	-14.40	32.50	26.06	-19.75	26.80	26.32	-1.81	21.80	21.43	-1.70	16.86	17.60	4.40	13.59	15.57	14.60	7.43	11.70	57.37	4.02	8.72	116.76	2.03	5.88	190.49
12	17	4.25	11.86	6.85	-42.25	17.07	17.09	0.11	23.68	19.81	-16.35	23.12	22.25	-3.79	25.29	21.70	-14.21	22.31	25.63	14.87	20.48	21.27	3.85	13.74	17.39	26.64	10.35	13.72	32.53	7.11	12.38	74.18
13	8	2.00	6.03	2.34	-61.25	9.60	10.05	4.71	14.95	12.15	-18.74	16.00	14.58	-8.99	20.20	16.44	-18.64	19.18	22.84	19.09	19.09	19.19	0.52	14.36	17.23	19.97	12.63	14.74	16.71	10.06	14.95	48.67
14	14	3.50	18.06	12.80	-29.19	24.11	22.71	-5.83	30.72	25.34	-17.54	28.02	27.25	-2.75	27.18	24.42	-10.15	22.72	25.01	10.07	19.77	21.16	7.02	12.19	16.59	36.12	8.03	12.57	56.64	4.85	10.06	107.26
15	10	2.50	6.77	2.08	-69.28	11.07	11.10	0.24	17.97	14.03	-21.93	19.68	17.62	-10.47	24.44	20.15	-17.56	23.59	28.72	13.29	24.32	23.76	-2.29	16.62	22.63	21.52	15.56	16.62	19.50	11.90	17.11	43.83
16	4	1.00	18.80	13.60	-27.66	25.17	22.93	-8.92	32.43	25.83	-20.37	29.65	28.08	-5.30	27.81	25.48	-8.39	23.27	25.13	7.96	20.53	22.16	8.02	12.82	18.28	44.85	7.85	13.40	70.79	4.51	9.70	115.09
17	12	3.00	18.52	16.43	-11.30	23.32	19.73	-15.37	28.45	21.80	-24.09	24.78	23.00	-7.17	20.31	20.59	1.39	16.43	17.33	5.53	14.32	16.47	14.98	8.34	14.28	71.06	4.37	9.80	124.15	2.16	5.48	154.06
18	12	3.00	2.06	0.11	-94.73	3.90	3.90	0.10	7.50	5.39	-28.18	9.40	7.72	-17.87	14.28	11.41	-20.08	15.34	18.65	21.57	17.86	17.83	-1.27	16.17	19.61	21.26	16.76	18.46	10.14	15.74	19.53	24.08
19	17	4.25	6.75	2.02	-70.04	11.29	10.82	-4.11	19.13	14.36	-24.92	21.59	18.96	-12.15	26.55	22.45	-15.44	26.44	28.57	8.08	29.04	27.19	-6.37	23.47	27.96	19.14	19.04	22.52	18.30	14.29	18.82	31.73
20	18	4.50	14.71	10.67	-27.46	20.73	18.45	-11.02	28.86	21.67	-24.90	27.74	24.89	-10.28	26.08	24.46	-6.21	22.77	24.25	6.50	21.67	22.93	5.82	14.15	21.24	50.09	8.48	14.89	75.66	4.76	9.45	98.84
21	18	4.50	8.86	3.89	-57.39	13.87	13.12	-5.41	22.49	16.91	-24.82	24.50	21.83	-11.74	28.15	24.36	-13.48	27.31	29.08	6.50	29.33	27.81	-5.17	22.77	28.10	23.40	17.12	21.72	26.89	11.98	16.81	40.29
22	31	7.75	3.43	0.55	-83.94	6.16	5.86	-4.97	11.49	8.31	-27.72	14.06	12.02	-14.65	19.76	16.37	-17.16	21.14	23.60	11.62	25.17	23.22	-7.77	22.79	25.94	13.83	21.49	22.77	5.92	18.68	21.34	14.22
23	11	2.75	11.97	6.94	-42.04	18.05	16.66	-7.69	27.18	20.50	-24.57	27.80	24.72	-11.10	28.82	25.78	-10.53	26.45	28.11	6.26	26.61	26.58	-0.12	18.80	25.59	36.10	12.54	18.70	49.17	7.80	13.12	68.26
24	19	5.00	5.14	1.52	-70.42	9.14	8.53	-6.65	16.98	12.16	-28.39	20.26	17.37	-14.29	24.52	21.91	-10.66	25.53	28.75	4.80	30.49	27.32	-10.39	26.06	30.21	15.89	19.71	23.09	17.11	14.04	16.75	19.30
	Area (km^2)	109.75																															
Volume of Rainfall (mm-km^2/hr)			1810.48	1452.05	-19.80	2065.88	1910.40	-8.41	2367.24	2024.22	-14.49	2078.21	2064.73	0.31	2028.13	1841.22	-9.13	1752.67	1898.32	8.20	1650.46	1666.60	0.98	1167.32	1438.77	23.26	892.98	1193.12	33.61	650.67	1058.10	62.62
Root Mean Square Error					3.75			2.36			4.29			2.13			2.60			2.24			1.34			3.80			3.54			4.13

APPENDIX G
Forecast of Spatial Distribution of Subcatchment Rainfall

Artificial Event No.139

Sub-Catchment No.	No. of Cell	Area	Time step 1			Time step 2			Time step 3			Time step 4			Time step 5			Time step 6			Time step 7			Time step 8		
			Actual	Predicted	% error	Actual	Predicted	% error	Actual	Predicted	% error	Actual	Predicted	% error	Actual	Predicted	% error	Actual	Predicted	% error	Actual	Predicted	% error	Actual	Predicted	% error
	(no.)	(km^2)	(mm/hr)	(mm/hr)	(%)	(mm/hr)	(mm/hr)	(%)	(mm/hr)	(mm/hr)	(%)	(mm/hr)	(mm/hr)	(%)	(mm/hr)	(mm/hr)	(%)	(mm/hr)	(mm/hr)	(%)	(mm/hr)	(mm/hr)	(%)	(mm/hr)	(mm/hr)	(%)
1	27	6.75	22.38	24.94	11.46	22.14	22.27	0.62	14.50	19.15	32.02	11.52	10.21	-11.35	8.44	5.57	-33.97	5.28	4.35	-17.58	2.06	3.78	83.67	1.07	4.24	298.24
2	35	8.75	21.56	24.99	15.90	24.57	23.24	-5.39	19.11	22.95	20.08	19.27	16.13	-16.30	16.97	14.58	-14.09	12.91	12.82	-0.73	6.18	9.70	56.90	3.77	7.37	95.39
3	28	7.00	13.36	16.78	25.55	17.30	16.29	-5.84	16.00	18.04	12.74	20.79	16.63	-20.03	22.59	20.35	-9.94	21.39	20.44	-4.44	12.90	17.04	32.08	9.46	11.89	25.68
4	36	9.00	20.61	23.75	15.26	20.17	20.81	3.18	12.43	17.08	37.48	8.75	8.46	-3.28	5.58	2.91	-47.93	3.08	1.55	-49.69	1.06	1.09	2.66	0.50	2.18	335.51
5	14	3.50	25.36	28.54	12.52	28.77	26.35	-8.42	20.78	25.27	21.62	17.95	16.26	-9.42	13.18	11.29	-14.36	8.48	7.76	-8.41	3.45	4.44	28.71	1.87	3.95	111.73
6	23	5.75	18.93	22.20	17.29	25.41	22.31	-12.22	23.08	25.44	10.25	27.94	22.44	-19.68	27.22	25.33	-6.94	23.47	22.89	-2.48	12.98	16.90	30.15	8.95	11.81	31.97
7	13	3.25	24.67	28.04	13.66	31.20	27.11	-13.11	25.34	28.62	12.94	25.46	21.73	-14.65	20.65	19.57	-5.23	14.85	14.76	-0.57	6.83	8.69	27.33	4.08	6.45	58.07
8	23	5.75	20.24	24.35	20.27	22.86	21.70	-5.10	15.57	19.71	26.60	11.93	11.79	-1.20	7.58	5.48	-27.69	4.28	2.46	-42.65	1.54	0.73	-52.71	0.77	0.93	21.04
9	19	4.75	6.07	6.74	11.00	10.19	8.24	-19.16	12.13	11.47	-5.49	21.39	15.71	-26.56	27.74	24.63	-11.21	32.42	27.18	-16.16	24.74	26.12	5.58	22.09	20.47	-7.35
10	6	1.50	10.32	12.08	17.14	15.95	13.47	-15.55	17.18	17.48	1.75	26.34	19.90	-24.46	30.75	27.83	-9.47	32.04	28.50	-11.05	21.61	24.70	14.30	17.45	18.12	3.82
11	23	5.75	22.12	25.48	15.19	29.04	24.60	-15.30	23.44	26.22	11.87	22.50	20.13	-10.53	16.76	16.96	1.15	11.26	11.32	0.47	4.89	5.32	8.77	2.82	4.00	41.91
12	17	4.25	14.87	16.66	12.05	22.84	18.54	-18.81	23.33	23.95	2.63	32.15	24.70	-23.18	33.10	31.25	-5.59	30.78	29.09	-5.48	18.64	22.37	19.99	13.92	16.12	15.80
13	8	2.00	8.79	9.35	6.36	14.72	11.51	-21.80	16.91	16.28	-3.73	27.63	20.24	-26.76	32.75	29.56	-9.73	35.23	30.48	-13.50	24.85	27.14	9.22	20.94	20.91	-0.15
14	14	3.50	19.92	22.59	13.39	28.72	23.64	-17.71	26.68	28.29	6.02	31.74	25.66	-19.17	28.64	28.26	-1.30	23.31	23.44	0.57	12.31	15.35	24.65	8.26	10.84	31.21
15	10	2.50	9.69	9.82	1.33	16.77	12.54	-25.24	19.28	18.40	-4.58	30.64	22.43	-26.79	34.26	31.74	-7.37	35.14	31.28	-10.98	23.74	26.51	11.66	19.42	20.46	5.34
16	4	1.00	19.96	22.65	13.49	29.08	23.63	-18.75	26.54	28.10	5.86	30.14	25.10	-16.73	25.50	26.35	3.32	19.60	20.43	4.19	9.81	11.95	21.81	6.33	8.53	34.72
17	12	3.00	16.78	20.03	19.37	23.52	19.47	-17.25	19.47	21.42	9.98	18.58	17.45	-6.10	13.06	14.33	9.78	8.43	8.53	1.18	3.56	3.00	-15.63	2.02	2.22	9.77
18	12	3.00	3.63	2.69	-25.90	7.15	4.89	-31.58	9.71	8.26	-14.92	19.59	13.68	-30.21	26.60	23.43	-11.90	33.43	26.90	-19.54	28.00	27.98	-0.09	27.21	24.13	-11.32
19	17	4.25	9.36	9.04	-3.51	16.76	12.07	-28.00	19.31	18.27	-5.39	29.90	22.27	-25.53	31.41	30.64	-2.48	30.77	28.70	-6.72	20.09	23.08	14.88	16.16	18.31	13.33
20	18	4.50	15.48	17.76	14.73	23.96	18.87	-21.26	22.32	23.29	4.35	25.07	21.78	-13.12	19.96	22.53	12.84	14.72	16.23	10.30	7.15	8.36	16.91	4.54	6.08	33.87
21	18	4.50	11.10	11.39	2.60	19.24	14.22	-26.13	21.01	20.44	-2.74	29.92	23.19	-22.49	29.04	29.84	2.75	26.34	26.13	-0.80	15.93	18.96	19.01	12.09	14.72	21.79
22	31	7.75	5.32	4.15	-21.91	10.23	6.90	-32.55	13.08	11.62	-11.18	23.78	16.95	-28.72	28.65	26.37	-7.96	32.50	27.57	-15.15	24.82	26.20	5.58	22.64	22.44	-0.88
23	11	2.75	13.92	15.35	10.23	22.86	17.52	-23.37	23.06	23.30	1.06	29.08	23.85	-17.99	25.49	27.72	8.75	20.76	22.14	6.61	11.20	13.66	21.97	7.74	10.15	31.04
24	19	5.00	6.93	6.56	-5.41	13.37	9.30	-30.49	15.62	14.89	-4.73	23.35	18.74	-19.74	22.24	24.81	11.53	20.26	21.04	3.86	12.49	14.85	18.88	9.71	12.07	24.24
	Area (km^2)	109.75																								
Volume of Rainfall (mm-km^2/hr)			1713.87	1934.18	12.85	2250.73	1950.05	-13.36	1993.11	2182.10	9.48	2395.76	1944.60	-18.83	2295.34	2150.65	-6.30	2072.06	1920.30	-7.32	1274.40	1486.48	16.64	995.30	1172.05	17.76
Root Mean Square Error					2.43			3.65			2.43			5.17			2.18			2.63			2.40			2.11

APPENDIX G
Forecast of Spatial Distribution of Subcatchment Rainfall

Artificial Event No.140

Sub-Catchment No.	No. of Cell (no.)	Area (km²)	Time step 1 Actual (mm/hr)	Time step 1 Predicted (mm/hr)	Time step 1 % error (%)	Time step 2 Actual (mm/hr)	Time step 2 Predicted (mm/hr)	Time step 2 % error (%)	Time step 3 Actual (mm/hr)	Time step 3 Predicted (mm/hr)	Time step 3 % error (%)	Time step 4 Actual (mm/hr)	Time step 4 Predicted (mm/hr)	Time step 4 % error (%)	Time step 5 Actual (mm/hr)	Time step 5 Predicted (mm/hr)	Time step 5 % error (%)	Time step 6 Actual (mm/hr)	Time step 6 Predicted (mm/hr)	Time step 6 % error (%)	Time step 7 Actual (mm/hr)	Time step 7 Predicted (mm/hr)	Time step 7 % error (%)	Time step 8 Actual (mm/hr)	Time step 8 Predicted (mm/hr)	Time step 8 % error (%)	Time step 9 Actual (mm/hr)	Time step 9 Predicted (mm/hr)	Time step 9 % error (%)	Time step 10 Actual (mm/hr)	Time step 10 Predicted (mm/hr)	Time step 10 % error (%)	Time step 11 Actual (mm/hr)	Time step 11 Predicted (mm/hr)	Time step 11 % error (%)	Time step 12 Actual (mm/hr)	Time step 12 Predicted (mm/hr)	Time step 12 % error (%)
1	27	8.75	3.93	12.63	221.44	5.12	4.76	-6.89	10.47	4.43	-57.65	12.02	5.95	-50.51	9.54	10.10	5.79	11.39	9.80	-13.97	12.59	12.95	2.85	13.49	11.68	-13.45	7.96	11.08	39.24	6.62	7.31	10.41	4.42	6.70	51.65	2.26	2.51	11.18
2	35	8.75	10.77	12.37	14.87	12.00	10.83	-9.70	20.81	11.80	-43.20	21.86	15.82	-27.16	16.43	19.55	19.00	17.68	16.36	-7.46	18.03	18.43	2.25	17.05	15.37	-9.87	9.05	10.41	15.09	6.61	5.82	-11.84	4.31	4.63	7.42	2.24	2.58	15.29
3	28	7.00	21.10	11.89	-43.68	19.86	17.53	-11.74	28.63	19.61	-31.51	28.92	25.08	-6.86	18.69	25.01	33.61	17.68	16.82	6.46	16.20	17.36	7.21	13.02	12.72	-2.26	5.95	5.08	-14.66	3.67	2.09	-43.12	2.26	1.23	-46.54	1.15	1.67	45.65
4	36	9.00	1.43	13.13	820.66	2.18	3.71	69.82	5.38	2.73	-49.23	7.17	2.56	-64.37	6.51	5.80	-13.83	8.85	6.86	-22.43	11.05	10.68	-3.34	13.80	11.27	-18.92	9.66	14.26	47.63	9.36	11.90	27.20	6.86	12.30	79.42	3.85	6.54	70.09
5	14	3.50	3.55	12.26	244.92	5.00	7.11	42.27	11.24	7.19	-35.99	14.98	8.99	-39.24	13.20	13.88	5.47	16.92	13.84	-18.25	20.35	18.84	-7.41	23.79	18.84	-20.80	15.68	19.06	21.92	13.92	14.50	4.13	10.22	13.84	35.48	5.95	8.56	43.87
6	23	5.75	13.41	8.77	-34.61	14.72	14.23	-3.31	25.28	17.40	-31.18	27.75	23.98	-13.58	22.28	26.80	20.29	23.85	22.53	-5.55	24.68	23.87	-3.29	23.10	20.79	-10.02	12.41	13.43	8.29	6.81	7.74	-12.15	6.00	5.52	-7.81	3.38	4.81	45.04
7	13	3.25	5.38	9.49	76.51	7.24	9.33	28.86	15.55	10.95	-29.60	20.03	14.86	-25.80	16.37	19.93	8.49	22.76	19.07	-16.21	26.81	23.95	-10.64	29.87	23.62	-20.95	18.97	21.38	12.68	15.67	15.33	-3.40	11.71	13.27	13.38	7.05	8.55	35.58
8	23	5.75	0.96	13.03	1224.47	1.68	6.01	257.54	4.70	4.87	3.52	7.27	3.83	-47.41	7.73	6.37	-17.60	11.47	8.22	-28.35	15.81	13.33	-15.68	22.02	15.47	-29.75	17.30	20.15	16.51	18.07	16.99	5.12	14.67	20.20	37.68	9.43	14.42	52.97
9	19	4.75	19.66	5.54	-71.82	17.52	16.19	-7.58	24.01	20.15	-16.06	23.49	26.44	12.54	17.83	24.48	36.90	16.20	18.06	17.88	14.86	15.23	2.36	11.47	11.46	0.04	5.21	4.22	-19.02	3.00	2.01	-33.13	1.95	0.81	-48.75	1.12	2.48	121.38
10	8	1.50	19.09	6.67	-65.06	16.43	17.25	-6.39	27.50	21.48	-21.87	28.05	26.70	2.32	21.53	28.15	30.73	20.88	22.32	6.69	19.97	19.96	-0.09	18.45	15.85	-3.64	7.99	7.20	-6.73	4.87	3.53	-27.45	3.20	1.75	-45.34	1.81	3.30	82.53
11	23	5.75	2.41	8.64	257.86	3.73	7.84	110.42	8.34	8.75	-4.32	13.84	10.84	-23.12	14.52	14.96	3.05	20.04	19.90	-20.68	26.20	21.87	-17.58	33.44	23.53	-29.64	24.48	25.06	2.44	23.03	20.90	-9.25	16.62	19.84	5.46	12.41	15.48	24.72
12	17	4.25	11.47	4.17	-63.65	12.94	13.16	1.70	23.01	18.01	-21.78	27.06	25.88	-4.45	23.67	28.19	19.09	25.95	24.84	-5.08	27.88	25.35	-9.07	29.72	23.32	-12.73	14.97	15.81	6.27	10.66	8.68	-9.02	7.67	6.41	-16.43	4.73	6.89	47.65
13	8	2.00	14.82	3.54	-76.13	14.81	14.10	-5.45	23.40	19.20	-17.93	25.52	26.94	5.55	21.11	26.91	27.51	21.18	22.40	8.89	21.16	20.09	-5.06	18.14	17.08	-5.81	9.17	9.18	0.07	5.81	5.01	-13.71	4.02	2.48	-38.36	2.44	4.30	76.53
14	14	3.50	6.86	5.05	-26.35	8.82	10.61	20.30	18.12	14.29	-21.15	23.48	20.52	-12.59	22.13	24.84	12.24	26.67	23.26	-12.76	31.08	26.98	-13.19	33.39	26.71	-19.98	20.81	22.36	7.48	18.56	15.47	-6.58	12.47	12.06	-3.12	7.92	10.56	33.60
15	10	2.50	10.39	1.71	-83.55	11.45	11.14	-2.72	19.93	16.61	-16.65	23.81	24.65	3.12	21.67	26.06	20.26	23.43	23.19	-1.01	25.19	22.44	-10.81	23.64	21.04	-11.01	13.18	14.36	8.97	9.06	8.81	-2.76	6.66	5.17	-22.63	4.26	6.72	54.11
16	4	1.00	4.26	4.55	6.80	6.01	8.95	48.81	13.69	12.08	-11.81	19.34	16.93	-12.51	19.73	21.53	9.10	25.45	21.40	-15.93	31.67	26.30	-16.96	36.92	27.56	-25.37	25.02	25.88	3.43	21.42	19.58	-8.61	16.94	16.38	-3.33	11.31	14.08	24.42
17	12	3.00	1.02	7.38	620.47	1.80	7.24	302.60	5.22	7.59	45.03	8.90	7.88	-13.66	10.89	10.42	-2.54	16.28	12.40	-23.62	23.60	17.91	-24.11	33.65	21.37	-36.51	27.90	25.58	-8.29	28.90	24.19	-16.29	25.48	24.15	-5.23	18.83	21.04	11.77
18	12	3.00	11.35	0.74	-93.47	10.68	8.79	-17.71	15.67	13.30	-15.14	17.04	19.83	16.36	14.46	19.30	33.57	13.93	16.65	19.56	13.64	13.29	-2.55	11.10	11.52	3.79	8.44	6.37	16.98	3.22	3.42	5.86	2.26	1.04	-54.26	1.47	2.84	92.92
19	17	4.25	5.88	0.55	-90.26	7.03	7.03	-0.01	13.98	12.02	-13.86	19.87	19.06	1.02	19.19	21.70	13.09	22.68	21.26	-6.26	26.67	22.30	-16.40	27.85	23.31	-16.29	17.40	19.85	14.04	13.11	13.81	3.78	10.44	9.01	-13.70	7.45	8.98	33.87
20	18	4.50	1.82	3.47	90.53	3.04	7.16	135.52	7.88	9.38	19.06	12.86	12.05	-4.84	14.68	15.58	6.12	20.88	17.06	-18.23	28.68	22.17	-22.69	37.64	25.38	-32.54	29.13	27.32	-6.21	27.71	23.48	-15.26	24.09	21.14	-12.23	18.01	19.38	7.65
21	18	4.50	4.05	0.68	-83.14	5.46	8.44	17.82	11.89	10.93	-8.06	17.17	17.06	-0.62	18.43	20.35	10.38	23.18	20.77	-10.38	28.78	23.33	-18.87	32.40	25.33	-21.82	21.76	23.53	8.10	17.04	17.27	-2.10	14.53	12.86	-12.85	10.83	12.81	21.45
22	31	7.75	6.89	0.41	-94.10	7.82	6.15	-18.16	13.07	10.86	-16.75	18.26	17.86	7.33	15.78	18.87	19.61	17.18	18.01	4.86	18.80	16.75	-11.42	17.91	16.81	-6.14	10.29	13.06	26.91	7.06	8.26	17.23	9.47	4.52	-17.45	3.87	5.86	54.40
23	11	2.75	2.89	1.53	-47.08	4.24	6.91	62.90	10.16	10.52	3.54	18.56	18.24	-2.07	17.43	18.86	8.87	23.28	18.96	-14.56	30.89	24.14	-21.10	37.29	29.86	-27.84	26.88	26.78	-0.50	23.62	21.16	-10.33	19.96	17.35	-13.10	14.70	16.54	12.46
24	19	5.00	1.78	0.12	-93.26	2.63	3.57	35.41	6.41	7.06	10.12	10.48	11.10	5.86	12.83	13.89	6.62	17.47	15.65	-10.41	23.69	19.34	-22.57	29.31	22.10	-24.63	22.98	23.44	7.30	19.28	19.04	-1.27	17.36	14.79	-14.88	14.21	16.32	7.79
	Area (km²)	108.75																																				
Volume of Rainfall (mm-km²/hr)			820.91	784.56	-4.43	904.80	984.25	8.78	1616.59	1234.25	-23.65	1917.74	1669.70	-11.89	1710.19	1969.85	15.19	1984.61	1838.15	-7.84	2295.51	2056.65	-10.41	2486.07	2016.00	-18.91	1605.40	1751.97	9.75	1352.45	1299.90	-3.89	1460.43	1088.52	-25.47	712.10	921.92	29.47
Root Mean Square Error					7.79			2.33			4.34			3.10			3.52			2.61			3.54			6.15			2.00			1.78			2.26			2.23

APPENDIX G
Forecast of Spatial Distribution of Subcatchment Rainfall

Artificial Event No.141

Sub-Catchment No.	No. of Cell	Area	Time step 1			Time step 2			Time step 3			Time step 4			Time step 5			Time step 6		
			Actual	Predicted	% error	Actual	Predicted	% error	Actual	Predicted	% error	Actual	Predicted	% error	Actual	Predicted	% error	Actual	Predicted	% error
	(no.)	(km^2)	(mm/hr)	(mm/hr)	(%)	(mm/hr)	(mm/hr)	(%)	(mm/hr)	(mm/hr)	(%)	(mm/hr)	(mm/hr)	(%)	(mm/hr)	(mm/hr)	(%)	(mm/hr)	(mm/hr)	(%)
1	27	6.75	1.89	3.43	81.21	3.77	3.97	5.18	4.31	3.93	-8.82	5.52	6.86	24.19	5.41	3.91	-27.76	6.42	7.50	16.83
2	35	8.75	5.32	12.83	141.10	9.03	9.30	3.06	9.16	12.01	31.15	11.15	12.14	8.89	9.61	9.67	0.56	10.68	10.06	-5.57
3	28	7.00	10.47	23.71	126.55	14.69	15.13	2.97	12.92	19.81	53.32	14.64	15.13	3.34	10.76	13.88	28.96	10.94	8.95	-18.24
4	36	9.00	0.90	0.96	6.71	2.14	2.38	11.15	2.79	1.45	-47.97	3.96	4.82	21.83	4.47	2.41	-46.16	5.82	7.77	33.55
5	14	3.50	2.63	5.83	121.52	5.70	6.07	6.59	6.90	7.12	3.19	9.67	10.27	6.25	10.09	8.27	-18.02	12.64	13.36	5.63
6	23	5.75	9.37	22.36	138.47	15.51	15.07	-2.79	15.39	21.35	38.75	19.40	18.58	-4.19	16.28	18.53	13.85	18.06	15.70	-13.06
7	13	3.25	4.71	11.94	153.62	9.66	9.73	0.73	11.21	13.40	19.54	15.71	15.10	-3.90	15.58	14.49	-6.97	19.09	17.76	-6.98
8	23	5.75	1.04	1.73	65.19	2.77	3.46	24.96	3.89	2.60	-35.86	6.14	6.04	-1.62	7.49	4.60	-40.02	10.38	11.47	10.46
9	19	4.75	15.61	29.09	86.35	20.50	19.58	-4.49	17.09	26.05	52.42	20.13	18.46	-8.26	13.91	20.37	46.50	13.94	11.02	-20.94
10	6	1.50	14.43	29.88	107.08	20.64	19.72	-4.47	16.33	27.10	47.87	22.08	20.25	-8.21	16.33	21.78	33.39	16.94	13.57	-19.93
11	23	5.75	2.97	8.19	176.10	7.03	7.87	12.05	9.06	10.32	14.02	14.02	12.99	-7.34	15.56	13.43	-13.68	20.60	18.77	-8.93
12	17	4.25	11.36	26.61	133.72	19.25	18.15	-5.74	19.34	26.84	38.75	25.73	22.39	-13.00	21.80	25.33	16.17	24.67	20.14	-18.38
13	8	2.00	14.65	29.59	102.00	21.80	20.13	-7.66	19.89	28.50	43.31	25.18	21.69	-13.87	19.15	24.94	30.19	20.40	16.11	-21.02
14	14	3.50	7.49	19.51	160.68	14.56	14.24	-2.23	16.20	21.27	31.29	22.94	20.26	-11.69	21.70	22.49	3.67	26.16	22.14	-15.35
15	10	2.50	12.87	27.65	114.78	21.14	19.31	-8.67	20.73	28.70	38.48	26.09	23.03	-18.01	23.11	27.82	20.37	25.97	20.41	-21.40
16	4	1.00	5.61	15.70	179.95	12.00	12.30	2.49	14.31	18.40	28.61	21.47	18.78	-12.56	21.85	21.50	-1.60	27.62	23.28	-15.73
17	12	3.00	1.85	5.98	222.88	5.00	6.66	33.09	7.06	8.03	13.54	12.06	10.65	-11.85	14.79	12.17	-17.75	20.98	18.17	-13.42
18	12	3.00	14.29	24.54	71.74	19.73	17.73	-10.18	17.00	24.82	46.01	21.66	18.47	-14.75	16.46	22.55	45.86	16.06	13.44	-16.39
19	17	4.25	9.59	22.26	132.22	17.77	16.54	-6.95	16.99	25.72	35.44	26.06	22.11	-21.28	25.32	28.36	11.99	30.32	23.63	-22.07
20	18	4.50	3.55	11.42	221.63	8.60	10.07	17.06	11.23	14.63	30.35	16.54	15.76	-15.02	20.84	19.54	-6.22	26.28	22.85	-19.21
21	18	4.50	7.47	19.30	158.31	15.13	14.80	-2.18	17.25	23.27	34.89	26.63	21.11	-20.76	25.76	27.35	6.16	32.17	24.96	-22.40
22	31	7.75	11.45	22.04	92.53	18.56	16.54	-10.91	18.00	24.60	37.76	25.36	20.10	-20.60	20.66	25.89	25.33	23.41	18.86	-19.43
23	11	2.75	5.41	15.90	193.93	12.03	12.77	6.14	14.72	19.74	34.09	23.62	19.28	-18.03	24.56	24.65	-0.06	32.01	26.16	-21.38
24	19	5.00	4.94	13.71	177.45	11.01	11.56	5.04	13.43	18.46	37.40	22.67	17.33	-23.58	23.69	24.46	3.74	31.19	23.53	-24.57
	Area (km^2)	109.75																		
Volume of Rainfall (mm-km^2/hr)			746.69	1670.63	123.74	1281.50	1267.05	-1.13	1329.97	1765.60	32.76	1844.23	1649.63	-10.56	1679.17	1798.50	7.11	2012.89	1725.72	-14.27
Root Mean Square Error					10.44			1.05			5.58			3.14			3.41			4.15

Sub-Catchment No.	Time step 7			Time step 8			Time step 9			Time step 10			Time step 11		
	Actual	Predicted	% error	Actual	Predicted	% error	Actual	Predicted	% error	Actual	Predicted	% error	Actual	Predicted	% error
	(mm/hr)	(mm/hr)	(%)	(mm/hr)	(mm/hr)	(%)	(mm/hr)	(mm/hr)	(%)	(mm/hr)	(mm/hr)	(%)	(mm/hr)	(mm/hr)	(%)
1	4.41	-15.12	6.54	7.55	15.50	7.22	7.36	1.76	6.36	9.14	43.76	5.82	8.16	5.64	
2	6.71	-1.71	6.04	6.05	0.14	4.66	3.40	-27.07	2.89	3.49	20.83	1.65	2.61	58.27	
3	6.99	-9.06	8.23	8.61	4.65	7.66	6.87	-10.64	5.76	7.77	34.77	4.23	5.29	25.17	
4	5.36	1.55	7.55	9.63	27.57	9.29	11.04	18.76	9.38	13.68	45.85	10.00	10.81	8.02	
5	10.91	3.56	13.35	14.39	7.84	14.32	14.62	2.08	12.81	16.34	27.61	11.43	12.82	12.17	
6	13.87	11.63	12.22	12.73	4.21	10.21	9.64	-5.56	7.09	8.90	25.56	4.55	6.60	44.87	
7	16.09	7.26	17.32	17.50	1.02	16.73	16.40	-1.96	13.65	16.58	21.52	10.82	12.95	22.01	
8	10.35	6.32	14.06	15.14	7.69	16.81	17.73	5.48	17.30	20.65	19.37	18.05	18.43	2.07	
9	10.70	34.38	6.06	6.59	8.96	3.85	3.42	-11.34	2.06	1.91	-7.46	0.93	1.72	85.67	
10	12.75	23.35	8.61	9.06	5.46	6.06	5.40	-10.82	3.55	3.95	11.22	1.81	3.17	75.11	
11	18.78	7.15	21.95	20.55	-8.40	22.42	21.17	-5.59	20.02	21.49	7.33	17.02	18.42	8.23	
12	20.41	22.30	15.84	15.98	2.16	12.12	12.15	0.24	8.08	9.40	16.64	4.72	7.22	52.89	
13	18.56	32.25	10.32	11.06	7.22	7.03	7.18	2.06	4.10	4.51	10.00	2.03	3.56	75.92	
14	22.39	15.32	20.45	20.09	-1.78	17.71	17.52	-1.05	13.25	15.34	15.73	9.01	12.09	34.18	
15	22.17	31.61	14.67	15.39	4.68	10.37	11.37	9.62	6.43	7.35	14.31	3.36	5.74	71.10	
16	24.45	13.10	24.14	22.60	-6.37	21.66	21.15	-3.23	17.38	19.03	9.48	12.58	15.68	24.58	
17	20.07	5.75	26.06	21.58	-13.96	26.27	23.68	-9.86	24.92	24.03	-3.55	22.13	22.48	1.56	
18	14.83	61.84	6.72	8.37	24.59	3.99	5.13	28.80	2.06	2.08	-0.22	0.86	1.51	74.76	
19	27.21	30.24	19.26	19.51	1.26	14.09	16.11	14.36	9.32	10.73	15.15	5.15	8.54	65.73	
20	25.92	9.62	26.06	24.02	-14.38	26.24	24.24	-7.59	22.38	21.97	-1.80	17.15	19.67	14.67	
21	28.86	23.06	23.25	22.14	-4.78	18.18	19.54	7.52	12.95	14.29	10.39	7.85	11.74	49.52	
22	21.90	48.32	12.15	13.91	14.55	7.96	10.50	31.90	4.75	5.71	20.09	2.32	4.31	85.60	
23	26.76	14.66	27.21	24.23	-10.96	23.33	22.88	-1.93	18.22	18.82	3.26	12.46	16.10	29.24	
24	29.09	22.76	24.05	22.00	-8.54	18.69	20.69	10.69	13.78	14.94	8.42	8.41	13.01	54.63	
Volume of Rainfall (mm-km^2/hr)	1732.95	17.15	1565.21	1572.23	0.45	1393.57	1417.30	1.70	1115.29	1294.60	16.06	1829.38	1055.50	-42.30	
Root Mean Square Error		3.52			1.62			1.26			1.89			2.27	

APPENDIX G
Forecast of Spatial Distribution of Subcatchment Rainfall

Artificial Event No.142																																			
Sub-Catchment No.	No. of Cell	Area		Time step 1			Time step 2			Time step 3			Time step 4			Time step 5			Time step 6			Time step 7			Time step 8			Time step 9			Time step 10		
			Actual	Predicted	% error	Actual	Predicted	% error	Actual	Predicted	% error	Actual	Predicted	% error	Actual	Predicted	% error	Actual	Predicted	% error	Actual	Predicted	% error	Actual	Predicted	% error	Actual	Predicted	% error	Actual	Predicted	% error
	(no.)	(km²)	(mm/hr)	(mm/hr)	(%)	(mm/hr)	(mm/hr)	(%)	(mm/hr)	(mm/hr)	(%)	(mm/hr)	(mm/hr)	(%)	(mm/hr)	(mm/hr)	(%)	(mm/hr)	(mm/hr)	(%)	(mm/hr)	(mm/hr)	(%)	(mm/hr)	(mm/hr)	(%)	(mm/hr)	(mm/hr)	(%)	(mm/hr)	(mm/hr)	(%)
1	27	6.75	29.67	26.16	-11.84	22.78	26.30	15.45	24.32	21.70	-10.81	19.09	22.90	19.96	15.56	17.39	11.76	14.33	13.40	-6.46	8.64	12.16	40.73	4.34	2.11	-51.46	1.84	0.80	-56.25	0.65	3.05	366.15
2	35	8.75	23.83	22.43	-5.87	21.89	24.52	13.02	24.74	22.42	-9.36	21.96	24.52	11.66	19.97	21.24	6.39	19.97	18.63	-6.71	14.03	17.91	27.58	8.02	6.09	-24.05	3.87	2.32	-39.98	1.58	5.06	221.48
3	28	7.00	12.72	13.55	6.51	13.64	16.18	18.61	16.46	16.86	2.61	16.31	18.36	12.57	16.34	17.96	9.91	17.67	17.21	-2.59	14.26	16.90	19.10	9.16	8.73	-4.68	5.06	3.48	-31.27	2.38	6.16	158.55
4	36	9.00	26.50	25.85	-2.45	19.20	24.13	25.68	20.62	19.19	-6.97	16.14	20.13	24.74	13.25	14.94	12.75	12.13	11.42	-5.85	7.45	10.27	37.89	3.85	2.11	-45.37	1.59	1.80	13.37	0.56	3.42	515.28
5	14	3.50	26.30	25.94	-1.40	22.41	26.37	17.65	25.97	23.06	-11.20	23.20	25.66	10.60	21.50	21.96	2.16	21.43	19.41	-9.45	16.54	18.82	21.14	9.26	7.62	-17.72	4.33	5.23	20.89	1.72	6.99	305.29
6	23	5.75	16.16	16.10	-0.37	17.18	19.93	15.99	21.41	20.52	-4.16	22.11	23.52	6.38	23.21	23.47	1.11	25.58	23.47	-8.27	22.07	24.01	8.78	15.17	14.92	-1.65	8.41	8.58	2.09	4.00	10.87	171.35
7	13	3.25	21.97	22.18	0.99	20.95	24.55	17.18	25.61	23.07	-9.93	25.22	26.61	5.50	25.60	24.95	-2.56	27.25	24.05	-11.77	22.58	24.37	7.91	15.19	13.68	-8.57	7.86	9.70	23.34	3.51	10.90	210.32
8	23	5.75	20.14	23.36	15.95	16.13	20.99	30.14	18.88	17.56	-6.97	16.93	19.46	14.89	15.97	16.38	2.56	16.92	14.39	-9.61	11.99	13.76	14.79	7.53	6.22	-17.35	3.48	6.04	73.68	1.39	6.10	338.86
9	19	4.75	3.89	4.11	5.80	5.37	7.18	33.74	7.43	9.65	29.82	9.33	10.27	10.03	11.69	12.47	6.74	14.73	14.14	-4.00	16.33	15.07	-7.68	13.92	15.57	11.89	9.57	10.26	7.23	5.74	12.17	112.18
10	6	1.50	7.33	7.55	3.03	9.23	11.33	22.83	12.29	13.77	12.02	14.36	16.48	7.82	16.83	17.52	4.11	20.15	18.96	-5.80	20.25	19.96	-1.31	15.81	16.97	7.34	9.97	10.23	2.60	5.44	12.43	128.39
11	23	5.75	17.92	19.54	9.03	16.95	20.44	20.59	21.34	19.23	-9.85	21.87	22.73	3.96	23.30	22.00	-5.57	25.42	22.04	-13.28	22.81	22.65	-0.68	16.71	15.75	-5.78	8.89	13.53	52.13	4.13	12.37	199.34
12	17	4.25	10.24	9.24	-9.76	12.21	14.09	15.40	16.38	16.39	0.05	19.16	19.58	2.28	22.69	21.96	-3.27	27.13	24.23	-10.68	28.00	25.96	-7.19	22.73	23.22	2.17	14.15	16.94	19.69	7.69	17.16	123.25
13	8	2.00	5.47	4.63	-15.43	7.30	8.81	20.79	10.16	11.61	14.24	12.80	13.29	3.79	16.20	16.16	-0.20	20.39	18.65	-8.55	23.06	20.30	-11.95	20.18	21.35	5.82	13.72	15.69	14.35	8.18	16.43	100.89
14	14	3.50	14.61	14.21	-2.79	15.88	18.45	16.16	20.78	19.44	-6.46	23.05	23.45	1.75	26.18	24.72	-5.56	30.15	26.34	-12.64	29.40	27.92	-5.03	22.88	22.52	-1.55	13.35	17.32	29.76	6.80	18.76	146.60
15	10	2.50	5.56	3.77	-32.24	7.46	8.49	13.79	10.66	11.46	7.55	13.89	13.77	-0.85	18.25	17.26	-5.43	23.42	20.72	-11.53	28.03	23.09	-17.64	26.01	26.40	1.51	17.96	21.89	21.88	10.94	20.52	87.53
16	4	1.00	14.04	14.10	0.42	15.03	17.60	17.06	19.91	18.35	-7.81	22.38	22.53	0.67	25.87	23.93	-7.52	29.96	25.83	-13.85	30.06	27.55	-8.34	24.13	23.55	-2.38	14.06	19.83	41.05	7.18	17.70	146.59
17	12	3.00	11.88	14.45	21.67	11.49	14.06	22.45	15.12	13.64	-9.75	16.54	16.64	0.60	18.94	17.28	-8.77	21.51	18.48	-14.13	21.58	19.38	-10.20	17.70	17.10	-3.41	9.90	16.90	70.64	4.91	13.22	169.34
18	12	3.00	1.78	0.60	-66.37	2.81	3.74	33.34	4.25	6.10	43.66	6.19	6.48	4.78	8.97	9.09	1.31	12.44	11.58	-6.96	17.12	13.26	-22.56	17.85	19.80	10.94	14.02	17.83	27.17	9.79	17.20	75.69
19	17	4.25	4.99	2.76	-44.61	6.64	7.07	6.56	9.70	9.75	0.45	13.10	12.35	-5.68	18.00	16.21	-9.93	23.69	20.44	-13.71	30.77	23.44	-23.83	31.28	30.21	-3.43	22.51	28.42	26.23	14.53	24.07	65.82
20	18	4.50	9.81	10.04	4.55	10.48	12.12	15.66	14.44	13.16	-8.89	17.24	16.73	-2.92	21.31	19.07	-10.49	25.84	21.87	-14.71	28.60	23.87	-16.56	25.64	24.69	-3.72	15.68	23.76	51.51	8.53	18.72	119.46
21	18	4.50	6.09	4.16	-31.66	7.87	8.25	7.80	11.08	10.63	-4.11	14.58	13.77	-5.56	19.65	17.51	-10.92	25.40	21.74	-14.40	32.25	24.76	-23.22	32.34	30.73	-4.97	22.57	29.36	30.09	14.15	24.09	70.28
22	31	7.75	2.63	0.96	-63.49	3.80	4.19	10.36	5.73	6.82	15.60	8.24	7.89	-4.31	12.02	11.19	-6.91	16.61	14.75	-11.22	23.59	17.29	-26.72	25.87	25.96	0.34	20.31	25.36	24.87	14.37	22.03	53.28
23	11	2.75	8.05	7.06	-12.25	9.46	10.59	11.92	13.39	12.49	-6.75	16.84	16.15	-4.05	21.78	19.43	-10.79	27.16	23.17	-14.70	32.27	25.81	-20.02	30.45	29.07	-4.53	19.78	27.84	39.72	11.46	22.23	93.96
24	19	6.00	3.11	1.41	-54.69	4.21	3.89	-7.66	6.50	6.01	-7.48	9.47	8.31	-12.29	14.18	12.22	-13.85	19.52	16.84	-13.76	28.84	20.01	-30.61	33.36	30.46	-8.64	25.13	32.15	27.94	17.23	24.37	41.36
	Area (km²)	109.75																																	
Volume of Rainfall (mm-km²/hr)			1565.59	1509.90	-3.56	1471.70	1735.53	17.93	1800.72	1716.48	-4.68	1828.96	1959.98	7.16	1972.30	1955.63	-0.85	2236.31	2006.47	-10.19	2215.31	2099.57	-5.22	1854.22	1762.70	-4.94	1186.82	1477.93	24.53	691.89	1417.27	104.84
Root Mean Square Error					1.54			2.61			1.58			1.84			1.40			2.61			4.19			1.36			4.38			7.78

APPENDIX G
Forecast of Spatial Distribution of Subcatchment Rainfall

Artificial Event No.143																																				
Sub-Catchment No.	No. of Cell	Area		Time step 1			Time step 2			Time step 3			Time step 4			Time step 5			Time step 6			Time step 7			Time step 8			Time step 9			Time step 10		
			Actual	Predicted	% error	Actual	Predicted	% error	Actual	Predicted	% error	Actual	Predicted	% error	Actual	Predicted	% error	Actual	Predicted	% error	Actual	Predicted	% error	Actual	Predicted	% error	Actual	Predicted	% error	Actual	Predicted	% error	Actual
	(no.)	(km^2)	(mm/hr)	(mm/hr)	(%)	(mm/hr)	(mm/hr)	(%)	(mm/hr)	(mm/hr)	(%)	(mm/hr)	(mm/hr)	(%)	(mm/hr)	(mm/hr)	(%)	(mm/hr)	(mm/hr)	(%)	(mm/hr)	(mm/hr)	(%)	(mm/hr)	(mm/hr)	(%)	(mm/hr)	(mm/hr)	(%)	(mm/hr)	(mm/hr)	(%)	(mm/hr)
1	27	6.75	20.12	26.54	31.95	22.06	21.85	-0.96	25.19	19.96	-20.79	18.41	19.86	7.87	17.22	16.54	-9.77	12.51	13.66	8.41	8.99	6.77	-24.67	7.42	6.76	-8.94	5.49	6.96	27.03	2.36	4.14	74.10	0.00
2	35	8.75	13.51	17.59	30.18	17.47	19.44	11.27	24.66	19.35	-21.54	19.86	22.65	14.03	21.36	17.57	-17.74	18.94	17.09	-9.80	15.86	14.30	-9.83	14.33	14.50	1.19	13.46	14.35	6.63	7.31	11.67	62.23	0.00
3	26	7.00	5.86	6.50	10.85	6.70	11.55	32.76	15.13	12.02	-20.56	13.33	16.56	24.25	16.37	12.66	-22.57	18.14	13.33	-26.53	18.24	17.35	-4.88	18.34	19.20	4.72	22.53	19.42	-13.81	15.81	20.93	32.40	0.00
4	36	9.00	21.67	30.17	39.24	23.83	22.41	-5.95	25.14	20.57	-18.18	18.12	18.63	2.80	16.56	15.66	-5.31	10.51	13.27	26.26	6.49	4.85	-25.21	4.90	4.00	-18.44	3.05	3.92	28.47	1.13	0.97	-14.50	0.00
5	14	3.50	19.23	25.73	33.81	25.35	24.40	-3.74	32.53	24.88	-23.52	25.87	26.39	2.00	27.14	22.21	-18.16	20.21	21.24	5.13	13.81	13.46	-2.54	11.06	11.31	2.09	8.28	10.36	25.22	3.65	4.99	36.49	0.00
6	23	5.75	8.95	9.10	2.87	14.02	16.01	14.14	23.82	18.28	-23.25	21.33	24.43	14.51	26.63	20.02	-24.82	26.70	21.86	-18.13	23.45	23.84	1.66	21.80	23.11	6.02	23.41	22.07	-5.74	14.59	20.03	37.25	0.00
7	13	3.25	14.86	16.67	25.63	22.25	22.51	1.14	32.91	24.88	-24.38	28.15	29.06	3.24	32.81	24.83	-24.31	27.44	25.66	-6.48	20.08	21.05	4.80	16.77	17.95	7.06	14.21	16.20	14.01	7.09	9.98	40.84	0.00
8	23	5.75	18.18	28.10	54.50	24.11	22.60	-6.27	28.50	22.79	-20.06	22.44	21.74	-3.14	23.17	19.57	-15.51	15.01	17.67	19.07	8.69	8.61	-0.88	6.33	5.86	-7.51	3.94	4.84	22.76	1.48	0.70	-52.40	0.00
9	19	4.75	1.62	0.28	-82.83	3.32	4.45	33.92	7.86	5.51	-29.99	8.21	9.53	16.02	12.80	8.27	-35.41	17.57	10.52	-40.16	19.49	19.95	2.36	20.76	22.33	7.57	32.13	22.75	-29.19	28.40	29.15	2.65	0.00
10	6	1.50	3.37	1.38	-58.91	6.29	7.93	26.22	13.19	9.77	-25.98	13.01	15.50	19.13	18.66	12.95	-30.59	22.84	15.50	-32.15	23.30	23.80	2.14	23.62	25.12	6.33	31.89	24.87	-22.03	24.66	28.32	14.78	0.00
11	23	5.75	14.07	18.94	34.60	22.26	21.38	-4.02	32.43	24.40	-24.75	28.28	27.41	-3.06	33.78	24.73	-26.81	26.20	25.56	-2.43	17.10	19.64	14.85	13.37	15.12	13.06	10.21	12.80	25.46	4.66	5.75	23.25	0.00
12	17	4.25	5.62	3.13	-44.32	10.53	11.48	9.06	20.56	15.16	-26.24	20.07	22.52	12.18	28.30	19.57	-30.85	30.67	23.43	-23.60	27.13	29.09	7.24	25.33	27.51	8.62	29.23	25.87	-11.49	19.67	25.17	27.99	0.00
13	8	2.00	2.60	0.36	-86.06	5.35	6.15	14.86	12.06	8.48	-29.72	12.51	14.28	14.07	19.29	12.63	-34.56	24.30	16.16	-33.49	24.34	25.54	4.92	24.42	26.23	7.39	33.72	25.70	-23.78	26.88	29.91	11.28	0.00
14	14	3.50	9.28	8.84	-4.77	16.26	16.91	3.98	28.21	21.12	-25.14	26.32	27.89	5.95	34.71	24.55	-29.27	32.64	27.75	-15.49	25.67	26.39	10.62	22.28	24.73	10.98	21.70	22.29	2.66	12.45	17.22	38.31	0.00
15	10	2.50	2.91	0.15	-94.85	6.32	6.61	4.55	14.24	10.05	-29.42	15.04	16.63	10.57	23.70	15.36	-35.19	28.40	20.06	-29.37	26.32	28.71	9.10	25.24	27.56	9.18	32.42	26.19	-19.21	24.26	28.48	17.39	0.00
16	4	1.00	9.80	10.18	3.86	17.54	17.60	0.32	29.75	22.30	-25.04	27.94	29.28	1.56	36.77	25.65	-30.25	32.61	28.73	-12.44	23.77	27.65	16.34	19.74	22.70	15.02	17.72	19.80	11.73	9.45	13.08	38.37	0.00
17	12	3.00	10.56	15.83	49.92	18.28	17.55	-3.99	27.25	21.02	-22.88	24.69	23.01	-6.80	31.07	22.10	-28.87	23.08	23.08	0.03	13.71	17.59	28.32	10.14	12.26	20.88	7.20	9.70	34.80	3.10	2.97	-4.22	0.00
18	12	3.00	0.77	0.00	-100.00	1.94	1.95	0.64	5.34	3.27	-38.82	6.17	6.58	6.75	11.07	6.70	-39.49	16.31	9.83	-39.71	17.83	19.28	8.08	18.85	20.85	10.62	31.05	21.16	-31.86	29.49	29.03	-1.57	0.00
19	17	4.25	2.94	0.58	-80.20	6.66	6.56	-1.44	14.87	10.75	-27.70	16.00	17.08	6.70	25.94	16.78	-35.30	29.48	22.25	-24.52	24.95	29.14	16.79	22.70	25.91	14.13	26.98	23.68	-12.23	18.96	23.74	25.17	0.00
20	18	4.50	7.58	8.55	12.73	14.77	14.54	-1.53	25.50	19.49	-23.56	24.71	24.04	-2.71	34.25	23.23	-32.17	29.12	26.34	-9.54	19.18	24.70	28.80	15.08	18.75	24.37	12.58	15.53	23.40	8.33	8.58	35.54	0.00
21	18	4.50	3.95	1.86	-53.08	8.65	8.58	-0.74	18.01	13.42	-25.52	18.94	19.78	4.45	29.63	19.43	-34.44	31.05	24.76	-20.28	24.30	29.50	21.39	21.13	24.93	17.98	22.72	22.07	-2.87	14.57	19.39	33.10	0.00
22	31	7.75	1.41	0.29	-79.64	3.38	3.14	-7.12	8.40	5.69	-32.26	9.51	10.15	6.65	16.69	10.52	-36.95	21.74	15.09	-30.58	20.67	23.60	14.17	20.17	22.72	12.62	28.73	21.81	-24.08	24.09	26.44	9.75	0.00
23	11	2.75	5.80	4.55	-21.58	12.03	11.95	-0.65	22.85	17.30	-24.27	23.08	23.33	1.08	33.98	22.59	-33.52	31.99	27.11	-15.26	22.90	26.67	26.21	18.90	23.03	21.85	17.83	19.69	10.45	10.07	14.06	39.78	0.00
24	19	5.00	2.23	0.91	-59.34	5.82	5.48	-2.52	12.65	9.91	-21.68	14.19	14.64	3.14	24.24	15.85	-34.63	25.36	21.17	-16.55	18.61	25.29	35.88	15.60	19.97	28.01	16.46	17.01	3.32	10.50	14.16	35.07	0.00
	Area (km^2)	109.75																																		
Volume of Rainfall (mm-km^2/hr)			1069.82	1298.55	21.38	1538.24	1566.15	1.81	2306.76	1769.00	-23.31	2042.36	2160.40	5.78	2582.22	1908.43	-26.17	2436.07	2068.68	-14.23	1965.68	2121.50	7.93	1763.75	1930.67	9.46	1940.38	1801.86	-7.14	1318.17	1619.70	22.80	0.00
Root Mean Square Error					3.97			1.09			5.33			1.59			7.57			5.14			3.10			2.33			4.39			3.45	

APPENDIX G
Forecast of Spatial Distribution of Subcatchment Rainfall

Artificial Event No.144																														
Sub-Catchment No.	No. of Cell	Area		Time step 1			Time step 2			Time step 3			Time step 4			Time step 5			Time step 6			Time step 7			Time step 8			Time step 9		
			Actual	Predicted	% error	Actual	Predicted	% error	Actual	Predicted	% error	Actual	Predicted	% error	Actual	Predicted	% error	Actual	Predicted	% error	Actual	Predicted	% error	Actual	Predicted	% error	Actual	Predicted	% error
	(no.)	(km^2)	(mm/hr)	(mm/hr)	(%)	(mm/hr)	(mm/hr)	(%)	(mm/hr)	(mm/hr)	(%)	(mm/hr)	(mm/hr)	(%)	(mm/hr)	(mm/hr)	(%)	(mm/hr)	(mm/hr)	(%)	(mm/hr)	(mm/hr)	(%)	(mm/hr)	(mm/hr)	(%)	(mm/hr)	(mm/hr)	(%)
1	27	6.75	2.89	1.63	-43.61	4.10	6.60	60.85	8.33	4.43	-46.77	13.00	10.04	-22.75	15.13	15.00	-0.86	22.29	16.87	-24.34	21.65	20.99	-3.07	27.76	21.21	-23.62	24.06	26.60	10.54
2	35	8.75	5.62	0.05	-99.09	7.43	10.28	38.38	13.43	8.09	-39.76	18.06	14.07	-22.08	18.19	18.54	1.90	22.54	19.11	-15.19	19.68	22.10	12.30	21.24	19.73	-7.14	16.14	21.37	32.38
3	28	7.00	6.71	0.00	-100.00	8.33	9.93	19.09	13.47	9.18	-31.91	15.61	12.22	-21.68	13.71	14.36	4.78	14.45	13.99	-3.15	11.43	15.21	33.05	10.67	12.22	14.54	7.24	11.60	60.37
4	36	9.00	2.61	4.05	54.97	3.60	6.58	82.94	7.33	4.48	-38.82	11.82	9.69	-18.00	14.02	14.26	1.70	21.11	16.48	-21.95	20.88	20.15	-3.48	26.58	21.27	-19.99	23.30	26.19	12.44
5	14	3.50	6.64	2.74	-58.72	8.44	13.24	56.91	15.28	10.16	-33.46	21.36	17.39	-18.58	21.95	22.36	1.87	27.89	23.16	-16.36	24.59	26.10	6.15	25.82	24.31	-5.83	19.64	25.24	28.53
6	23	5.75	11.48	0.31	-97.27	13.55	17.50	29.17	21.31	15.46	-27.46	24.57	20.47	-16.71	21.13	22.86	8.17	21.56	21.15	-1.89	16.79	21.93	30.55	14.54	17.45	19.97	9.49	14.93	57.34
7	13	3.25	11.46	2.87	-74.96	13.52	18.89	39.69	22.23	15.62	-29.75	27.78	22.80	-17.93	25.56	26.61	4.10	28.24	25.66	-9.13	23.19	27.25	17.48	21.25	23.44	10.26	14.67	21.29	45.10
8	23	5.75	5.56	6.10	9.84	6.74	10.88	61.51	12.06	8.43	-30.16	17.26	14.19	-17.76	17.91	18.35	2.43	22.88	19.83	-13.33	20.65	22.11	7.11	21.39	21.67	1.27	16.46	22.02	33.76
9	19	4.75	11.48	2.11	-81.67	11.99	12.83	6.94	15.59	13.61	-12.72	14.13	12.26	-13.20	9.65	10.79	11.87	7.47	8.76	17.30	4.92	7.81	58.57	3.25	5.58	71.43	1.73	4.00	130.76
10	6	1.50	12.57	0.23	-98.14	13.83	15.75	13.88	19.39	15.58	-19.65	19.27	16.43	-14.74	14.37	16.03	11.59	12.33	13.72	11.24	8.64	13.03	50.91	6.29	9.42	49.61	3.60	6.80	88.87
11	23	5.75	13.15	7.17	-45.47	14.56	19.94	36.98	22.91	16.88	-26.32	28.03	23.04	-17.81	24.98	25.92	3.74	26.56	24.87	-6.35	21.45	25.56	19.14	18.43	22.08	19.78	12.36	18.40	48.81
12	17	4.25	18.50	4.07	-77.99	19.62	23.16	18.07	27.35	21.73	-20.56	27.83	24.17	-13.15	21.00	23.83	13.48	18.28	20.06	9.70	13.00	18.85	45.00	9.40	13.67	45.51	5.44	9.12	67.87
13	8	2.00	16.89	4.49	-73.43	17.23	18.84	9.36	22.33	18.96	-15.07	20.57	18.25	-11.27	14.16	16.39	15.73	11.06	13.00	17.58	7.35	11.45	55.75	4.81	7.93	64.82	2.57	4.89	90.08
14	14	3.50	18.35	5.56	-69.68	19.82	24.84	25.31	29.05	22.18	-23.64	31.86	27.07	-15.02	25.72	28.19	9.63	24.27	24.93	2.73	18.16	24.37	34.20	14.05	18.93	34.72	8.62	13.87	61.00
15	10	2.50	22.38	9.72	-56.57	21.87	23.77	8.68	27.53	23.43	-14.89	24.96	22.71	-9.02	16.75	19.98	19.28	12.64	15.37	21.57	8.26	13.07	58.19	5.10	8.82	73.00	2.64	4.64	75.69
16	4	1.00	19.65	8.55	-56.50	20.71	25.93	25.19	30.03	23.15	-22.92	33.05	27.98	-15.36	26.56	28.90	8.80	24.88	25.88	3.21	18.59	24.83	33.56	14.01	19.55	39.50	8.51	13.73	61.28
17	12	3.00	14.67	11.46	-21.91	15.01	19.47	29.72	22.11	17.18	-22.29	25.77	21.35	-17.14	21.63	22.78	5.33	21.38	21.61	1.09	16.63	21.10	26.85	12.91	17.99	39.31	8.19	12.99	58.60
18	12	3.00	16.07	11.72	-27.11	14.75	15.60	5.79	16.64	16.68	0.28	13.06	13.09	0.25	7.66	9.68	26.45	4.92	6.61	34.22	2.92	4.88	67.41	1.55	3.30	113.05	0.71	1.83	155.40
19	17	4.25	28.16	17.91	-36.42	25.71	27.39	6.54	30.74	26.68	-13.21	27.04	25.48	-5.77	17.50	21.74	24.18	12.71	16.22	27.64	8.18	13.23	61.71	4.80	8.93	86.06	2.44	4.01	64.45
20	18	4.50	22.01	14.27	-35.18	21.43	25.47	18.86	29.16	23.31	-20.08	30.68	26.26	-14.39	23.32	25.88	10.97	20.42	22.57	10.55	14.75	20.74	40.66	10.12	16.17	59.87	5.85	9.63	64.60
21	18	4.50	29.03	18.42	-36.53	26.57	28.74	8.18	32.48	27.48	-15.39	29.69	27.37	-7.81	19.88	24.17	21.56	15.05	18.71	24.28	9.96	15.72	57.86	6.06	10.99	81.78	3.17	5.18	63.17
22	31	7.75	23.99	18.92	-21.11	21.02	21.90	4.16	23.39	22.26	-4.82	18.72	18.96	1.33	11.13	14.85	31.58	7.35	10.06	36.82	4.49	7.49	66.96	2.46	4.97	102.29	1.19	2.15	79.68
23	11	2.75	26.65	16.22	-39.14	25.26	28.55	12.99	32.70	26.65	-18.50	32.15	28.36	-11.77	22.95	26.60	15.88	18.66	21.91	17.40	12.88	19.31	49.93	8.26	14.20	71.93	4.52	7.48	65.47
24	19	5.00	31.89	24.94	-21.79	26.55	27.19	2.38	29.61	26.46	-10.63	24.89	24.53	-1.46	15.14	20.07	32.55	10.16	14.63	44.00	6.28	11.09	76.51	3.25	7.49	130.09	1.55	2.20	42.33
	Area (km^2)	109.75																												
Volume of Rainfall (mm-km^2/hr)			1559.06	842.55	-45.96	1577.19	1891.40	19.92	2191.45	1725.32	-21.27	2351.45	2032.60	-13.56	1936.68	2131.95	10.08	1982.54	1945.92	-1.85	1601.67	1970.28	23.01	1504.19	1667.23	10.84	1094.95	1487.27	35.83
Root Mean Square Error					8.82			3.36			4.76			3.40			2.44			2.83			4.36			3.99			3.99

APPENDIX G
Forecast of Spatial Distribution of Subcatchment Rainfall

Artificial Event No.145

Sub-Catchment No.	No. of Cell	Area	Actual	Time step 1 Predicted	% error	Actual	Time step 2 Predicted	% error	Actual	Time step 3 Predicted	% error	Actual	Time step 4 Predicted	% error	Actual	Time step 5 Predicted	% error	Actual	Time step 6 Predicted	% error	Actual	Time step 7 Predicted	% error	Actual	Time step 8 Predicted	% error	Actual	Time step 9 Predicted	% error	Actual	Time step 10 Predicted	% error	Actual	Time step 11 Predicted	% error
	(no.)	(km^2)	(mm/hr)	(mm/hr)	(%)	(mm/hr)	(mm/hr)	(%)	(mm/hr)	(mm/hr)	(%)	(mm/hr)	(mm/hr)	(%)	(mm/hr)	(mm/hr)	(%)	(mm/hr)	(mm/hr)	(%)	(mm/hr)	(mm/hr)	(%)	(mm/hr)	(mm/hr)	(%)	(mm/hr)	(mm/hr)	(%)	(mm/hr)	(mm/hr)	(%)	(mm/hr)	(mm/hr)	(%)
1	27	6.75	4.71	5.96	27.02	6.37	4.78	-24.95	8.96	4.68	-47.78	16.02	6.54	-59.17	17.32	18.06	-7.15	13.23	17.94	35.67	15.89	14.63	-7.97	15.41	16.80	8.96	15.35	15.49	0.86	15.25	15.49	1.56	13.22	14.42	9.12
2	36	8.75	12.83	8.68	-32.31	14.85	11.67	-20.03	18.25	13.13	-28.07	27.12	15.70	-42.12	25.74	23.97	-6.87	16.60	24.17	43.88	17.60	16.54	-6.03	15.24	18.21	19.46	13.35	15.18	13.70	11.39	13.86	21.78	8.34	9.79	17.46
3	28	7.00	24.93	13.06	-47.59	24.33	19.76	-18.77	25.70	22.08	-14.11	31.11	23.83	-23.41	25.27	25.34	0.29	13.73	22.65	65.04	12.17	13.17	8.19	9.26	12.57	35.78	7.02	9.18	30.83	4.93	7.31	48.15	2.94	2.57	-12.67
4	36	9.00	1.81	5.15	183.96	2.86	3.00	4.94	4.63	2.21	-52.25	9.70	3.14	-67.67	12.28	10.82	-11.90	10.95	13.52	23.48	16.32	13.61	-9.86	16.32	17.01	4.24	17.95	17.37	-3.22	21.31	18.58	-12.79	21.80	20.66	-5.24
5	14	3.50	4.64	5.74	23.79	6.67	6.90	3.50	9.93	7.19	-27.60	18.33	9.24	-49.62	21.62	19.23	-11.08	17.97	22.04	26.93	22.30	18.77	-15.81	21.85	23.17	6.06	21.77	21.82	0.26	23.45	21.85	-6.84	21.32	21.28	-0.19
6	23	5.75	17.07	8.90	-47.84	19.17	16.38	-14.57	22.99	19.81	-13.84	31.85	22.91	-28.06	30.10	26.13	-6.54	16.76	27.67	47.53	19.14	18.20	-4.96	15.74	19.84	26.09	12.90	15.80	22.46	10.71	13.49	25.97	7.41	8.24	11.22
7	13	3.25	7.23	5.66	-21.68	9.87	9.92	0.43	14.06	11.71	-16.71	23.91	14.58	-39.03	27.07	24.05	-11.19	20.29	28.42	30.20	24.81	20.72	-16.81	22.71	25.21	11.01	21.06	22.61	7.37	21.15	21.53	1.81	17.58	18.98	7.93
8	23	5.75	1.39	5.11	267.74	2.40	4.73	97.50	4.19	3.70	-11.63	9.25	4.12	-55.44	13.07	10.71	-18.05	12.46	13.99	12.28	16.91	15.43	-18.41	20.50	20.56	0.24	22.70	21.54	-5.11	29.62	23.24	-21.53	32.13	26.83	-16.47
9	19	4.75	25.33	12.13	-52.11	22.94	19.52	-14.92	22.77	23.65	3.87	24.03	25.03	4.13	18.84	20.56	9.10	9.27	17.22	85.81	7.68	9.74	26.84	5.29	7.56	42.96	3.54	4.88	37.82	2.31	3.02	30.70	1.22	0.09	-92.22
10	6	1.50	24.51	11.57	-52.81	24.09	20.55	-14.70	25.67	25.00	-2.60	29.96	27.16	-9.39	25.13	25.57	1.74	13.45	22.77	69.22	11.99	13.32	11.06	8.79	12.23	39.13	6.33	8.55	35.17	4.47	6.18	38.36	2.58	1.43	-44.53
11	23	5.75	3.48	4.33	24.27	5.38	7.57	40.85	8.57	8.56	-0.06	16.34	10.43	-36.18	21.14	16.35	-13.20	17.82	21.63	21.43	24.37	19.32	-20.73	23.98	24.99	4.23	23.71	23.94	1.00	27.42	23.88	-12.91	25.78	24.16	-6.29
12	17	4.25	15.63	6.98	-55.37	17.78	16.04	-9.81	21.59	21.16	-1.96	29.24	24.50	-16.22	28.50	26.82	-5.87	17.84	26.45	49.98	18.13	17.44	-3.83	14.52	18.76	29.18	11.45	14.56	27.12	8.56	11.75	22.83	6.46	6.71	3.84
13	8	2.00	20.05	8.96	-55.30	20.33	17.64	-13.25	22.29	22.96	3.03	26.28	25.50	-2.96	23.03	23.33	1.29	12.58	21.15	68.14	11.54	12.79	10.82	8.46	11.68	38.07	6.04	8.16	35.14	4.41	5.70	29.15	2.59	1.48	-43.04
14	14	3.50	9.59	5.00	-47.85	12.40	12.31	-0.72	16.85	16.18	-3.96	26.28	19.59	-25.48	28.78	25.89	-10.06	20.21	27.54	36.31	23.33	20.30	-12.99	20.30	24.06	18.60	17.54	20.50	16.88	16.69	18.30	9.65	12.87	14.44	12.26
15	10	2.50	14.75	5.89	-60.07	16.24	14.40	-11.33	19.18	20.19	5.28	24.40	23.34	-4.34	23.39	22.48	-3.88	13.81	21.70	57.09	13.74	14.21	3.41	10.50	14.22	35.45	7.81	10.61	35.88	6.27	7.87	25.46	3.99	3.70	-7.24
16	4	1.00	6.21	3.75	-39.60	8.74	10.03	14.70	12.80	13.18	2.89	21.66	16.15	-25.43	25.83	22.85	-11.53	19.60	25.48	29.99	24.43	20.35	-16.72	22.21	25.25	13.68	20.06	22.53	12.31	20.81	20.90	0.44	17.32	16.58	7.24
17	12	3.00	1.60	3.58	123.67	2.77	6.34	128.55	4.89	6.63	35.76	10.25	7.43	-27.46	14.96	12.29	-17.92	13.91	15.65	11.90	21.07	16.18	-23.19	21.70	22.12	1.92	22.37	22.48	0.49	29.02	23.25	-19.87	29.86	25.93	-13.18
18	12	3.00	16.02	6.76	-57.80	16.04	12.00	-20.19	15.44	16.93	9.64	16.23	19.03	17.21	13.52	14.68	8.60	6.76	12.74	88.53	5.79	7.96	37.28	3.93	5.84	48.66	2.58	3.73	45.88	1.73	1.95	12.47	0.92	0.13	-85.49
19	17	4.25	8.58	2.64	-69.23	10.50	9.48	-9.72	13.61	14.84	9.05	19.02	18.05	-5.08	20.35	18.38	-6.71	13.21	19.23	45.61	14.47	14.19	-1.86	11.61	16.53	33.79	9.06	12.61	38.03	8.12	9.96	22.72	5.66	6.67	21.26
20	18	4.50	3.00	2.58	-14.09	4.67	7.37	57.84	7.50	9.57	27.55	13.87	11.44	-17.55	18.58	15.91	-14.37	15.53	18.95	22.06	21.47	17.27	-19.54	20.49	22.67	10.65	19.38	21.58	11.39	22.74	20.90	-8.09	20.96	21.22	1.25
21	18	4.50	6.26	1.95	-68.86	8.30	8.33	0.33	11.56	13.06	13.15	17.62	16.12	-8.52	20.36	17.93	-11.96	14.32	19.71	37.68	16.91	15.51	-8.32	14.30	18.24	27.58	11.82	15.53	31.41	11.55	13.25	14.69	8.79	10.83	23.22
22	31	7.75	10.31	3.42	-66.95	11.11	8.90	-19.96	12.94	14.06	8.63	15.73	16.81	6.98	16.21	14.67	-3.53	8.81	14.34	62.80	8.75	10.12	15.67	6.53	9.42	44.41	4.72	7.01	48.62	3.84	4.89	27.13	2.45	2.34	-4.46
23	11	2.75	4.50	2.05	-54.58	6.51	8.03	23.35	9.78	11.75	20.11	16.49	14.41	-12.61	20.61	17.99	-12.70	15.85	20.60	29.97	20.32	17.26	-15.04	18.28	21.68	18.59	16.19	19.52	20.59	17.38	17.85	2.72	14.58	16.45	12.84
24	19	5.00	2.99	0.54	-81.94	4.28	4.74	10.57	6.40	8.35	30.34	10.29	10.48	1.81	13.12	10.89	-17.00	9.86	12.97	31.48	12.61	11.85	-6.05	10.93	14.63	33.86	9.19	13.23	43.86	9.88	11.68	18.18	8.03	11.20	39.33
	Area (km^2)	109.75																																	
Volume of Rainfall (mm-km^2/hr)			1079.27	653.97	-39.41	1215.24	1119.48	-7.88	1494.19	1393.15	-6.76	2154.05	1631.85	-24.24	2229.87	2062.70	-7.50	1542.32	2159.82	40.04	1797.80	1655.52	-7.91	1620.37	1895.05	16.95	1485.52	1668.17	12.30	1539.32	1545.72	0.42	2132.43	1347.15	-36.83
Root Mean Square Error					6.78			2.31			2.17			5.65			2.05			6.29			2.63			2.91			2.32			2.46			1.84

APPENDIX G
Forecast of Spatial Distribution of Subcatchment Rainfall

Artificial Event No.146																							
Sub-Catchment No.	No. of Cell	Area		Time step 1			Time step 2			Time step 3			Time step 4			Time step 5			Time step 6			Time step 7	
			Actual	Predicted	% error	Actual	Predicted	% error	Actual	Predicted	% error	Actual	Predicted	% error	Actual	Predicted	% error	Actual	Predicted	% error	Actual	Predicted	% error
	(no.)	(km^2)	(mm/hr)	(mm/hr)	(%)	(mm/hr)	(mm/hr)	(%)	(mm/hr)	(mm/hr)	(%)	(mm/hr)	(mm/hr)	(%)	(mm/hr)	(mm/hr)	(%)	(mm/hr)	(mm/hr)	(%)	(mm/hr)	(mm/hr)	(%)
1	27	6.75	22.11	28.70	29.83	19.75	20.05	1.50	16.89	18.96	12.24	12.22	14.97	22.55	8.89	9.03	1.58	4.42	4.50	1.70	2.37	0.73	-69.10
2	35	8.75	22.95	28.90	25.92	20.56	22.29	8.42	19.13	20.85	9.01	14.84	17.77	19.72	11.94	11.07	-7.31	6.81	5.72	-15.96	3.99	2.07	-48.14
3	28	7.00	15.72	21.27	35.27	13.70	18.29	33.56	13.53	15.43	13.98	11.00	13.56	23.31	9.58	8.42	-12.10	6.16	4.18	-32.12	3.87	2.76	-28.60
4	36	9.00	17.94	24.63	37.30	17.90	16.99	-5.11	16.13	17.67	9.54	12.35	14.64	18.53	9.35	10.43	11.58	4.75	6.79	42.84	2.67	2.39	-10.55
5	14	3.50	22.64	28.33	25.15	23.79	21.78	-8.45	23.96	23.71	-1.06	20.17	21.69	7.50	17.15	16.26	-5.15	10.08	11.55	14.61	6.25	5.96	-4.63
6	23	5.75	19.50	24.37	24.97	19.55	21.67	10.82	21.21	21.63	1.98	18.87	20.93	10.92	17.71	15.57	-12.10	12.11	11.05	-8.71	8.16	7.81	-4.26
7	13	3.25	22.33	27.22	21.89	24.46	22.80	-6.80	26.84	25.47	-5.12	24.38	24.90	2.11	22.79	19.88	-12.78	15.12	15.55	2.83	10.25	10.27	0.23
8	23	5.75	15.64	20.60	31.69	18.72	15.77	-15.72	20.14	19.32	-4.08	18.21	18.47	1.44	16.34	15.84	-3.04	10.00	13.13	31.23	6.60	8.32	25.94
9	19	4.75	6.96	9.97	43.27	7.08	11.61	64.09	8.81	9.29	5.51	8.80	9.51	8.08	9.72	7.94	-18.26	8.30	6.73	-18.86	6.46	7.77	20.21
10	6	1.50	11.40	15.25	33.77	11.51	15.85	37.75	13.58	14.15	4.19	12.94	14.32	10.61	13.38	11.22	-16.17	10.44	8.65	-17.13	7.63	8.27	8.30
11	23	5.75	17.83	21.24	19.10	22.13	18.66	-15.69	26.53	23.47	-11.54	26.35	24.42	-7.31	26.70	21.97	-17.70	19.15	19.86	3.72	14.14	15.50	9.62
12	17	4.25	14.57	17.45	19.78	16.36	18.17	11.04	20.38	19.42	-4.72	20.60	20.93	1.60	22.25	18.25	-17.98	17.92	16.46	-8.10	13.81	15.42	11.71
13	8	2.00	9.23	11.69	26.65	10.16	13.70	34.82	13.17	12.90	-2.04	13.72	14.10	2.79	15.61	12.66	-18.87	13.59	11.98	-11.89	10.94	13.10	19.74
14	14	3.50	18.01	21.12	17.28	21.10	20.39	-3.37	25.88	23.76	-8.22	25.97	25.37	-2.32	27.32	22.34	-18.26	20.96	20.14	-3.92	15.85	17.24	8.75
15	10	2.50	9.39	10.66	13.49	11.32	13.39	18.33	15.67	14.41	-8.06	17.42	16.89	-3.07	21.02	16.67	-20.70	19.33	17.61	-8.92	16.50	19.46	17.95
16	4	1.00	16.82	19.13	13.69	21.13	18.90	-10.54	27.03	23.80	-11.95	28.29	26.18	-7.47	30.77	24.35	-20.86	24.24	23.38	-3.57	18.96	20.63	8.81
17	12	3.00	12.12	13.34	10.11	17.19	13.13	-23.67	22.98	19.10	-16.90	25.38	21.63	-14.79	28.49	22.03	-22.68	22.69	22.50	-0.85	18.58	20.21	8.75
18	12	3.00	3.84	4.89	27.47	4.56	7.67	68.27	6.75	6.54	-3.10	7.92	7.87	-0.66	10.39	8.66	-16.68	10.79	10.43	-3.42	9.91	14.07	41.97
19	17	4.25	8.26	7.94	-3.98	11.03	11.25	2.05	16.49	14.27	-13.44	19.85	18.13	-8.67	25.90	19.96	-22.91	25.90	23.45	-9.49	24.19	26.58	9.89
20	18	4.50	11.72	11.93	1.80	16.74	13.50	-19.35	23.78	19.66	-17.33	27.62	23.45	-15.10	33.24	24.58	-26.07	29.08	26.43	-9.11	25.29	25.91	2.45
21	18	4.50	9.27	8.77	-5.36	12.80	11.88	-7.18	19.13	16.24	-15.13	23.13	20.54	-11.22	29.98	22.58	-24.69	29.44	26.18	-11.09	27.46	28.63	4.26
22	31	7.75	4.96	4.82	-2.89	6.52	8.08	23.97	10.10	9.02	-10.71	12.53	11.80	-5.84	17.20	13.89	-19.24	18.58	17.61	-5.22	18.16	22.07	21.53
23	11	2.75	11.02	10.84	-1.62	15.56	13.35	-14.19	22.75	19.03	-16.35	26.98	23.31	-13.59	33.63	24.85	-26.09	31.00	27.55	-11.13	27.73	28.41	2.43
24	19	5.00	5.21	3.25	-37.73	8.36	6.87	-17.86	14.38	11.62	-19.17	19.80	16.70	-15.70	29.22	21.26	-27.25	32.88	27.58	-16.13	34.63	32.11	-7.28
	Area (km^2)	109.75																					
Volume of Rainfall (mm-km^2/hr)			1584.04	1937.85	22.34	1724.44	1749.60	1.46	1979.78	1909.65	-3.54	1936.99	1950.57	0.70	2053.12	1712.15	-16.61	1668.94	1577.10	-5.50	1377.55	1441.53	4.64
Root Mean Square Error					3.72			2.66			2.16			2.15			4.65			2.07			1.88

APPENDIX G
Forecast of Spatial Distribution of Subcatchment Rainfall

Artificial Event No.147

Sub-Catchment No.	No. of Cell	Area	Time step 1			Time step 2			Time step 3			Time step 4			Time step 5			Time step 6			Time step 7			Time step 8			Time step 9		
			Actual	Predicted	% error	Actual	Predicted	% error	Actual	Predicted	% error	Actual	Predicted	% error	Actual	Predicted	% error	Actual	Predicted	% error	Actual	Predicted	% error	Actual	Predicted	% error	Actual	Predicted	% error
	(no.)	(km²)	(mm/hr)	(mm/hr)	(%)	(mm/hr)	(mm/hr)	(%)	(mm/hr)	(mm/hr)	(%)	(mm/hr)	(mm/hr)	(%)	(mm/hr)	(mm/hr)	(%)	(mm/hr)	(mm/hr)	(%)	(mm/hr)	(mm/hr)	(%)	(mm/hr)	(mm/hr)	(%)	(mm/hr)	(mm/hr)	(%)
1	27	6.75	30.86	29.25	-5.21	34.12	24.72	-27.56	21.50	22.56	4.94	13.71	18.41	34.25	11.93	10.07	-15.65	8.10	7.97	-1.60	3.67	2.98	-18.77	1.85	1.94	5.18	0.93	2.72	192.20
2	35	8.75	27.12	26.70	-1.54	34.67	25.36	-26.85	24.47	27.08	10.68	18.15	21.20	16.77	18.99	15.81	-16.75	14.85	16.24	9.34	8.17	8.83	8.07	4.75	4.81	1.32	2.61	4.26	63.19
3	28	7.00	15.51	17.29	11.48	22.60	17.82	-21.17	17.71	21.64	22.22	15.35	16.12	5.02	19.45	16.60	-14.63	17.54	19.85	13.21	11.87	13.45	13.35	8.03	8.17	1.76	4.81	6.39	32.87
4	36	9.00	28.42	27.19	-4.33	30.93	22.35	-27.74	19.26	19.02	-1.24	11.51	16.85	46.35	9.25	8.24	-10.94	6.12	5.19	-15.19	2.59	1.79	-30.79	1.26	1.34	6.37	0.64	2.30	256.24
5	14	3.50	31.62	28.67	-9.32	40.05	27.50	-31.33	28.04	28.09	0.20	19.20	23.99	24.99	18.15	15.52	-14.48	13.82	13.95	0.97	6.96	7.71	10.70	3.67	4.29	10.96	2.18	4.11	88.59
6	23	5.75	21.23	20.22	-4.76	32.00	23.40	-26.89	25.70	29.09	13.21	21.64	23.21	7.25	26.38	21.67	-17.84	24.10	25.34	5.16	15.86	18.46	16.38	10.69	11.19	4.67	6.66	8.87	33.15
7	13	3.25	28.61	25.58	-10.58	40.40	27.77	-31.27	30.84	31.58	2.41	23.33	26.75	14.68	24.90	20.58	-17.35	21.16	21.41	1.19	12.24	14.40	17.68	7.59	8.16	7.53	4.65	6.77	45.43
8	23	5.75	25.15	23.55	-6.37	31.47	21.63	-31.29	21.88	20.57	-6.00	14.05	19.06	35.79	12.30	11.15	-9.32	9.25	8.06	-12.89	4.40	4.27	-3.05	2.40	2.40	-0.16	1.40	2.49	77.12
9	19	4.75	5.89	5.97	1.48	11.14	8.83	-20.76	10.71	13.26	23.80	11.45	10.44	-8.84	18.65	15.71	-15.81	21.48	21.58	0.47	19.35	20.70	6.97	16.50	17.07	3.42	11.98	14.75	23.16
10	6	1.50	10.55	10.43	-1.08	18.38	14.18	-22.84	16.53	20.23	22.38	16.19	15.73	-2.80	23.67	19.57	-17.34	24.93	25.53	2.42	19.90	22.08	10.98	15.46	15.92	2.97	10.52	12.98	23.38
11	23	5.75	24.88	21.21	-14.74	36.26	24.11	-33.49	28.43	27.72	-2.48	21.13	24.74	17.08	22.09	18.80	-14.91	19.32	18.80	-2.65	11.18	13.85	23.94	7.08	8.04	13.62	4.61	6.53	41.48
12	17	4.25	15.19	12.50	-17.70	26.13	18.79	-28.11	23.31	26.71	14.57	21.55	21.90	1.61	29.40	23.61	-19.71	30.49	29.60	-2.92	23.04	26.15	13.48	17.49	18.11	3.53	12.24	14.64	19.55
13	8	2.00	8.50	6.99	-17.79	15.99	11.90	-25.60	15.31	18.39	20.09	15.72	14.84	-5.64	24.40	19.70	-19.26	27.80	26.54	-4.54	24.08	25.66	6.59	20.18	20.26	0.39	14.91	17.24	15.58
14	14	3.50	21.13	17.50	-17.19	34.03	23.58	-30.72	28.83	30.88	7.11	24.40	26.17	7.25	29.88	24.18	-19.07	28.91	28.20	-2.45	19.59	23.26	18.77	13.81	14.80	7.20	9.38	11.81	25.91
15	10	2.50	9.11	6.00	-34.16	17.69	12.51	-29.27	17.34	20.14	16.13	17.68	16.99	-3.88	27.11	21.40	-21.08	31.53	28.68	-9.03	27.25	29.01	6.45	23.08	23.05	-0.13	17.70	19.62	10.87
16	4	1.00	20.94	16.60	-20.71	33.99	22.96	-32.40	28.97	29.98	3.46	23.99	26.23	9.31	28.56	23.43	-17.99	27.67	26.65	-3.69	18.36	22.48	22.41	12.86	14.25	10.80	8.91	11.30	26.82
17	12	3.00	17.94	14.39	-19.80	27.80	17.86	-35.76	22.90	21.29	-7.03	17.19	20.33	18.30	18.16	16.08	-11.43	16.79	15.73	-6.32	10.05	13.18	31.16	6.66	7.95	19.35	4.69	6.20	32.10
18	12	3.00	3.15	1.73	-45.19	6.97	5.13	-26.33	7.58	8.99	18.58	8.97	7.93	-11.61	16.50	13.47	-18.40	22.02	19.70	-10.55	23.15	23.22	0.30	22.64	22.69	0.22	18.88	21.19	12.24
19	17	4.25	8.58	4.35	-49.36	17.11	11.41	-33.35	17.21	19.05	10.69	17.39	17.18	-1.22	26.47	20.83	-21.30	31.92	27.76	-13.03	26.12	30.06	6.88	24.71	24.65	-0.24	20.33	21.29	4.73
20	18	4.50	15.50	10.86	-29.96	26.60	17.23	-35.22	23.73	23.50	-0.96	19.76	21.94	11.06	23.67	20.06	-15.18	24.13	22.59	-6.38	16.49	21.13	28.15	12.05	13.96	15.85	9.01	10.99	21.98
21	18	4.50	10.37	5.66	-45.49	19.97	13.17	-34.03	19.55	21.02	7.54	18.78	19.24	2.45	26.90	21.48	-20.16	31.35	27.62	-11.89	26.09	29.21	11.94	22.11	22.76	2.95	18.04	19.21	6.47
22	31	7.75	4.67	1.90	-59.35	9.99	6.70	-32.92	10.67	12.08	13.21	11.85	11.18	-5.66	20.35	16.09	-20.98	26.92	22.84	-15.16	27.15	27.14	-0.03	26.34	25.38	-3.67	22.91	23.31	1.76
23	11	2.75	13.43	8.40	-37.44	24.49	16.09	-34.30	22.92	23.83	3.94	20.50	21.89	6.79	26.81	22.00	-17.96	29.17	26.62	-8.75	21.90	26.40	20.57	17.14	18.80	9.66	13.32	15.24	14.42
24	19	5.00	5.96	1.75	-70.73	12.78	7.80	-39.00	13.58	14.15	4.15	13.66	14.32	4.81	20.66	17.05	-17.46	26.35	22.42	-14.90	23.68	26.78	13.08	21.66	22.17	2.34	19.44	18.96	-2.45
	Area (km²)	109.75																											
Volume of Rainfall (mm-km²/hr)			1965.52	1745.53	-12.09	2831.37	1991.72	-29.65	2243.48	2391.88	6.61	1829.84	2048.40	11.94	2237.45	1854.43	-17.12	2236.93	2129.33	-4.81	1670.19	1842.37	10.31	1317.11	1357.60	3.07	994.96	1174.05	18.00
Root Mean Square Error					3.03			8.25			2.09			2.63			4.07			2.07			2.50			0.80			1.91

APPENDIX G
Forecast of Spatial Distribution of Subcatchment Rainfall

Artificial Event No.148																														
Sub-Catchment No.	No. of Cell	Area	Time step 1			Time step 2			Time step 3			Time step 4			Time step 5			Time step 6			Time step 7			Time step 8			Time step 9		
			Actual	Predicted	% error	Actual	Predicted	% error	Actual	Predicted	% error	Actual	Predicted	% error	Actual	Predicted	% error	Actual	Predicted	% error	Actual	Predicted	% error	Actual	Predicted	% error	Actual	Predicted	% error
	(no.)	(km^2)	(mm/hr)	(mm/hr)	(%)	(mm/hr)	(mm/hr)	(%)	(mm/hr)	(mm/hr)	(%)	(mm/hr)	(mm/hr)	(%)	(mm/hr)	(mm/hr)	(%)	(mm/hr)	(mm/hr)	(%)	(mm/hr)	(mm/hr)	(%)	(mm/hr)	(mm/hr)	(%)	(mm/hr)	(mm/hr)	(%)
1	27	6.75	2.93	3.70	26.03	4.87	2.70	-44.53	7.46	8.46	13.40	11.99	9.98	-16.79	17.80	14.37	-19.25	19.01	16.71	-12.13	20.58	17.12	-16.79	24.50	18.69	-23.72	20.81	20.10	-3.39
2	35	8.75	5.60	3.89	-32.93	7.95	5.42	-31.76	10.83	10.24	-5.42	14.97	13.33	-10.93	17.70	16.39	-7.42	16.39	15.77	-3.79	14.62	14.97	2.35	14.47	14.91	3.04	10.45	14.07	34.65
3	28	7.00	7.08	2.89	-59.22	7.87	6.59	-16.20	9.64	7.58	-21.31	11.47	11.33	-1.26	10.66	11.69	9.62	8.51	8.57	0.75	6.32	7.31	15.75	5.25	6.48	23.41	3.26	4.86	49.07
4	36	9.00	2.59	5.46	110.86	4.67	3.15	-32.46	7.08	9.79	38.22	11.77	10.24	-13.01	19.65	14.96	-23.90	22.54	19.17	-14.95	25.84	20.44	-20.88	32.61	22.58	-30.78	29.40	24.80	-15.65
5	14	3.50	6.65	8.16	22.66	10.12	7.88	-22.17	13.60	15.58	14.45	19.56	17.06	-12.79	26.88	21.59	-19.70	27.21	23.86	-12.31	25.99	23.87	-8.14	27.53	24.14	-12.29	21.35	24.07	12.73
6	23	5.75	11.85	8.13	-31.43	13.76	12.67	-7.94	16.17	15.24	-5.73	19.15	18.51	-3.37	19.11	19.37	1.39	15.86	16.23	2.32	11.63	14.25	20.44	9.90	12.41	25.44	6.23	10.06	61.42
7	13	3.25	11.53	11.12	-3.59	15.33	13.06	-14.81	18.63	19.53	4.84	23.93	21.39	-10.61	28.44	24.44	-14.06	26.25	24.53	-6.55	21.92	23.35	6.50	20.48	22.05	7.71	14.28	20.32	42.22
8	23	5.75	5.42	8.90	63.96	8.85	6.97	-21.30	11.61	14.86	28.02	17.10	15.02	-12.17	26.46	19.52	-26.25	28.81	23.93	-16.97	29.17	25.20	-13.64	32.92	26.32	-20.05	27.32	27.28	-0.17
9	19	4.75	12.15	7.35	-39.54	10.32	12.78	23.90	10.02	8.27	-17.48	9.31	10.40	11.65	6.49	7.93	22.26	4.30	3.92	-8.85	2.37	2.53	6.81	1.49	1.42	-4.90	0.73	0.36	-51.05
10	6	1.50	13.20	7.63	-42.15	12.64	13.80	9.20	13.24	11.28	-14.79	13.50	14.27	5.66	10.72	12.45	16.12	7.70	7.87	2.13	4.74	5.93	25.16	3.30	4.15	25.86	1.77	2.17	22.66
11	23	5.75	12.96	14.25	9.79	17.47	15.23	-12.84	20.07	21.73	8.31	25.26	22.13	-12.42	31.51	24.97	-20.74	29.91	26.41	-11.70	24.96	25.63	3.49	23.43	24.45	4.37	16.61	22.90	37.84
12	17	4.25	18.99	13.98	-26.39	19.42	20.22	4.16	20.00	19.07	-4.65	20.90	21.01	0.54	18.44	19.53	5.88	14.13	14.93	5.65	9.16	12.19	33.14	6.73	9.28	37.95	3.82	6.48	69.56
13	8	2.00	17.61	11.96	-31.98	15.67	18.26	16.52	15.05	13.61	-9.58	14.24	15.36	7.89	10.67	12.51	17.23	7.39	7.65	3.54	4.22	5.46	29.70	2.75	3.41	24.11	1.40	1.53	8.66
14	14	3.50	18.54	15.79	-14.82	21.21	20.36	-3.99	22.85	22.93	0.33	25.76	24.30	-5.66	26.14	24.68	-5.66	21.84	22.00	0.75	15.66	19.59	25.03	12.70	16.60	30.76	7.88	13.71	74.05
15	10	2.50	23.01	17.36	-24.57	20.71	23.54	13.64	19.13	18.46	-3.52	17.60	18.95	6.43	13.72	15.69	14.36	9.63	10.60	10.05	5.44	7.89	45.06	3.51	5.06	44.19	1.79	2.75	53.79
16	4	1.00	19.63	18.20	-7.27	23.08	21.80	-5.56	24.44	25.08	2.60	27.64	25.48	-7.83	29.34	26.13	-10.95	25.15	24.63	-2.08	18.26	22.50	23.20	15.00	19.43	29.50	9.46	16.50	74.36
17	12	3.00	14.23	16.12	13.24	18.76	16.58	-11.64	19.91	21.79	9.46	23.67	21.03	-11.90	30.01	22.97	-23.46	28.53	25.07	-12.15	22.91	24.97	8.97	20.85	23.42	12.29	14.56	21.68	50.28
18	12	3.00	16.85	13.85	-17.82	12.47	18.06	44.84	10.35	10.45	0.93	6.34	10.25	22.93	5.12	6.81	32.92	3.12	3.09	-1.01	1.47	1.53	3.50	0.80	0.49	-38.66	0.35	0.03	-90.53
19	17	4.25	28.49	23.26	-18.37	25.36	28.10	10.79	22.03	22.68	2.96	19.92	21.21	6.47	15.79	17.66	11.85	11.28	13.25	17.41	6.34	10.33	62.96	4.10	6.92	68.60	2.12	4.46	110.23
20	18	4.50	21.58	20.89	-3.21	24.97	23.32	-6.60	24.46	25.49	4.21	26.45	24.31	-8.12	28.49	24.33	-14.58	24.57	23.98	-2.41	17.27	22.42	29.86	13.82	19.29	39.57	8.63	16.56	91.81
21	18	4.50	29.06	24.39	-16.07	27.49	28.77	4.65	24.32	25.12	3.27	22.87	23.34	2.06	19.69	20.51	4.16	14.81	16.90	14.10	8.82	14.02	58.90	6.05	10.25	69.35	3.30	7.43	125.01
22	31	7.75	24.61	20.52	-16.62	19.18	24.44	27.43	15.55	16.66	7.12	12.82	15.05	17.41	8.84	11.13	25.80	5.84	7.02	20.21	3.01	4.77	58.87	1.82	2.56	40.87	0.90	1.32	46.75
23	11	2.75	26.41	23.49	-11.04	27.78	27.24	-1.97	25.96	26.66	2.70	26.24	25.17	-4.07	25.32	23.74	-6.25	20.41	21.53	5.48	13.19	19.06	44.52	9.76	15.25	56.22	5.69	12.13	113.27
24	19	5.00	31.47	26.43	-16.03	28.05	29.20	4.10	22.31	24.26	8.72	19.30	20.78	7.67	15.94	17.40	9.14	11.63	14.77	26.95	6.35	12.34	94.19	4.03	8.74	116.86	2.08	6.38	206.87
	Area (km^2)	109.75																												
Volume of Rainfall ($mm\text{-}km^2/hr$)			1576.50	1367.68	-13.25	1648.99	1634.53	-0.88	1701.78	1764.42	3.68	1913.44	1841.55	-3.76	2065.21	1899.75	-8.01	1855.69	1778.68	-4.15	1546.32	1649.35	6.66	1513.33	1513.60	0.02	1136.02	1387.60	22.15
Root Mean Square Error					3.68			2.39			1.50			1.76			3.42			2.07			3.35			3.88			4.21

APPENDIX G
Forecast of Spatial Distribution of Subcatchment Rainfall

Artificial Event No.149																														
Sub-Catchment No.	No. of Cell	Area		Time step 1			Time step 2			Time step 3			Time step 4			Time step 5			Time step 6			Time step 7			Time step 8			Time step 9		
			Actual	Predicted	% error	Actual	Predicted	% error	Actual	Predicted	% error	Actual	Predicted	% error	Actual	Predicted	% error	Actual	Predicted	% error	Actual	Predicted	% error	Actual	Predicted	% error	Actual	Predicted	% error
	(no.)	(km^2)	(mm/hr)	(mm/hr)	(%)	(mm/hr)	(mm/hr)	(%)	(mm/hr)	(mm/hr)	(%)	(mm/hr)	(mm/hr)	(%)	(mm/hr)	(mm/hr)	(%)	(mm/hr)	(mm/hr)	(%)	(mm/hr)	(mm/hr)	(%)	(mm/hr)	(mm/hr)	(%)	(mm/hr)	(mm/hr)	(%)	(mm/hr)	(mm/hr)	(%)
1	27	6.75	27.02	28.27	4.63	32.66	25.68	-20.76	23.36	26.50	13.46	22.13	22.03	-0.45	15.83	20.38	28.74	12.47	14.10	13.14	9.25	10.37	12.19	4.59	4.30	-6.40	2.48	2.27	-8.53
2	35	6.75	21.82	22.58	3.49	30.14	23.71	-21.34	24.93	27.20	9.11	25.63	23.96	-6.52	18.71	24.23	29.46	15.86	17.15	8.18	13.00	13.89	6.83	6.91	6.22	-10.04	4.20	3.60	-14.27
3	28	7.00	11.80	12.58	6.66	18.39	15.80	-14.09	17.43	19.87	14.00	19.25	18.58	-3.53	14.03	19.80	41.15	12.53	14.04	12.01	11.07	11.95	7.90	6.16	5.32	-13.56	4.15	3.31	-20.25
4	36	9.00	23.48	27.44	16.82	27.78	23.50	-15.39	19.26	22.79	18.35	18.33	18.92	3.22	14.14	17.21	21.70	11.69	13.25	13.40	9.18	10.39	13.22	4.66	5.98	23.11	2.68	4.34	61.61
5	14	3.50	23.14	25.71	11.09	31.45	24.65	-20.98	25.24	27.48	8.87	26.33	24.31	-7.66	21.41	24.71	15.38	19.48	19.69	1.07	17.31	17.24	-0.37	10.02	11.21	11.90	6.27	8.31	32.69
6	23	5.75	14.49	14.96	3.24	23.15	18.72	-19.14	22.29	24.45	9.69	25.52	23.21	-9.06	20.54	25.73	25.27	19.92	20.21	1.43	19.39	18.94	-2.34	11.82	12.37	4.66	8.41	9.04	7.56
7	13	3.25	19.22	20.95	8.99	28.76	22.62	-21.35	25.61	27.48	7.33	28.57	25.42	-11.02	24.26	27.55	13.53	23.83	22.79	-4.37	23.44	21.55	-8.07	14.68	15.85	7.97	10.22	12.25	19.92
8	23	5.75	17.17	22.18	29.19	22.84	19.37	-15.18	17.80	19.96	12.13	18.78	17.83	-5.04	16.70	17.97	7.60	16.18	16.10	-0.47	15.50	14.91	-3.83	9.74	11.87	21.84	6.35	10.28	61.88
9	19	4.75	3.50	3.93	12.04	6.89	7.36	6.83	8.33	10.40	24.86	10.87	11.13	2.32	9.10	12.77	40.33	9.96	10.63	6.66	11.43	10.77	-5.80	7.81	8.51	8.94	6.74	7.31	8.46
10	6	1.50	6.60	6.72	1.84	12.05	10.98	-8.84	13.41	15.72	17.17	16.68	16.03	-3.89	13.73	18.50	34.76	14.32	14.90	4.03	15.36	14.70	-4.32	9.99	10.53	5.49	7.95	8.38	5.43
11	23	5.75	15.24	17.43	14.38	23.26	18.23	-21.65	21.02	22.27	5.91	24.28	21.23	-12.58	22.60	23.78	5.21	24.08	21.69	-9.93	26.21	21.94	-16.27	18.12	19.54	7.84	13.57	16.81	23.90
12	17	4.25	8.98	8.14	-9.39	16.08	12.93	-19.60	17.42	19.22	10.37	21.82	19.56	-10.35	19.33	23.38	20.93	21.21	20.21	-4.75	24.20	21.15	-12.63	16.84	18.42	9.38	13.86	15.29	10.33
13	8	2.00	4.84	4.28	-11.60	9.41	8.55	-9.15	11.19	13.06	16.77	14.71	13.94	-5.24	13.00	16.78	29.06	14.77	14.60	-1.12	17.69	15.56	-12.01	12.65	14.13	11.63	11.14	12.20	9.55
14	14	3.50	12.65	12.61	-0.34	21.26	16.56	-22.13	21.42	22.99	7.33	25.98	22.70	-12.64	23.50	26.61	13.21	25.49	23.45	-8.00	28.52	24.29	-14.84	19.77	21.36	8.04	15.63	17.78	13.71
15	10	2.50	4.62	3.36	-30.28	9.60	7.89	-17.83	11.63	12.96	11.43	15.73	14.18	-9.87	14.85	17.82	19.99	17.91	16.69	-6.79	23.07	18.89	-18.11	17.68	19.83	12.18	16.35	17.74	8.49
16	4	1.00	11.95	12.13	1.46	20.16	15.40	-23.60	20.29	21.43	5.62	24.93	21.48	-13.87	23.68	25.58	7.99	26.87	23.68	-11.24	31.20	25.25	-19.07	22.61	24.10	6.61	18.32	20.88	13.92
17	12	3.00	9.80	11.60	18.34	15.67	11.97	-23.65	14.79	14.85	0.39	18.00	15.14	-15.88	18.54	17.96	-3.13	21.81	18.68	-14.37	26.87	20.55	-23.52	20.82	21.68	4.11	17.17	20.43	18.95
18	12	3.00	1.56	1.19	-23.57	3.51	4.10	16.93	4.86	6.28	29.27	7.08	7.39	4.47	6.72	8.87	31.87	8.60	8.78	2.15	12.02	10.27	-14.59	9.70	12.37	27.49	9.96	11.84	18.84
19	17	4.25	4.23	2.35	-44.34	8.54	6.21	-27.24	10.47	10.91	4.16	14.59	12.49	-14.42	14.89	16.45	10.53	19.31	17.15	-11.18	27.38	20.76	-24.16	23.07	25.38	9.99	23.15	23.73	2.48
20	18	4.50	7.95	7.77	-2.22	13.97	10.09	-27.79	14.60	14.61	0.01	18.83	15.61	-17.14	19.72	19.70	-0.12	24.45	20.63	-15.62	32.32	23.72	-26.62	26.28	26.56	1.04	23.48	24.85	5.82
21	18	4.50	5.11	3.37	-34.08	9.96	6.98	-29.88	11.74	11.96	1.86	16.11	13.50	-16.22	16.77	17.84	6.38	21.77	18.87	-13.32	30.85	22.78	-26.14	26.20	27.69	5.70	25.93	25.94	0.02
22	31	7.75	2.25	1.02	-54.60	4.81	4.08	-15.20	6.36	7.07	11.23	9.25	8.48	-8.31	9.43	11.03	16.94	12.65	11.88	-6.06	18.84	14.76	-21.65	16.37	19.61	19.79	17.57	18.84	7.21
23	11	2.75	6.69	5.48	-18.09	12.45	8.80	-29.30	13.86	14.04	1.26	18.49	15.43	-16.57	19.37	20.01	3.33	24.60	20.93	-14.93	33.62	24.58	-26.88	27.84	28.45	2.18	26.01	26.51	1.93
24	19	5.00	2.53	0.95	-62.38	5.38	2.94	-45.45	6.91	6.17	-10.72	10.26	8.08	-21.25	11.99	11.82	-1.45	17.62	14.93	-15.27	29.10	19.93	-31.53	28.22	28.59	1.31	31.52	28.21	-10.51
	Area (km^2)	109.75																												
Volume of Rainfall (mm-km^2/hr)			1382.30	1458.02	5.48	2021.17	1627.10	-19.50	1818.40	1998.58	9.91	2075.02	1908.83	-8.01	1798.56	2110.50	17.34	1891.69	1832.00	-3.16	2129.86	1843.07	-13.47	1544.45	1655.38	7.18	1331.22	1435.98	7.87
Root Mean Square Error					1.79			3.95			1.80			2.13			3.20			1.95			4.66			1.49			1.88

APPENDIX G
Forecast of Spatial Distribution of Subcatchment Rainfall

Artificial Event No.150

Sub-Catchment No.	No. of Cell	Area	Time step 1			Time step 2			Time step 3			Time step 4			Time step 5			Time step 6		
			Actual	Predicted	% error	Actual	Predicted	% error	Actual	Predicted	% error	Actual	Predicted	% error	Actual	Predicted	% error	Actual	Predicted	% error
	(no.)	(km^2)	(mm/hr)	(mm/hr)	(%)	(mm/hr)	(mm/hr)	(%)	(mm/hr)	(mm/hr)	(%)	(mm/hr)	(mm/hr)	(%)	(mm/hr)	(mm/hr)	(%)	(mm/hr)	(mm/hr)	(%)
1	27	6.75	5.71	11.10	94.57	7.84	2.64	-66.27	8.43	7.68	-8.88	7.23	6.17	-14.69	11.56	5.48	-52.61	12.05	10.19	-15.47
2	35	8.75	5.67	5.00	-11.81	8.48	4.38	-48.37	10.63	7.74	-27.21	10.73	10.21	-4.86	19.19	11.20	-41.62	21.61	19.33	-10.56
3	28	7.00	3.10	0.30	-90.20	5.25	4.64	-11.67	8.01	4.59	-42.67	9.89	10.35	4.73	20.62	13.53	-34.38	25.94	22.44	-13.49
4	36	9.00	8.27	20.60	149.06	9.98	5.32	-46.68	9.04	11.22	24.14	6.54	6.83	4.37	8.66	4.86	-44.02	7.67	6.61	-13.83
5	14	3.50	12.32	17.91	45.36	15.60	8.81	-43.53	15.66	14.96	-4.43	12.66	13.31	5.14	17.61	11.86	-32.62	15.77	16.49	4.57
6	23	5.75	7.65	2.87	-62.41	11.41	8.30	-27.20	14.89	10.26	-31.08	15.79	16.63	5.27	27.29	19.20	-29.67	28.78	28.12	-2.31
7	13	3.25	14.07	13.48	-4.24	18.42	11.33	-38.48	19.90	16.54	-16.89	17.37	18.27	5.16	24.72	17.98	-27.29	22.05	24.18	9.67
8	23	5.75	16.43	28.72	74.80	18.11	12.47	-31.14	15.18	18.17	19.73	10.24	12.54	22.41	11.55	9.35	-19.04	8.52	9.35	9.83
9	19	4.75	2.58	0.19	-92.64	4.43	5.83	31.65	7.39	3.66	-50.43	10.12	11.18	10.41	20.62	15.85	-23.11	24.09	22.29	-7.48
10	6	1.50	4.19	0.00	-100.00	6.89	7.20	4.57	10.57	5.93	-43.87	13.24	14.40	8.74	25.54	18.97	-25.74	28.85	27.12	-6.01
11	23	5.75	20.94	21.52	2.77	24.55	15.86	-35.41	23.28	20.95	-10.00	17.90	20.04	11.96	21.53	16.18	-15.53	16.33	20.68	26.64
12	17	4.25	9.39	1.50	-84.03	13.65	11.11	-18.58	17.86	11.72	-34.38	19.11	20.44	6.94	30.84	23.95	-22.34	29.66	31.25	5.37
13	8	2.00	5.07	0.00	-100.00	8.02	8.20	2.24	12.01	6.81	-43.26	14.74	15.84	7.47	26.43	20.58	-22.15	27.44	27.36	-0.29
14	14	3.50	14.78	7.92	-46.39	19.72	13.82	-29.91	22.68	16.91	-25.47	21.24	22.71	6.90	30.41	24.09	-20.77	26.53	30.26	14.15
15	10	2.50	8.05	0.28	-96.52	11.79	10.73	-9.02	16.14	10.04	-37.81	18.16	19.44	7.04	29.00	23.64	-18.49	26.95	29.12	8.03
16	4	1.00	19.37	12.95	-33.14	24.23	16.50	-31.91	25.68	20.20	-21.33	22.14	24.08	8.72	28.67	24.25	-15.41	22.73	28.43	25.03
17	12	3.00	26.91	26.69	-0.80	28.70	20.02	-30.27	24.52	23.36	-4.74	17.03	20.59	20.94	17.48	17.68	1.19	11.29	16.58	46.81
18	12	3.00	2.83	0.03	-98.82	4.61	5.56	20.48	7.51	3.95	-47.41	10.12	11.05	9.22	18.45	15.35	-16.80	18.84	19.11	1.44
19	17	4.25	11.89	2.18	-81.70	15.97	13.38	-16.23	19.78	13.51	-31.65	20.14	21.77	8.09	27.92	24.71	-11.49	22.59	27.58	22.06
20	18	4.50	25.71	18.64	-27.49	29.00	20.27	-30.12	27.43	22.86	-16.67	21.23	24.25	14.23	23.46	23.06	-1.67	15.93	23.26	46.11
21	18	4.50	16.14	5.86	-64.92	20.46	15.91	-22.25	23.29	16.86	-27.62	21.81	23.76	8.93	27.87	25.81	-8.13	21.05	27.81	31.15
22	31	7.75	6.36	0.43	-93.31	9.12	8.86	-2.92	12.62	8.10	-35.82	14.52	16.78	8.89	22.14	19.44	-12.17	19.25	22.06	14.62
23	11	2.75	21.76	11.80	-45.77	26.02	16.78	-27.83	26.96	20.72	-23.16	22.90	25.34	10.65	27.14	25.67	-5.42	19.37	27.05	39.86
24	19	5.00	18.08	8.00	-55.75	21.06	16.96	-19.54	22.11	17.25	-21.99	19.23	22.07	14.77	21.33	22.81	6.93	13.85	21.42	54.64
	Area (km^2)	109.75																		
Volume of Rainfall (mm-km^2/hr)			1219.35	1041.32	-14.60	1545.13	1109.98	-28.16	1700.68	1361.02	-19.97	1577.11	1705.00	8.11	2295.45	1814.83	-20.94	2102.22	2272.00	8.08
Root Mean Square Error					6.93			5.14			4.44			1.72			4.99			3.99

Sub-Catchment No.	Time step 7			Time step 8			Time step 9			Time step 10		
	Actual	Predicted	% error	Actual	Predicted	% error	Actual	Predicted	% error	Actual	Predicted	% error
	(mm/hr)	(mm/hr)	(%)	(mm/hr)	(mm/hr)	(%)	(mm/hr)	(mm/hr)	(%)	(mm/hr)	(mm/hr)	(%)
1	13.86	10.16	-26.71	10.71	10.54	-1.65	7.34	9.74	32.72	5.11	8.66	69.59
2	26.66	19.05	-28.53	22.58	19.33	-14.40	16.89	16.25	-3.83	12.77	13.12	2.74
3	35.14	24.29	-30.87	33.17	26.03	-21.52	27.52	22.63	-17.79	22.80	18.18	-20.28
4	7.66	5.58	-27.17	5.19	5.22	0.49	3.05	5.39	76.80	1.89	6.14	224.28
5	15.96	13.07	-18.08	11.22	11.07	-1.34	6.73	8.69	29.12	4.31	7.99	85.25
6	33.56	25.90	-22.81	27.72	24.49	-11.67	19.54	18.57	-4.95	14.42	13.59	-5.76
7	22.22	18.95	-14.70	15.84	15.58	-1.61	9.46	10.87	14.95	6.11	8.61	40.82
8	7.29	5.75	-21.14	4.38	3.87	-11.72	2.18	3.54	62.52	1.21	5.23	330.68
9	30.69	24.46	-20.30	28.59	26.03	-8.93	22.34	22.20	-0.64	18.27	15.94	-12.74
10	35.64	27.85	-22.41	31.75	28.02	-11.75	23.85	22.67	-4.95	18.73	16.18	-13.58
11	14.35	13.82	-3.68	9.07	9.52	4.89	4.67	5.99	28.25	2.72	5.57	104.77
12	31.97	27.44	-14.17	25.11	24.55	-2.22	16.27	17.10	5.08	11.46	10.93	-4.63
13	31.56	26.73	-15.31	26.68	26.05	-2.38	18.57	19.95	7.45	13.91	12.91	-7.20
14	26.26	23.76	-9.50	18.83	19.14	1.64	11.07	12.22	10.45	7.19	8.09	12.51
15	28.23	25.83	-8.50	22.02	23.07	4.79	13.86	15.87	14.50	9.69	9.13	-5.76
16	20.73	20.30	-2.05	13.78	14.73	6.85	7.38	8.58	16.20	4.48	5.85	30.66
17	8.64	9.23	6.85	4.86	4.95	1.93	2.14	2.68	25.17	1.12	3.46	208.09
18	21.39	20.06	-6.23	18.39	20.39	10.87	12.70	15.97	25.66	9.66	9.19	-4.89
19	21.04	21.49	2.18	14.81	16.82	13.55	8.20	9.69	18.18	5.24	4.53	-13.53
20	12.77	14.37	12.55	7.63	8.62	12.96	3.57	4.13	15.59	1.98	3.12	57.51
21	18.47	19.83	7.37	12.24	14.13	15.46	6.33	7.32	15.61	3.83	3.38	-11.72
22	19.10	19.39	1.51	14.52	16.99	17.05	8.69	11.20	28.97	5.95	5.29	-11.14
23	16.16	18.01	11.43	10.11	11.75	16.13	4.94	5.70	15.46	2.84	3.13	10.12
24	10.68	13.30	24.56	6.39	7.82	22.24	2.88	2.90	0.72	1.59	0.79	-50.72
Area (km^2)												
Volume of Rainfall (mm-km^2/hr)	2234.57	1919.57	-14.10	1748.90	1691.00	-3.31	1171.71	1250.85	6.75	851.23	921.07	8.21
Root Mean Square Error			4.33			2.23			1.80			2.25